

UNCLASSIFIED

AD NUMBER
ADB043539
NEW LIMITATION CHANGE
TO Approved for public release, distribution unlimited
FROM Distribution authorized to U.S. Gov't. agencies only; Test and Evaluation; Dec 1979. Other requests shall be referred to U.S. Army Armament Research and Development Weapons Systems Lab., Dover, NJ 07801.
AUTHORITY
USARDC ltr, 10 Apr 1984

THIS PAGE IS UNCLASSIFIED

AD

B043539

AUTHORITY

USFADC Ltr 10 APR 84



**② LEVEL III**

AD

AD-E400 384

AD B O 4 3 5 3 9

TECHNICAL REPORT ARLCD-TR-79030

**FUZE GEAR-TRAIN ANALYSIS**

G. G. LOWEN  
CITY COLLEGE OF NEW YORK

F. R. TEPPER  
ARRADCOM

DDC  
RECEIVED  
JAN 29 1980  
B

DECEMBER 1979



**US ARMY ARMAMENT RESEARCH AND DEVELOPMENT COMMAND**  
**LARGE CALIBER**  
**WEAPON SYSTEMS LABORATORY**  
**DOVER, NEW JERSEY**

DDC FILE COPY

Distribution limited to US Government agencies only because of test and evaluation, December 1979. Other requests for this document must be referred to Commander, ARRADCOM, ATTN: DRDAR-TSS, Dover, New Jersey 07801.

79 12 20 031  
THIS DOCUMENT IS BEST QUALITY PRACTICABLE  
THE COPY FURNISHED TO DDC CONTAINED A  
SIGNIFICANT NUMBER OF PAGES WHICH DO NOT  
REPRODUCE LEGIBLY.

The views, opinions, and/or findings contained in this report are those of the author(s) and should not be construed as an official Department of the Army position, policy or decision, unless so designated by other documentation.

Destroy this report when no longer needed. Do not return to the originator.

The citation in this report of the names of commercial firms or commercially available products or services does not constitute official endorsement or approval of such commercial firms, products, or services by the United States Government.

## **DISCLAIMER NOTICE**

**THIS DOCUMENT IS BEST QUALITY  
PRACTICABLE. THE COPY FURNISHED  
TO DDC CONTAINED A SIGNIFICANT  
NUMBER OF PAGES WHICH DO NOT  
REPRODUCE LEGIBLY.**

UNCLASSIFIED

SECURITY CLASSIFICATION OF THIS PAGE (When Data Entered)

REPORT DOCUMENTATION PAGE		READ INSTRUCTIONS BEFORE COMPLETING FORM
1. REPORT NUMBER Technical Report ARI.CD-TR-79030	2. GOVT ACQUISITION NO.	3. RECIPIENT'S CATALOG NUMBER ⑨ Technical report
4. TITLE (and Subtitle) ⑥ Fuze Gear-Train Analysis	5. FUNDING NUMBERS (if applicable)	
7. AUTHOR(S) ⑩ G. G. Lowen / City College of New York F.R. Tepper / ARRADCOM	6. PERFORMING ORG. REPORT NUMBER	
9. PERFORMING ORGANIZATION NAME AND ADDRESS Commander, ARRADCOM LCWSL (DRDAR-LCN) Dover, NJ 07801	8. CONTRACT OR GRANT NUMBER(s)	
11. CONTROLLING OFFICE NAME AND ADDRESS Commander, ARRADCOM TSD, STINFO (DRDAR-TSS) Dover, NJ 07801	10. PROGRAM ELEMENT, PROJECT, TASK AREA & WORK UNIT NUMBERS	
14. MONITORING AGENCY NAME & ADDRESS (if different from Controlling Office) ⑬ 481	12. REPORT DATE ⑪ December 1979	
	13. NUMBER OF PAGES 478	
	16. SECURITY CLASS. (of this report) Unclassified	
16. DISTRIBUTION STATEMENT (of this Report) Distribution limited to U.S. Government agencies only because of test and evaluation, December 1979. Other requests for this document must be referred to Commander, ARRADCOM, ATTN: DRDAR-TSS, Dover, NJ 07801.	15. SECURITY CLASS. (of abstract) Unclassified	
17. DISTRIBUTION STATEMENT (of the abstract entered in Block 20, if different from Report) ⑮ 5811	18. DECLASSIFICATION/DOWNGRADING SCHEDULE	
18. SUPPLEMENTARY NOTES ⑰ ML R400 884	DDC RECEIVED JAN 29 1980	
19. KEY WORDS (Continue on reverse side if necessary and identify by block number) Clock gear                      Safing and arming Involute gear                  Timing Ogival gear Gear train	B	
20. ABSTRACT (Continue on reverse side if necessary and identify by block number) This report documents the development of the tools needed to compare the efficiency of fuze-related gear trains designed to operate in a spin environment. Computer models have been developed for two and three pass step-up designs with clock (ogival) and involute tooth shapes. Using appropriate moment input-output relationships, the computer programs develop point and cycle efficiency for each type of gear train. Pivot friction partially caused by centrifugal force on the gear and pinion combinations during spin, and		

DD FORM 1473, 1 JAN 73 EDITION OF 1 NOV 65 IS OBSOLETE

UNCLASSIFIED

SECURITY CLASSIFICATION OF THIS PAGE (When Data Entered)

410 103

UNCLASSIFIED

SECURITY CLASSIFICATION OF THIS PAGE(When Data Entered)

20. Abstract (continued)

tooth-to-tooth contact friction are considered. All models allow a variety of parameter variations.

UNCLASSIFIED

SECURITY CLASSIFICATION OF THIS PAGE(When Data Entered)

## TABLE OF CONTENTS

	<u>Page No.</u>
Introduction	1
Point Efficiency and Cycle Efficiency	2
Description of Study	3
<b>Appendixes</b>	
A Step-up Gear Trains with Involute Teeth	A-1
B Design of Unequal Addendum Involute Gear Sets with Standard Center Distances	B-1
C Computer Models for Step-up Gear Trains with Involute Teeth	C-1
D Geometry of General Clock Gear Tooth	D-1
E Kinematics and Moment Input-Output Relationship for Single Step-up Gear Mesh with Clock Teeth	E-1
F Computer Models for Single Step-up Gear Mesh with Clock Teeth	F-1
G Kinematics of Two and Three Step-up Gear Trains with Clock Teeth	G-1
H Moment Input-Output Relationships for Two and Three Step-up Gear Trains with Teeth Operating in a Spin Environment	H-1
I Computer Models for Two and Three Step-up Gear Trains with Clock Teeth Operating in a Spin Environment	I-1

### Distribution List

<b>ACCESSION for</b>		
NTIS	White Section	<input type="checkbox"/>
DDC	Buff Section	<input checked="" type="checkbox"/>
UNANNOUNCED		<input type="checkbox"/>
JUSTIFICATION		
BY		
DISTRIBUTION/AVAILABILITY CODES		
Dist. AVAIL. and/or SPECIAL		
<b>B</b>	<i>23</i>	

LIST OF TABLES

<u>Table</u>	<u>Title</u>	<u>Page</u>
H-1	Possible Combinations of Phases for Three Pass Step-up Gear Train as Shown in Figure G-1	H-2
H-2	Possible Combinations of Phases for Two Pass Step-up Gear Train as Shown in Figure A-10	H-3

LIST OF FIGURES

<u>Figure</u>	<u>Title</u>	<u>Page</u>
A-1	Determination of Direction of Contact Friction Forces by Velocity Analysis	A-2
A-2	Free Body Diagrams of Pivot Shafts	A-5
A-3	Moments due to Friction Components Always Oppose Motion	A-7
A-4	Free Body Diagram for Single Step-Up Involute Gear Mesh	A-10
A-5	Basic Configuration for Involute Three Step-Up Gear Train in Spin Environment	A-19
A-6	Free Body Diagram of Pinion 4	A-21
A-7	Equilibrium of Gear and Pinion Set No.3	A-28
A-8	Free Body Diagram of Gear and Pinion Set No.2	A-35
A-9	Free Body Diagram of Gear No.1	A-42
A-10	Basic Configuration for Involute Two Step-Up Gear Train in Spin Environment	A-48
A-11	Free Body Diagram of Pinion No.3	A-49
A-12	Free Body Diagram of Gear and Pinion Set No.2	A-56
A-13	Free Body Diagram of Gear No.1	A-64
A-14	Pivot Hole Relationships	A-70

<u>Figure</u>	<u>Title</u>	<u>Page</u>
A-15	Involute Mesh Geometry	A-75
B-1	Relationship between Pinion Pitch Radius $r_p$ , Rack Cutter Addendum A and Resulting Pinion Root Radius $r_r$	B-4
B-2	Minimum Root Radius $r_{rm}$ for Rack Cutter with Sharp Corner	B-5
B-3	Rack Cutter with Corner Radius $r_c$ (Effective Addendum of Cutter is Decreased)	B-6
D-1	Geometry of Ogival Tooth	D-2
E-1	Round on Round Phase of Contact (Gear Drives Pinion)	E-2
E-2	Round on Flat Phase of Contact (Gear Drives Pinion)	E-11
E-3	Sensing Geometry for Contact of Subsequent Tooth Mesh	E-19
E-4	Flat of Gear Contacts Round of Pinion	E-23
E-5	Free Body Diagram for Round on Round Phase	E-27
E-6	Free Body Diagram for Round on Flat Phase	E-34
G-1	Basic Configuration for Ogival Three Step-Up Gear Train in Spin Environment	G-2
G-2	Round on Round Phase for Mesh No.1	G-5
G-3	Round on Flat Phase for Mesh No.1	G-13
G-4	Round on Round Phase for Mesh No.2	G-24
G-5	Round on Flat Phase for Mesh No.2	G-31

<u>Figure</u>	<u>Title</u>	<u>Page</u>
H-1	Free Body Diagram of Pinion No.4 Mesh No.3: Round on Round	H-7
H-2	Free Body Diagram of Gear and Pinion No.3 Mesh No.3: Round on Round Mesh No.2: Round on Round	H-12
H-3	Free Body Diagram of Gear and Pinion No.2 Mesh No.2: Round on Round. Mesh No.1: Round on Round	H-19
H-4	Free Body Diagram of Gear No.1 Mesh No.1: Round on Round	H-26
H-5	Free Body Diagram of Gear and Pinion No.2 Mesh No.2: Round on Round Mesh No.1: Round on Flat	H-32
H-6	Free Body Diagram of Gear No.1 Mesh No.1: Round on Flat	H-39
H-7	Free Body Diagram of Gear and Pinion No.3 Mesh No.3: Round on Round Mesh No.2: Round on Flat	H-45
H-8	Free Body Diagram of Gear and Pinion No.2 Mesh No.2: Round on Flat Mesh No.1: Round on Flat	H-52
H-9	Free Body Diagram of Gear and Pinion No.2 Mesh No.2: Round on Flat Mesh No.1: Round on Round	H-60

<u>Figure</u>	<u>Title</u>	<u>Page</u>
H-10	Free Body Diagram of Pinion No.4 Mesh No.3: Round on Flat	H-68
H-11	Free Body Diagram of Gear and Pinion No.3 Mesh No.3: Round on Flat Mesh No.2: Round On Flat	H-74
H-12	Free Body Diagram of Gear and Pinion No.3 Mesh No.3: Round on Flat Mesh No.2: Round on Round	H-83
H-13	Free Body Diagram of Pinion No.3 Mesh No.2: Round on Round	H-94
H-14	Free Body Diagram of Pinion No.3 Mesh No.2: Round on Flat	H-103

## INTRODUCTION

This project provides the computer programs needed to compare the efficiency of fuze-related gear trains operating in a spin environment. Specifically, two and three pass stop-up computer models with both involute and ogival (clock) tooth shapes were developed.

By using appropriate moment input-output relationships, the computer programs allow the determination of point and cycle efficiencies. Pivot friction, partly due to the centrifugal forces on the gear and pinion combinations, is considered in addition to tooth-to-tooth contact friction. The models derived allow a wide variety of parameter variations.

The main body of this report consists of nine appendixes, each of which contains a detailed analysis of each combination of tooth forms, the number of passes, and the spin environment. The derivation of moment relationships, pivot friction, gear tooth geometry, and the direct-contact mechanism kinematics are also included. The computer programs used are listed and instructions in their use and in interpreting the results are given.

The point efficiency  $\epsilon_P$  is defined as

$$\epsilon_P = \frac{M_{OREF}}{M_{in}} \quad (1)$$

where  $M_{in}$  represents the instantaneous input moment to the gear train.  $M_{OREF}$  stands for the instantaneous equilibrant output moment  $M_o$  after it has been referred to the input shaft by way of the instantaneous angular velocity ratio

$$K_{RATIO} = \left| \frac{\dot{\psi}}{\dot{\phi}} \right|. \quad (2)$$

In the above,

$\dot{\psi}$  = instantaneous angular velocity of the output gear

$\dot{\phi}$  = instantaneous angular velocity of the input gear

Equation 1 then becomes

$$\epsilon_P = K_{RATIO} \frac{M_o}{M_{in}} \quad (3)$$

The cycle efficiency  $\epsilon_C$  represents the ratio of the work available at the output shaft to that done by the input moment during one tooth cycle of the input gear. Thus,

$$\epsilon_C = \frac{\int M_o d\psi}{\int M_{in} d\phi} \quad (4)$$

The quantities  $d\psi$  and  $d\phi$  represent infinitesimal rotations of the output and input gears, respectively.

## DESCRIPTION OF STUDY

### Appendix A

Appendix A furnishes the background, as well as the derivations, for the moment input-output expressions for two and three pass step-up gear trains (where in each mesh the gear is the driver) with involute teeth and unity contact ratio.

Section 1 shows the development of a sign convention for the direction of the contact point friction force. It is based on the direction of the relative velocity between the contact points on the gear and pinion teeth. Section 2 discusses how to deal with the normal and friction forces at the gear and pinion pivots of single and multiple mesh trains. Section 3 shows the application of the above results to the moment input-output analysis of a single mesh. The frame is assumed stationary for this case, and the external loads are confined to the driving input moment and the equilibrating output moment.

The basic geometry of the three pass step-up gear train, mounted on a rotating fuze body, is formulated in section 4 for use in the moment input-output analysis. Force and moment equilibria of the individual component gears, which also account for the centrifugal forces, lead to the desired expression. Section 5 includes a similar derivation for a two pass step-up gear train with

involute teeth. In order to be able to continuously compute the moment relationships for these trains, a method for determining the simultaneous locations of the contact points of all the meshes had to be worked out. Such a method is given in section 6 together with certain angular relationships of the pivot locations on the model fuze body.

The kinematic relationships in involute gear trains are relatively simple compared to those in ogival trains because of the constant transmission ratio and the invariant direction of the line-of-action in each individual mesh.

#### Appendix B

To avoid the severe undercutting of pinions which generally is associated with step-up gear meshes, it is necessary to use non-standard involute gearing. Appendix B shows both the theory and the necessary steps for the design of unequal addendum gears and pinions of unity contact ratio. In addition, a numerical example is given.

#### Appendix C

This appendix contains four computer programs which make it possible to determine the point and cycle efficiencies of three gear combinations containing unequal addendum involute meshes with

unity contact ratio. In each case, the structure of the program is thoroughly discussed and a sample run is used to interpret the results. The names of these programs and their relationship to work described in the other appendixes are given below:

1. Program INVOL 1 : Design of unequal addendum involute gear and pinion set with unity contact ratio.

This program is based on the work in Appendix B. Five sample computations, which are used in other programs, are shown.

2. Program INVOL 2 : Point and cycle efficiencies for single pass involute step-up gear mesh with unity contact ratio.

This program is based on the work in section 3 of Appendix A.

3. Program INVOL 3 : Point and cycle efficiencies for three pass involute step-up gear train in spin environment. (All meshes have unity contact ratio).

This program is based on the work in sections 4 and 6 of Appendix A.

4. Program INVOL 4 : Point and cycle efficiencies for two pass involute step-up gear train in spin environment. (All meshes have unity contact ratio).

This program is based on the work in sections 5 and 6 of Appendix A.

## Appendix D

This appendix describes the geometry of an ogival tooth in which each side of the tooth profile has a circular arc blending tangentially into a radial straight line flank. The basic tooth nomenclature is defined and methods for determining the required tooth parameters are given.

## Appendix E

Section 1 of Appendix E gives all necessary kinematic derivations for a single step-up mesh with ogival teeth. The motion of an ogival mesh consists of two phases. On first contact, the circular arc portion of the driving gear tooth makes contact with the circular arc portion of the driven pinion tooth. Later in the cycle, and up to the point of final disengagement, the circular arc portion of the gear tooth contacts the straight line portion of the pinion tooth. These phases of motion were named "round on round" and "round on flat," respectively. Equivalent four-link mechanism models were used for both regimes to obtain expressions for the pinion output angles, for transition angles, for output angular velocities and for contact-point relative velocities. In addition, a sensing expression was developed which allows the computer determination of that position of a given mesh at which the subsequent mesh comes into engagement. (Because of the variable transmission ratio of ogival meshes, there is only one set of teeth in contact at any one time).

Section 2 of this appendix shows derivations of moment input-output expressions for both phases of contact of a single ogival mesh. Again, while pivot friction is considered in addition to contact friction, the frame is assumed to be stationary for this single mesh.

### Appendix F

Two computer programs which deal with the kinematics and the moment input-output relationships of a single pass step-up gear mesh with clock teeth are given in this appendix. The structure of each of these programs is again discussed in detail and sample runs are used to explain their input and output parameters. The names of these programs and their relationships to work in other sections are given below:

1. Program CLOCK 1 : Kinematics of a single step-up gear mesh with clock teeth.

This program is based on work in Appendix D as well as on work in section 1 of Appendix E. In addition, it has been used to check the geometry of the ogival meshes which were used in programs CLOCK 2, CLOCK 3 and CLOCK 4 (See Appendix I for the latter two).

2. Program CLOCK 2 : Point and cycle efficiencies for single pass step-up gear mesh with clock teeth.

This program is based on work in section 2 of Appendix E.

## Appendix G

When one considers the kinematic relationships of ogival meshes which are mounted on a fuse body as parts of two or three pass step-up trains, it becomes necessary to account for the relative positions of the individual meshes on the fuse body. Appendix G gives the appropriate derivations for each of the three meshes of a three-pass train. The model of the fuse body is identical with that used for involute step-up trains.

## Appendix H

This appendix shows the derivations of moment input-output expressions for two and three pass step-up gear trains with ogival teeth which must operate in a spin environment.

Because of the increase in rotational speed associated with each tooth mesh, increasingly more sets of teeth will come into engagement in the second and third meshes as one set of teeth moves through one complete contact cycle in the first (i.e., the input) mesh. With two phases of motion for each mesh, there will be eight contact combinations in a three-pass train. Section 1 of Appendix H gives a derivation for the moment input-output expression of each of these eight cases.

Section 2 shows similar work for the four contact combinations which are associated with two pass step-up gear trains with ogival teeth.

Both analyses account for the effects of the centrifugal forces.

## Appendix I

This appendix contains two computer programs which allow the determination of point and cycle efficiencies for two and three pass step-up gear meshes with clock teeth. As for other programs, the origins of their mathematical formulations are thoroughly discussed. In addition, their input and output parameters are explained with the help of a sample run. The names of these programs as well as their relationships to work in other appendixes are given below:

1. Program CLOCK 3 : Point and cycle efficiencies for three pass clock (ogival) step-up gear train in spin environment.

This program is based on work given in Appendix G as well as in section 1 of Appendix H. The general fuze geometry is that described in section 6 of Appendix A.

2. Program CLOCK 4 : Point and cycle efficiencies for two pass clock (ogival) step-up gear train in spin environment.

The kinematics of this program is again based on work given in Appendix G. The moment input-output relationships are from section 2 of Appendix H.

## APPENDIX A

### STEP-UP GEAR TRAINS WITH INVOLUTE TEETH

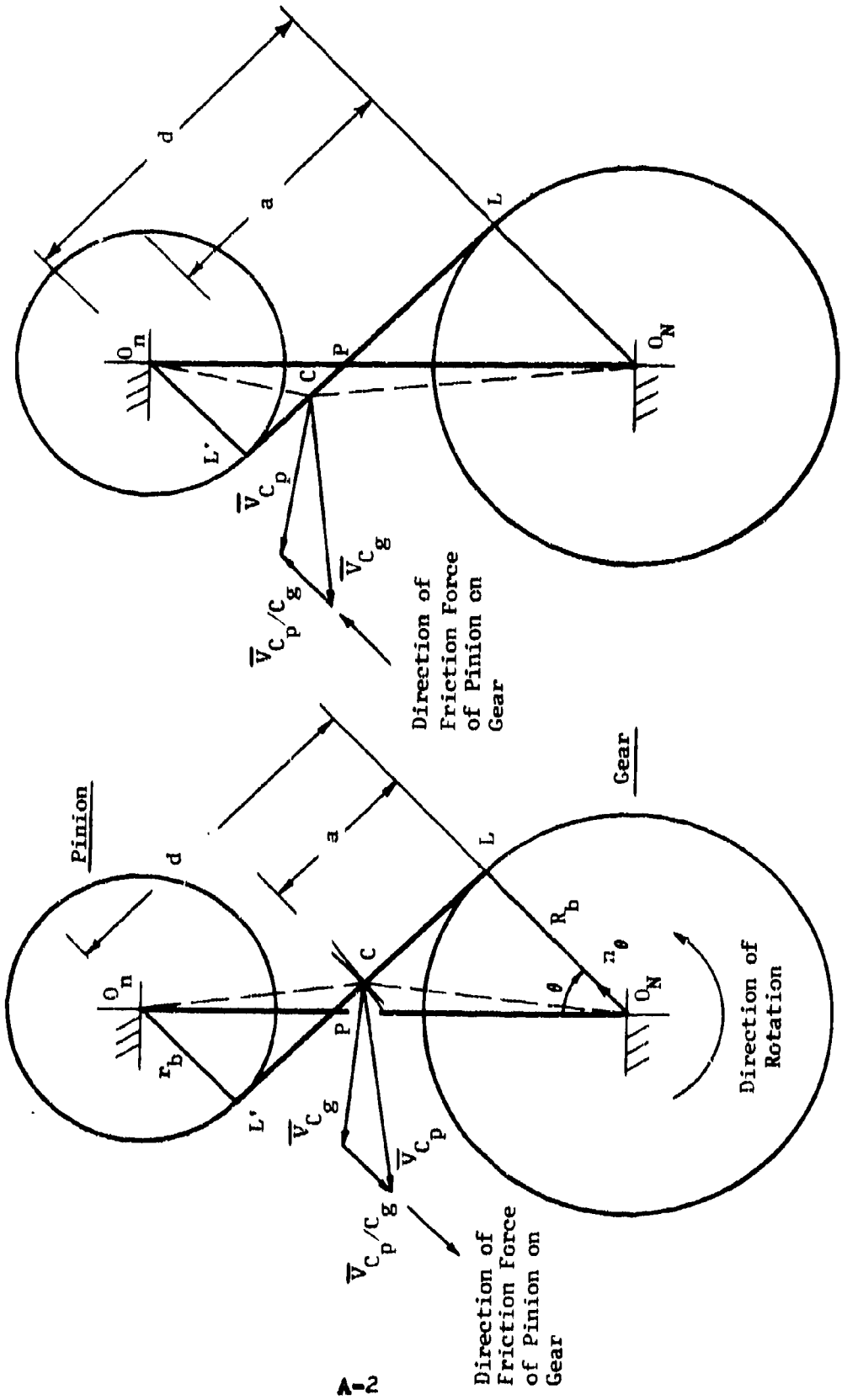
#### 1. DIRECTION OF FRICTION FORCE AT TOOTH-TO-TOOTH CONTACT

Figure A-1 uses the base circle and the line-of-action configuration of an involute mesh, in which the gear drives the pinion, to determine the direction of the friction forces at contact point C before and after the contact point passes through pitch point P. Distance d represents the length of the line-of-action between base circle tangent points L and L'. The distance between contact point C and point L along the line-of-action is measured by length a.

Further:

- $\theta$  = actual (rolling) pressure angle
- $R_b$  = gear base radius
- $r_b$  = pinion base radius

The friction force of the pinion tooth on the gear tooth, for example, will have the direction of the relative velocity,  $\bar{v}_{C_p / C_g}$ , of the contact point on the pinion tooth,  $C_p$ , with respect to the coincident contact point on the gear tooth,  $C_g$ . (The friction force of the gear tooth on the pinion tooth has the opposite direction.) This relative velocity changes direction at the pitch point, where it becomes instantaneously zero.



Contact Before Pitch Point  
(Approach)

Contact After Pitch Point  
(Recess)

FIGURE A-1. DETERMINATION OF DIRECTION OF CONTACT FRICTION FORCES BY VELOCITY ANALYSIS

Figure A-1 shows contact before the pitch point (during approach). To obtain the direction of the relative velocity,  $\mathbf{V}_{C_p/C_g}$ , by a graphical analysis, one makes use of the velocity equation

$$\mathbf{V}_{C_p} = \mathbf{V}_{C_p/C_g} + \mathbf{V}_{C_g} \quad (\text{A-1})$$

where  $\mathbf{V}_{C_p}$  = velocity of point  $C_p$  on pinion tooth with direction normal to line  $O_n - C$

$\mathbf{V}_{C_p/C_g}$  = relative velocity between point  $C_p$  and point  $C_g$ . The direction of this velocity is normal to the line of action.

$\mathbf{V}_{C_g}$  = velocity of point  $C_g$  on gear tooth with direction normal to line  $O_n - C$ . The magnitude of this velocity was arbitrarily chosen.

The graphical construction, according to Eq (A1), shows that  $\mathbf{V}_{C_p/C_g}$  has the direction opposite to that of the unit vector  $\mathbf{n}_\theta$  shown at point  $O_n$ . As stated earlier, this represents

the friction force on the gear tooth during approach.

Figure A-1b shows the same graphical analysis for contact during recess. Once the pitch point is passed, both the relative velocity,  $\bar{V}_{C_p/C_g}$ , and the friction force of the pinion on the gear have the direction of the positive unit vector  $\bar{n}_\theta$ .

2. ASSUMPTIONS CONCERNING NORMAL AND FRICTION  
FORCES AT PIVOTS

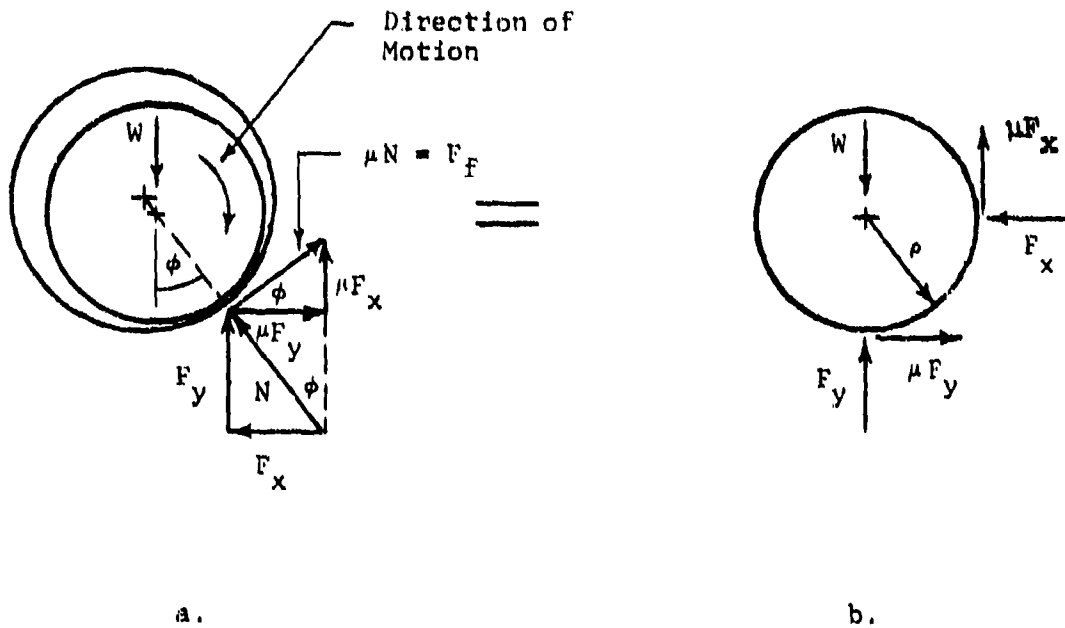


FIGURE A-2 FREE-BODY DIAGRAMS OF PIVOT SHAFTS

Figure A-2a shows a pivot shaft which is loaded by a known external force,  $W$ , and rotates in a clockwise direction. Due to friction between the shaft and the bearing, contact is made at an angle,  $\phi = \tan^{-1} \mu$ , where  $\mu$  is the associated coefficient of friction.  $N$  is the normal contact

force. The friction force  $F_f = \mu N$  opposes the clockwise rotation by creating a counterclockwise moment.

$N$  may be resolved into the components  $F_x$  and  $F_y$ . The associated  $x$  and  $y$  components of the friction force are  $\mu F_y$  and  $\mu F_x$ , respectively.

The directions of the components of  $N$  and  $F_f$  are drawn in the same manner in Fig. A-2b in a somewhat more convenient representation. When the direction of the resultant external force,  $W$ , is not known, contact is possible anywhere on the periphery of the bearing and the components  $F_x$  and  $F_y$  of the normal contact force cannot be drawn with certainty in the free body diagram. The direction of the friction components must still oppose the motion.

Figure A-3 shows two general possibilities of drawing the free body diagram of a pivot which rotates in a clockwise direction. In either case, the moments of the friction components oppose the rotation while  $F_x$  and  $F_y$  may be positive or negative. Assume now, for example, that Fig. A-3a shows the wrong direction for  $F_x$  and that the solution of the applicable equilibrium equation will reverse the sign of  $F_x$ . This will automatically reverse the sign of the friction component  $\mu F_x$  also. Since contact is now made on the opposite

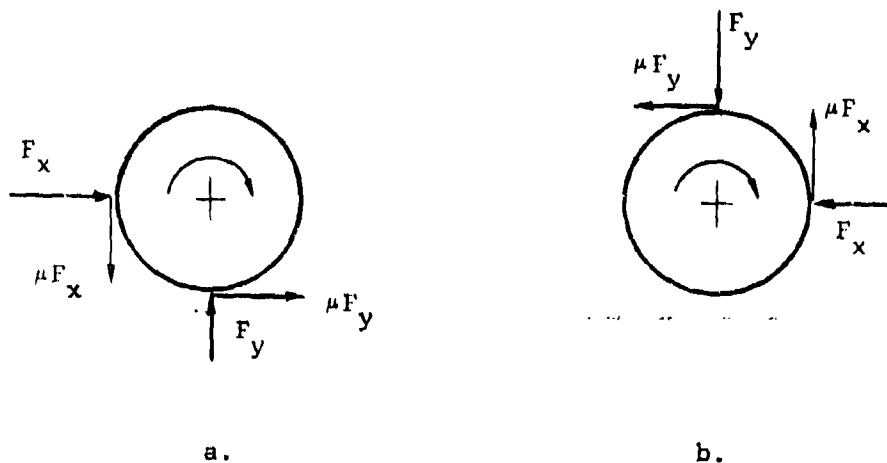


FIGURE A-3 MOMENTS DUE TO FRICTION COMPONENTS  
ALWAYS OPPOSE MOTION

side of the pivot, the correct sign of the friction component is automatically assured.

The total friction moment then is expressed by

$$M_f = \pm \mu \rho \sqrt{F_x^2 + F_y^2} \quad (\text{A-2})$$

where  $\rho$  is the pivot radius. The sign of the above is chosen so that the rotation is opposed. In case  $F_x$  and  $F_y$  contain required terms that cannot be factored out of the square root of equation (A-2), the friction moment is conservatively overstated by the use of the absolute values of  $F_x$  and  $F_y$ .

$$M_f = \pm \mu p \left( |F_x| + |F_y| \right) \quad (A-3a)$$

If the expressions for  $F_x$  and  $F_y$  consist of sums of positive and negative terms, then  $F_x$  and  $F_y$  are presented as the sums of the absolute values of these terms. A conservative pivot friction moment becomes, similar to equation (A-3a),

$$M_f = \pm \mu p \left( \tilde{F}_x + \tilde{F}_y \right) \quad (A-3b)$$

The tildes represent the sums of the absolute values of the component terms.

### 3. MOMENT INPUT-OUTPUT RELATIONSHIP FOR SINGLE STEP-UP

#### GEAR MESH WITH INVOLUTE TEETH

Figure A-4 shows free body diagrams of the gear and the pinion of a single mesh where the gear is driven by a counterclockwise input moment  $M_{in}$ . It is desired to find the equilibrating output moment  $M_o$ .

#### a. UNIT VECTORS

The unit vector directed from point  $O_N$  to point L is given by

$$\bar{n}_\theta = \sin\theta\bar{i} + \cos\theta\bar{j} \quad (A-4)$$

where  $\theta$  represents the actual pressure angle, regardless of tooth modification. The unit vector directed along the line of action from point L to point L' is given by

$$\bar{n}_{\theta T} = -\cos\theta\bar{i} + \sin\theta\bar{j} \quad (A-5)$$

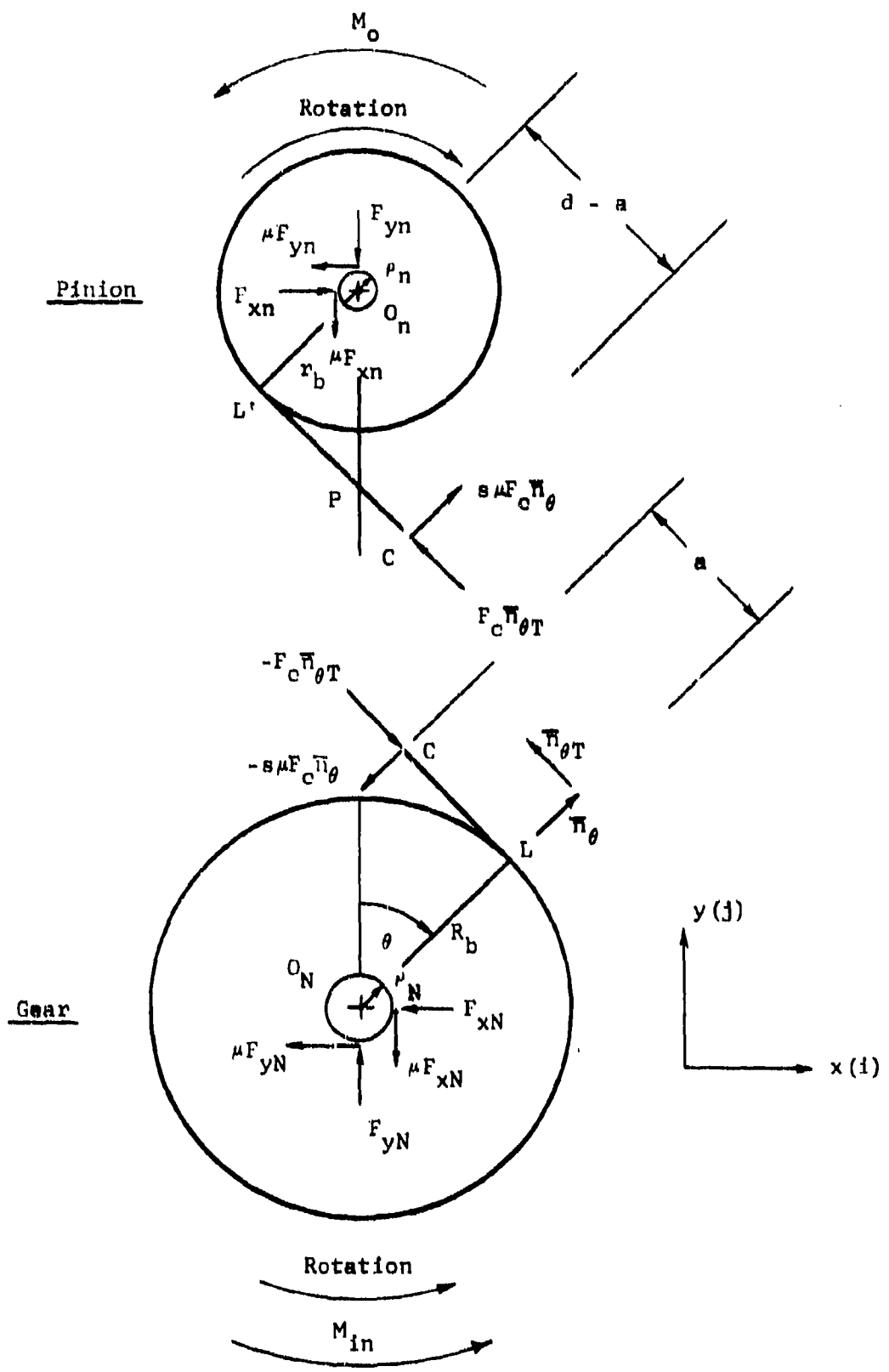


FIGURE A-4. FREE BODY DIAGRAM FOR SINGLE STEP-UP INVOLUTE GEAR MESH  
A-10

b. NOMENCLATURE AND SIGNUM CONVENTION

$F_{xN}, F_{yN}$  = x and y components of normal force acting on gear pivot

$\mu F_{xN}, \mu F_{yN}$  = friction force components acting on gear pivot. Directions chosen to result in friction moments which oppose motion. (See part 2).

$F_{xn}, F_{yn}$  = x and y components of normal force acting on pinion pivot

$\mu F_{xn}, \mu F_{yn}$  = friction force components acting on pinion pivot

$\mu$  = coefficient of friction

$F_c$  = normal contact force between gear and pinion.

The force of the pinion on the gear is  $(-)F_c \bar{n}_{\theta T}$ , while the normal force of the gear on the pinion becomes  $F_c \bar{n}_{\theta T}$ .

$\mu F_c$  = tooth contact friction force. The analysis in Section 1 shows that the friction force of the pinion on the gear, before the pitch point, acts in the direction of  $(-)\bar{n}_{\theta}$ . Therefore

$-s \mu F_c \bar{n}_{\theta}$  = friction force on gear with

$s$  = +1 for a <  $\overline{LP}$  (approach) (A-6)

and

$$s = -1 \text{ for } a > \overline{LP} \text{ (recess)} \quad (\text{A-7})$$

while

$$s = 0 \text{ for } a = \overline{LP} \text{ (at pitch point)} \quad (\text{A-8})$$

Further,

$r_N, r_n$  = gear and pinion pivot radii

$R_b, r_b$  = gear and pinion base circle radii

c. FORCE ANALYSIS OF THE GEAR

By inspecting Figure A-4, one sees that force equilibrium of the gear is expressed by

$$-F_c \bar{n}_{\theta T} - s \mu F_c \bar{n}_\theta - F_{xN} \bar{i} - \mu F_{xN} \bar{j} + F_{yN} \bar{j} - \mu F_{yN} \bar{i} = 0 \quad (A-9)$$

Similarly, moment equilibrium of the gear is given by

$$M_{in} \bar{k} - r_N \mu \sqrt{F_{xN}^2 + F_{yN}^2} \bar{k} + R_b \bar{n}_\theta \times (-) F_c \bar{n}_{\theta T} + (R_b \bar{n}_\theta + a \bar{n}_{\theta T}) \times (-) s \mu F_c \bar{n}_\theta = 0 \quad (A-10)$$

Note the use of equation (A-2) to express the friction moment at the gear pivot.

With the help of equations (A-4) and (A-5) one may write equations (A-9) and (A-10) in scalar form. Thus,

$$F_c \cos \theta - \mu s F_c \sin \theta - F_{xN} - \mu F_{yN} = 0 \quad (A-11)$$

$$-F_c \sin \theta - \mu s F_c \cos \theta + F_{yN} - \mu F_{xN} = 0 \quad (A-12)$$

Equation (A-10) becomes

$$M_{in} - \rho_N \mu \sqrt{F_{xN}^2 + F_{yN}^2} - R_b F_c + \mu s a F_c = 0 \quad (A-13)$$

Simultaneous solution of equations (A-11) and (A-12) for

$F_{xN}$  and  $F_{yN}$  gives

$$F_{xN} = F_c \frac{(1 - \mu^2 s) \cos \theta - \mu(1 + s) \sin \theta}{1 + \mu^2} \quad (A-14)$$

and

$$F_{yN} = F_c \frac{(1 - \mu^2 s) \sin \theta + \mu(1 + s) \cos \theta}{1 + \mu^2} \quad (A-15)$$

When the above expressions are substituted into the moment equation (A-13) and if one notes that  $s^2$  always equals +1, the following expression for  $F_c$  is obtained:

$$F_c = \frac{M_{in}}{R_b + \mu(\rho_N - as)} \quad (A-16)$$

d. FORCE ANALYSIS OF THE PINION

Force equilibrium of the pinion is assured by

$$F_c \bar{n}_{\theta T} + \mu s F_c \bar{n}_{\theta} + F_{xn} \bar{i} - F_{yn} \bar{j} - \mu F_{xn} \bar{j} - \mu F_{yn} \bar{i} = 0, \quad (A-17)$$

while moment equilibrium is given by

$$M_o \bar{k} + r_n \mu \sqrt{F_{xn}^2 + F_{yn}^2} \bar{k} + [-r_b \bar{n}_{\theta} - (d - a) \bar{n}_{\theta T}] \times (F_c \bar{n}_{\theta T} + \mu s F_c \bar{n}_{\theta}) = 0 \quad (A-18)$$

In scalar form, the above become

$$-F_c \cos \theta + \mu s F_c \sin \theta + F_{xn} - \mu F_{yn} = 0 \quad (A-19)$$

$$F_c \sin \theta + \mu s F_c \cos \theta - \mu F_{xn} - F_{yn} = 0 \quad (A-20)$$

$$M_o + \mu r_n \sqrt{F_{xn}^2 + F_{yn}^2} - r_b F_c + \mu s (d - a) F_c = 0 \quad (A-21)$$

Equations (A-19) and (A-20) are now solved simultaneously for  $F_{xn}$  and  $F_{yn}$ . This gives

$$F_{xn} = F_c \frac{(1 + \mu^2 s) \cos \theta + \mu(1 - s) \sin \theta}{1 + \mu^2} \quad (\text{A-22})$$

and

$$F_{yn} = F_c \frac{(1 + \mu^2 s) \sin \theta - \mu(1 - s) \cos \theta}{1 + \mu^2} \quad (\text{A-23})$$

Equations (A-22) and (A-23) are then substituted into the moment equation (A-21). This furnishes the following expression for the normal contact force,  $F_c$ . (Again,  $s^2$  always equals +1.):

$$F_c = \frac{M_o}{r_b - \mu [r_n + s(d - a)]} \quad (\text{A-24})$$

e. MOMENT INPUT-OUTPUT RELATIONSHIP

The equilibrant moment,  $M_o$ , may be expressed as a function of the input moment,  $M_{in}$ , after equations (A-16) and (A-24) have been set equal to each other. Thus,

$$M_o = \frac{M_{in} \left\{ r_b - \mu \left[ \rho_n + s(d - a) \right] \right\}}{R_b + \mu \left[ \rho_N - sa \right]} \quad (A-25)$$

The input-output relationship may also then be expressed in terms of

$$M_o = M_{in} \frac{r_b}{R_b} E_2 \quad (A-26)$$

$$\text{where } E_2 = \frac{1 - \frac{\mu \left[ \rho_n + s(d - a) \right]}{r_b}}{1 + \frac{\mu \left( \rho_N - sa \right)}{R_b}},$$

and represents the efficiency of moment transmission of a single step-up mesh with involute teeth.

#### 4. MOMENT INPUT-OUTPUT RELATIONSHIP FOR THREE STEP-UP GEAR TRAIN IN SPIN ENVIRONMENT

Figure A-5 shows the basic configuration of the three step-up gear train for which the relationship between the equilibrant output moment  $M_{o4}$ , acting on pinion 4, and the input moment  $M_{in}$ , acting on gear 1, is to be found.

The body-fixed x-y coordinate system has its origin at the spin axis, C, of the fuze body, and its x-axis coincides with the line C- $O_1$ , where  $O_1$  represents the pivot axis of the input gear-spin rotor combination. Points  $O_2$ ,  $O_3$  and  $O_4$  represent the pivot axes of gear and pinion no. 2, gear and pinion no. 3, and pinion no. 4, respectively. Further,

- $R_i$  = distance from the spin axis to the various pivot axes
- $R_{bi}$  = base radii of gears
- $r_{bi}$  = base radii of pinions
- $\beta_1$  = angle between positive x-axis and line of centers  $O_1-O_2$
- $\beta_2$  = angle between positive x-axis and line of centers  $O_2-O_3$
- $\beta_3$  = angle between positive x-axis and line of centers  $O_3-O_4$
- $\gamma_1$  = angle between positive x-axis and lines C- $O_1$

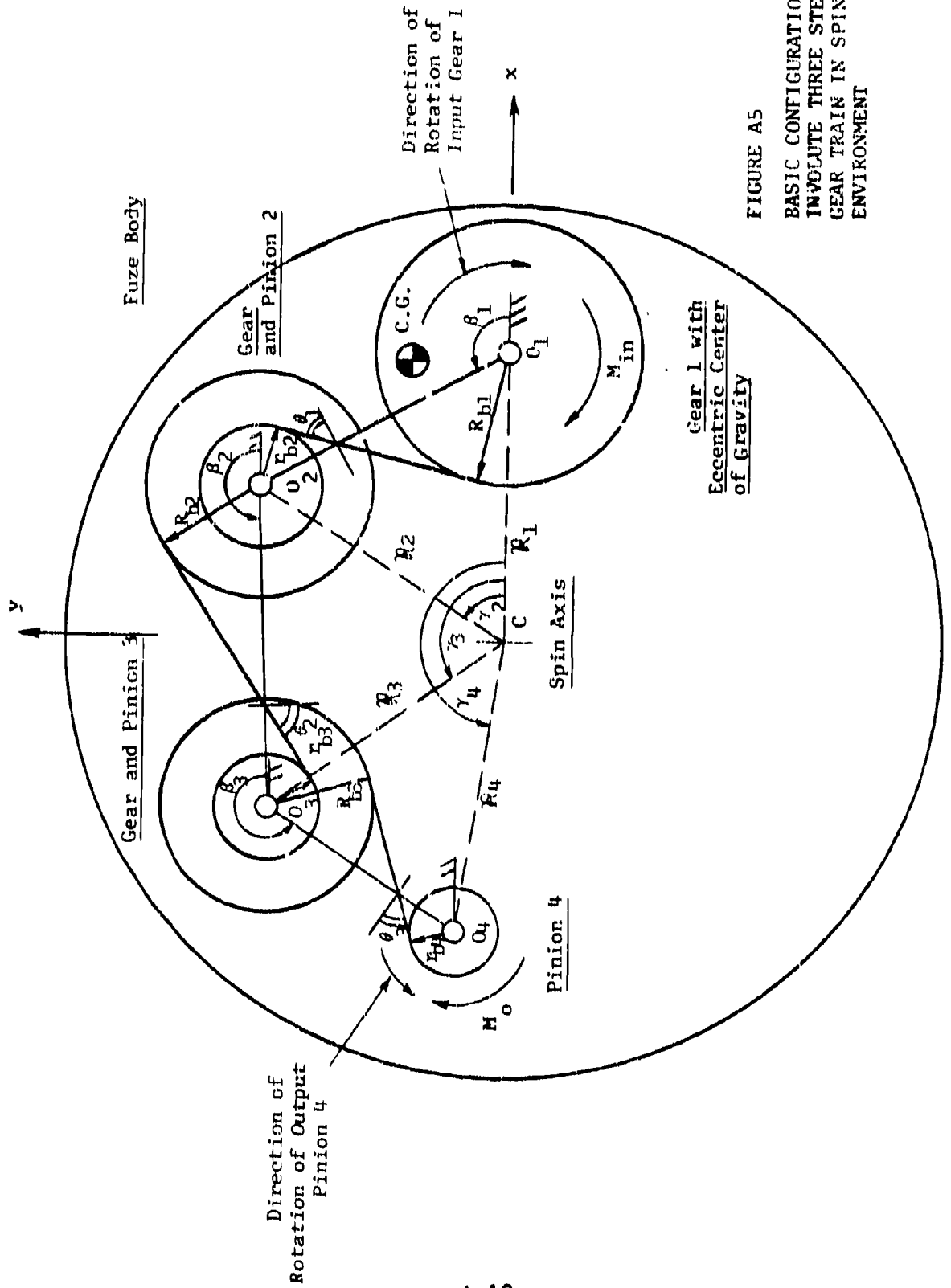


FIGURE A5  
 BASIC CONFIGURATION FOR  
 INVOLUTE THREE STEP-UP  
 GEAR TRAIN IN SPIN  
 ENVIRONMENT

- $\theta_1$  = pressure angle of mesh between gear no. 1 and pinion no. 2  
 $\theta_2$  = pressure angle of mesh between gear no. 2 and pinion no. 3  
 $\theta_3$  = pressure angle of mesh between gear no. 3 and pinion no. 4

To obtain the moment input-output relationship of the total train, the input-output relationships of the individual components must first be obtained. The following equilibrium analyses include pivot as well as contact friction forces, in addition to loads due to the centrifugal forces on the individual components. The directions of the tooth-to-tooth friction forces are chosen according to the rules of Section 1 of this appendix, using an appropriate signum convention. The direction of the pivot friction forces is chosen according to Section 2 and, to avoid difficulties with the direction of the associated friction moment, equation (A-3b) will be used.

a. EQUILIBRIUM OF PINION 4

Figure A-6 shows a free body diagram of pinion 4. The contact between gear 3 and pinion 4 is shown before contact point  $C_3$  has passed through pitch point  $P_3$ . The unit vector  $\bar{n}_{34}$  is along the line-of-action in the direction of the contact force of the gear on the pinion.

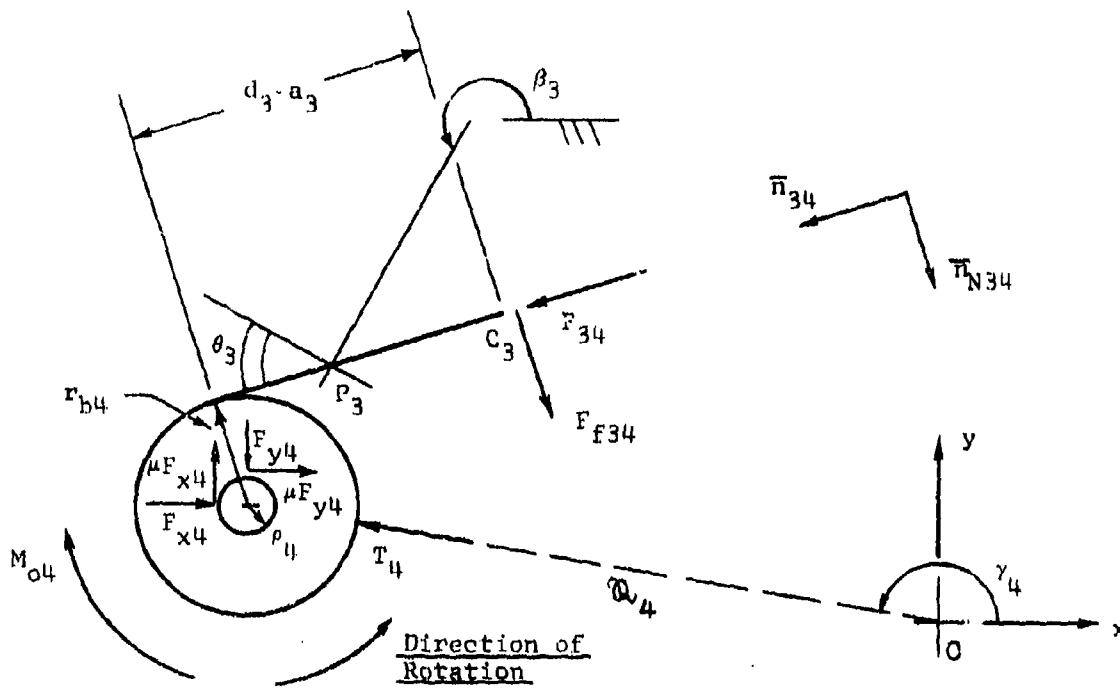


FIGURE A-6. FREE BODY DIAGRAM OF PINION 4

Thus,

$$\bar{n}_{34} = \sin(\beta_3 + \theta_3)\bar{I} - \cos(\beta_3 + \theta_3)\bar{J} \quad (\text{A-27})$$

The unit vector normal to the line-of-action is given by

$$\bar{n}_{N34} = \cos(\beta_3 + \theta_3)\bar{I} + \sin(\beta_3 + \theta_3)\bar{J} \quad (\text{A-28})$$

The contact force  $\bar{F}_{34}$  then becomes

$$\bar{F}_{34} = F_{34} \bar{n}_{34} \quad (\text{A-29})$$

The friction force of gear 3 on pinion 4 is given by

$$\bar{F}_{f34} = \mu s_3 F_{34} \bar{n}_{N34} \quad (\text{A-30})$$

where  $s_3 = +1$ , for contact before the pitch point

$s_3 = 0$ , for contact at the pitch point

$s_3 = -1$ , for contact after the pitch point

(See also Section 1.)

The normal forces on the pivot shaft are given by

$$\bar{F}_{x4} = F_{x4} \bar{I} \quad (A-31)$$

and

$$\bar{F}_{y4} = -F_{y4} \bar{J} \quad (A-32)$$

The associated pivot friction forces are given by  $\mu F_{x4} \bar{J}$  and  $\mu F_{y4} \bar{I}$  for the indicated direction of rotation. The centrifugal force  $T_4$  on the pinion is represented by

$$\bar{T}_4 = T_4 (\cos \gamma_4 \bar{I} + \sin \gamma_4 \bar{J}) \quad (A-33)$$

where

$$T_4 = R_4 \omega^2 m_4 \quad (A-34a)$$

with

$$\omega = \text{spin angular velocity} \quad (A-34b)$$

and

$$m_4 = \text{mass of pinion 4} \quad (A-34c)$$

The force equilibrium equation is given by

$$\begin{aligned} F_{34} \bar{N}_{34} + \mu_B F_{34} \bar{N}_{34} + T_4 (\cos \gamma_4 \bar{I} + \sin \gamma_4 \bar{J}) + F_{x4} \bar{I} \\ + \mu F_{y4} \bar{I} + \mu F_{x4} \bar{J} - F_{y4} \bar{J} = 0 \end{aligned} \quad (A-35)$$

Moment equilibrium is given by the following expression, in which the pivot friction moment is expressed according to Equation (A-3b):

$$-M_{o4} - \rho_4 \nu (\tilde{F}_{x4} + \tilde{F}_{y4}) + r_{b4} F_{34} - \mu s_3 (d_3 - a_3) F_{34} = 0 \quad (A-36)$$

where  $\rho_4$  represents the pivot radius.  $d_3$  is the length of the line-of-action of the mesh from points of tangency to the base circles.  $a_3$  is the distance on the line of action from the gear point of tangency to the contact point  $C_3$ .

Equation (A-35) gives the following component equations:

$$F_{34} \sin(\beta_3 + \theta_3) + \mu s_3 F_{34} \cos(\beta_3 + \theta_3) + T_4 \cos \gamma_4 + F_{x4} + \mu F_{y4} = 0 \quad (A-37)$$

$$-F_{34} \cos(\beta_3 + \theta_3) + \mu s_3 F_{34} \sin(\beta_3 + \theta_3) + T_4 \sin \gamma_4 - F_{y4} + \mu F_{x4} = 0 \quad (A-38)$$

Simultaneous solution of the above for  $F_{x4}$  and  $F_{y4}$  results in

$$F_{x4} = \frac{1}{1 + \mu^2} \left\{ -T_4 [\cos \gamma_4 + \mu \sin \gamma_4] - F_{34} [(1 + \mu^2 s_3) \sin(\beta_3 + \theta_3) - \mu(1 - s_3) \cos(\beta_3 + \theta_3)] \right\} \quad (A-39)$$

and

$$F_{y4} = \frac{1}{1 + \mu^2} \left\{ T_4 [\sin \gamma_4 - \mu \cos \gamma_4] - F_{34} [(1 + \mu^2 s_3) \cos(\beta_3 + \theta_3) + \mu(1 - s_3) \sin(\beta_3 + \theta_3)] \right\} \quad (A-40)$$

To obtain conservative values for the pivot friction moment in equation (A-36) according to equation (A-3b), one substitutes the largest possible values for  $F_{x4}$  and  $F_{y4}$ . This is accomplished by making the signs of  $T_4$  and  $F_{34}$  positive and by using the absolute values of their respective coefficients in Equations (A-39) and (A-40). Equation (A-36) then becomes

$$-M_{o4} - \mu p_4 (T_4 A_1 + F_{34} A_2 + T_4 A_3 + F_{34} A_4) + r_{b4} F_{34} - \mu s_3 (d_3 - a_3) F_{34} = 0 \quad (A-41)$$

where

$$A_1 = \left| \frac{\sin \gamma_4 - \mu \cos \gamma_4}{1 + \mu^2} \right| \quad (A-42)$$

$$A_2 = \left| \frac{(1 + \mu^2 s_3) \cos(\beta_3 + \theta_3) + \mu(1 - s_3) \sin(\beta_3 + \theta_3)}{1 + \mu^2} \right| \quad (\text{A-43})$$

$$A_3 = \left| \frac{\cos \gamma_4 + \mu \sin \gamma_4}{1 + \mu^2} \right| \quad (\text{A-44})$$

$$A_4 = \left| \frac{(1 + \mu^2 s_3) \sin(\beta_3 + \theta_3) - \mu(1 - s_3) \cos(\beta_3 + \theta_3)}{1 + \mu^2} \right| \quad (\text{A-45})$$

Finally equation (A-41) is solved for  $F_{34}$

$$F_{34} = \frac{M_{o4}}{D_1} + \frac{T_4 C_1}{D_1} \quad (\text{A-46})$$

where

$$C_1 = \mu r_4 (A_1 + A_3) \quad (\text{A-47})$$

$$D_1 = r_{b4} - \mu [s_3 (d_3 - a_3) + r_4 (A_2 + A_4)] \quad (\text{A-48})$$

b. EQUILIBRIUM OF GEAR AND PINION SET NO. 3

Figure A-7 shows the free body diagram of gear and pinion set no. 3. Contact point  $C_3$ , between pinion 4 and gear 3, is, as shown previously in Figure A-6, before pitch point  $P_3$ . The normal force, along the line-of-action, is given [see equation (A-29)] by

$$\bar{F}_{43} = -F_{34} \bar{N}_{34} \quad (A-49)$$

and the associated friction force  $\bar{F}_{f43}$  is given [see equation (A-30)] by

$$\bar{F}_{f43} = -\mu_3 F_{34} \bar{N}_{34} \quad (A-50)$$

The unit vectors along (and perpendicular to) the line-of-action of gear 2 and pinion 3 are given by

$$\bar{N}_{23} = -\sin(\beta_2 - \theta_2) \bar{I} + \cos(\beta_2 - \theta_2) \bar{J} \quad (A-51)$$

and

$$\bar{N}_{N23} = -\cos(\beta_2 - \theta_2) \bar{I} - \sin(\beta_2 - \theta_2) \bar{J} \quad (A-52)$$

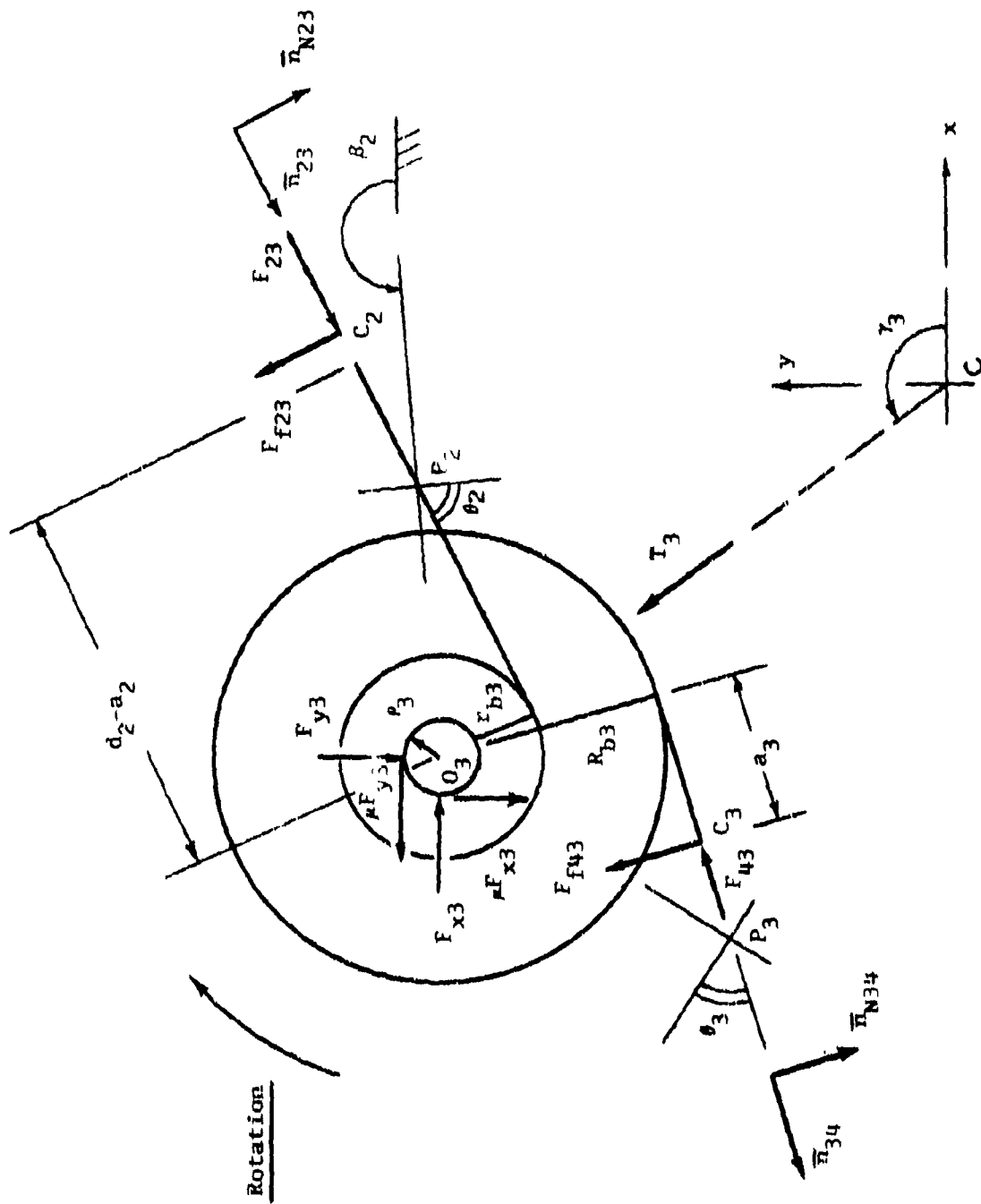


FIGURE A-7. EQUILIBRIUM OF GEAR AND PINION SET NO. 3

The contact point  $C_2$  between gear 2 and pinion 3 is also shown before pitch point  $P_2$  is passed.

The normal contact force between these teeth then becomes

$$\bar{F}_{23} = F_{23} \bar{n}_{23} \quad (A-53)$$

The associated friction force is given by

$$\bar{F}_{f23} = -\mu s_2 F_{23} \bar{n}_{23} \quad (A-54)$$

where  $s_2 = +1$  for contact before pitch point  $P_2$

$s_2 = 0$  for contact at pitch point  $P_2$

$s_2 = -1$  for contact after pitch point  $P_2$

The normal forces on the pivot shaft are given by

$$\bar{F}_{x3} = F_{x3} \bar{i} \quad (A-55)$$

and

$$\bar{F}_{y3} = -F_{y3} \bar{j} \quad (A-56)$$

The associated pivot friction forces are represented by  $(-)\mu F_{y3} \bar{i}$

and  $(-)\mu F_{x3}\bar{J}$  for the indicated direction of gear rotation.

The centrifugal force,  $\bar{T}_3$ , on the assembly is given by

$$\bar{T}_3 = T_3(\cos\gamma_3\bar{I} + \sin\gamma_3\bar{J}) \quad (A-57)$$

where

$$T_3 = R_3\omega^2 m_3 \quad (A-58a)$$

with

$$m_3 = \text{mass of pinion and gear 3} \quad (A-58b)$$

Force equilibrium is given by

$$\begin{aligned} F_{23}\bar{N}_{23} - \mu_{S2}F_{23}\bar{N}_{N23} - F_{34}\bar{a}_{34} - \mu_{S3}F_{34}\bar{N}_{N34} + T_3(\cos\gamma_3\bar{I} + \sin\gamma_3\bar{J}) \\ + F_{x3}\bar{I} - \mu F_{y3}\bar{I} - F_{y3}\bar{J} - \mu F_{x3}\bar{J} = 0 \end{aligned} \quad (A-59)$$

Moment equilibrium requires

$$\begin{aligned} R_{b3}F_{34} - \mu_{S3}a_3F_{34} - r_{b3}F_{23} + \mu_{S2}(d_2 - a_2)F_{23} \\ + \mu p_3(\tilde{F}_{x3} + \tilde{F}_{y3}) = 0 \end{aligned} \quad (A-60)$$

Note the use of equation (A-3b) for the pivot friction moment.

$p_3$  represents the pivot radius and length  $d_2$  is the length of the

line-of-action between the points of tangency to the base circles.

$a_2$  is the distance along the line-of-action from the gear point of tangency to the contact point  $C_2$ .

The component form of equation (A-59) is represented by the following two expressions:

$$\begin{aligned} -F_{23}\sin(\beta_2 - \theta_2) + \mu s_2 F_{23}\cos(\beta_2 - \theta_2) - F_{34}\sin(\beta_3 + \theta_3) \\ - \mu s_3 F_{34}\cos(\beta_3 + \theta_3) + T_3\cos\gamma_3 + F_{x3} - \mu F_{y3} = 0 \end{aligned} \quad (A-61)$$

and

$$\begin{aligned} F_{23}\cos(\beta_2 - \theta_2) + \mu s_2 F_{23}\sin(\beta_2 - \theta_2) + F_{34}\cos(\beta_3 + \theta_3) \\ - \mu s_3 F_{34}\sin(\beta_3 + \theta_3) + T_3\sin\gamma_3 - F_{y3} - \mu F_{x3} \\ = 0 \end{aligned} \quad (A-62)$$

Simultaneous solution of the above for  $F_{x3}$  and  $F_{y3}$  leads to

$$\begin{aligned} F_{x3} = \frac{1}{1 + \mu^2} \left\{ F_{23} \left[ (1 + \mu^2 s_2)\sin(\beta_2 - \theta_2) + \mu(1 - s_2)\cos(\beta_2 - \theta_2) \right] \right. \\ \left. + T_3 \left[ \mu\sin\gamma_3 - \cos\gamma_3 \right] + F_{34} \left[ (1 - \mu^2 s_3)\sin(\beta_3 + \theta_3) \right. \right. \\ \left. \left. + \mu(1 + s_3)\cos(\beta_3 + \theta_3) \right] \right\} \end{aligned} \quad (A-63)$$

and

$$F_{y3} = \frac{1}{1 + \mu^2} \left\{ F_{23} \left[ (1 + \mu^2 a_2) \cos(\beta_2 - \theta_2) + \mu(a_2 - 1) \sin(\beta_2 - \theta_2) \right] \right. \\ \left. + T_3 \left[ \sin \gamma_3 + \mu \cos \gamma_3 \right] + F_{34} \left[ (1 - \mu^2 a_3) \cos(\beta_3 + \theta_3) \right. \right. \\ \left. \left. - \mu(a_3 + 1) \sin(\beta_3 + \theta_3) \right] \right\} \quad (A-64)$$

Now, equations (A-63) and (A-64) are substituted into the moment equation (A-60) with consideration of the pivot friction moment according to equation (A-3b). This gives

$$R_{b3} F_{34} - \mu a_3 a_3 F_{34} - r_{b3} F_{23} + \mu a_2 (d_2 - a_2) F_{23} \\ + \mu a_3 \left[ F_{23} (A_5 + A_8) + T_3 (A_6 + A_9) + F_{34} (A_7 + A_{10}) \right] \\ = 0 \quad (A-65)$$

where

$$A_5 = \left| \frac{(1 + \mu^2 a_2) \cos(\beta_2 - \theta_2) + \mu(a_2 - 1) \sin(\beta_2 - \theta_2)}{1 + \mu^2} \right| \quad (A-66)$$

$$A_6 = \left| \frac{\sin \gamma_3 + \mu \cos \gamma_3}{1 + \mu^2} \right| \quad (A-67)$$

$$A_7 = \left| \frac{(1 - \mu^2 s_3) \cos(\beta_3 + \theta_3) - \mu(1 + s_3) \sin(\beta_3 + \theta_3)}{1 + \mu^2} \right| \quad (A-68)$$

$$A_8 = \left| \frac{(1 + \mu^2 s_2) \sin(\beta_2 - \theta_2) + \mu(1 - s_2) \cos(\beta_2 - \theta_2)}{1 + \mu^2} \right| \quad (A-69)$$

$$A_9 = \left| \frac{\mu \sin \gamma_3 - \cos \gamma_3}{1 + \mu^2} \right| \quad (A-70)$$

$$A_{10} = \left| \frac{(1 - \mu^2 s_3) \sin(\beta_3 + \theta_3) + \mu(1 + s_3) \cos(\beta_3 + \theta_3)}{1 + \mu^2} \right| \quad (A-71)$$

Finally equation (A-65) is solved for  $F_{23}$

$$F_{23} = \frac{F_{34} C_2 + T_3 C_3}{D_2} \quad (A-72)$$

where

$$C_2 = R_{b3} - \mu [s_3 a_3 - r_3 (A_7 + A_{10})] \quad (A-73)$$

$$C_3 = \mu r_3 (A_6 + A_9) \quad (A-74)$$

$$D_2 = r_{b3} - \mu [s_2 (d_2 - a_2) + r_3 (A_5 + A_8)] \quad (A-75)$$

c. EQUILIBRIUM OF GEAR AND PINION SET NO. 2

Figure A-8 shows the free body diagram of gear and pinion set no. 2. The contact point  $C_2$ , between gear 2 and pinion 3, is again shown before the pitch point  $P_2$  is passed. (See also Figure A-7.) The normal force, along the line-of-action, becomes with equation (A-72)

$$F_{32} = -F_{23}\bar{n}_{23} \quad (A-76)$$

The associated friction force,  $F_{f32}$ , is given by

$$F_{f32} = \mu_2 F_{23}\bar{n}_{N23} \quad (A-77)$$

The unit vectors along (and perpendicular to) the line-of-action of gear 1 and pinion 2 are given by

$$\bar{n}_{12} = \sin(\beta_1 + \theta_1)\bar{I} - \cos(\beta_1 + \theta_1)\bar{J} \quad (A-78)$$

and

$$\bar{n}_{N12} = \cos(\beta_1 + \theta_1)\bar{I} + \sin(\beta_1 + \theta_1)\bar{J} \quad (A-79)$$

The contact point  $C_1$ , between gear 1 and pinion 2 is also shown before pitch point  $P_1$  is passed.

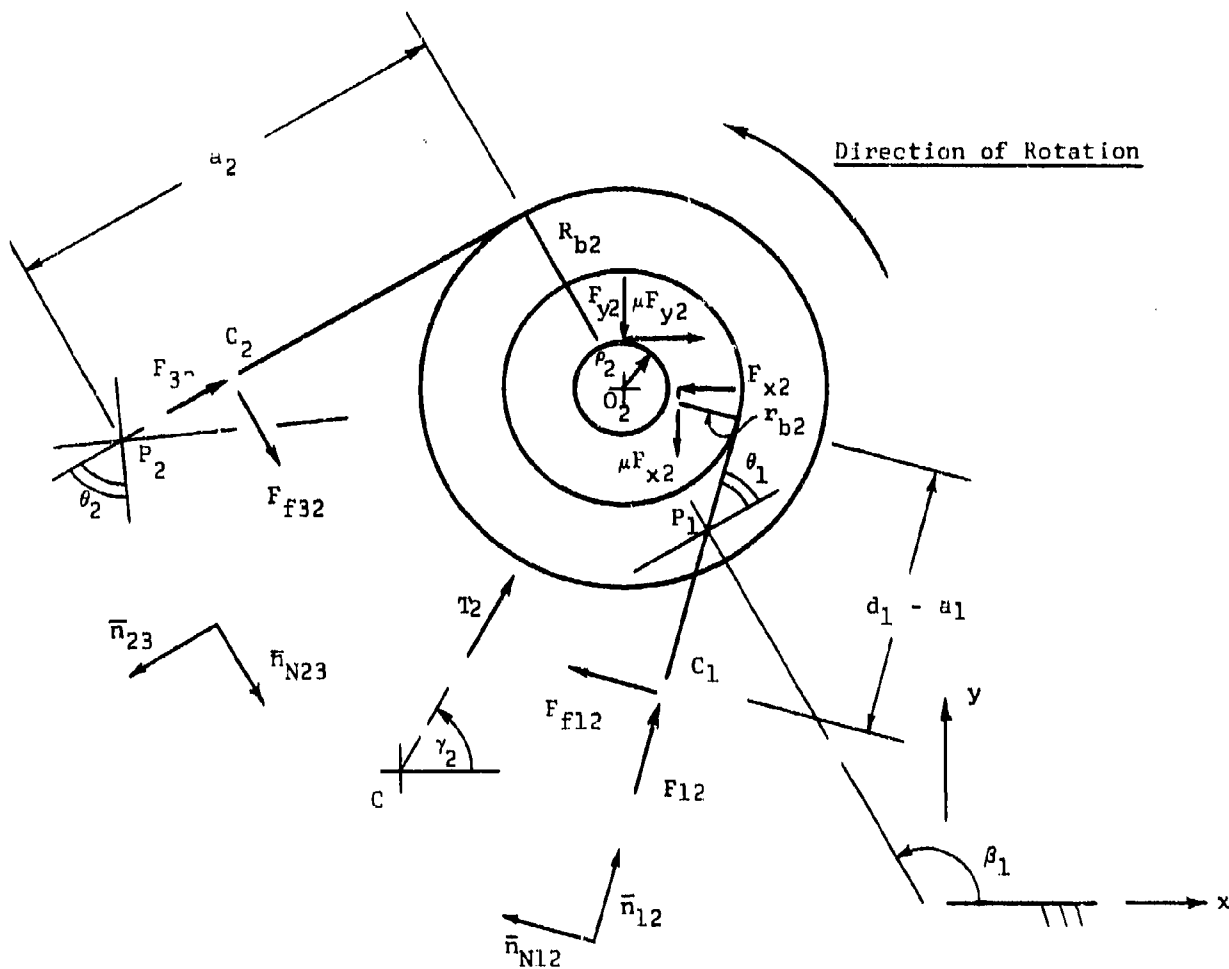


FIGURE A8, FREE BODY DIAGRAM OF GEAR AND PINION SET NO. 2

The normal contact force between the teeth of this mesh becomes

$$\bar{F}_{12} = F_{12} \bar{n}_{12}, \quad (A-80)$$

while the associated friction force is given by  
(See Section 1 of this Appendix.)

$$\bar{F}_{f12} = \mu s_1 F_{12} \bar{n}_{N12} \quad (A-81)$$

where  $s_1 = +1$  for contact before pitch point  $P_1$

$s_1 = 0$  for contact at pitch point  $P_1$

$s_1 = -1$  for contact after pitch point  $P_1$

The normal forces on the pivot shaft are

$$\bar{F}_{x2} = -F_{x2} \bar{i} \quad (A-82)$$

and

$$\bar{F}_{y2} = -F_{y2} \bar{j} \quad (A-83)$$

The associated pivot friction forces are again chosen such that

their friction moments oppose the indicated rotation.

The centrifugal force,  $T_2$ , on this gear and pinion assembly is given by

$$\bar{T}_2 = T_2(\cos\gamma_2\bar{i} + \sin\gamma_2\bar{j}) \quad (A-84)$$

$$\text{where } T_2 = R_2\omega^2 m_2 \quad (A-85a)$$

with

$$m_2 = \text{mass of gear and pinion set no. 2} \quad (A-85b)$$

Force equilibrium is given by

$$\begin{aligned} -F_{23}\bar{n}_{23} + \mu_{s2}F_{23}\bar{n}_{N23} + F_{12}\bar{n}_{12} + \mu_{s1}F_{12}\bar{n}_{N12} \\ + T_2(\cos\gamma_2\bar{i} + \sin\gamma_2\bar{j}) - F_{x2}\bar{i} - F_{y2}\bar{j} + \mu_{Fy2}\bar{i} - \mu_{Fx2}\bar{j} \\ = 0 \end{aligned} \quad (A-86)$$

Moment equilibrium is given by

$$\begin{aligned} -R_{b2}F_{23} + \mu_{s2}a_2F_{23} + r_{b2}F_{12} - \mu_{s1}(d_1 - a_1)F_{12} \\ - \mu_{F2}(\bar{F}_{x2} + \bar{F}_{y2}) = 0 \end{aligned} \quad (A-87)$$

Again, equation (A-3b) is used to account for the pivot friction moment.  $\rho_2$  represents the pivot radius.  $d_1$  is the length of the line-of-action between the points of tangency to the base circles, and  $a_1$  is the distance from the point of tangency of the gear to the contact point  $C_1$ .

The component form of equation (A-86) is given by

$$\begin{aligned}
 &F_{23} \sin(\beta_2 - \theta_2) - \mu s_2 F_{23} \cos(\beta_2 - \theta_2) + F_{12} \sin(\beta_1 + \theta_1) \\
 &+ \mu s_1 F_{12} \cos(\beta_1 + \theta_1) + T_2 \cos \gamma_2 - F_{x2} + \mu F_{y2} \\
 &= 0 \qquad \qquad \qquad (A-88)
 \end{aligned}$$

$$\begin{aligned}
 &-F_{23} \cos(\beta_2 - \theta_2) - \mu s_2 F_{23} \sin(\beta_2 - \theta_2) - F_{12} \cos(\beta_1 + \theta_1) \\
 &+ \mu s_1 F_{12} \sin(\beta_1 + \theta_1) + T_2 \sin \gamma_2 - F_{y2} - \mu F_{x2} \\
 &= 0 \qquad \qquad \qquad (A-89)
 \end{aligned}$$

Simultaneous solution of the above furnishes

$$\begin{aligned}
 F_{x2} = \frac{1}{1 + \mu^2} &\left\{ -F_{12} \left[ \mu(1 - s_1) \cos(\beta_1 + \theta_1) - (1 + \mu^2 s_1) \sin(\beta_1 + \theta_1) \right] \right. \\
 &+ T_2 \left[ \mu \sin \gamma_2 + \cos \gamma_2 \right] \\
 &\left. + F_{23} \left[ (1 - \mu^2 s_2) \sin(\beta_2 - \theta_2) - \mu(1 + s_2) \cos(\beta_2 - \theta_2) \right] \right\} \\
 &\qquad \qquad \qquad (A-90)
 \end{aligned}$$

and

$$F_{y2} = \frac{1}{1 + \mu^2} \left\{ -F_{12} \left[ \mu(1 - s_1) \sin(\beta_1 + \theta_1) + (1 + \mu^2 s_1) \cos(\beta_1 + \theta_1) \right] \right. \\ \left. + T_2 \left[ \sin \gamma_2 - \mu \cos \gamma_2 \right] \right. \\ \left. + F_{23} \left[ -\mu(1 + s_2) \sin(\beta_2 - \theta_2) - (1 - \mu^2 s_2) \cos(\beta_2 - \theta_2) \right] \right\} \quad (A-91)$$

Now, equations (A-90) and (A-91) are substituted into the moment equation (A-87). With consideration of the pivot friction moment according to equation (A-3b), this gives

$$-R_{b2} F_{23} + \mu s_2 a_2 F_{23} + r_{b2} F_{12} - \mu s_1 (d_1 - a_1) F_{12} \\ - \mu p_2 \left[ F_{12} (A_{11} + A_{14}) + T_2 (A_{12} + A_{15}) + F_{23} (A_{13} + A_{16}) \right] \\ = 0 \quad (A-92)$$

In the above

$$A_{11} = \left| \frac{\mu(1 - s_1) \sin(\beta_1 + \theta_1) + (1 + \mu^2 s_1) \cos(\beta_1 + \theta_1)}{1 + \mu^2} \right| \quad (A-93)$$

$$A_{12} = \left| \frac{\sin \gamma_2 - \mu \cos \gamma_2}{1 + \mu^2} \right| \quad (A-94)$$

$$A_{13} = \left| \frac{\mu(1 + s_2)\sin(\beta_2 - \theta_2) + (1 - \mu^2 s_2)\cos(\beta_2 - \theta_2)}{1 + \mu^2} \right| \quad (\text{A-95})$$

$$A_{14} = \left| \frac{\mu(1 - s_1)\cos(\beta_1 + \theta_1) - (1 + \mu^2 s_1)\sin(\beta_1 + \theta_1)}{1 + \mu^2} \right| \quad (\text{A-96})$$

$$A_{15} = \left| \frac{\mu \sin \gamma_2 + \cos \gamma_2}{1 + \mu^2} \right| \quad (\text{A-97})$$

$$A_{16} = \left| \frac{(1 - \mu^2 s_2)\sin(\beta_2 - \theta_2) - \mu(1 + s_2)\cos(\beta_2 - \theta_2)}{1 + \mu^2} \right| \quad (\text{A-98})$$

Finally, equation (A-92) is solved for  $F_{12}$

$$F_{12} = \frac{F_{23}C_4 + T_2C_5}{D_3} \quad (\text{A-99})$$

where

$$C_4 = R_{b2} - \mu \left[ s_2 a_2 - p_2 (A_{13} + A_{16}) \right] \quad (\text{A-100})$$

$$C_5 = \mu p_2 (A_{12} + A_{15}) \quad (\text{A-101})$$

$$D_3 = r_{b2} - \mu \left[ s_1 (d_1 - a_1) + p_2 (A_{11} + A_{14}) \right] \quad (\text{A-102})$$

d. EQUILIBRIUM OF GEAR NO. 1

Figure A-9 shows the free body diagram of gear no. 1, the input gear.

The contact point  $C_1$  is identical with that shown in Figure A-8.

The normal force on gear no. 1 is given by (See equation (A-80).)

$$\bar{F}_{21} = -F_{12}\bar{N}_{12} \quad (A-103)$$

The associated friction force is

$$\bar{F}_{f21} = -\mu s_1 F_{12}\bar{N}_{12} \quad (A-104)$$

The normal forces on the pivot shaft are given by

$$\bar{F}_{x1} = -F_{x1}\bar{I} \quad (A-105)$$

and

$$\bar{F}_{y1} = F_{y1}\bar{J} \quad (A-106)$$

The associated pivot friction forces are chosen in such a direction that their moments oppose the indicated rotation.

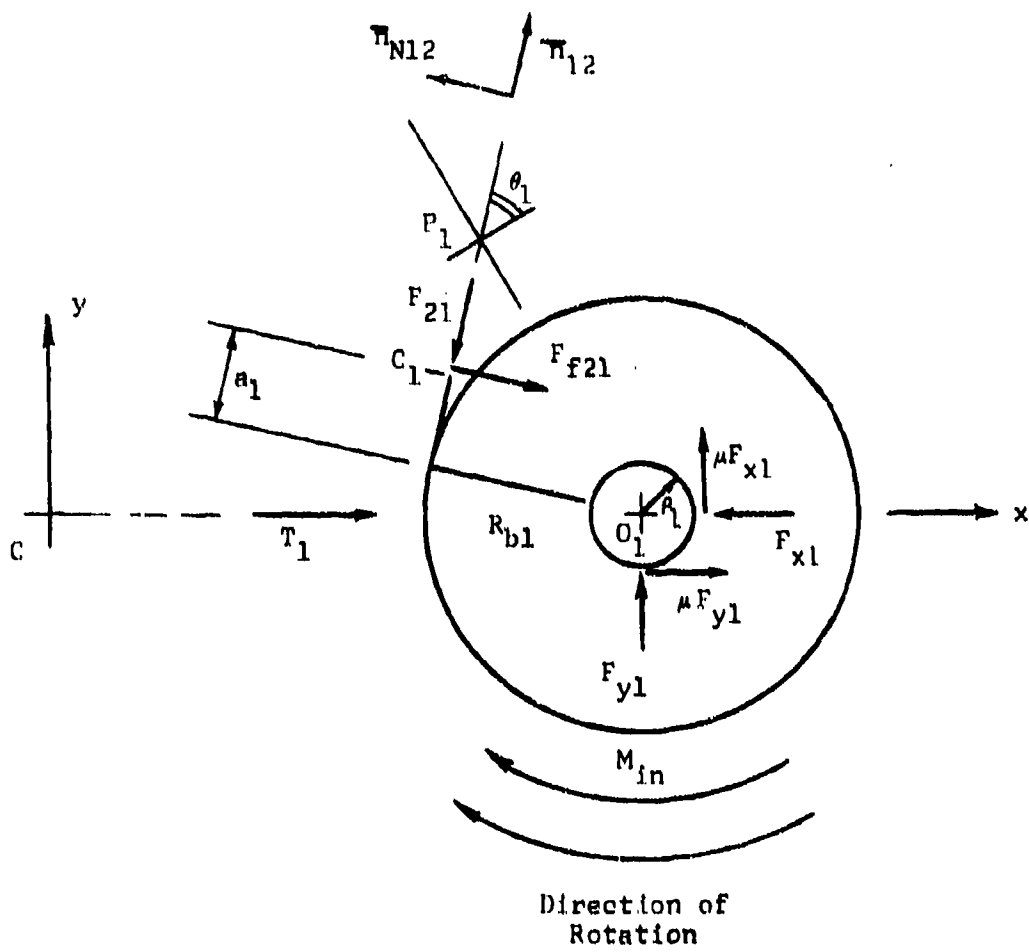


FIGURE A9. FREE BODY DIAGRAM OF GEAR 1

The centrifugal force  $\bar{T}_1$  on gear 1 is given by

$$\bar{T}_1 = T_1 \bar{I} \quad (A-107)$$

where

$$T_1 = \mathcal{Q}_1 \omega^2 m_1 \quad (A-108a)$$

$$m_1 = \text{mass of gear 1} \quad (A-108b)$$

Force equilibrium is given by

$$-F_{12} \bar{H}_{12} - \mu_{s1} F_{12} \bar{N}_{12} + T_1 \bar{I} - F_{x1} \bar{I} + F_{y1} \bar{J} + \mu_{f1} F_{y1} \bar{I} + \mu_{f1} F_{x1} \bar{J} = 0 \quad (A-109)$$

Moment equilibrium is found from

$$R_{b1} F_{12} - \mu_{s1} a_1 F_{12} - M_{in} + \mu_{f1} (\tilde{F}_{x1} + \tilde{F}_{y1}) = 0 \quad (A-110)$$

The form of equation (A-3b) is again utilized to obtain the pivot friction moment.  $\rho_1$  represents the pivot radius of gear 1.

The component form of equation (A-109) becomes

$$\begin{aligned}
 -F_{12}\sin(\beta_1 + \theta_1) - \mu s_1 F_{12}\cos(\beta_1 + \theta_1) - F_{x1} + \mu F_{y1} + T_1 \\
 = 0
 \end{aligned}
 \tag{A-111}$$

and

$$\begin{aligned}
 F_{12}\cos(\beta_1 + \theta_1) - \mu s_1 F_{12}\sin(\beta_1 + \theta_1) + F_{y1} + \mu F_{x1} \\
 = 0
 \end{aligned}
 \tag{A-112}$$

Simultaneous solution of equations (A-111) and (A-112) furnishes the forces on the pivot, i.e.,

$$F_{x1} = \frac{-F_{12}[(1 - \mu^2 s_1)\sin(\beta_1 + \theta_1) + \mu(1 + s_1)\cos(\beta_1 + \theta_1)] + T_1}{1 + \mu^2}
 \tag{A-113}$$

$$F_{y1} = \frac{F_{12}[\mu(1 + s_1)\sin(\beta_1 + \theta_1) - (1 - \mu^2 s_1)\cos(\beta_1 + \theta_1)] - \mu T_1}{1 + \mu^2}
 \tag{A-114}$$

Equations (A-113) and (A-114) are now substituted into the moment equation (A-110) in the following manner: (Again, the method of equation (A-3b) is applied.)

$$R_{b1}F_{12} - \mu s_1 a_1 F_{12} - M_{in} + \mu p_1 [F_{12}(A_{17} + A_{19}) + T_1(A_{18} + A_{20})] = 0 \quad (A-115)$$

where

$$A_{17} = \left| \frac{(1 - \mu^2 s_1) \sin(\beta_1 + \theta_1) + \mu(1 + s_1) \cos(\beta_1 + \theta_1)}{1 + \mu^2} \right| \quad (A-116)$$

$$A_{18} = \left| \frac{1}{1 + \mu^2} \right| \quad (A-117)$$

$$A_{19} = \left| \frac{\mu(1 + s_1) \sin(\beta_1 + \theta_1) - (1 - \mu^2 s_1) \cos(\beta_1 + \theta_1)}{1 + \mu^2} \right| \quad (A-118)$$

$$A_{20} = \left| \frac{\mu}{1 + \mu^2} \right| \quad (A-119)$$

Finally, equation (A-115) is solved for  $F_{12}$

$$F_{12} = \frac{M_{in}}{D_4} - \frac{T_1 C_6}{D_4} \quad (A-120)$$

where

$$C_6 = \mu p_1 (A_{18} + A_{20}) \quad (A-121)$$

$$D_4 = R_{b1} - \mu [s_1 a_1 - p_1 (A_{17} + A_{19})] \quad (A-122)$$

e. INPUT-OUTPUT RELATIONSHIP

To obtain the input-output relationship for the complete gear train, equation (A-120) is now equated to equation (A-99).

This furnishes

$$F_{23} = \frac{D_3}{C_4 D_4} (M_{in} - T_1 C_6) - T_2 \frac{C_5}{C_4} \quad (A-123)$$

Further, the above is equated to equation (A-72). This results in the following expression for  $F_{34}$

$$F_{34} = \frac{D_2 D_3}{C_2 C_4 D_4} (M_{in} - T_1 C_6) - T_2 \frac{C_5 D_2}{C_2 C_4} - T_3 \frac{C_3}{C_2} \quad (A-124)$$

Finally, equation (A-124) is equated to equation (A-46).

This establishes the input-output relationship

$$M_{o4} = \frac{D_1 D_2 D_3}{C_2 C_4 D_4} (M_{in} - T_1 C_6) - T_2 \frac{C_5 D_1 D_2}{C_2 C_4} - T_3 \frac{C_3 D_1}{C_2} - T_4 C_1 \quad (A-125)$$

5. MOMENT INPUT-OUTPUT RELATIONSHIP FOR INVOLUTE TWO STEP-UP  
GEAR TRAIN IN SPIN ENVIRONMENT

Figure A-10 shows the basic configuration of a two step-up gear train with involute teeth for which the relationship between the equilibrant output moment,  $M_{o3}$ , acting on pinion 3, and the input moment,  $M_{in}$ , acting on gear 1 is to be found. All nomenclature is identical with that used in Section 4 in connection with the three step-up gear train.

Again, the general relationship between input and output is found by assembling the input-output relationships of the individual component gears.

a. EQUILIBRIUM OF PINION 3

Figure A-11 shows the free body diagram of pinion 3. The contact point  $C_2$  between gear 2 and pinion 3 is shown before the pitch point  $P_2$  is passed.

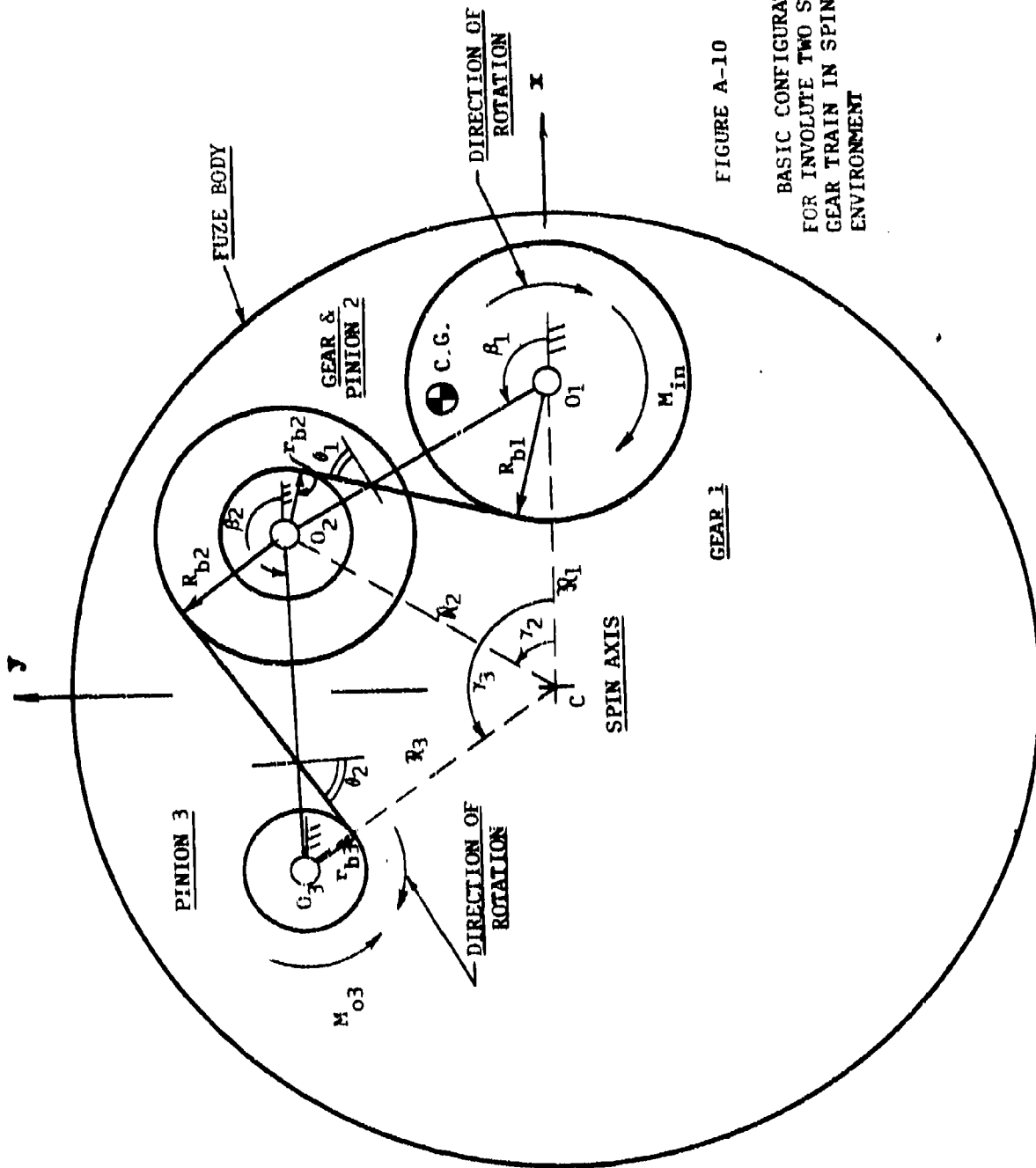


FIGURE A-10

BASIC CONFIGURATION  
FOR INVOLUTE TWO STEP-UP  
GEAR TRAIN IN SPIN  
ENVIRONMENT

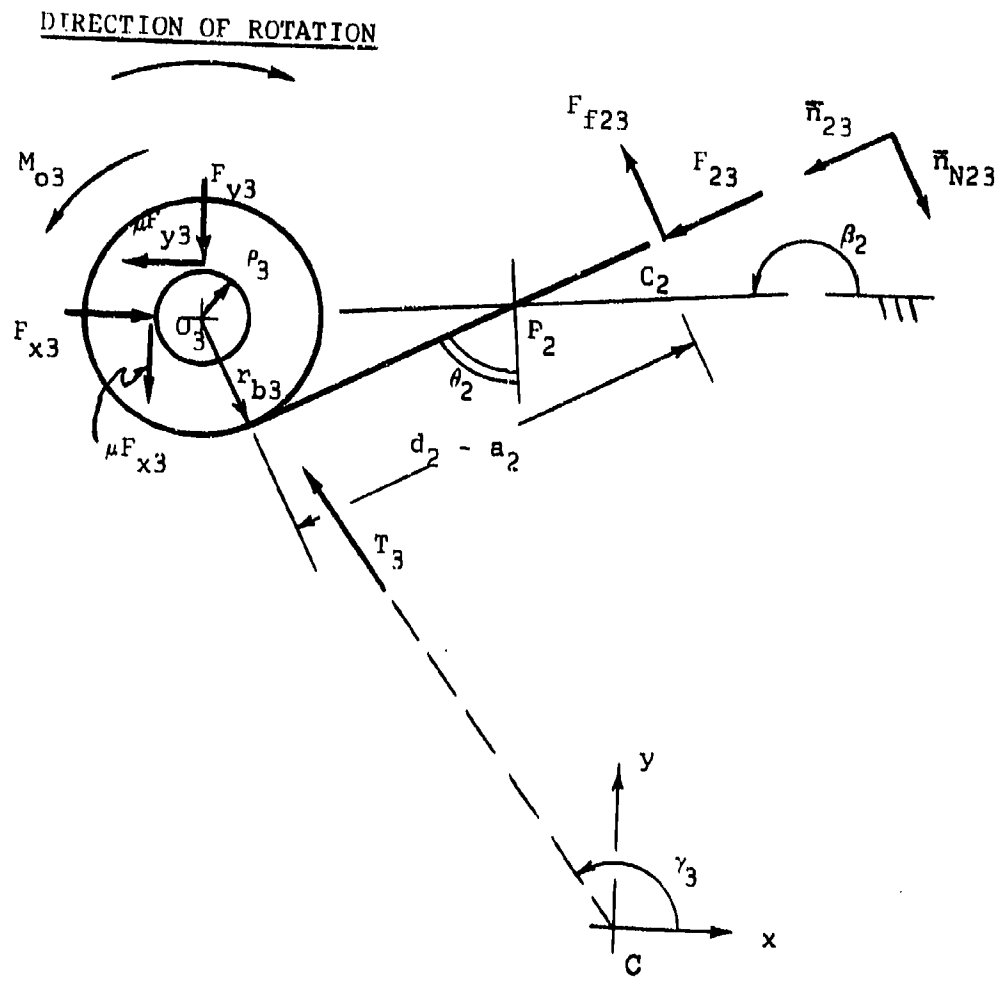


FIGURE A-11 FREE BODY DIAGRAM OF PINION 3

As in equation (A-53), the normal force between the teeth of gear 2 and pinion 3 is given by

$$\bar{F}_{23} = F_{23} \bar{n}_{23} \quad (A-126)$$

The associated friction force is given by equation (A-54), i.e.,

$$\bar{F}_{f23} = -\mu s_2 F_{23} \bar{n}_{N23} \quad (A-127)$$

where  $s_2 = +1$  , for contact before pitch point  $P_2$

$s_2 = 0$  , for contact at pitch point  $P_2$

$s_2 = -1$  , for contact after pitch point  $P_2$

The unit vectors in equations (A-126) and (A-127) were defined by equations (A-51) and (A-52), respectively. The normal forces on the pivot shaft are given by

$$\bar{F}_{x3} = F_{x3} \bar{i} \quad (A-128)$$

and

$$\bar{F}_{y3} = -F_{y3} \bar{j} \quad (A-129)$$

The pivot friction forces become  $(-)\mu F_{y3}\bar{i}$  and  $(-)\mu F_{x3}\bar{j}$  for the indicated direction of rotation.

As in equation (A-57), the centrifugal force on the pinion is given by

$$\bar{T}_3 = T_3(\cos\gamma_3\bar{i} + \sin\gamma_3\bar{j}) \quad (A-130)$$

where

$$T_3 = R_3\omega^2 m_3 \quad (A-131)$$

with

$$m_3 = \text{mass of pinion 3} \quad (A-132)$$

Force equilibrium is given by

$$\begin{aligned} F_{23}\bar{n}_{23} - \mu s_2 F_{23}\bar{n}_{23} + T_3(\cos\gamma_3\bar{i} + \sin\gamma_3\bar{j}) + F_{x3}\bar{i} \\ - \mu F_{y3}\bar{i} - F_{y3}\bar{j} - \mu F_{x3}\bar{j} = 0 \end{aligned} \quad (A-133)$$

Moment equilibrium is obtained from

$$M_{o3} - r_{b3}F_{23} + \mu s_2(d_2 - a_2)F_{23} + \mu F_3(\tilde{F}_{x3} + \tilde{F}_{y3}) = 0 \quad (A-134)$$

Note the use of equation (A-3b) for the pivot friction moment.

$r_3$  represents the pivot radius.  $d_2$  is the length of the line of action between the points of tangency to the base circles of pinion 3 and gear 2.  $a_2$  is the distance along the line-of-action from the gear point of tangency to contact point  $C_2$ .

The x and y components of equation (A-133) are given by

$$-F_{23}\sin(\beta_2 - \theta_2) + \mu s_3 F_{23}\cos(\beta_2 - \theta_2) + T_3\cos\gamma_3 + F_{x3} - \mu F_{y3} = 0, \quad (A-135)$$

and

$$F_{23}\cos(\beta_2 - \theta_2) + \mu s_3 F_{23}\sin(\beta_2 - \theta_2) + T_3\sin\gamma_3 - F_{y3} - \mu F_{x3} = 0 \quad (A-136)$$

Simultaneous solution of these expressions for  $F_{x3}$  and  $F_{y3}$  yields

$$F_{x3} = \frac{1}{1 + \mu^2} \left\{ F_{23} \left[ (1 + \mu^2 s_2)\sin(\beta_2 - \theta_2) + \mu(1 - s_2)\cos(\beta_2 - \theta_2) \right] + T_3 \left[ \mu\sin\gamma_3 - \cos\gamma_3 \right] \right\} \quad (A-137)$$

and

$$F_{y3} = \frac{1}{1 + \mu^2} \left\{ F_{23} \left[ (1 + \mu^2 s_2) \cos(\beta_2 - \theta_2) + \mu(s_2 - 1) \sin(\beta_2 - \theta_2) \right] + T_3 \left[ \sin \gamma_3 + \mu \cos \gamma_3 \right] \right\} \quad (A-138)$$

Now, equations (A-137) and (A-138) are substituted into the moment equation (A-134), with the pivot friction moment given according to the formulation of equation (A-3b):

$$M_{o3} - r_{b3} F_{23} + \mu s_2 (d_2 - s_2 F_{23}) + \mu p_3 \left[ F_{23} (A_1 + A_3) + T_3 (A_2 + A_4) \right] = 0 \quad (A-139)$$

where

$$A_1 = \left| \frac{(1 + \mu^2 s_2) \cos(\beta_2 - \theta_2) + \mu(s_2 - 1) \sin(\beta_2 - \theta_2)}{1 + \mu^2} \right| \quad (A-140)$$

$$A_2 = \left| \frac{\sin \gamma_3 + \mu \cos \gamma_3}{1 + \mu^2} \right| \quad (A-141)$$

$$A_3 = \left| \frac{(1 + \mu^2 s_2) \sin(\beta_2 - \theta_2) + \mu(1 - s_2) \cos(\beta_2 - \theta_2)}{1 + \mu^2} \right| \quad (A-142)$$

$$A_4 = \left| \frac{\mu \sin \gamma_3 - \cos \gamma_3}{1 + \mu^2} \right| \quad (\text{A-143})$$

Finally, equation (A-139) is solved for  $F_{23}$

$$F_{23} = \frac{M_{o3}}{D_1} + T_3 \frac{C_1}{D_1} \quad (\text{A-144})$$

where

$$C_1 = \mu p_3 (A_2 + A_4) \quad (\text{A-145})$$

$$D_1 = r_{b3} - \mu \left[ a_2 (d_2 - a_2) + p_3 (A_1 + A_3) \right] \quad (\text{A-146})$$

b. EQUILIBRIUM OF GEAR AND PINION SET NO. 2

Figure A-12 shows the free body diagram of gear and pinion set no. 2. The contact point,  $C_2$ , between gear 2 and pinion 3 is again shown before the pitch point,  $P_2$ . With equation (A-126), the normal force between the teeth of this mesh becomes

$$\bar{F}_{32} = -F_{23}\bar{n}_{23} \quad (A-147)$$

The associated friction force is the negative of equation (A-127), i.e.,

$$\bar{F}_{f32} = \mu s_2 F_{23}\bar{n}_{23} \quad (A-148)$$

Similar to equation (A-80), the normal force between gear 1 and pinion 2 is given by

$$\bar{F}_{12} = F_{12}\bar{n}_{12} \quad (A-149)$$

(See equation (A-78) for the definition of unit vector  $\bar{n}_{12}$ .)

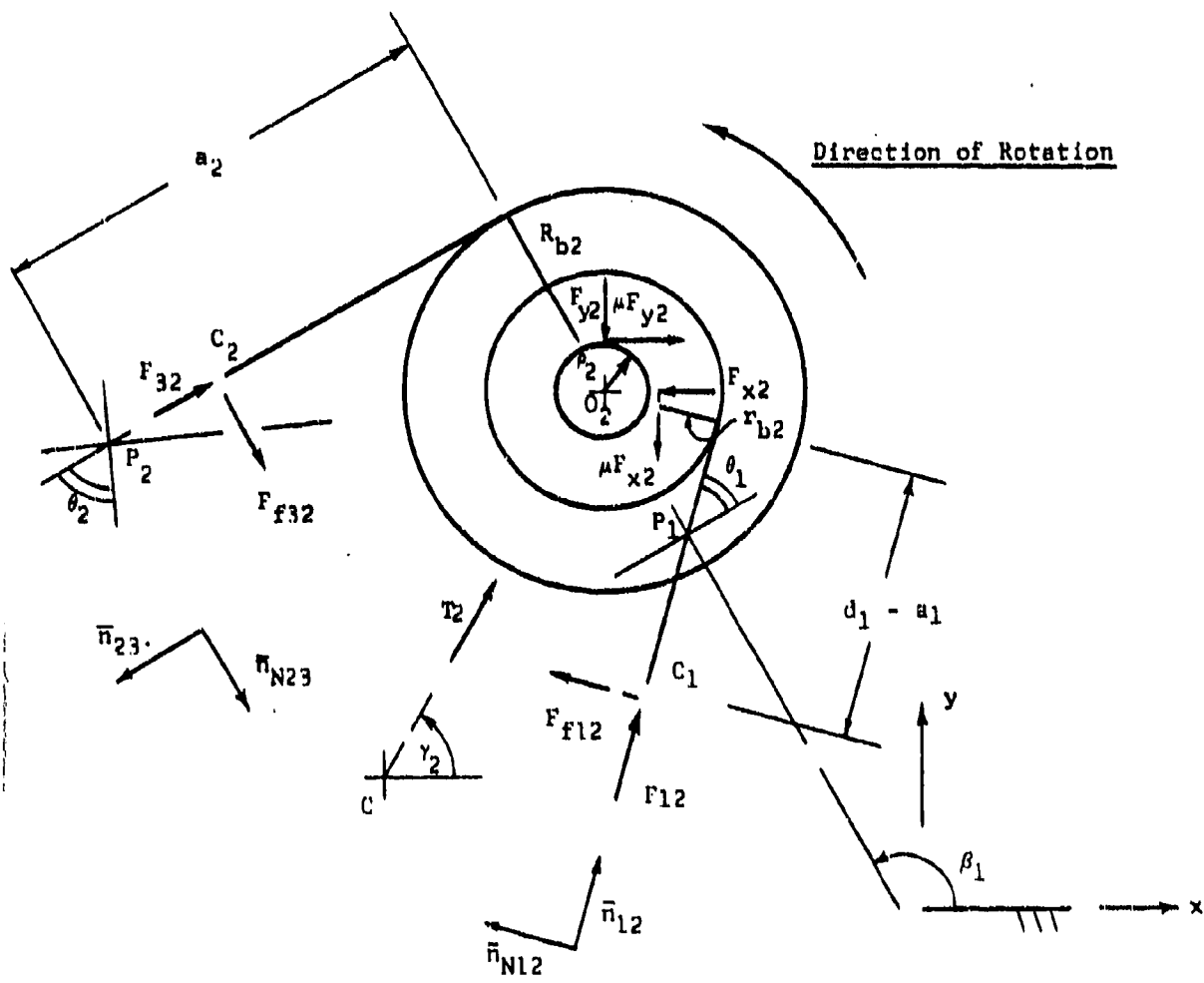


FIGURE A-12 FREE BODY DIAGRAM OF GEAR AND PINION SET NO. 2

Figure A-12 shows the contact point  $C_1$  before the pitch point  $P_1$  is passed.

The associated friction force is given by

$$\bar{F}_{f12} = \mu s_1 F_{12} \bar{H}_{N12} \quad (A-150)$$

where  $s_1 = +1$ , for contact before pitch point  $P_1$

$s_1 = 0$ , for contact at pitch point  $P_1$

$s_1 = -1$ , for contact after pitch point  $P_1$

The unit vector  $\bar{H}_{N12}$  is given by equation (A-79).

The normal forces on the pivot shaft are given by

$$F_{x2} = -F_{x2} \bar{I} \quad (A-151)$$

and

$$F_{y2} = -F_{y2} \bar{J} \quad (A-152)$$

The associated friction forces  $\mu F_{y2} \bar{I}$  and  $(-)\mu F_{x2} \bar{J}$  were chosen so that their moments oppose the indicated rotation.

The centrifugal force on this gear and pinion assembly is expressed by

$$\vec{T}_2 = T_2(\cos\gamma_2\vec{i} + \sin\gamma_2\vec{j}) \quad (\text{A-153})$$

$$\text{where } T_2 = \mathcal{Q}_2\omega^2 m_2 \quad (\text{A-154})$$

$$m_2 = \text{mass of gear and pinion set no. 2} \quad (\text{A-155})$$

Force equilibrium is given by

$$\begin{aligned} -F_{23}N_{23} + \mu_s F_{23}N_{23} + F_{12}N_{12} + \mu_s F_{12}N_{12} \\ + T_2(\cos\gamma_2\vec{i} + \sin\gamma_2\vec{j}) - F_{x2}\vec{i} + \mu F_{y2}\vec{i} - F_{y2}\vec{j} - \mu F_{x2}\vec{j} \\ = 0 \end{aligned} \quad (\text{A-156})$$

Moment equilibrium is given by

$$\begin{aligned} -R_{b2}F_{23} + \mu_s a_2 F_{23} + r_{b2}F_{12} - \mu_s (d_1 - a_1)F_{12} \\ - \mu p_2(\tilde{F}_{x2} + \tilde{F}_{y2}) = 0 \end{aligned} \quad (\text{A-157})$$

Again, equation (A-3b) is used to obtain a conservative pivot friction moment.  $p_2$  represents the pivot radius.  $d_1$  and  $a_1$  are similar to the previously used distances along the lines of action of the other meshes.

The component form of equation (A-156) becomes

$$\begin{aligned}
 &F_{23}\sin(\beta_2 - \theta_2) - \mu s_2 F_{23}\cos(\beta_2 - \theta_2) + F_{12}\sin(\beta_1 + \theta_1) \\
 &+ \mu s_1 F_{12}\cos(\beta_1 + \theta_1) + T_2\cos\gamma_2 - F_{x2} + \mu F_{y2} = 0 \quad (A-158)
 \end{aligned}$$

and

$$\begin{aligned}
 &-F_{23}\cos(\beta_2 - \theta_2) - \mu s_2 F_{23}\sin(\beta_2 - \theta_2) - F_{12}\cos(\beta_1 + \theta_1) \\
 &+ \mu s_1 F_{12}\sin(\beta_1 + \theta_1) + T_2\sin\gamma_2 - F_{y2} - \mu F_{x2} = 0 \quad (A-159)
 \end{aligned}$$

Simultaneous solution of the above expressions for  $F_{x2}$  and  $F_{y2}$  gives

$$\begin{aligned}
 F_{x2} = \frac{1}{1 + \mu^2} \left\{ -F_{12} \left[ \mu(1 - s_1)\cos(\beta_1 + \theta_1) - (1 + \mu^2 s_1)\sin(\beta_1 + \theta_1) \right] \right. \\
 + T_2 \left[ \mu\sin\gamma_2 + \cos\gamma_2 \right] \\
 \left. + F_{23} \left[ (1 - \mu^2 s_2)\sin(\beta_2 - \theta_2) - \mu(1 + s_2)\cos(\beta_2 - \theta_2) \right] \right\} \quad (A-160)
 \end{aligned}$$

$$F_{y2} = \frac{1}{1 + \mu^2} \left\{ -F_{12} \left[ \mu(1 - s_1) \sin(\beta_1 + \theta_1) + (1 + \mu^2 s_1) \cos(\beta_1 + \theta_1) \right] \right. \\
+ T_2 \left[ \sin \gamma_2 - \mu \cos \gamma_2 \right] \\
\left. + F_{23} \left[ -\mu(1 + s_2) \sin(\beta_2 - \theta_2) - (1 - \mu^2 s_2) \cos(\beta_2 - \theta_2) \right] \right\}$$

(A-161)

Now equations (A-160) and (A-161) are substituted into the moment equation (A-157) with the pivot friction moment formulated again according to equation (A-3b):

$$\begin{aligned}
 & -R_{b2}F_{23} + \mu s_2 a_2 F_{23} + r_{b2}F_{12} - \mu s_1 (d_1 - a_1)F_{12} \\
 & - \mu P_2 \left[ F_{12}(A_5 + A_8) + T_2(A_6 + A_9) + F_{23}(A_7 + A_{10}) \right] = 0
 \end{aligned}
 \tag{A-162}$$

where

$$A_5 = \left| \frac{\mu(1 - s_1)\sin(\beta_1 + \theta_1) + (1 + \mu^2 s_1)\cos(\beta_1 + \theta_1)}{1 + \mu^2} \right|
 \tag{A-163}$$

$$A_6 = \left| \frac{\mu \sin \gamma_2 - \cos \gamma_2}{1 + \mu^2} \right|
 \tag{A-164}$$

$$A_7 = \left| \frac{\mu(1 + s_2)\sin(\beta_2 - \theta_2) + (1 - \mu^2 s_2)\cos(\beta_2 - \theta_2)}{1 + \mu^2} \right|
 \tag{A-165}$$

$$A_8 = \left| \frac{\mu(1 - s_1)\cos(\beta_1 + \theta_1) - (1 + \mu^2 s_1)\sin(\beta_1 + \theta_1)}{1 + \mu^2} \right|
 \tag{A-166}$$

$$A_9 = \left| \frac{\mu \sin \gamma_2 + \cos \gamma_2}{1 + \mu^2} \right|
 \tag{A-167}$$

$$A_{10} = \left| \frac{(1 - \mu^2 s_2) \sin(\beta_2 - \theta_2) - \mu(1 + s_2) \cos(\beta_2 - \theta_2)}{1 + \mu^2} \right| \quad (\text{A-168})$$

Finally equation (A-162) is solved for  $F_{12}$

$$F_{12} = \frac{F_2 C_2}{D_2} + \frac{T_2 C_3}{D_2} \quad (\text{A-169})$$

where

$$C_2 = R_{b2} - \mu \left[ s_2 s_2 - \rho_2 (A_7 + A_{10}) \right] \quad (\text{A-170})$$

$$C_3 = \mu \rho_2 (A_6 + A_9) \quad (\text{A-171})$$

$$D_2 = r_{b2} - \mu \left[ s_1 (d_1 - a_1) + \rho_2 (A_5 + A_8) \right] \quad (\text{A-172})$$

c. EQUILIBRIUM OF GEAR NO. 1

Figure A-13 shows the free body diagram of gear no. 1, the input gear.

The contact point,  $C_1$ , corresponds to that shown in Figure A-12.

According to equation (A-149), the normal contact force between pinion 2 and gear 1 becomes

$$\bar{F}_{21} = -F_{12}\bar{n}_{12} \quad (A-173)$$

The associated friction force is the negative of equation (A-150), i.e.,

$$\bar{F}_{f21} = -\mu S_1 F_{12}\bar{n}_{N12} \quad (A-174)$$

The normal forces on the pivot shaft are given by

$$\bar{F}_{x1} = -F_{x1}\bar{i} \quad (A-175)$$

and

$$\bar{F}_{y1} = F_{y1}\bar{j} \quad (A-176)$$

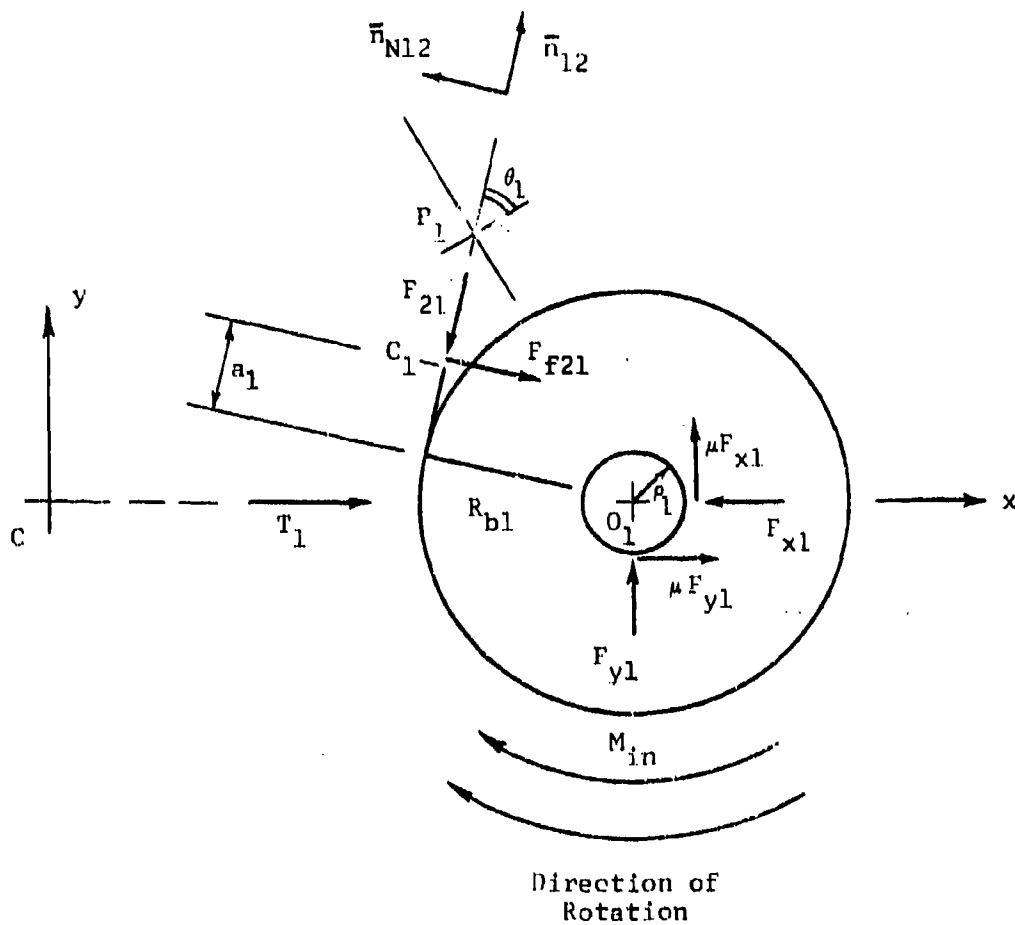


FIGURE A-13. FREE BODY DIAGRAM OF GEAR 1

The associated friction forces  $\mu F_{y1}\bar{i}$  and  $\mu F_{x1}\bar{j}$  were chosen with such directions that their moments oppose rotation due to input moment  $M_{in}$ .

Centrifugal force  $\bar{T}_1$  on gear 1 is given by

$$\bar{T}_1 = T_1\bar{i} \quad (A-177)$$

where, as with equation (A-107)

$$T_1 = R_1\omega^2 m_1 \quad (A-178)$$

and

$$m_1 = \text{mass of gear 1} \quad (A-179)$$

Force equilibrium of gear 1 is given by

$$\begin{aligned} -F_{12}\bar{n}_{12} - \mu s_1 F_{12}\bar{n}_{N12} + T_1\bar{i} - F_{x1}\bar{i} + F_{y1}\bar{j} + \mu F_{y1}\bar{i} \\ + \mu F_{x1}\bar{j} = 0 \end{aligned} \quad (A-180)$$

Moment equilibrium is given by

$$R_{b1}F_{12} - \mu s_1 a_1 F_{12} - M_{in} + \mu r_1 (\hat{F}_{x1} + \hat{F}_{y1}) = 0 \quad (A-181)$$

Note that equations (A-180) and (A-181) have the same forms as equations (A-109) and (A-110).

The force component expressions are the same as given by equations (A-111) and (A-112), and their simultaneous solution for the pivot forces is identical to that given by equations (A-113) and (A-114), i.e.,

$$F_{x1} = \frac{-F_{12} \left[ (1 - \mu^2 s_1) \sin(\beta_1 + \theta_1) + \mu(1 + s_1) \cos(\beta_1 + \theta_1) \right] + T_1}{1 + \mu^2} \quad (\text{A-182})$$

and

$$F_{y1} = \frac{F_{12} \left[ \mu(1 + s_1) \sin(\beta_1 + \theta_1) - (1 - \mu^2 s_1) \cos(\beta_1 + \theta_1) \right] - \mu T_1}{1 + \mu^2} \quad (\text{A-183})$$

Equations (A-182) and (A-183) are now substituted into equation (A-181) according to the method of equation (A-3b)

$$\begin{aligned} R_{b1} F_{12} - \mu s_1 s_1 F_{12} - M_{1n} + \mu \rho_1 \left[ F_{12} (A_{11} + A_{13}) + T_1 (A_{12} + A_{14}) \right] \\ = 0 \end{aligned} \quad (\text{A-184})$$

where

$$A_{11} = \left| \frac{(1 - \mu^2 s_1) \sin(\beta_1 + \theta_1) + \mu(1 + s_1) \cos(\beta_1 + \theta_1)}{1 + \mu^2} \right| \quad (\text{A-185})$$

$$A_{12} = \left| \frac{1}{1 + \mu^2} \right| \quad (\text{A-186})$$

$$A_{13} = \left| \frac{\mu(1 + s_1) \sin(\beta_1 + \theta_1) - (1 - \mu^2 s_1) \cos(\beta_1 + \theta_1)}{1 + \mu^2} \right| \quad (\text{A-187})$$

$$A_{14} = \left| \frac{\mu}{1 + \mu^2} \right| \quad (\text{A-188})$$

Finally, equation (A-184) is solved for  $F_{12}$

$$F_{12} = \frac{M_{1n}}{D_3} - \frac{T_1 C_4}{D_3} \quad (\text{A-189})$$

where

$$C_4 = \mu \rho_1 (A_{12} + A_{14}) \quad (\text{A-190})$$

$$D_3 = R_{b1} - \mu [s_1 a_1 - \rho_1 (A_{11} + A_{13})] \quad (\text{A-191})$$

d. INPUT-OUTPUT RELATIONSHIP

To obtain the input-output relationship for the complete gear train, equation (A-189) is now set equal to equation (A-169).

This furnishes

$$F_{23} = \frac{D_2}{C_2 D_3} [M_{1n} - T_1 C_4] - T_2 \frac{C_3}{C_2} \quad (A-192)$$

The above is then set equal to equation (A-144). This results in the input-output moment relationship

$$M_{o3} = \frac{D_1 D_2}{C_2 D_3} [M_{1n} - T_1 C_4] - T_2 \frac{C_3 D_1}{C_2} - T_3 C_1 \quad (A-193)$$

6. AUXILIARY GEOMETRIC AND KINEMATIC EXPRESSIONS FOR TWO AND THREE STEP-UP GEAR TRAINS WITH INVOLUTE TEETH

a. NOMENCLATURE FOR INVOLUTE GEAR TEETH

$R_{pi}, r_{pi}$  = pitch radii of gear and pinion of  $i^{\text{th}}$  gear and pinion set

$R_{bi}, r_{bi}$  = base radii of gear and pinion of  $i^{\text{th}}$  gear and pinion set

$R_{oi}, r_{oi}$  = outside radii of gear and pinion of  $i^{\text{th}}$  gear and pinion set

$\theta_j$  = effective pressure angle of  $j^{\text{th}}$  mesh

$\mathcal{R}_i$  = distance from spin axis to pivot of  $i^{\text{th}}$  gear and pinion set

b. ANGULAR RELATIONSHIPS BETWEEN PIVOT HOLES

Figure A-14 shows the angular relationships between the lines connecting the pivot holes as well as the spin center. (See also Figures A-5 and A-10.) The following serves to determine the angles  $\gamma_1$  and  $\beta_1$  for certain combinations of gears and pinions as well as spin radii  $\mathcal{R}_1$ .

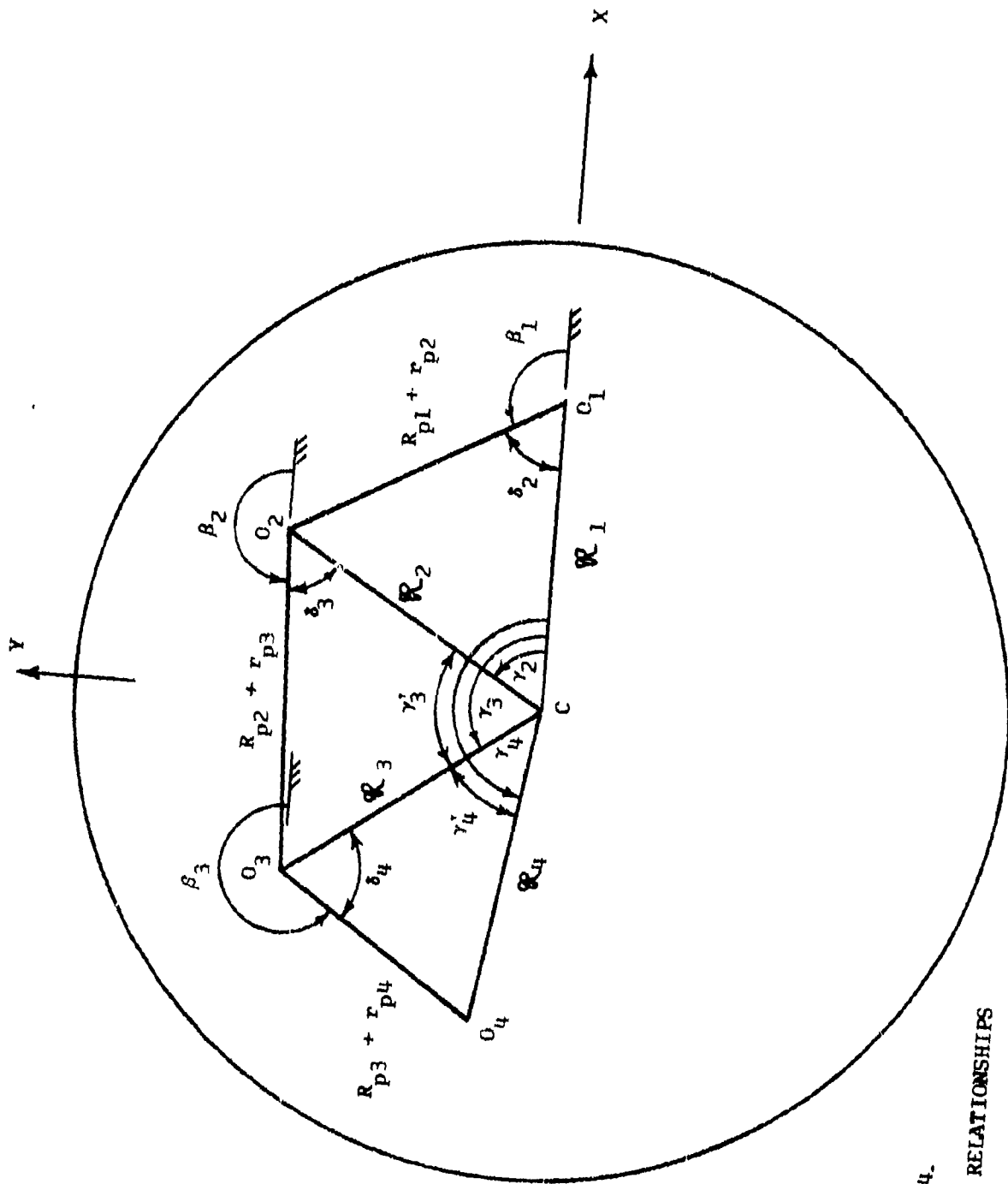


FIGURE A-14.  
PIVOT HOLE RELATIONSHIPS

ANGLE  $\gamma_1$

From

$$(R_{p1} + r_{p2})^2 = R_1^2 + R_2^2 - 2R_1R_2\cos\gamma_2$$

one obtains

$$\gamma_2 = \cos^{-1} \left[ \frac{R_1^2 + R_2^2 - (R_{p1} + r_{p2})^2}{2R_1R_2} \right] \quad (\text{A-194})$$

Similarly, from

$$\gamma_3' = \cos^{-1} \left[ \frac{R_2^2 + R_3^2 - (R_{p2} + r_{p3})^2}{2R_2R_3} \right]$$

one obtains

$$\gamma_3 = \gamma_2 + \gamma_3' \quad (\text{A-195})$$

Also with

$$\gamma_4' = \cos^{-1} \left[ \frac{R_3^2 + R_4^2 - (R_{p3} + r_{p4})^2}{2R_3R_4} \right]$$

one obtains

$$\gamma_4 = \gamma_3 + \gamma_4' \quad (\text{A-196})$$

ANGLES  $\delta_1$

Since

$$R_2^2 = (R_{p1} + r_{p2})^2 + R_1^2 - 2(R_{p1} + r_{p2})R_1 \cos \delta_2$$

$$\delta_2 = \cos^{-1} \left[ \frac{(R_{p1} + r_{p2})^2 + R_1^2 - R_2^2}{2R_1(R_{p1} + r_{p2})} \right] \quad (\text{A-197})$$

Similarly,

$$\delta_3 = \cos^{-1} \left[ \frac{(R_{p2} + r_{p3})^2 + R_2^2 - R_3^2}{2R_2(R_{p2} + r_{p3})} \right] \quad (\text{A-198})$$

and

$$\delta_4 = \cos^{-1} \left[ \frac{(R_{p3} + r_{p4})^2 + R_3^2 - R_4^2}{2R_3(R_{p3} + r_{p4})} \right] \quad (\text{A-199})$$

ANGLES  $\beta_1$

With Equation (A-197)

$$\beta_1 = \pi - \delta_2 \quad (\text{A-200})$$

Further, with Equations (A-194) and (A-198)

$$\beta_2 = \gamma_2 + (\pi - \delta_3) \quad (\text{A-201})$$

Finally, with Equations (A-195) and (A-199)

$$\beta_3 = \gamma_3 + (\pi - \delta_4) \quad (\text{A-202})$$

c. DETERMINATION OF CONTACT POINT C FOR VARIOUS MESHES

Figure A-15 shows the points of interest along the line of action of an involute gear which drives an involute pinion.

Points L and L' are the points of tangency to the base circles of radius  $R_b$  and  $r_b$ , respectively, and the distance  $d = LL'$ . Initial contact is made at point M, where the line of action intersects the pinion addendum circle of radius  $r_o$ . Final contact corresponds to point N. Here the line of action intersects the gear addendum circle of radius  $R_o$ .

The position of the instantaneous contact point C with respect to point L, i.e., the length,  $a$ , is expressed with the help of instantaneous angle  $\alpha$  which has its origin at the line  $O_1L$ . Then,

$$a = LC = R_b \alpha \quad (A-203)$$

A computer procedure for the determination of instantaneous angle  $\alpha$  of any mesh must first find the associated initial and final angles of contact  $\alpha_{in}$  and  $\alpha_{fin}$ . In addition, it must contain a method for incrementing angle  $\alpha$ . The following shows such a procedure for each of the meshes of a two pass and a three pass step-up gear train, together with a means of obtaining the signs of the signum terms.

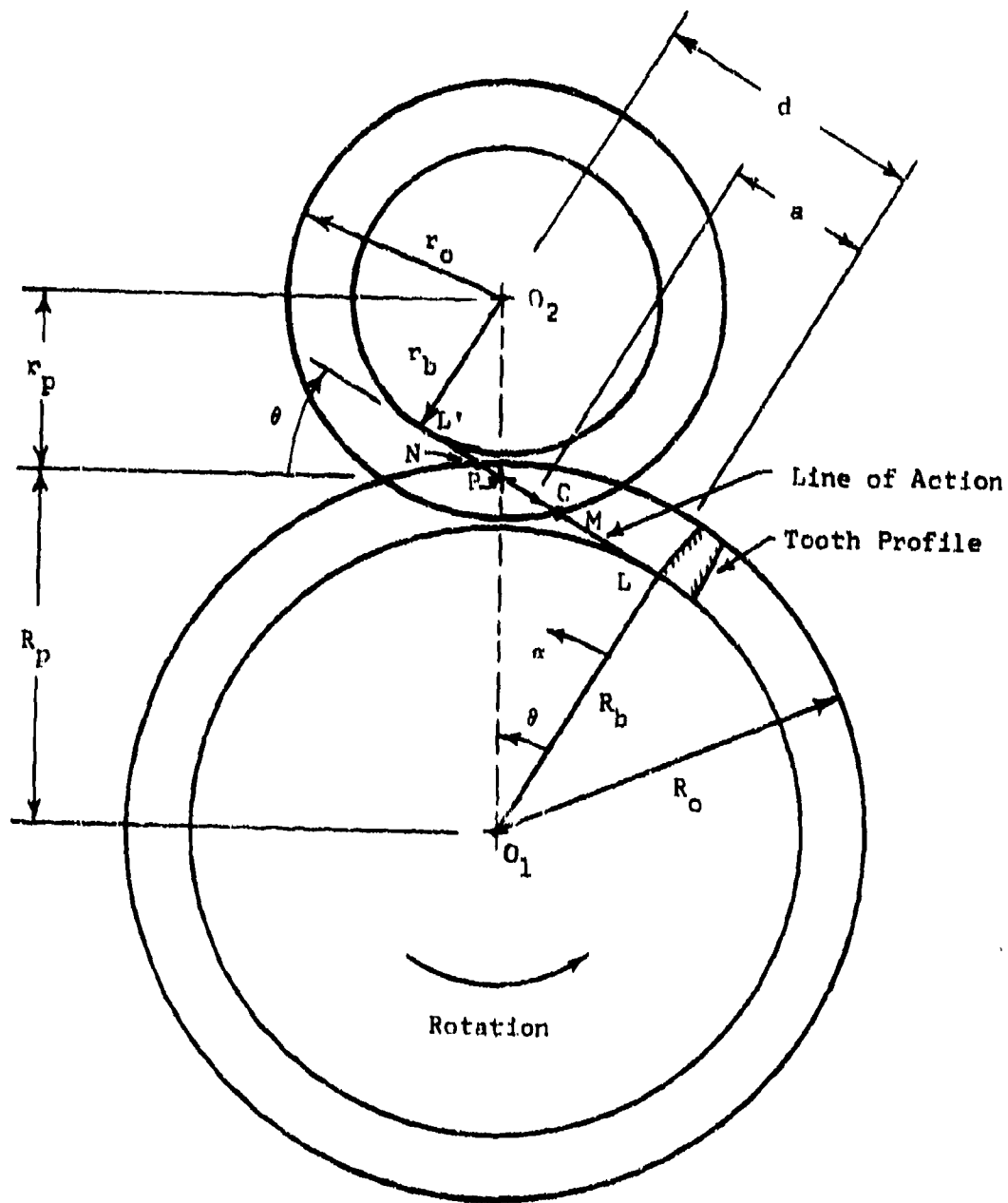


FIGURE A-15.  
INVOLUTE MESH GEOMETRY

1.) MESH OF GEAR 1 AND PINION 2

The total length,  $d_1 = LL'$ , is given by

$$d_1 = (R_{b1} + r_{b1}) \tan \theta_1 \quad (A-204)$$

The initial angle of contact,  $\alpha_{1IN}$ , is obtained from

$$\alpha_{1in} = \frac{ML}{R_{b1}} = \frac{(R_{b1} + r_{b2}) \tan \theta_1 - \sqrt{r_{o2}^2 - r_{b2}^2}}{R_{b1}} \quad (A-205)$$

Similarly, the final angle of contact,  $\alpha_{1FIN}$ , is given by

$$\alpha_{1fin} = \frac{\sqrt{R_{o1}^2 - R_{b1}^2}}{R_{b1}} \quad (A-206)$$

The magnitude of the increment  $\Delta\alpha_1$  depends on whether one deals with a two step-up or a three step-up gear train.

Assuming that a two step-up train is involved and that one wishes to compute the length  $a_2$  of mesh 2  $K_2$  times after the first contact, the angular increment,  $\Delta\alpha_{22}$ , has the magnitude

$$\Delta \alpha_{22} = \frac{\alpha_{2fin} - \alpha_{2in}}{K_2} \quad (A-207)$$

(The second subscript refers to a two step-up configuration.)

Because of the transmission ratio between gear sets 1 and 2, the associated angular increment of gear 1 will be smaller than  $\Delta \alpha_{22}$ , i.e.,

$$\Delta \alpha_{12} = \Delta \alpha_{22} \frac{r_{b2}}{R_{b1}} \quad (A-208)$$

The instantaneous angle,  $\alpha_1$ , will then be given by

$$\alpha_1 = \alpha_{1in} + j_{12} \Delta \alpha_{12} \quad (A-209)$$

and, the instantaneous distance,  $a_1$ , becomes

$$a_1 = R_{b1} (\alpha_{1in} + j_{12} \Delta \alpha_{12}) \quad (A-210)$$

In the above,  $j_{12}$  represents the number of times the angle  $\alpha_1$  has been incremented. While the total number of increments depends on the length of contact, the incrementing of  $\alpha_1$  comes to an end when  $\alpha_1 \geq \alpha_{1fin}$ . This also corresponds to a complete mechanism

cycle. Since mesh 2 goes through  $R_{b1}/r_{b2}$  times as many cycles as mesh no. 1, the angle  $\alpha_2$  has to be re-initialized to  $\alpha_{2in}$  when  $\alpha_1 \geq \alpha_{2fin}$  i.e., after  $K_2$  increments. (For simplicity it is assumed that the motion starts when all meshes are at their initial contact angles,  $\alpha_{in}$ .)

When a three step-up gear train is involved, one must make sure that enough computations are made for mesh 3. Assuming that  $K_3$  increments are to be made, one obtains

$$\Delta\alpha_{33} = \frac{\alpha_{3fin} - \alpha_{3in}}{K_3} \quad (A-211)$$

The associated angular increments for meshes 2 and 1 then become

$$\Delta\alpha_{23} = \Delta\alpha_{33} \frac{r_{b3}}{R_{b2}} \quad (A-212)$$

and

$$\Delta\alpha_{13} = \Delta\alpha_{33} \frac{r_{b3}}{R_{b2}} \times \frac{r_{b2}}{R_{b1}} \quad (A-213)$$

For this case the instantaneous distance  $a_1$  becomes

$$a_1 = R_{b1} (\alpha_{1in} + J_{13} \Delta\alpha_{13}) \quad (A-214)$$

$j_{13}$  stands for the number of times  $\alpha_1$  has been incremented at any given instant. This incrementing again ends when  $\alpha_1 \geq \alpha_{1fin}$ . Meshes 2 and 3 are re-initialized to  $\alpha_{2in}$  and  $\alpha_{3in}$  as often as is necessary to complete one cycle for mesh no. 1.

The sign of  $s_1$  is best obtained from the fact that at pitch point  $P_1$

$$\alpha_{1p} = \frac{LP}{R_{b1}} = \frac{R_{b1} \tan \theta_1}{R_{b1}} = \tan \theta_1 \quad (A-215)$$

then for

$$\begin{aligned} \alpha_1 < \tan \theta_1 : s_1 &= +1 \\ \alpha_1 = \tan \theta_1 : s_1 &= 0 \\ \alpha_1 > \tan \theta_1 : s_1 &= -1 \end{aligned} \quad (A-216)$$

## 2.) MESH OF GEAR 2 AND PINION 3

Similar to the previous section.

$$d_2 = (R_{b2} + r_{b3}) \tan \theta_2 \quad (\text{A-217})$$

$$\alpha_{2in} = \frac{(R_{b2} + r_{b3}) \tan \theta_2 - \sqrt{r_{o3}^2 - r_{b3}^2}}{R_{b2}} \quad (\text{A-218})$$

$$\alpha_{2fin} = \frac{\sqrt{R_{o2}^2 - R_{b2}^2}}{R_{b2}} \quad (\text{A-219})$$

For a two step-up gear train, the instantaneous length,  $a_2$ , becomes

$$a_2 = R_{b2}(\alpha_{2in} + J_{22} \Delta \alpha_{22}) \quad (\text{A-220})$$

where  $\Delta \alpha_{22}$  is given by Equation (A-207) and

$$J_{22} = 1, 2, \dots, K_2.$$

When  $\alpha_2 \geq \alpha_{2fin}$  it must be re-initialized to  $\alpha_{2in}$  until mesh no. 1 has completed its full cycle.

For a three step-up gear train, the length,  $a_2$ , becomes

$$a_2 = R_{b2}(\alpha_{2in} + j_{23}\Delta\alpha_{23}) \quad (A-221)$$

with  $\Delta\alpha_{23}$  given by Equation (A-212).  $j_{23}$  stands for the number of times  $\alpha_2$  has been incremented and again depends on the length of contact. Re-initialization follows the same rule as given above.

The sign of  $s_2$  is obtained as follows: (See Equation (A-215).)

For

$$\begin{aligned} \alpha_2 < \tan\theta_2 : s_2 &= +1 \\ \alpha_2 = \tan\theta_2 : s_2 &= 0 \\ \alpha_2 > \tan\theta_2 : s_2 &= -1 \end{aligned} \quad (A-222)$$

### 3.) MESH OF GEAR 3 AND PINION 4

Again, in the same vein as in Section 1,

$$d_3 = (R_{b3} + r_{b4}) \tan \theta_3 \quad (\text{A-223})$$

$$a_{3in} = \frac{(R_{b3} + r_{b4}) \tan \theta_3 - \sqrt{r_{o4}^2 - r_{b4}^2}}{R_{b3}} \quad (\text{A-224})$$

$$a_{3fin} = \frac{\sqrt{R_{o3}^2 - R_{b3}^2}}{R_{b3}} \quad (\text{A-225})$$

The instantaneous length,  $a_3$ , is given by

$$a_3 = R_{b3}(a_{3in} + j_{33} \Delta a_{33}) \quad (\text{A-226})$$

where  $\Delta a_{33}$  is given by Equation (A-211) and  $j_{33} = 1, 2, \dots, K_3$ .

Whenever  $a_3 \geq a_{3fin}$  it must be re-initialized until mesh no. 1

completed its full cycle.

The sign of  $s_3$  is again obtained with the help of an expression

Equation (A-215):

$$a_3 < \tan \theta_3 : s_3 = +1$$

$$a_3 = \tan \theta_3 : s_3 = 0$$

$$a_3 > \tan \theta_3 : s_3 = -1$$

(A-227)

## APPENDIX B

### DESIGN OF UNEQUAL ADDENDUM INVOLUTE GEAR SETS WITH STANDARD CENTER DISTANCES

One of the ways of preventing undercutting in pinions with small numbers of teeth, which must mesh with gears of unequal and larger numbers of teeth, is to decrease the pinion dedendum together with the gear addendum by the necessary amount. To maintain standard working depth for such a mesh, the addendum of the pinion as well as the dedendum of the gear are increased by the same amount. (This, of course, presupposes that the gear is not undercut by this modification.) This can be accomplished without any change in the standard base and pitch radii or the associated standard center distance by "withdrawing" the hob during the cutting of the pinion and feeding it "deeper" when the gear is cut. In this way the pinion, which has its outside radius increased by the hob withdrawal distance, will have a larger than standard circular tooth thickness at its standard pitch circle. The outside radius of the gear is decreased by the same amount. Because the cutter is fed to full depth, the gear tooth thickness at the standard pitch circle will be less than standard.

The following gives the design steps for this type of gearing and illustrates them by way of an example.

## 1. STANDARD GEAR NOMENCLATURE

- $N$  = number of teeth of gear
- $n$  = number of teeth of pinion
- $\theta$  = pressure angle
- $P_d = \frac{N}{2R_p} = \frac{n}{2r_p}$  = diametral pitch
- $P_{cs}$  = standard circular pitch at pitch circle, where also
- $$P_{cs} = \frac{\pi}{P_d}$$
- $R_p, r_p$  = pitch radii of gear and pinion, respectively
- $R_b$  =  $R_p \cos \theta$ , base circle radius of gear
- $r_b$  =  $r_p \cos \theta$ , base circle radius of pinion
- $T_{cs}, t_{cs}$  =  $\frac{P_{cs}}{2}$ , circular tooth thickness of gear and pinion,  
respectively, at standard pitch circles
- $\frac{1}{P_d}$  = standard gear addendum
- $\frac{1.157}{P_d}$  = standard gear dedendum

## 2. DETERMINATION OF HOB WITHDRAWAL DISTANCE C

Figure B-1 indicates the relationship between the pinion pitch radius,  $r_p$ , its root radius,  $r_r$ , and the rack cutter addendum  $A$ . The root radius is formed by the addendum line of the cutter tooth, so that

$$r_r = r_p - A \quad (B-1)$$

In order to avoid undercutting, the addendum line of a sharp cornered cutter must not pass below point L, the tangent point of the line of action and the base circle (see Figure B-2).

The minimum root radius,  $r_{rm}$ , becomes for this case

$$r_{rm} = r_p \cos \theta = r_p \cos^2 \theta \quad (B-2)$$

When the rack tooth corner is rounded off with a radius  $r_c$ , as shown in Figure B-3, the effective addendum line of the cutter tooth moves up the distance  $r_c(1 - \sin \theta)$ . To avoid undercutting with this type of cutter, the effective addendum line must not pass the base circle below point L in Figure B-2. This allows a reduction of the minimum allowable root radius to

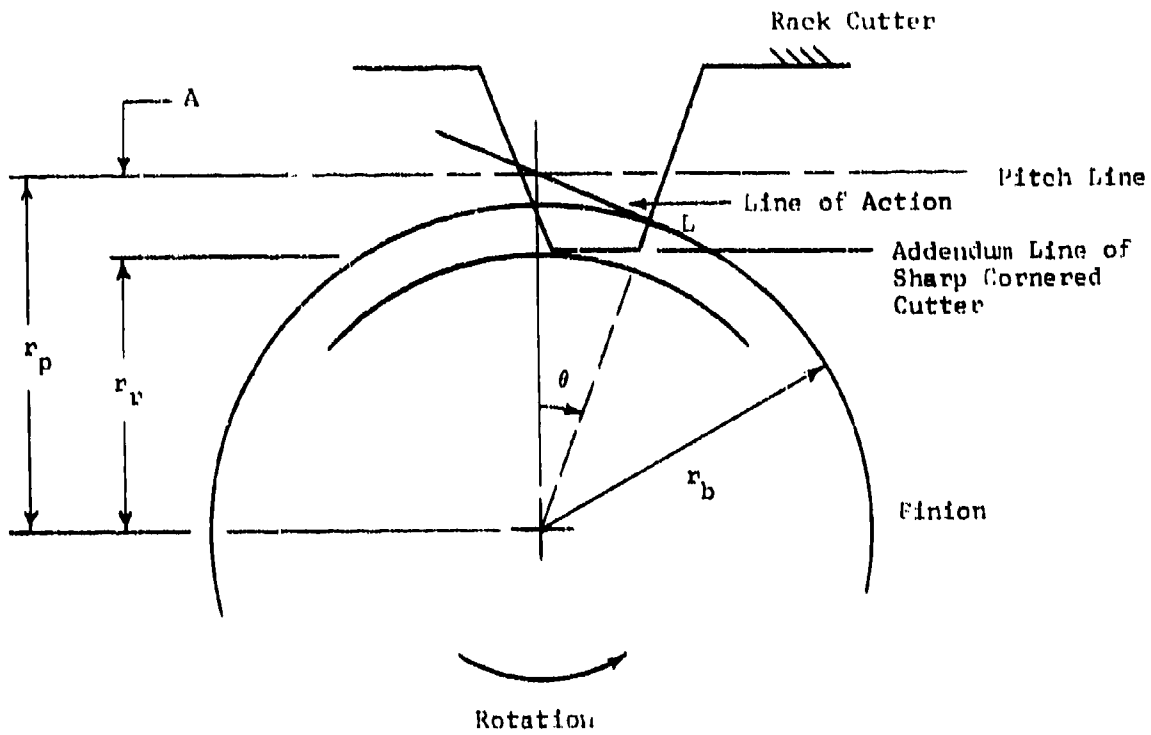


FIGURE B-1

RELATIONSHIP BETWEEN PINION PITCH RADIUS,  $r_p$ , RACK CUTTER ADDENDUM A AND RESULTING PINION ROOT RADIUS,  $r_r$

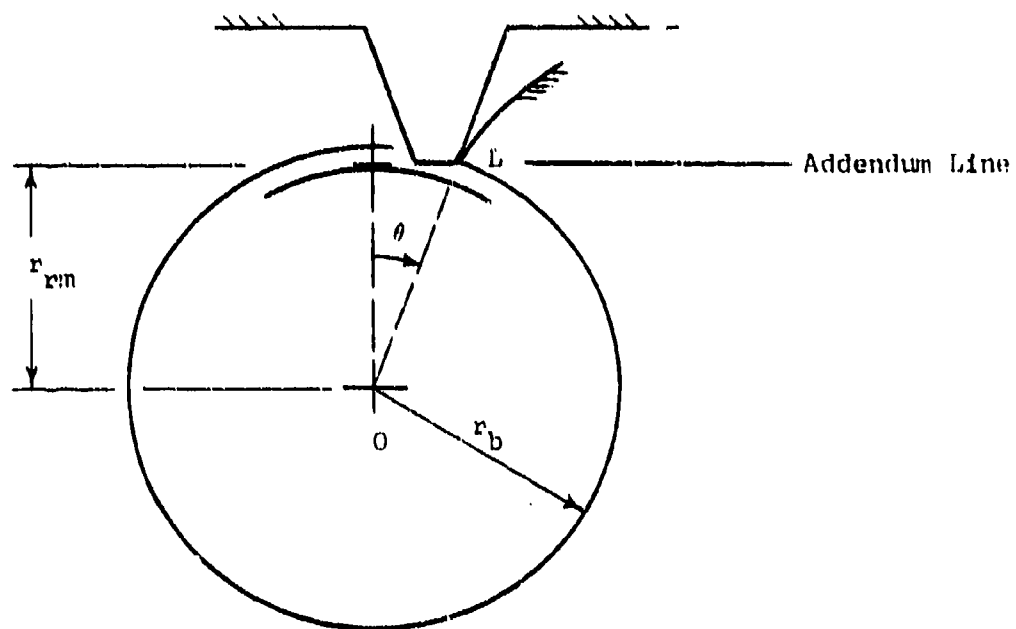


FIGURE B-2

MINIMUM ROOT RADIUS,  $r_{min}$ , FOR RACK CUTTER WITH SHARP CORNER

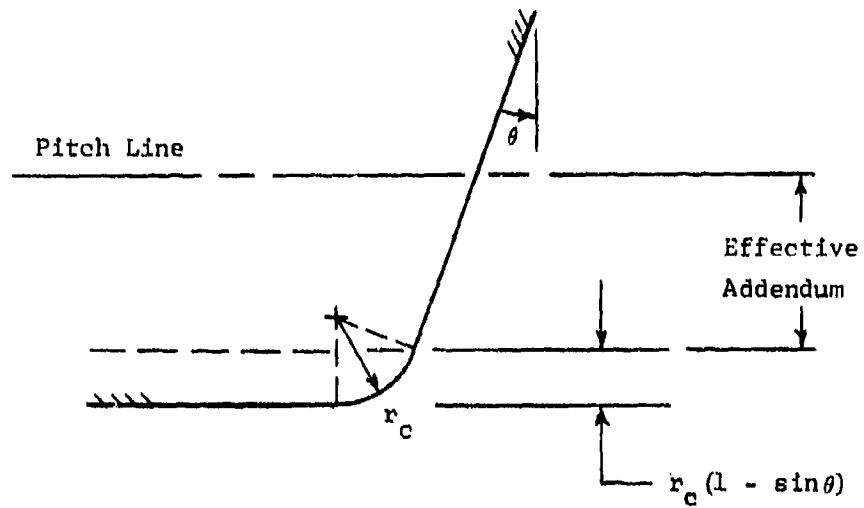


FIGURE B-3

RACK CUTTER WITH CORNER RADIUS,  $r_c$ , (EFFECTIVE ADDENDUM OF CUTTER IS DECREASED)

$$r_{rnc} = r_p \cos^2 \theta - r_c (1 - \sin \theta) \quad (B-3)$$

By common usage the corner radius may either be

$$r_c = .1 t_s = \frac{.05 \pi}{P_d}, \quad (B-4)$$

or it is chosen such that the second term in Equation (B-3) becomes

$$r_c (1 - \sin \theta) \approx \frac{.157}{P_d} \quad (B-5)$$

(This makes for an effective cutter addendum of  $1/P_d$ .)

Hob withdrawal becomes necessary if the root radius, obtained by setting the cutter to standard depth, is smaller than the minimum given by Equation (B-3). Thus, the hob withdrawal  $C$  is obtained from Equations (B-1) and (B-3), i.e.,

$$C = r_{rnc} - r_r \quad (B-6)$$

With the cutter addendum  $A = 1.157/P_d$ , and using the expression of Equation (B-4) for the rack corner radius, Equation (B-6) becomes

$$C = \frac{1}{P_d} (1 + .157 \sin \theta) - r_p \sin^2 \theta \quad (B-7)$$

If Equation (B-5) is used, with the same definition of the cutter addendum, one obtains for C

$$C = \frac{1}{P_d} - r_p \sin^2 \theta \quad (B-7)$$

### 3. OUTSIDE RADII OF PINION AND GEAR BLANKS

The outside radius of the pinion blank becomes

$$r_o = r_p + \frac{1}{P_d} + C \quad (B-8)$$

The outside radius of the gear blank becomes

$$R_o = R_p + \frac{1}{P_d} - C \quad (B-9)$$

#### 4. TOOTH THICKNESS AT PITCH CIRCLES OF PINION AND GEAR

Since the thickness of the hobtooth at the pinion pitch circle will be reduced by the amount  $2C\tan\theta$ , due to the withdrawal  $C$ , the circular thickness of the pinion tooth at this location will be increased by this amount, i.e.,

$$t_c = t_{cs} + 2C\tan\theta \quad (B-10)$$

The gear tooth thickness will be decreased to

$$T_c = T_{cs} - 2C\tan\theta \quad (B-11)$$

at its pitch circle.

## 5. TOOTH THICKNESS AT OUTSIDE AND BASE RADII BY INVOLUTOMETRY

The circular tooth thickness at an arbitrary radius of an involute tooth may be obtained if the tooth thickness, radius, and pressure angle of any other location, such as the pitch circle, are known together with the pressure angle at the arbitrary radius. [See Equation (5-5), pg. 80, E. Buckingham: Analytical Mechanics of Gears, McGraw-Hill Book Co., Inc. New York, 1949.]

Accordingly, the circular tooth thickness,  $t_o$ , at the outside radius of the pinion, may be obtained from

$$t_o = t_c \frac{r_o}{r_p} - 2r_o(\text{INV}\theta_{OP} - \text{INV}\theta) \quad (\text{B-12})$$

where

$\text{INV}\theta = \tan\theta - \theta$ , the involute function corresponding to the pressure angle  $\theta$

$\theta$  = pressure angle of mesh. This is also the pressure angle at the pitch circle.

$\theta_{OP} = \cos^{-1} \frac{r_b}{r_o}$ , the pressure angle associated with the outside radius of the pinion

Similarly, the circular tooth thickness,  $T_o$ , at the outside radius of the gear is obtained from:

$$T_o = T_c \frac{R_o}{R_p} - 2R_o(\text{INV}\theta_{OG} - \text{INV}\theta) \quad (\text{B-13})$$

where

$$\theta_{OG} = \cos^{-1} \frac{R_b}{R_o}, \text{ the pressure angle associated with the outside radius of the gear}$$

The tooth thickness at the base circle radius of the modified pinion is given by

$$t_b = t_c \cos\theta + 2r_p \text{INV}\theta \quad (\text{B-14})$$

This becomes for the gear

$$T_b = T_c \cos\theta + 2R_g \text{INV}\theta \quad (\text{B-15})$$

(The above is only of theoretical interest in case the inter-tooth space is not cut below the base circle radius.)

## 6. EXPRESSIONS FOR CONTACT RATIO AND PINION OUTSIDE RADIUS FOR

### UNITY CONTACT RATIO

The expression for contact ratio [Equation 4-19, pg. 72, E. Buckingham: Analytical Mechanics of Gears] is given by

$$m_p = \frac{\sqrt{R_o^2 - R_b^2} + \sqrt{r_o^2 - r_b^2} - (R_b + r_b)\tan\theta}{p_{cs}\cos\theta} \quad (B-16)$$

If the contact ratio of a certain mesh is larger than unity, and one wishes to reduce it to unity by reducing the outside radius of the pinion, one may find this new pinion outside radius with the help of

$$r_o' = \sqrt{r_b^2 + \left[ p_{cs}\cos\theta + (R_b + r_b)\tan\theta - \sqrt{R_o^2 - R_b^2} \right]^2} \quad (B-17)$$

7. EXAMPLE

Design a pinion and a gear with the following specifications:

$$P_d = 44, \quad N = 42, \quad n = 8, \quad \theta = 20^\circ$$

This gives

$$R_p = .47727 \text{ in. (1.212 cm)} \quad r_p = .09091 \text{ in. (.231 cm)}$$

$$R_b = R_p \cos 20^\circ = .44848 \text{ in. (1.139 cm)} \quad r_b = .08542 \text{ in. (.217 cm)}$$

$$P_{cs} = \frac{\pi}{44} = .07140 \text{ in. (.181 cm)} \quad T_{cs} = t_{cs} = .03570 \text{ in. (.091 cm)}$$

According to Equation (B-7), the hob withdrawal,  $C$ , is computed as

$$C = \frac{1}{44} - .09091 \sin^2 20^\circ = .012093 \text{ in. (.031 cm)}$$

Then, according to Equations (B-8) and (B-9)

$$r_o = .09091 + .022727 + .012093 = .12573 \text{ in. (.319 cm)}$$

$$R_o = .47727 + .022727 - .012093 = .48790 \text{ in. (1.239 cm)}$$

The new tooth thickness at the pitch radii is found with the help of Equations (B-10) and (B-11)

$$t_c = .03570 + 2(.012093)\tan 20^\circ = .04450 \text{ in. (.113 cm)}$$

$$T_c = .03570 - 2(.012093)\tan 20^\circ = .02689 \text{ in. (.068 cm)}$$

For the purposes of the present analysis, the pinion outside radius is now reduced to obtain a contact ratio of unity. With Equation (B-17)

$$r'_o = .110 \text{ in. (.279 cm)} \quad \text{This is essentially the unmodified pinion radius of } .113 \text{ in. (.287 cm).}$$

Now compute the circular tooth thickness at the outside radii  $r'_o$  and  $R_o$  using the following data in Equations (B-12) and (B-13):

$$\theta = 20^\circ \qquad \text{INV } 20^\circ = .01490$$

$$\theta_{OP} = \cos^{-1} \frac{.08542}{.110} = 39.0509^\circ \qquad \text{INV } 39.0509^\circ = .12969$$

$$\theta_{OG} = \cos^{-1} \frac{.44848}{.48790} = 23.1889^\circ \qquad \text{INV } 23.1889^\circ = .02365$$

Then

$$t_o = .04450 \left( \frac{.110}{.09091} \right) - 2(.110)(.12969 - .0149) = .02860 \text{ in. (.073 cm)}$$

and

$$T_o = .02689 \left( \frac{.4879}{.47727} \right) - 2(.4879)(.02365 - .0149) = .01896 \text{ in. (.048 cm)}$$

These are sufficient to allow for rounding off the teeth.

Finally, check that the gear is not undercut. The actual root radius of the gear is

$$R_o = \frac{2.157}{P_d} = .4879 - .04902 = .4389 \text{ in. (1.115 cm)}$$

The minimum permissible root radius without undercutting, according to Equations (B-3) and (B-4), is computed from

$$\begin{aligned} R_{rm} &= R_p \cos^2 \theta - \frac{.05\pi}{P_d} (1 - \sin \theta) = .47727(.883) - .0023 \\ &= .419 \text{ in. (1.064 cm)} \end{aligned}$$

Thus, the gear is not undercut.

## APPENDIX C

### COMPUTER MODELS FOR STEP-UP GEAR TRAINS WITH INVOLUTE TEETH

The present appendix contains descriptions, listings, and sample outputs of the following involute gear-train-related computer programs:

1. Program INVOL 1 : Design of unequal addendum involute gear and pinion set with unity contact ratio.
2. Program INVOL 2 : Point and cycle efficiencies for single pass involute step-up gear mesh with unity contact ratio.
3. Program INVOL 3 : Point and cycle efficiencies for three pass involute step-up gear train in spin environment. (All meshes have unity contact ratio).
4. Program INVOL 4 : Point and cycle efficiencies for two pass involute step-up gear train in spin environment. (All meshes have unity contact ratio).

The relevant background, the input parameters, the manner of the computations and the form of the output of each program are discussed in detail. The program proper forms the last part of each section.

1. Program INVOL 1: Design of Unequal Addendum Involute Gear  
and Pinion Set with Unity Contact Ratio.

The program INVOL 1 is based on Appendix B which shows the design equations for unequal addendum involute gear sets with standard center distances.

The nomenclature of the program is chosen to coincide as much as possible with that of Appendix B.

a. Input Parameters (See also Program INVOL 1, below)

The following parameters represent the input data of the program:

PSUBD     -      $P_d$  , the diametral pitch  
NG         -      $N_G$  , the number of teeth of the gear  
NP         -      $N_P$  , the number of teeth of the pinion  
THETAD    -      $\theta$  , the pressure angle of the mesh as well as  
            of the hob (in degrees)  
ISTOP      -     arbitrary single-digit integer for multiple data  
            sets. Must be zero for last set of data.

b. Computations

The program computes the following quantities (where not otherwise indicated, consult Section 1 of Appendix B for nomenclature):

CAPRP      -      $R_p$   
RP         -      $r_p$   
CAPRB      -      $R_b$   
RB         -      $r_b$

PSUBC	-	$p_c$
TSTAND	-	$t_{cs}$
C	-	hob withdrawal distance. See eq (B-7)
RO	-	$r_o$ , See eq (B-8). This is the original pinion blank radius.
CAPRO	-	$R_o$ , see eq (B-9)
TC	-	$t_o$ , see eq (B-10)
CAPTC	-	$T_o$ , see eq (B-11)
TB	-	$t_b$ , see eq (B-14). Note also the computation of the involute function at the end of the program.
CAPTB	-	$T_b$ , see eq (B-15)
ROFIN	-	$r'_o$ , see eq (B-17). This is the pinion outside radius for unity contact ratio.
THETOG	-	$\theta_{OG}$ , according to expression associated with eq (B-13)
THETOP	-	$\theta_{OP}$ , according to expression associated with eq (B-12)
CAPTO	-	$T_o$ , see eq (B-13)
TO	-	$t_o$ , see eq (B-12). Computed with ROFIN.
CRATIO	-	$m_p$ , see eq (B-16). This is the original contact ratio, which uses the unmodified pinion blank radius RO.
CRFIN	-	represents the contact ratio when computed with the final pinion blank radius ROFIN.
ROOT	-	actual root radius of pinion
CAPROOT	-	actual root radius of gear
CAPRMIN	-	$R_{rm}$ , see equations (B-3) and (B-4)

c. Output of Program

The output of the program is best explained by means of the first sample computations which are shown at the end of the program. This example is identical with that given in section 7 of Appendix B. The output lists the following:

I. The input parameters, PSUBD, NG, NP, and pressure angle, THETAD, are printed out.

II. The above is followed by computational results for

CAPRP

RP

CAPRB

TSTAND

C

CAPRO

RO, this is the original pinion blank radius before the unity contact ratio modification.

CRATIO, note that for the given case, this original contact ratio equals 1.3

ROFIN, the pinion outside radius which corresponds to unity contact ratio

CRFIN, this, of course, has to be unity because of the use of ROFIN. This computation serves as a check.

CAPTC, this tooth thickness, as well as the following one, is useful for strength computations

TC

THEOGD, this pressure angle, as well as the following one, corresponds to the final outside radii of the gear and pinion, respectively, and is needed for the computations of the tooth thicknesses at the outside radii

THEOPD

CAPTO, this tooth thickness at the outside radius of the gear, as well as the following one for the pinion, must be sufficiently large to allow for the presence of a tip radius

TO

CAPTB

TB

CAPROOT

ROOT

CAPRMIN

The values of the last five parameters are to some extent interconnected. First, it is important to see whether the gear is undercut. This does not occur as long as CAPROOT is larger than CAPRMIN, i.e., the actual root radius is larger than the minimum allowable one. The gear tooth thickness at the base circle is of interest for strength purposes. Since, for the given case, CAPRB = .44849 in. (1.139 cm) and CAPROOT = .4388 in. (1.115 cm) the base circle lies above the root circle, and the greatest cross-section of the tooth is approximately equal to CAPTB. TB is called the theoretical

pinion tooth thickness at the base circle since it is possible that the base circle lies below the minimum allowable root circle of the pinion. In such a case, the actual tooth may be weaker than indicated by this dimension. For the present case,  $RB = .08543$  in. (.217 cm) and  $ROOT = .07671$  in. (.195 cm), and therefore, the base circle, which lies above the root circle, gives a good indication of the actual tooth cross-section at the root.

Program INVOL 1

This program contains five different sets of gears. This will be of use in programs INVOL 2, INVOL 3 and INVOL 4.

```

1      PROGRAM INVOL 1 (INPUT,OUTPUT,TAPES=INPUT,TAPE6=OUTPUT)

```

```

C      DESIGN OF UNEQUAL ADDENDUM INVOLUTE GEAR AND PINION SET
C      WITH UNITY CONTACT RATIO

```

```

5      REAL*INV

```

```

1      READ(5,2)PSUBD,NG,MP,THETAD,ISTOP
2      FORMAT(F10.4,2I10.4,10.4,9X,11)

```

```

10     PI = 3.14159

```

```

2      Z = PI/180.

```

```

      THETA = THETAD*Z

```

```

      CAPRP = NG/(2.*PSUBD)

```

```

      RP = NP/(2.*PSUBD)

```

```

      CAPRB = CAPRP*COS(LHETA)

```

```

      RB = RP*COS(LHETA)

```

```

      PSUBC = PI/PSUBD

```

```

      TSTAND = PSUBC/2.

```

```

      C = 1./PSUBD - RP*SIN(THETA)*SIN(THETA)

```

```

      CAPRO = CAPRP + 1./PSUBD - C

```

```

      RO = RP - 1./PSUBD - C

```

```

      CAPTC = TSTAND - 2.*C*TAN(LHETA)

```

```

      IC = TSTAND - 2.*C*TAN(LHETA)

```

```

      CAPTB = CAPTC*COS(LHETA) + 2.*CAPRB*INV(THETA)

```

```

      IB = IC*COS(THETA) - 2.*RB*INV(THETA)

```

```

      ROFIN = SORT(RB*RB + (PSUBC*COS(THETA) + (CAPRB + RB)*TAN(THETA)

```

```

1      - SORT((CAPRO+CAPRO - CAPRB*CAPRB)*2)

```

```

      THEOG = ACOS(CAPRB/CAPRO)

```

```

      THEOG = THEOG/Z

```

```

      THEOP = ACOS(RB/ROFIN)

```

```

      THEOPD = THEOP//

```

```

      CAPTO = CAPTC*CAPRO/CAPRB - 2.0*CAPRO*(INV(THETOG) - INV(THETA))

```

```

      IO = IC*ROFIN/RO - 2.*ROFIN*INV(THETOP) - INV(THETA)

```

```

      CRATIO = (SORT(CAPRO*CAPRO - CAPRB*CAPRB) + SORT(RO*RO - RB*RB)

```

```

1      - (CAPRB + RB)*TAN(THETA))/(PSUBC*COS(THETA))

```

```

      CRFIN = (SORT((CAPRO+CAPRO - CAPRB*CAPRB) + SORT(ROFIN*ROFIN

```

```

1      - RB*RB) - (CAPRB + RB)*TAN(THETA))/(PSUBC*COS(THETA))

```

```

      ROOT = RO - 2.157/PSUBD

```

```

      CAPROOI = CAPRO - 2.157/PSUBD

```

```

      CAPRMN = CAPRP*COS(THETA)*COS(THETA) - .05*PI*(1. - SIN(THETA))/

```

```

1      PSUBD

```

```

      WRITE(6,3)PSUBD,NG,MP,THETAD

```

```

3      FORMAT(10I10,10F10.4,10.4,9X,11)

```

```

16     **F9.5**PINION NUMBER OF TEETH (MP) =.13/*OPRESSURE ANGLE (THE

```

```

21A) **F6.2)

```

```

45     WRITE(6,4)CAPRP,RP

```

```

4      FORMAT(10GEAR PITCH RADIUS (CAPRP) =.F9.5,3X,PINION PITCH RADIUS

```

```

1      (RP) =.F9.5)

```

```

      WRITE(6,5)CAPRB,RB

```

```

5      FORMAT(10GEAR BASE RADIUS (CAPRB) =.F9.5,3X,PINION BASE RADIUS (

```

```

1      RB) =.F9.5)

```

```

      WRITE(6,6)TSTAND

```

```

6      FORMAT(10STANDARD TOOTH THICKNESS AT PITCH RADII (TSTAND) =.F9.5)

```

```

      WRITE(7,7)C

```

74/74 - OPT=1

FUNCTION INV

REAL FUNCTION INV(META)  
INV = JAN(META) -- META  
RETURN  
END

55 / FORMAT(0H08 WITHDRAWAL DISTANCE (C) =%F8.5)  
WRITE(6,8)CAPRO,HO

8 FORMAT(0GEAR BLANK RADIUS (CAPRO) =%F9.5,3X,0ORIGINAL PINION 0LA  
LWK RADIUS (RO) =%F9.5)

60 WRITE(6,9)CRATIO  
Y FORMAT(00ORIGINAL CONTACT RATIO (CRATIO) =%F6.3)  
WRITE(6,10)ROFIN

10 FORMAT(0PINION OUTSIDE RADIUS FOR UNITY CONTACT RATIO (ROFIN) =%  
F9.5)  
WRITE(6,11)CRFIN

11 FORMAT(0FINAL CONTACT RATIO (CRFIN) =%F6.3)  
WRITE(6,12)CAPTC,TC

65 12 FORMAT(0GEAR TOOTH THICKNESS AT PITCH CIRCLE (CAPTC) =%F9.5,3X,  
1PINION TOOTH THICKNESS AT PITCH CIRCLE (TC) =%F8.5)

70 WRITE(6,13)THEOD,THEOPD  
13 FORMAT(0GEAR PRESSURE ANGLE AT OUTSIDE RADIUS (THEOD) =%F9.5,  
13X,0PINION PRESSURE ANGLE AT FINAL OUTSIDE RADIUS (THEOPD) =%

F9.5)  
WRITE(6,14)CAPTO,TO

14 FORMAT(0GEAR TOOTH THICKNESS AT OUTSIDE RADIUS (CAPTO) =%F8.5,  
13X,0PINION TOOTH THICKNESS AT FINAL OUTSIDE RADIUS (TO) =%F8.5)

75 WRITE(6,15)CAPTB,TB  
15 FORMAT(0GEAR TOOTH THICKNESS AT BASE CIRCLE (CAPTB) =%F8.5,3X,  
1THEORETICAL PINION TOOTH THICKNESS AT BASE CIRCLE (TB) =%F8.5)

WRITE(6,16)CAPROOT,CAPRMIN  
16 FORMAT(0RADIUS OF ROOT CIRCLE OF GEAR (CAPROOT) =%F8.5,3X,  
1MINIMUM ALLOWABLE RADIUS OF ROOT CIRCLE OF GEAR (CAPRMIN) =%F8.5

80 2)  
IF (CAPROOT .GE. CAPRMIN)WRITE(6,17)

IF (CAPROOT .LT. CAPRMIN)WRITE(6,18)  
17 FORMAT(0THE GEAR IS NOT UNDERCUT\*)

85 18 FORMAT(0THE GEAR IS UNDERCUT\*)  
WRITE(6,19)ROOT

19 FORMAT(0RADIUS OF ROOT CIRCLE OF PINION (ROOT) =%F8.5)  
IF (ISTOP .EQ. 0)GO TO 9999

90 GO TO 1  
9999 STOP  
END

0 10

DIAMETRIC PITCH (PSUDO) = 44.00

GEAR NUMBER OF TEETH (NB) = 42

PINION NUMBER OF TEETH (NP) = 8

PRESSURE ANGLE (PFA) = 20.00

GEAR PITCH RADIUS (CRPW) = .37727 PINION PITCH RADIUS (RP) = .09051

GEAR BASE RADIUS (CRPB) = .34889 PINION BASE RADIUS (RPB) = .08243

STANDARD TOOTH THICKNESS AT PITCH RADII (DISTAND) = .87570

FOR WITHDRAWAL DISTANCE (C) = .91289

GEAR BLANK RADIUS (CRB) = .34741 ORIGINAL PINION BLANK RADIUS (RBO) = .12573

ORIGINAL CONTACT RATIO (CAR10) = 1.242

PINION OUTSIDE RADIUS FOR UNITY CONTACT RATIO (RPOUK) = .11000

FINAL CONTACT RATIO (CARFIN) = 1.098

GEAR TOOTH THICKNESS AT HIGH CIRCLE (CARHC) = .02498 PINION TOOTH THICKNESS AT PINION CIRCLE (IC) = .04450

GEAR PRESSURE ANGLE AT OUTSIDE RADIUS (THEO00) = 23.18094 PINION PRESSURE ANGLE AT FINAL OUTSIDE RADIUS (THEO0N) = 39.05893

GEAR TOOTH THICKNESS AT OUTSIDE RADIUS (CAR00) = .01594 PINION TOOTH THICKNESS AT FINAL OUTSIDE RADIUS (IC0) = .02868

GEAR TOOTH THICKNESS AT BASE CIRCLE (CAR10) = .03164 THEORETICAL PINION TOOTH THICKNESS AT BASE CIRCLE (IB) = .04437

RADIUS OF ROOT CIRCLE OF GEAR (CARR00) = .43005 MINIMUM ALLOWABLE RADIUS OF ROOT CIRCLE OF GEAR (CARBMIN) = .41909

THE GEAR IS NOT UNDERCUT

RADIUS OF ROOT CIRCLE OF PINION (RPO0) = .07571

DIAMETRAL PITCH (IN) = 65.00  
GEAR NUMBER OF PITCH (NO) = 27  
PITCH NUMBER OF TEETH (NP) = 9  
PRESSURE ANGLE (T-P/A) = 20.00  
TEETH PITCH RADIUS (CAPR) = .20769 PINION PITCH RADIUS (RP) = .06923  
GEAR BASE RADIUS (CRBT) = .19217 PINION BASE RADIUS (RB) = .06586  
STANDARD TOOTH THICKNESS AT PITCH RADIUS (STAND) = .62417  
ADD ADDITIONAL DISTANCE (C) = .00729  
GEAR BEAM RADIUS (CRB) = .21579 ORIGINAL PINION BEAM RADIUS (RO) = .03199  
ORIGINAL CONTACT RATIO (CRATIO) = 1.371  
PINION OUTSIDE RADIUS FOR UNIT CONTACT RATIO (ROF1) = .04009  
PINION CONTACT RATIO (CR1) = 1.000  
GEAR TOOTH THICKNESS AT PITCH CIRCLE (CRP1) = .01666 PINION TOOTH THICKNESS AT PINION CIRCLE (IC1) = .02067  
GEAR PRESSURE ANGLE AT OUTSIDE RADIUS (THEO1) = 25.25332 PINION PRESSURE ANGLE AT FINAL OUTSIDE RADIUS (THEO2) = 36.85942  
GEAR TOOTH THICKNESS AT OUTSIDE RADIUS (CRP2) = .01267 PINION TOOTH THICKNESS AT FINAL OUTSIDE RADIUS (IC2) = .02024  
GEAR TOOTH THICKNESS AT BASE CIRCLE (CRB1) = .02754 THEORETICAL PINION TOOTH THICKNESS AT BASE CIRCLE (IB1) = .02963  
RADIUS OF ROOT CIRCLE OF GEAR (CRRO1) = .18261 MINIMUM ALLOWABLE RADIUS OF ROOT CIRCLE OF GEAR (CARMIN) = .10101  
THE GEAR IS NOT INTERFERED  
RADIUS OF ROOT CIRCLE OF PINION (RRO1) = .05472

GEOMETRICAL PITCH (PSUBOT) = 77.80

GEAR NUMBER OF PETH (NBT) = 27

PINION NUMBER OF PETH (NPT) = 9

PRESSURE ANGLE (THETA) = 20.00

GEAR PITCH RADIUS (CAPRT) = .17532 PINION PITCH RADIUS (RPT) = .05944

GEAR BASE RADIUS (CAPRB) = .16479 PINION BASE RADIUS (RBT) = .05492

STANDARD TOOTH THICKNESS AT PITCH RADIUS (TS1AND) = .02940

TOOTH WITHDRAWAL DISTANCE (D) = .00015

GEAR BEAM RADIUS (CAPBC) = .10210 ORBITAL PINION BEAM RADIUS (RBO) = .01750

ORIGINAL CONTACT RATIO (CRATIO) = 1.371

PINION OUTSIDE RADIUS FOR UNITY CONTACT RATIO (ROFTN) = .04020

FINAL CONTACT RATIO (CAPFIN) = 1.900

GEAR TOOTH THICKNESS AT PITCH CIRCLE (CAPFC) = .01592 PINION TOOTH THICKNESS AT PITCH CIRCLE (FC) = .02488

GEAR PRESSURE ANGLE AT OUTSIDE RADIUS (THCOSH) = 25.25382 PINION PRESSURE ANGLE AT FINAL OUTSIDE RADIUS (THCOPH) = 36.45992

GEAR TOOTH THICKNESS AT OUTSIDE RADIUS (CAPTO) = .01976 PINION TOOTH THICKNESS AT FINAL OUTSIDE RADIUS (THO) = .01710

GEAR TOOTH THICKNESS AT BASE CIRCLE (CAPTB) = .01907 THEORETICAL PINION TOOTH THICKNESS AT BASE CIRCLE (TBL) = .02501

RADIUS OF ROOT CIRCLE OF GEAR (CAPROCT) = .15815 MINIMUM ALLOWABLE RADIUS OF ROOT CIRCLE OF GEAR (CAPRMIN) = .15347

THE GEAR IS NOT UNDERST

RADIUS OF ROOT CIRCLE OF PINION (ROOFT) = .04957

DIAMETRAL PITCH (PCURD) = 44.00

GEAR NUMBER OF PETH (NG) = 56

PINION NUMBER OF TEEH (NP) = 8

PRESSURE ANGLE (PETA) = 20.00

GEAR PITCH RADIUS (CAPM) = .63636 PINION PITCH RADIUS (AP) = .09891

GEAR BASE RADIUS (CAPMB) = .59799 PINION BASE RADIUS (BP) = .08943

STANDARD TOOTH THICKNESS AT PITCH RADIUS (SIAND) = .03570

MOD WITHORAL D-TANCE (C) = .01209

GEAR BLANK RADIUS (CAPMD) = .04700 ORIGINAL PINION BLANK RADIUS (RO) = .12573

ORIGINAL CONTACT RATIO (CRATIO) = 1.349

PINION OUTSIDE RADIUS FOR UNITY CONTACT RATIO (ROFIN) = .10970

FINAL CONTACT RATIO (CNFIN) = 1.000

GEAR TOOTH THICKNESS AT PITCH CIRCLE (CAPIC) = .02690 PINION TOOTH THICKNESS AT PITCH CIRCLE (PC) = .04450

GEAR PRESSURE ANGLE AT OUTSIDE RADIUS (INCOD) = 22.04455 PINION PRESSURE ANGLE AT FINAL OUTSIDE RADIUS (THEOD) = 30.85337

GEAR TOOTH THICKNESS AT OUTSIDE RADIUS (CAPID) = .01991 PINION TOOTH THICKNESS AT FINAL OUTSIDE RADIUS (TO) = .02901

GEAR TOOTH THICKNESS AT BASE CIRCLE (CAPTB) = .04310 THEORETICAL PINION TOOTH THICKNESS AT BASE CIRCLE (TB) = .04437

RADIUS OF ROOT CIRCLE OF GEAR (CAPROO) = .59798 MINIMUM ALLOWABLE RADIUS OF ROOT CIRCLE OF GEAR (CAPRMIN) = .55957

THE GEAR IS NOT UNDERCUT

RADIUS OF ROOT CIRCLE OF PINION (ROO) = .07671

DIAMETRAL PITCH (PSUBD) = 65.00  
 GEAR NUMBER OF TEETH (NG) = 56  
 PINION NUMBER OF TEETH (NP) = 8  
 PRESSURE ANGLE (THETA) = 20.00  
 GEAR PITCH RADIUS (CAPHP) = .43677 PINION PITCH RADIUS (RP) = .06154  
 GEAR BASE RADIUS (CAPRB) = .40479 PINION BASE RADIUS (RB) = .05783  
 STANDARD TOOTH THICKNESS AT PITCH RADIUS (ISTAND) = .02417  
 HOB WITHDRAWAL DISTANCE (C) = .00619  
 GEAR BLANK RADIUS (CAPBO) = .43797 ORIGINAL PINION BLANK RADIUS (RBO) = .06511  
 ORIGINAL CONTACT RATIO (CRATIO) = 1.349  
 PINION OUTSIDE RADIUS FOR UNITY CONTACT RATIO (ROFIN) = .07426  
 FINAL CONTACT RATIO (CFIN) = 1.008  
 GEAR TOOTH THICKNESS AT PITCH CIRCLE (CAPIC) = .01821 PINION TOOTH THICKNESS AT PITCH CIRCLE (IC) = .03012  
 GEAR PRESSURE ANGLE AT OUTSIDE RADIUS (THEOOP) = 22.44465 PINION PRESSURE ANGLE AT FINAL OUTSIDE RADIUS (TO) = .01464  
 GEAR TOOTH THICKNESS AT OUTSIDE RADIUS (CAPLO) = .01287 PINION TOOTH THICKNESS AT FINAL OUTSIDE RADIUS (TO) = .01464  
 GEAR TOOTH THICKNESS AT BASE CIRCLE (CAPTB) = .02918 THEORETICAL PINION TOOTH THICKNESS AT BASE CIRCLE (TB) = .03003  
 RADIUS OF ROOT CIRCLE OF GEAR (CAPROOT) = .49478 MINIMUM ALLOWABLE RADIUS OF ROOT CIRCLE OF GEAR (CAPRMIN) = .37879  
 THE GEAR IS NOT UNDERCUT  
 RADIUS OF ROOT CIRCLE OF PINION (RROOT) = .05192

2. Program INVOL 2: Point and Cycle Efficiencies for Single  
Pass Involute Step-Up Gear Mesh With  
Unity Contact Ratio

The program INVOL 2 is based on section 3 of Appendix A, which gives the moment input-output relationship for a single step-up gear mesh with involute teeth. The mesh has unity contact ratio. Again, the nomenclature of the program is chosen to coincide as much as possible with that of the original derivation. The contact geometry is adapted from section 6c of Appendix A.

a. Input Parameters (See also program in section d below)

The following parameters represent the input data of the program. Most of these are taken from the results of INVOL 1 since the moment expressions are for unity contact ratio only.

CAPRP =  $R_p$ , the pitch radius of the gear

RP =  $r_p$ , the pitch radius of the pinion

CAPRO =  $R_o$ , the outside radius of the gear

ROFIN =  $R'_o$ , see eq. (B-17). This is the pinion outside radius  
for unity contact ratio.

RHOCAPN =  $\rho_N$ , the pivot radius of the gear

RHON =  $\rho_N$ , the pivot radius of the pinion

MU =  $\mu$ , the coefficient of friction at both pivots as well as  
at the gear and pinion contact point

K, range divisor, i.e., it represents the number of times the  
output moment and the efficiency are computed between  
initial and final contact of the gear and the pinion

ISTOP, arbitrary single digit for multiple data sets. It must be zero for the last set of data.

b. Computations

Both point and cycle efficiencies are based on eq. (A-25). With the help of eq. (3), the point efficiency becomes

$$\epsilon_p = \frac{\{r_b - \mu [r_n + s(d-a)]\}}{\{R_b + \mu [r_N - sa]\}} \frac{\dot{\psi}}{\dot{\phi}} \quad (C-1)$$

Since the angular velocity is constant for involute gears, and may be expressed in terms of the base circle radii  $R_b$  and  $r_b$ ,

$$K_{ratio} = \frac{\dot{\psi}}{\dot{\phi}} = \frac{R_b}{r_b} \quad (C-2)$$

Therefore,

$$\epsilon_p = E_2 \quad (\text{POINTEF}) \quad (C-3)$$

as given by eq. (A-26).

The cycle efficiency expression is based on eq. (4). If one replaces both integrals by summations, one obtains

$$\epsilon_c = \frac{\sum M_o \Delta\psi}{\sum M_{in} \Delta\phi} \quad (C-4)$$

where  $\Delta\phi$  and  $\Delta\psi$  now represent incremental changes in the input and output angles, respectively. The input moment is constant

over the total interval. Also

$$\Sigma \Delta \varphi = \alpha_{FIN} - \alpha_{IN} \quad (C-5)$$

(See eqs. (A205) and (A206).)

The increment  $\Delta \psi$  is also constant and may therefore be taken outside the summation sign. It is expressed with the help of  $\Delta \varphi$

$$\Delta \psi = \Delta \alpha = \frac{\alpha_{FIN} - \alpha_{IN}}{K} = \text{DELALPH} \quad (C-6)$$

(This is an adaptation of eq. (A-207) to the single step-up mesh.)

With the above

$$\Delta \psi = K_{\text{ratio}} \Delta \alpha \quad (C-7)$$

Substitution into eq. (C-4) gives

$$\epsilon_o = \frac{K_{\text{ratio}} \Delta \alpha \Sigma M_o}{M_{in} (\alpha_{FIN} - \alpha_{IN})} \quad (C-8)$$

Since

$$\epsilon_p = K_{\text{ratio}} \frac{M_o}{M_{in}} \quad (C-9)$$

one obtains for the cycle efficiency

$$\epsilon_o = \frac{\Delta \alpha \Sigma \epsilon_p}{(\alpha_{FIN} - \alpha_{IN})} \quad (\text{CYCLEFF}) \quad (C-10)$$

To arrive at expressions for both POINTEF and CYCLEFF in the program, the following other important computations are necessary:

$$\text{ALPHIN} = \alpha_{\text{IN}}, \text{ see eq. (A-205)}$$

$$\text{ALPHFIN} = \alpha_{\text{FIN}}, \text{ see eq. (A-206)}$$

$$D = d, \text{ see eq. (A-204)}$$

$$A = a, \text{ see eq. (A-203)}$$

The signum value  $s$  is obtained according to eqs. (A-215) and (A-216), which are alternate ways of expressing eqs. (A-6) to (A-8).

c. Output of Program (see Program INVOL 2, below)

The output of the program is best explained by means of the single sample computation which is shown at the end of the program. This example uses the data of the first sample output of INVOL 1. The output lists the following:

I. Input Parameters

The input parameters CAPRP, RP, CAPRO, RO and THETAD are reproduced. In addition, the following dimensions, which were selected from a practical viewpoint, are shown:

$$\text{RHOCAPN} = \rho_M = .060 \text{ in. (.152 cm)}$$

$$\text{RHON} = \rho_n = .030 \text{ in. (.076 cm)}$$

$$\text{MU} = \mu = .2$$

$$K = 25 \quad (\text{no substantial changes in cycle efficiency were encountered for larger values of } K)$$

## II. Computed Values

The point efficiency is listed as a function of the angle  $\alpha$ , while the cycle efficiency is computed for the interval from  $\alpha_{IN}$  to  $\alpha_{FIN}$ . The signum parameter,  $s$ , is listed for checking purposes.

Program INVOL 2

C-21



GEAR PITCH RADIUS (CARPP) = .47727 PINION PITCH RADIUS (RPI) = .09001  
GEAR OUTSIDE RADIUS (CARPO) = .49791 PINION OUTSIDE RADIUS FOR UNITY CONTACT RATIO (RPSIM) = .11000

POSSURE ANGLE IN DEGREES (THETA) = 20.00

GEAR PIVOT RADIUS (RHOCAON) = .040 PINION PIVOT RADIUS (RHON) = .030

COEFFICIENT OF FRICTION (MU) = .20

RANGE DIVISOR (K) = 25

ALPHAD = 15.07	S = 1.0	POINTEF = .7905
ALPHAD = 16.72	S = 1.0	POINTEF = .7979
ALPHAD = 18.66	S = 1.0	POINTEF = .8054
ALPHAD = 20.34	S = 1.0	POINTEF = .8129
ALPHAD = 21.34	S = 1.0	POINTEF = .8204
ALPHAD = 22.69	S = 1.0	POINTEF = .8279
ALPHAD = 24.63	S = 1.0	POINTEF = .8355
ALPHAD = 26.37	S = 1.0	POINTEF = .8430
ALPHAD = 28.72	S = 1.0	POINTEF = .8506
ALPHAD = 30.06	S = 1.0	POINTEF = .8582
ALPHAD = 32.46	S = 1.0	POINTEF = .8658
ALPHAD = 34.75	S = 1.0	POINTEF = .8735
ALPHAD = 36.89	S = 1.0	POINTEF = .8811
ALPHAD = 39.63	S = 1.0	POINTEF = .8888
ALPHAD = 42.77	S = 1.0	POINTEF = .8965
ALPHAD = 46.12	S = 1.0	POINTEF = .9042
ALPHAD = 49.66	S = 1.0	POINTEF = .9100
ALPHAD = 53.40	S = 1.0	POINTEF = .9153
ALPHAD = 57.15	S = 1.0	POINTEF = .9206
ALPHAD = 61.69	S = 1.0	POINTEF = .9260
ALPHAD = 66.83	S = 1.0	POINTEF = .9314
ALPHAD = 72.17	S = 1.0	POINTEF = .9367
ALPHAD = 77.52	S = 1.0	POINTEF = .9401
ALPHAD = 83.96	S = 1.0	POINTEF = .9435
ALPHAD = 90.20	S = 1.0	POINTEF = .9470

CYCLE EFFICIENCY = .8566

3. Program INVOL 3: Point and Cycle Efficiencies for Three  
Pass Involute Step-Up Gear Train in  
Spin Environment (All Meshes Have Unity  
Contact Ratio)

The program INVOL 3 is based on section 4 of Appendix A, which derives the moment input-output relationship for a three pass step-up gear train operating in a spin environment. Again, all meshes have unity contact ratio. As previously, the nomenclature of the program is chosen to coincide as closely as possible with that of the original derivations. The expressions for the contact geometry and other auxiliary geometric terms may be found in section 6 of Appendix A.

a. Input Parameters (see Program INVOL 3, below)

The following parameters represent the input data for the program. Those which involve gear dimensions only must be obtained from the results of INVOL 1 since the moment expressions are derived for unity contact ratio only.

MU =  $\mu$ , the coefficient of friction at all pivots and at  
all tooth contact points

RPM, revolutions per minute of the fuze body

CAPRP1 =  $R_{p1}$

CAPRP2 =  $R_{p2}$

CAPRP3 =  $R_{p3}$

RP2 =  $r_{p2}$

RP3 =  $r_{p3}$

RP4 =  $r_{p4}$

THETA1 =  $\theta_1$

THETA2 =  $\theta_2$

THETA3 =  $\theta_3$

ISTOP, arbitrary single digit integer for multiple data set.

It must be zero for last set of data.

R1 =  $R_1$

R2 =  $R_2$

R3 =  $R_3$

R4 =  $R_4$

RHO1 =  $\rho_1$

RHO2 =  $\rho_2$

RHO3 =  $\rho_3$

RHO4 =  $\rho_4$

CAPRB1 =  $R_{b1}$

CAPRB2 =  $R_{b2}$

CAPRB3 =  $R_{b3}$

RB2 =  $r_{b2}$

RB3 =  $r_{b3}$

RB4 =  $r_{b4}$

CAPRO1 =  $R_{o1}$

CAPRO2 =  $R_{o2}$

CAPRO3 =  $R_{o3}$

RO2 =  $r'_{o2}$

RO3 =  $r'_{o3}$

RO4 =  $r'_{o4}$

M1 =  $m_1$ , mass of input gear 1

M2 =  $m_2$ , mass of gear and pinion 2

- $M_3 = m_3$ , mass of gear and pinion 3  
 $M_4 = m_4$ , mass of pinion 4  
 $MD = md^2$ , the "mass-distance" product contained in the expression  
for the input moment  $M_{in}$   
 $K = K_3$ , the range divisor which is associated with gear 3,  
the driving gear of the last mesh (see eq. (A-211))

b. Computations (see COMMENT cards in program)

I. Computation of MIN, GAMMAS and BETAS

To start with, the program computes the input moment

$$MIN = M_{in} = md^2 \omega^2 \quad (C-11)$$

Subsequently, the angles  $\gamma_2, \gamma_3, \gamma_4$  and  $\beta_1, \beta_2, \beta_3$  are established according to the expressions given in section 6b of Appendix A.

II. Determination of Gear Train Constants

The determination of the gear train constants consists of the following:

RATIO =  $K_{ratio}$ . (see eq. (2)). Since the angular velocity is constant, this parameter may be expressed in terms of the applicable base radii, i.e.,

$$\frac{R_{b1} \times R_{b2} \times R_{b3}}{r_{b2} \times r_{b3} \times r_{b4}}$$

TEST1, TEST2 and TEST3 represent the tangent functions of the mesh pressure angles, which are used in conjunction with the values of the signum functions, s.

D1, D2 and D3 are given by eqs. (A-204), (A-217) and (A-223), respectively, and represent the distances between the points of tangency to the base circles along the lines-of-action of the three meshes.

MTOT = 0 represents the initialization of the sum of the output moments. This is used for the determination of the cycle efficiency.

### III. Determination of Initial and Final Values of ALPHAS, Initialization of ALPHAS and Centrifugal Forces

The determination of the initial and final angles of rotation is accomplished with the help of subroutine ALPHA, at the end of the program, which makes use of eqs. (A-205), (A-206), (A-218), (A-219), (A-224) and (A-225). Thus, the initial values of the individual angles of rotation, ALPHA1, ALPHA2 and ALPHA3 are represented by AL1IN, AL2IN and AL3IN, while the final angles are given by AL1FIN, AL2FIN and AL3FIN.

The angular increments of gears 3, 2 and 1, i.e., DELAL3, DELAL2 and DELAL1, are determined with the help of eqs. (A-211) - (A-213), respectively.

The centrifugal forces, which act on the pivots of the various gear and/or pinion assemblies, are obtained by way of eqs. (A-33), (A-57), (A-84) and (A-107).

### IV. Point and Cycle Efficiencies (See "output moment" in PROGRAM)

Both point and cycle efficiencies are based on eq. (A-125) for the output moment  $MO4 = M_{O4}$ .

The point efficiency is computed directly in the manner of eq. (3), i.e.,

$$\eta_p = K_{ratio} \frac{M_{O4}}{M_{in}} = \text{POINTEP} \quad (\text{C-12})$$

The cycle efficiency is treated in the manner of eq. (C-8), i.e.,

$$\eta_p = \frac{K_{ratio} \Delta \alpha_1 \Sigma M_{O4}}{M_{in} (\alpha_{1FIN} - \alpha_{1IN})} = \text{CYCLEFF} \quad (\text{C-13})$$

The program gives the summation as

$$MTOT = \Sigma M_{O4} \quad (\text{C-14})$$

#### V. Gear Train Motion Model

The simulation of the gear train motion, which is necessary for the computation of both POINTEP and CYCLEFF, is found in a loop which starts with statement label no. 14 (card no. 116) and ends with card no. 199. As discussed earlier, the motions of the individual driving gears are initialized at their respective angles, AL1IN, AL2IN and AL3IN. (This starting of the total train is arbitrary and is done only for convenience. There is an infinite number of other starting combinations each of which produces a different starting point efficiency.) The position of each mesh is subsequently incremented by the appropriate DELAL1, DELAL2 or DELAL3. When the angle ALPHA1 reaches the magnitude AL1FIN, CYCLEFF is determined, and the computation is ended. Since meshes 2 and 3 go through numerous cycles while mesh 1 goes through one cycle, they have

to be reset to their initial angles of rotation once their respective final angles have been reached. This is accomplished by the conditional statements on cards 116 and 117.

The values of the signum functions  $s_1$ ,  $s_2$  and  $s_3$  are determined continuously according to eqs. (A-216), (A-222) and (A-227).

The instantaneous positions of the contact  $A_1 = a_1$ ,  $A_2 = a_2$ , and  $A_3 = a_3$  are determined for each of the meshes by an appropriate adaptation of eq. (A-203). (See also eqs. (A-214), (A-220) and (A-226).)

The determination of the instantaneous output moment,  $M_{O4} = M_{O4}$ , requires the continuous computation of the variable quantities  $A_1$  to  $A_{20}$ ,  $C_1$  to  $C_6$  and  $D_1$  to  $D_4$ , which are given originally in conjunction with the various equilibrium conditions in section 4 of Appendix A. The program uses the following nomenclature for these variables:

AA1 to AA20  
CC1 to CC6  
DD1 to DD4

c. Output (see Program INVOL 3, below)

Again, the output of the program is best explained by means of the sample computation which is shown at the end of the program. This example uses the gear data of the first three sample computations of program INVOL 1. The output lists the following:

## I. Input Parameters

### Mesh No. 1

$$\text{CAPRP1} = R_{p1} = .47727 \text{ in. (1.212 cm)}$$

$$\text{CAPRB1} = R_{b1} = .44849 \text{ in. (1.139 cm)}$$

$$\text{CAPRO1} = R_{o1} = .48791 \text{ in. (1.239 cm)}$$

$$\text{RP2} = r_{p2} = .09091 \text{ in. (.231 cm)}$$

$$\text{RB2} = r_{b2} = .08543 \text{ in. (.217 cm)}$$

$$\text{RO2} = r'_{o2} = .11000 \text{ in. (.279 cm) (This is an ROFIN as given by INVOL 1.)}$$

Also,

$$\text{THETA1} = \theta_1 = 20^\circ$$

### Mesh No. 2

$$\text{CAPRP2} = R_{p2} = .20769 \text{ in. (.527 cm)}$$

$$\text{CAPRB2} = R_{b2} = .19517 \text{ in. (.496 cm)}$$

$$\text{CAPRO2} = R_{o2} = .21579 \text{ in. (.548 cm)}$$

$$\text{RP3} = r_{p3} = .06923 \text{ in. (.176 cm)}$$

$$\text{RB3} = r_{b3} = .06506 \text{ in. (.165 cm)}$$

$$\text{RO3} = r'_{o3} = .08089 \text{ in. (.205 cm)}$$

Also,

$$\text{THETA2} = \theta_2 = 20^\circ$$

### Mesh No. 3

$$\text{CAPRP3} = R_{p3} = .17532 \text{ in. (.445 cm)}$$

$$\text{CAPRB3} = R_{b3} = .16475 \text{ in. (.418 cm)}$$

$$\text{CAPRO3} = R_{o3} = .18216 \text{ in. (.463 cm)}$$

$$\text{RP4} = r_{p4} = .05844 \text{ in. (.148 cm)}$$

$$\text{RB4} = r_{b4} = .05492 \text{ in. (.139 cm)}$$

$$\text{RO4} = r'_{o4} = .06828 \text{ in. (.173 cm)}$$

Also,

$$\text{THETA3} = \theta_3 = 20^\circ$$

In addition,

$$\text{MU} = \mu = .2$$

$$\text{RPM} = 1000$$

$$\text{M1} = m_1 = .51079 \times 10^{-4} \text{ lb-sec}^2/\text{in.} \quad (8.943 \text{ g})$$

$$\text{M2} = m_2 = .17413 \times 10^{-4} \text{ lb-sec}^2/\text{in.} \quad (3.049 \text{ g})$$

$$\text{M3} = m_3 = .69788 \times 10^{-5} \text{ lb-sec}^2/\text{in.} \quad (1.222 \text{ g})$$

$$\text{M4} = m_4 = .7745 \times 10^{-6} \text{ lb-sec}^2/\text{in.} \quad (0.136 \text{ g})$$

$$\text{R1} = R_1 = .75 \text{ in.} \quad (1.905 \text{ cm})$$

$$\text{R2} = R_2 = .75 \text{ in.} \quad (1.905 \text{ cm})$$

$$\text{R3} = R_3 = .75 \text{ in.} \quad (1.905 \text{ cm})$$

$$\text{R4} = R_4 = .75 \text{ in.} \quad (1.905 \text{ cm})$$

$$\text{RHO1} = \rho_1 = .060 \text{ in.} \quad (.152 \text{ cm})$$

$$\text{RHO2} = \rho_2 = .030 \text{ in.} \quad (.076 \text{ cm})$$

$$\text{RHO3} = \rho_3 = .025 \text{ in.} \quad (.064 \text{ cm})$$

$$\text{RHO4} = \rho_4 = .020 \text{ in.} \quad (.051 \text{ cm})$$

$$\text{MD} = md^2 = .15 \times 10^{-4} \text{ lb-sec}^2 \text{ in.} \quad (16.944 \text{ g-cm}^2)$$

$$\text{K} = 25$$

## II. Computed Values

The point efficiency is given as a function of the angle  $\alpha_1$ , together with the signum parameters  $s_1$ ,  $s_2$  and  $s_3$  (given for checking purposes). The cycle efficiency is shown at the end of the output. In addition, the input moment, MIN, is printed out.

Program INVOL 3

C-32

```

1      PROGRAM INVOL 3(INPUT,OUTPUT,TAPES=INPUT,TAPE6=OUTPUT)
C      POINT AND CYCLE EFFICIENCIES FOR THREE PASS INVOLUTE STEP-UP
C      IN SPIN ENVIRONMENT (ALL WFSHES HAVE UNITY CONTACT RATIO)
5      C
C      REAL MIN,MU,M1,M2,M3,M4,M03,M04,MTOT,MD
C      READ AND WRITE INPUT DATA
10     READ(5,1)MU,RPM,CAPRP1,CAPRP2,CAPRP3,RP2,RP3,RP4,THETA1,
1      THETA2,THETA3,ISTOP
      READ(5,2)R1,R2,R3,R4
      READ(5,3)RH01,RH02,RH03,RH04
      READ(5,4)CAPR01,CAPR02,CAPR03,RP2,RP3,RP4
      READ(5,5)CAPR01,CAPR02,CAPR03,RP2,RP3,RP4
      READ(5,6)M1,M2,M3,M4
      READ(5,7)MD,K
      PI = 3.14159
      OMEGA = RPM*2.3PI/60.
20     OM2 = OMEGA*OMEGA
      1 FORMAT(F16.3,F10.076FIN.573F10.47I1)
      2 FORMAT(4F10.4)
      3 FORMAT(4F10.4)
      4 FORMAT(6F10.5)
      5 FORMAT(6F10.5)
      6 FORMAT(4E10.2)
      7 FORMAT(E10.2/I3)
30     C      COMPUTATION OF MIN, GAMMAS AND RETAS
C
C      MIN = MD*OM2
      GAMMA2 = ACOS((R1*R1 + R2*R2 - (CAPRP1*RP2)*(CAPRP1*RP2)) /
1      (2.*R1*R2))
      GAMMA3 = ACOS((R2*R2 + R3*R3 - (CAPRP2*RP3)*(CAPRP2*RP3)) /
1      (2.*R2*R3))
      GAMMA4 = ACOS((R3*R3 + R4*R4 - (CAPRP3*RP4)*(CAPRP3*RP4)) /
1      (2.*R3*R4))
      GAMMA5 = GAMMA3 + GAMMA4
      DELTA2 = ACOS(((CAPRP1*RP2)*(CAPRP1*RP2) + R1*R1 - R2*R2) /
1      (2.*R1*(CAPRP1 + RP2)))
      DELTA3 = ACOS(((CAPRP2*RP3)*(CAPRP2*RP3) + R2*R2 - R3*R3) /
1      (2.*R2*(CAPRP2 + RP3)))
      DELTA4 = ACOS(((CAPRP3*RP4)*(CAPRP3*RP4) + R3*R3 - R4*R4) /
1      (2.*R3*(CAPRP3 + RP4)))
      BETA1 = PI - DELTA2
      BETA2 = GAMMA2 + PI - DELTA3
      BETA3 = GAMMA3 + PI - DELTA4
50     WRITE(6,8)MIN,MU,RPM,CAPRP1,CAPRP2,CAPRP3,RP2,RP3,RP4,THETA1,
1      THETA2,THETA3
      WRITE(6,9)R1,R2,R3,R4,M1,M2,M3,M4
      WRITE(6,10)RH01,RH02,RH03,RH04
      WRITE(6,11)CAPR01,CAPR02,CAPR03,RP2,RP3,RP4

```

```

55      WRITE(6,12)(CAPR01,CAPR02,CAPR03,MO2,RO3,RO4
      WRITE(6,13)MO,K
      R FORMAT(1E+5X,EMIX) = F12.5,3X,MMU = F6.3,3X,OPPM = F6.0//
      1X,CAPR01 = F8.5,3X,CAPR02 = F6.5,3X,CAPR03 = F8.5//6X,
      2X,RO2 = F8.5,3X,RO3 = F.5 X,RO4 = F8.5//6X,
      3*THETA1 = F6.3,3X,THETA2 = F.3,3X,THETA3 = F9.3//
9      FORMAT(6X,OR1 = F7.5,3X,OR2 = F7.5,3X,OR3 = F7.5,3X,OR4 = F7.5
      1//6X,OM) = E15.5,3X,OP = E15.5,3X,OM3 = E15.5,3X
      2*OM4 = E15.5//
      10 FORMAT(6X,ORMO1 = F7.5,3X,ORMO2 = F7.5,3X,ORMO3 = F7.5,3X,
      1*ORMO4 = F7.5//
      11 FORMAT(6X,CAPR01 = F7.5,3X,CAPR02 = F7.5,3X,CAPR03 = F7.5,
      13X,OR02 = F7.5,3X,OR01 = F7.5,3X,OR04 = F7.5//
      12 FORMAT(6X,CAPR01 = F7.5,3X,CAPR02 = F7.5,3X,CAPR03 = F7.5,3X
      1*OR02 = F7.5,3X,OR03 = F7.5,3X,OR04 = F7.5//
      13 FORMAT(6X,MO = E10.3//6X,ORANGE DIVISOR = F14//)
70      C
      C CONVERSION TO RADIAN
      C
      Z = PI/180.
      THETA1 = THETA1*Z
      THETA2 = THETA2*Z
      THETA3 = THETA3*Z
      C
      C DETERMINATION OF GEAR TRAIN CONSTANTS
      C
      RATIO = CAPR03*CAPR02*CAPR01/(RO2*RO3*OR04)
      TEST1 = TAN(THETA1)
      TEST2 = TAN(THETA2)
      TEST3 = TAN(THETA3)
      D1 = (CAPR01 * RO2)*TAN(THETA1)
      D2 = (CAPR02 * RO3)*TAN(THETA2)
      D3 = (CAPR03 * RO4)*TAN(THETA3)
      MTO2 = 0.
      C
      C DETERMINATION OF INITIAL AND FINAL VALUES OF ALPHAS
      C
      CALL ALPHA(CAPR01,RO2,THETA1,CAPR01,PO2,AL1IN,AL1FIN)
      CALL ALPHA(CAPR02,RO3,THETA2,CAPR02,PO3,AL2IN,AL2FIN)
      CALL ALPHA(CAPR03,RO4,THETA3,CAPR03,PO4,AL3IN,AL3FIN)
      DELAL3 = (AL3FIN - AL3IN)/K
      DELAL2 = DELAL3*RO3/CAPR02
      DELAL1 = DELAL2*RO2/CAPR01
      C
      C INITIALIZATION OF ALPHAS
      C
      ALPHA1 = AL1IN
      ALPHA2 = AL2IN
      ALPHA3 = AL3IN
      C
      C CENTRIFUGAL FORCE
      C

```

110 T1 = M1\*Z1\*OM2  
 T2 = M2\*Z2\*OM2  
 T3 = M3\*N3\*OM2  
 T4 = M4\*OM2

115 DENOM = 1. + MU\*RU

120 C UPDATE VALUES OF ALPHA3

125 IF (ALPHA2 .GT. ZERO) ALPHA2 = ALPH1  
 IF (ALPHA3 .GT. ZERO) ALPHA3 = ALPH1

130 C TEST TO DETERMINE IF CONTACT POINT IS IN APPROACH OR RECESS

135 IF APPROACH S = 1.  
 IF RECESS S = -1.  
 AT PITCH POINT S = 0.

140 IF (ALPHA1 .EQ. TEST1) S1 = 1.  
 IF (ALPHA2 .EQ. TEST2) S2 = 1.  
 IF (ALPHA3 .EQ. TEST3) S3 = 1.  
 IF (ALPHA1 .GT. TEST1) S1 = -1.  
 IF (ALPHA2 .GT. TEST2) S2 = -1.  
 IF (ALPHA3 .GT. TEST3) S3 = -1.  
 IF (ALPHA1 .EQ. TEST1) S1 = 0.  
 IF (ALPHA2 .EQ. TEST2) S2 = 0.  
 IF (ALPHA3 .EQ. TEST3) S3 = 0.

145 C DETERMINATION OF IMPUL FOR MOMENT EXPRESSIONS

150 A1 = ALPHA1\*CAPR01  
 A2 = ALPHA2\*CAPR02  
 A3 = ALPHA3\*CAPR03  
 A41 = ABS((S1\*OM2\*(GAMMA2) - MU\*OM2\*(GAMMA3))/DENOM)  
 A42 = ABS((1. - S3)\*MU\*OM2)\*COS(BETA3 - THETA3) + MU\*(1. - S3)  
 1\* SIN(BETA3 - THETA3) / DENOM  
 A43 = ABS((COS(GAMMA4) + MU\*SIN(GAMMA4)) / DENOM)  
 A44 = ABS((1. - S3)\*MU\*OM2)\*SIN(BETA3 - THETA3) - MU\*(1. - S3)  
 1\* COS(BETA3 - THETA3) / DENOM  
 A45 = ABS((1. - MU\*OM2)\*S1)\*COS(BETA2 - THETA2) + MU\*(S2 - 1.)  
 1\* SIN(BETA2 - THETA2) / DENOM  
 A46 = ABS((SIN(GAMMA3) + MU\*OM2)\*S1)\*COS(BETA3 - THETA3) / DENOM  
 A47 = ABS((1. - MU\*OM2)\*S1)\*COS(BETA3 - THETA3) - MU\*(1. - S3)  
 1\* SIN(BETA3 - THETA3) / DENOM  
 A48 = ABS((1. - MU\*OM2)\*S1)\*SIN(BETA2 - THETA2) + MU\*(1. - S2)  
 1\* COS(BETA2 - THETA2) / DENOM  
 A49 = ABS((MU\*SIN(GAMMA3) - COS(GAMMA3)) / DENOM)  
 A50 = ABS((1. - MU\*OM2)\*S1)\*SIN(BETA3 - THETA3) / DENOM  
 A51 = ABS((MU\*(1. - S1)\*SIN(BETA1 - THETA1) + (1. - S1)\*OM2\*OM2)  
 1\* COS(BETA1 - THETA1)) / DENOM  
 A52 = ABS((SIN(GAMMA2) - MU\*OM2\*(GAMMA2)) / DENOM)  
 A53 = ABS((MU\*(1. - S2)\*SIN(BETA2 - THETA2) + (1. - S2)\*OM2\*OM2)  
 1\* COS(BETA2 - THETA2)) / DENOM

```

160 AA14 = ABS((MU*(1.-S1)) * COS(BETA1 * THETA1)) - (1. - MU * MU * S1)
    1 * SIN(BETA1 * THETA1) / DENOM
165 AA15 = ABS((MU * SIN(GAMMA2)) * COS(GAMMA2)) / DENOM
    AA16 = ABS((1. - MU * MU * S1) * SIN(BETA2 * THETA2)) - MU * (1. - S2)
    1 * COS(BETA2 * THETA2) / DENOM
    AA17 = ABS((1. - MU * MU * S1) * SIN(BETA1 * THETA1)) * MU * (1. - S1)
    AA18 = ABS(1. / DENOM)
    AA19 = ABS((MU * (1. - S1)) * SIN(BETA1 * THETA1)) - (1. - MU * MU * S1)
    1 * COS(BETA1 * THETA1) / DENOM
    AA20 = ABS(MU / DENOM)
170 DD1 = RHA - MU * (S3 * (D3 - A3)) * RHO4 * (A2 - AA5)
    DD2 = -MU * (RHO3 * (AA5 - AA8) * S2 * (D2 - A2)) * PR3
    DD3 = R92 - MU * (S1 * (D1 - A1)) * RHO2 * (A11 - AA14)
    DD4 = CAPR81 - MU * (S * A1) - RHO1 * (AA17 - AA19)
175 CC1 = MU * RHO4 * (AA1 - AA3)
    CC2 = CAPR83 - MU * (S3 * A3) - RHO3 * (AA7 - AA10)
    CC3 = MU * RHO3 * (A36 - AA9)
    CC4 = CAPR82 - MU * (S2 * A2) - RHO2 * (A13 - AA16)
    CC5 = MU * RHO2 * (AA12 - AA15)
    CC6 = MU * RHO1 * (AA18 - AA20)
180
C OUTPUT MOMENT
C
    ALPHA10 = ALPHA1 * 129. / PI
    W04 = (D1 * D2 * D03) / (CC2 * CC4 * RHO4 * (MIN(T1 * CC6) - T2 * CC5 * D0) * D02)
    1 / (CC2 * CC4) - T3 * CC3 * D01 / CC2 - T4 * CC1
    POINTEF = RATIO * W04 / MIN
    WRITE(6,15) ALPHA10, S1, S2, S3, POINTEF
185 15 FORMAT(1X, 'ALPHA1 =', F4.2, ' (DEG)', ' S1 =', F5.1, ' S2 =', F5.1,
    13 * S3 =', F5.1, ' S3, POINT EFFICIENCY =', F7.5)
    M107 = M107 * MU
C
C ADVANCE GEAR TRAIN TO NEXT POS. F104
C
    ALPHA1 = ALPHA1 * DELA1
    IF (ALPHA1 .GT. ALIFIN) GO TO 16
    ALPHA2 = ALPHA2 * DELA2
    ALPHA3 = ALPHA3 * DELA3
    GO TO 14
200 16 CYCLEFF = RATIO * DELA1 * M107 / (MIN * (ALIFIN - ALPHA1))
    WRITE(6,17) CYCLEFF
    17 FORMAT(1X, 'CYCLE EFFICIENCY =', F5.3)
    IF (I1STOP .NE. 0) GO TO 190
    STOP
    END
205

```

9-36

SUBROUTINE ALPHA 76/76 OPT=1

FTM 4.6-428

99/96/7A 18.01.15

PAGE 1

```
1 SUBROUTINE ALPHA(CAPR8,RR,THETA,CAPRO,RO,ALIN,ALFIN)
C THIS SUBROUTINE COMPUTES THE INITIAL AND FINAL VALUES OF ALPHAS
C
5 ALIN = ((CAPR8 + RR)*TAN(THETA) - SQRT(DO*RO - RR*RR))/CAPR8
ALFIN = SQRT(CAPRO*CAPRO - CAPR8*CAPR8)/CAPR8
RETURN
END
```

0-37

WIS = -16442.00 MU = .200 MM = 1000

CAP001 = -47727 CAP002 = -20760 CAP003 = -17532

BP2 = -80001 BP3 = -84003 BP4 = -85444

INETA1 = 48.888 INETA2 = 28.888 INETA3 = 28.888

R1 = .75000 R2 = .75000 R3 = .75000 R4 = .75000

W1 = -210700 W2 = -171300 W3 = -697800 W4 = -776540

RM01 = 80000 RM02 = 83000 RM03 = 82500 RM04 = 82000

CAP001 = 64009 CAP002 = 19517 CAP003 = 16475 RM3 = 80500 RM4 = 85497

CAP001 = 11791 CAP002 = 21570 CAP003 = 18216 RM2 = 11000 RM3 = 80000 RM4 = 84820

RB = 1500-44

RANGE DIVISOR = 25

ALPHA1 = 15.97 (DE6)	S1 = 1.0	S2 = 1.0	S3 = 1.0	POINT EFFICIENCY = 37862
ALPHA1 = 16.01 (DE6)	S1 = 1.0	S2 = 1.0	S3 = 1.0	POINT EFFICIENCY = 37597
ALPHA1 = 16.04 (DE6)	S1 = 1.0	S2 = 1.0	S3 = 1.0	POINT EFFICIENCY = 36117
ALPHA1 = 16.08 (DE6)	S1 = 1.0	S2 = 1.0	S3 = 1.0	POINT EFFICIENCY = 36642
ALPHA1 = 16.11 (DE6)	S1 = 1.0	S2 = 1.0	S3 = 1.0	POINT EFFICIENCY = 36172
ALPHA1 = 16.16 (DE6)	S1 = 1.0	S2 = 1.0	S3 = 1.0	POINT EFFICIENCY = 36787
ALPHA1 = 16.19 (DE6)	S1 = 1.0	S2 = 1.0	S3 = 1.0	POINT EFFICIENCY = 40247
ALPHA1 = 16.21 (DE6)	S1 = 1.0	S2 = 1.0	S3 = 1.0	POINT EFFICIENCY = 40791
ALPHA1 = 16.26 (DE6)	S1 = 1.0	S2 = 1.0	S3 = 1.0	POINT EFFICIENCY = 41361
ALPHA1 = 16.29 (DE6)	S1 = 1.0	S2 = 1.0	S3 = 1.0	POINT EFFICIENCY = 41896
ALPHA1 = 16.31 (DE6)	S1 = 1.0	S2 = 1.0	S3 = 1.0	POINT EFFICIENCY = 42456
ALPHA1 = 16.35 (DE6)	S1 = 1.0	S2 = 1.0	S3 = 1.0	POINT EFFICIENCY = 43021
ALPHA1 = 16.34 (DE6)	S1 = 1.0	S2 = 1.0	S3 = 1.0	POINT EFFICIENCY = 43591
ALPHA1 = 16.31 (DE6)	S1 = 1.0	S2 = 1.0	S3 = 1.0	POINT EFFICIENCY = 44166
ALPHA1 = 16.05 (DE6)	S1 = 1.0	S2 = 1.0	S3 = 1.0	POINT EFFICIENCY = 44695
ALPHA1 = 16.04 (DE6)	S1 = 1.0	S2 = 1.0	S3 = 1.0	POINT EFFICIENCY = 44752
ALPHA1 = 16.52 (DE6)	S1 = 1.0	S2 = 1.0	S3 = 1.0	POINT EFFICIENCY = 44669
ALPHA1 = 16.55 (DE6)	S1 = 1.0	S2 = 1.0	S3 = 1.0	POINT EFFICIENCY = 44464
ALPHA1 = 16.54 (DE6)	S1 = 1.0	S2 = 1.0	S3 = 1.0	POINT EFFICIENCY = 44318
ALPHA1 = 16.82 (DE6)	S1 = 1.0	S2 = 1.0	S3 = 1.0	POINT EFFICIENCY = 44171
ALPHA1 = 16.05 (DE6)	S1 = 1.0	S2 = 1.0	S3 = 1.0	POINT EFFICIENCY = 44822
ALPHA1 = 16.04 (DE6)	S1 = 1.0	S2 = 1.0	S3 = 1.0	POINT EFFICIENCY = 43872
ALPHA1 = 16.72 (DE6)	S1 = 1.0	S2 = 1.0	S3 = 1.0	POINT EFFICIENCY = 43721
ALPHA1 = 16.75 (DE6)	S1 = 1.0	S2 = 1.0	S3 = 1.0	POINT EFFICIENCY = 43569
ALPHA1 = 16.74 (DE6)	S1 = 1.0	S2 = 1.0	S3 = 1.0	POINT EFFICIENCY = 43415
ALPHA1 = 16.85 (DE6)	S1 = 1.0	S2 = 1.0	S3 = 1.0	POINT EFFICIENCY = 43240
ALPHA1 = 16.89 (DE6)	S1 = 1.0	S2 = 1.0	S3 = 1.0	POINT EFFICIENCY = 43195
ALPHA1 = 16.92 (DE6)	S1 = 1.0	S2 = 1.0	S3 = 1.0	POINT EFFICIENCY = 43153
ALPHA1 = 16.96 (DE6)	S1 = 1.0	S2 = 1.0	S3 = 1.0	POINT EFFICIENCY = 43126
ALPHA1 = 16.96 (DE6)	S1 = 1.0	S2 = 1.0	S3 = 1.0	POINT EFFICIENCY = 43304
ALPHA1 = 16.99 (DE6)	S1 = 1.0	S2 = 1.0	S3 = 1.0	POINT EFFICIENCY = 43808
ALPHA1 = 17.07 (DE6)	S1 = 1.0	S2 = 1.0	S3 = 1.0	POINT EFFICIENCY = 44476
ALPHA1 = 17.06 (DE6)	S1 = 1.0	S2 = 1.0	S3 = 1.0	POINT EFFICIENCY = 44871
ALPHA1 = 17.09 (DE6)	S1 = 1.0	S2 = 1.0	S3 = 1.0	POINT EFFICIENCY = 45478
ALPHA1 = 17.12 (DE6)	S1 = 1.0	S2 = 1.0	S3 = 1.0	POINT EFFICIENCY = 46275
ALPHA1 = 17.16 (DE6)	S1 = 1.0	S2 = 1.0	S3 = 1.0	POINT EFFICIENCY = 46806
ALPHA1 = 17.19 (DE6)	S1 = 1.0	S2 = 1.0	S3 = 1.0	POINT EFFICIENCY = 47502
ALPHA1 = 17.23 (DE6)	S1 = 1.0	S2 = 1.0	S3 = 1.0	POINT EFFICIENCY = 48122
ALPHA1 = 17.29 (DE6)	S1 = 1.0	S2 = 1.0	S3 = 1.0	POINT EFFICIENCY = 48758
ALPHA1 = 17.29 (DE6)	S1 = 1.0	S2 = 1.0	S3 = 1.0	POINT EFFICIENCY = 49393
ALPHA1 = 17.33 (DE6)	S1 = 1.0	S2 = 1.0	S3 = 1.0	POINT EFFICIENCY = 50196
ALPHA1 = 17.33 (DE6)	S1 = 1.0	S2 = 1.0	S3 = 1.0	POINT EFFICIENCY = 50798

Q  
J  
D



AL 0001	19.78	00E.0	51	1.0	52	1.0	POINT EFFICIENCY = .48037
AL 0002	19.78	00E.0	51	1.0	52	1.0	POINT EFFICIENCY = .48675
AL 0003	19.78	00E.0	51	1.0	52	1.0	POINT EFFICIENCY = .49320
AL 0004	19.77	00E.0	51	1.0	52	1.0	POINT EFFICIENCY = .50626
AL 0005	19.78	00E.0	51	1.0	52	1.0	POINT EFFICIENCY = .51299
AL 0006	19.83	00E.0	51	1.0	52	1.0	POINT EFFICIENCY = .51954
AL 0007	19.87	00E.0	51	1.0	52	1.0	POINT EFFICIENCY = .52636
AL 0008	19.90	00E.0	51	1.0	52	1.0	POINT EFFICIENCY = .53333
AL 0009	19.96	00E.0	51	1.0	52	1.0	POINT EFFICIENCY = .54028
AL 0010	19.97	00E.0	51	1.0	52	1.0	POINT EFFICIENCY = .54842
AL 0011	20.00	00E.0	51	1.0	52	1.0	POINT EFFICIENCY = .55678
AL 0012	20.04	00E.0	51	1.0	52	1.0	POINT EFFICIENCY = .56576
AL 0013	20.07	00E.0	51	1.0	52	1.0	POINT EFFICIENCY = .57517
AL 0014	20.10	00E.0	51	1.0	52	1.0	POINT EFFICIENCY = .58508
AL 0015	20.14	00E.0	51	1.0	52	1.0	POINT EFFICIENCY = .59546
AL 0016	20.17	00E.0	51	1.0	52	1.0	POINT EFFICIENCY = .60645
AL 0017	20.21	00E.0	51	1.0	52	1.0	POINT EFFICIENCY = .61806
AL 0018	20.24	00E.0	51	1.0	52	1.0	POINT EFFICIENCY = .63028
AL 0019	20.27	00E.0	51	1.0	52	1.0	POINT EFFICIENCY = .64311
AL 0020	20.31	00E.0	51	1.0	52	1.0	POINT EFFICIENCY = .65656
AL 0021	20.36	00E.0	51	1.0	52	1.0	POINT EFFICIENCY = .67077
AL 0022	20.38	00E.0	51	1.0	52	1.0	POINT EFFICIENCY = .68573
AL 0023	20.41	00E.0	51	1.0	52	1.0	POINT EFFICIENCY = .70131
AL 0024	20.46	00E.0	51	1.0	52	1.0	POINT EFFICIENCY = .71769
AL 0025	20.44	00E.0	51	1.0	52	1.0	POINT EFFICIENCY = .73487
AL 0026	20.51	00E.0	51	1.0	52	1.0	POINT EFFICIENCY = .75285
AL 0027	20.56	00E.0	51	1.0	52	1.0	POINT EFFICIENCY = .77163
AL 0028	20.59	00E.0	51	1.0	52	1.0	POINT EFFICIENCY = .79121
AL 0029	20.61	00E.0	51	1.0	52	1.0	POINT EFFICIENCY = .81169
AL 0030	20.65	00E.0	51	1.0	52	1.0	POINT EFFICIENCY = .83306
AL 0031	20.68	00E.0	51	1.0	52	1.0	POINT EFFICIENCY = .85534
AL 0032	20.71	00E.0	51	1.0	52	1.0	POINT EFFICIENCY = .87854
AL 0033	20.75	00E.0	51	1.0	52	1.0	POINT EFFICIENCY = .90267
AL 0034	20.78	00E.0	51	1.0	52	1.0	POINT EFFICIENCY = .92773
AL 0035	20.82	00E.0	51	1.0	52	1.0	POINT EFFICIENCY = .95374
AL 0036	20.85	00E.0	51	1.0	52	1.0	POINT EFFICIENCY = .98071
AL 0037	20.88	00E.0	51	1.0	52	1.0	POINT EFFICIENCY = .10066
AL 0038	20.92	00E.0	51	1.0	52	1.0	POINT EFFICIENCY = .10263
AL 0039	20.95	00E.0	51	1.0	52	1.0	POINT EFFICIENCY = .10461
AL 0040	20.94	00E.0	51	1.0	52	1.0	POINT EFFICIENCY = .10673
AL 0041	21.02	00E.0	51	1.0	52	1.0	POINT EFFICIENCY = .10897
AL 0042	21.05	00E.0	51	1.0	52	1.0	POINT EFFICIENCY = .11132
AL 0043	21.09	00E.0	51	1.0	52	1.0	POINT EFFICIENCY = .11377
AL 0044	21.12	00E.0	51	1.0	52	1.0	POINT EFFICIENCY = .11632
AL 0045	21.15	00E.0	51	1.0	52	1.0	POINT EFFICIENCY = .11897
AL 0046	21.18	00E.0	51	1.0	52	1.0	POINT EFFICIENCY = .12172
AL 0047	21.22	00E.0	51	1.0	52	1.0	POINT EFFICIENCY = .12457
AL 0048	21.26	00E.0	51	1.0	52	1.0	POINT EFFICIENCY = .12752
AL 0049	21.29	00E.0	51	1.0	52	1.0	POINT EFFICIENCY = .13057
AL 0050	21.32	00E.0	51	1.0	52	1.0	POINT EFFICIENCY = .13372
AL 0051	21.36	00E.0	51	1.0	52	1.0	POINT EFFICIENCY = .13697
AL 0052	21.39	00E.0	51	1.0	52	1.0	POINT EFFICIENCY = .14032
AL 0053	21.43	00E.0	51	1.0	52	1.0	POINT EFFICIENCY = .14377
AL 0054	21.44	00E.0	51	1.0	52	1.0	POINT EFFICIENCY = .14732
AL 0055	21.49	00E.0	51	1.0	52	1.0	POINT EFFICIENCY = .15097
AL 0056	21.54	00E.0	51	1.0	52	1.0	POINT EFFICIENCY = .15472
AL 0057	21.59	00E.0	51	1.0	52	1.0	POINT EFFICIENCY = .15857
AL 0058	21.63	00E.0	51	1.0	52	1.0	POINT EFFICIENCY = .16252
AL 0059	21.64	00E.0	51	1.0	52	1.0	POINT EFFICIENCY = .16667
AL 0060	21.70	00E.0	51	1.0	52	1.0	POINT EFFICIENCY = .17092
AL 0061	21.73	00E.0	51	1.0	52	1.0	POINT EFFICIENCY = .17527
AL 0062	21.74	00E.0	51	1.0	52	1.0	POINT EFFICIENCY = .17982
AL 0063	21.80	00E.0	51	1.0	52	1.0	POINT EFFICIENCY = .18457



ALPHA1 = 24.07 (DEG)	S1 = -1.0	S2 = 1.0	S3 = 1.0	POINT EFFICIENCY = .65544
ALPHA1 = 24.10 (DEG)	S1 = -1.0	S2 = 1.0	S3 = 1.0	POINT EFFICIENCY = .65964
ALPHA1 = 24.13 (DEG)	S1 = -1.0	S2 = 1.0	S3 = 1.0	POINT EFFICIENCY = .66528
ALPHA1 = 24.17 (DEG)	S1 = -1.0	S2 = 1.0	S3 = 1.0	POINT EFFICIENCY = .67115
ALPHA1 = 24.20 (DEG)	S1 = -1.0	S2 = 1.0	S3 = 1.0	POINT EFFICIENCY = .67646
ALPHA1 = 24.24 (DEG)	S1 = -1.0	S2 = 1.0	S3 = 1.0	POINT EFFICIENCY = .68180
ALPHA1 = 24.27 (DEG)	S1 = -1.0	S2 = 1.0	S3 = 1.0	POINT EFFICIENCY = .68718
ALPHA1 = 24.30 (DEG)	S1 = -1.0	S2 = 1.0	S3 = 1.0	POINT EFFICIENCY = .69260
ALPHA1 = 24.34 (DEG)	S1 = -1.0	S2 = 1.0	S3 = -1.0	POINT EFFICIENCY = .69968
ALPHA1 = 24.37 (DEG)	S1 = -1.0	S2 = 1.0	S3 = -1.0	POINT EFFICIENCY = .70709
ALPHA1 = 24.40 (DEG)	S1 = -1.0	S2 = 1.0	S3 = -1.0	POINT EFFICIENCY = .71449
ALPHA1 = 24.44 (DEG)	S1 = -1.0	S2 = 1.0	S3 = -1.0	POINT EFFICIENCY = .72149
ALPHA1 = 24.47 (DEG)	S1 = -1.0	S2 = 1.0	S3 = -1.0	POINT EFFICIENCY = .72828
ALPHA1 = 24.51 (DEG)	S1 = -1.0	S2 = 1.0	S3 = -1.0	POINT EFFICIENCY = .73467
ALPHA1 = 24.54 (DEG)	S1 = -1.0	S2 = 1.0	S3 = -1.0	POINT EFFICIENCY = .74067

CYCLE EFFICIENCY = .661

4. Program INVOL 4: Point and Cycle Efficiencies for Two  
Pass Involute Step-Up Gear Train in  
Spin Environment (All Meshes Have  
Unity Contact Ratio)

The program INVOL 4 is based on section 5 of Appendix A, which derives the moment input-output relationship for a two pass step-up gear train, operating in a spin environment. Here again, all meshes have unity contact ratio. INVOL 4 is very similar to INVOL 3 in its construction. Again, the expressions for the contact geometry and other auxiliary geometric terms may be found in section 6 of Appendix A.

a. Input Parameters (see Program INVOL 4, below)

The following parameters represent the input data for the program. Those which involve gear dimensions only must be obtained from the results of INVOL 1 since the moment expressions are again derived for unity contact ratio only.

MU =  $\mu$ , coefficient of friction at all pivots and at all  
tooth contact points

RPM, revolutions per minute of the fuze body

CAPRP1 =  $R_{p1}$

CAPRP2 =  $R_{p2}$

RF2 =  $r_{p2}$

RP3 =  $r_{p3}$

THETA1 =  $\theta_1$

THETA2 =  $\theta_2$

ISTOP, arbitrary single digit integer for multiple data sets.

It must be zero for last set of data.

$$R1 = R_1$$

$$R2 = R_2$$

$$R3 = R_3$$

$$RHO1 = \rho_1$$

$$RHO2 = \rho_2$$

$$RHO3 = \rho_3$$

$$CAPRB1 = R_{b1}$$

$$CAPRB2 = R_{b2}$$

$$RB2 = r_{b2}$$

$$RB3 = r_{b3}$$

$$CAPRO1 = R_{o1}$$

$$CAPRO2 = R_{o2}$$

$$RO2 = r'_{o2}$$

$$RO3 = r'_{o3}$$

$$M1 = m_1, \text{ mass of input gear 1}$$

$$M2 = m_2, \text{ mass of gear and pinion 2}$$

$$M3 = m_3, \text{ mass of pinion 3}$$

$$MD = md^2, \text{ "mass-distance" product contained in the following expression for the input moment } M_{1n}$$

$$K = K_2, \text{ the range divisor which is associated with gear 2, the driving gear of the last mesh for this case (see eq. (A-207))}$$

b. Computations (see COMMENT cards in program)

I. Computation of MIN, Gammas and Betas

To start with, the program computes the input moment

$$MIN = M_{in} = md\omega^2 \quad (C-15)$$

The program computes the angles  $\gamma_2$ ,  $\gamma_3$  and  $\beta_1$ ,  $\beta_2$  according to the expressions given in section 6b of Appendix A.

II. Determination of the Gear Train Constants

The determination of the gear train constants consists of the following:

RATIO =  $K_{ratio}$  (see eq. (2)). Since the angular velocity is constant, this parameter may be expressed in terms of the applicable base radii, i.e.,

$$\frac{R_{b1} \times R_{b2}}{r_{b2} \times r_{b3}}$$

TEST1 and TEST2 represent the tangent functions of the mesh pressure angles, which are used in conjunction with the values of the signum functions  $s$ .

D1, and D2 are given by eqs. (A-204) and (A-217), respectively, and represent the distances between the points of tangency to the base circles along the lines-of-action of the two meshes.

MTOT = 0 represents the initialization of the sum of the output moments. This is used for the determination of the cycle efficiency.

### III. Determination of Initial and Final Values of ALPHAS.

#### Initialization of ALPHAS and Centrifugal Forces

The determination of the initial and final angles of rotation is accomplished with the help of subroutine ALPHA, at the end of the program, which makes use of eqs. (A-205), (A-206) as well as (A-218) and (A-219). Thus, the initial values of the individual angles of rotation, ALPHA1 and ALPHA2, are represented by AL1IN and AL2IN, respectively, while the final ones are given by AL1FIN and AL2FIN.

The angular increments of gears 2 and 1, i.e., DELAL2 and DELAL1, are determined with the help of eqs. (A-207) and (A-208), respectively.

The centrifugal forces, which act on the pivots of the various gear and/or pinion assemblies, are obtained by way of eqs. (A-131), (A-154) and (A-178).

### IV. Point and Cycle Efficiencies (See "output moment" in program)

Both point and cycle efficiencies are based on eq. (A-193) for the output moment  $M_{O3} = M_{O3}$ .

The point efficiency is computed directly in the manner of eq. (3), i.e.,

$$\eta_p = K_{ratio} \frac{M_{O3}}{M_{in}} = \text{POINTEF} \quad (\text{C-16})$$

The cycle efficiency is treated in the manner of eq. (C-13), i.e.,

$$\epsilon_0 = \frac{K_{ratio} \Delta \alpha_1 \Sigma M_{O3}}{M_{in} (\alpha_{1FIN} - \alpha_{1IN})} = CYCLEFF \quad (C-17)$$

The program gives the summation as

$$MTOT = \Sigma M_{O3} \quad (C-18)$$

#### V. Gear Train Motion Model

The simulation of the gear train motion, which is necessary for the computation of both POINTEF and CYCLEFF, is found in a loop which begins with statement label no. 14 (card no. 98) and ends with card no. 161.

As discussed earlier, the motions of the individual driving gears are initialized at their respective angles, AL1IN and AL2IN.

(This starting of the total train is arbitrary and is done only for convenience. There is an infinite number of other starting combinations, each of which produces a different starting point efficiency.) The position of each mesh is subsequently incremented by the appropriate DELAL1 or DELAL2. When the angle ALPHA1 reaches the magnitude AL1FIN, CYCLEFF is determined, and the computation is ended. Since mesh 2 goes through a number of cycles while mesh 1 goes through one cycle, mesh 2 has to be reset to its starting position, AL2IN, once the angle AL2FIN has been reached. This is accomplished by the conditional statement on card no. 98.

The values of the signum functions  $s_1$  and  $s_2$  are determined continuously according to eqs. (A-216) and (A-222).

The instantaneous positions of the contact,  $A1 = a_1$  and  $A2 = a_2$ , are determined for each of the meshes by appropriate

adaptations of eq. (A-203). (See also eqn. (A-214) and (A-220).)

The determination of the instantaneous output moment,  $M_{O3} = M_{O3}$ , requires the continuous computation of the variable quantities  $A_1$  to  $A_{14}$ ,  $C_1$  to  $C_4$  and  $D_1$  to  $D_3$ , which are given originally in conjunction with the various equilibrium conditions in section 5 of Appendix A. The program uses the following nomenclature for these variables:

AA1 to AA14

CC1 to CC4

DD1 to DD3

c. Output (see Program INVOL 4, below)

The output of the program is again best explained with the help of the sample computation shown at the end of the program. This example uses the gear data of the fourth and fifth sample computations of program INVOL 1. The output lists the following:

I. Input Parameters

Mesh No. 1

CAPRP1 =  $R_{p1}$  = .63636 in. (1.616 cm)

CAPRB1 =  $R_{b1}$  = .59799 in. (1.519 cm)

CAPRO1 =  $R_{o1}$  = .64700 in. (1.643 cm)

RP2 =  $r_{p2}$  = .09091 in. (0.231 cm)

RB2 =  $r_{b2}$  = .08543 in. (0.217 cm)

RO2 =  $r'_{o2}$  = .1097 in. (0.279 cm) (This is a ROFIN as given by INVOL 1.)

Also

THETA1 =  $\theta_1$  =  $20^\circ$

Mesh No. 2

$$\text{CAPRP2} = R_{p2} = .43077 \text{ in. (1.094 cm)}$$

$$\text{CAPRB2} = R_{b2} = .40479 \text{ in. (1.028 cm)}$$

$$\text{CAPRO2} = R_{o2} = .43977 \text{ in. (1.117 cm)}$$

$$\text{RP3} = r_{p3} = .06154 \text{ in. (0.156 cm)}$$

$$\text{RB3} = r_{b3} = .05783 \text{ in. (0.147 cm)}$$

$$\text{RO3} = r_{o3} = .07426 \text{ in. (0.189 cm)}$$

Also

$$\text{THETA2} = \theta_2 = 20^\circ$$

In addition,

$$\text{MU} = \mu = .2$$

$$\text{RPM} = 1000$$

$$\text{M1} = m_1 = .51079 \times 10^{-4} \text{ lb-sec}^2/\text{in. (8.943 g)}$$

$$\text{M2} = m_2 = .17413 \times 10^{-4} \text{ lb-sec}^2/\text{in. (3.049 g)}$$

$$\text{M3} = m_3 = .69788 \times 10^{-5} \text{ lb-sec}^2/\text{in. (1.222 g)}$$

$$\text{R1} = R_1 = .75 \text{ in. (1.905 cm)}$$

$$\text{R2} = R_2 = .75 \text{ in. (1.905 cm)}$$

$$\text{R3} = R_3 = .75 \text{ in. (1.905 cm)}$$

$$\text{RHO1} = \rho_1 = .060 \text{ in. (0.152 cm)}$$

$$\text{RHO2} = \rho_2 = .030 \text{ in. (0.076 cm)}$$

$$\text{RHO3} = \rho_3 = .025 \text{ in. (0.064 cm)}$$

$$\text{MD} = md^2 = .15 \times 10^{-4} \text{ lb-sec}^2 \text{ in. (16.944 g-cm}^2\text{)}$$

$$\text{K} = 25$$

## II. Computed Values

The point efficiency is given as a function of the angle  $\alpha_1$ , together with the signum parameters  $s_1$  and  $s_2$  (given for checking purposes). The cycle efficiency is shown at the end of the output. In addition, the input moment, MIN, is printed out.

Program INVOL 4

C-51

PROGRAM INVOL 4 (INPUT,CUTFRIT,TAPES=INPUT,TAPE6=OUTPUT)  
 POINT AND CYCLE EFFICIENCIES FOR TWO PASS INVOLUTE STEP-UP GEAR TRAIN  
 IN SPIR ENVIRONMENT (ALL WFSHES HAVE UNITY CONTACT RATIO)

REAL MIN,MU,M1,M2,M3,MQ3,MTOT,MD

READ AND WRITE INPUT DATA

100 READ(5,1)MU,RP1,CAPPR1,CAPPR2,RP2,RP3,TMET1,TMET2,ISTOP

READ(5,2)R1,R2,R3

READ(5,3)RM01,RM02,RM03

READ(5,4)CAPR1,CAPR2,RR2,RR3

READ(5,5)CAPR1,CAPR2,RR2,RR3

READ(5,6)M1,M2,M3

READ(5,7)MD,K

1 FORMAT(F10.3,F10.0/4F10.5/2F10.4/11)

2 FORMAT(3F10.5)

3 FORMAT(3F10.5)

4 FORMAT(4F10.5)

5 FORMAT(4F10.5)

6 FORMAT(3F10.4)

7 FORMAT(F10.4/13)

PI = 3.14159

OMEGA = RPM\*2\*PI/60

OM2 = OMEGA\*OMEGA

0-52

C COMPUTATION OF MIN, GAMMAS AND BETAS

MIN = MU\*OM2

GAMMA2 = ACOS((R1\*R1 + R2\*R2 - (CAPR1\*RP2)+(CAPR1\*RP2))/

142.\*R1.\*R2))

GAMMA3 = ACOS((R2\*R2 + R3\*R3 - (CAPR2\*RP3)+(CAPR2\*RP3))/

142.\*R2.\*R3))

GAMMA1 = GAMMA2 + GAMMA3

DELTA2 = ACOS(((CAPR1\*RP2)+(CAPR1\*RP2) + R1\*R1 - R2\*R2)/

142.\*R1.\*(CAPR1 + RP2))

DELTA3 = ACOS(((CAPR2\*RP3)+(CAPR2\*RP3) + R2\*R2 - R3\*R3)/

142.\*R2.\*(CAPR2 + RP3))

BETA1 = PI - DELTA2

BETA2 = GAMMA2 + PI - DELTA3

WRITE(6,8)MIN,MU,RP1,CAPR1,CAPR2,RP2,RP3,TMET1,TMET2

WRITE(6,9)R1,R2,R3,M1,M2,M3

WRITE(6,10)RM01,RM02,RM03

WRITE(6,11)CAPR1,CAPR2,RR2,RR3

WRITE(6,12)CAPR1,CAPR2,RR2,RR3

WRITE(6,13)MD,K

A FORMAT(10,5)X,MIN = F12.5,3X,MU = F6.3,3X,RP1 = F6.0/6X,

1,CAPR1 = F8.5,3X,CAPR2 = F8.5/6X,RP2 = F8.5,3X,RP3 = F8.5/6X,

9 FORMAT(6)X,R1 = F7.5,3X,R2 = F7.5,3X,R3 = F7.5/6X,M1 = F7.5/6X,

12.5,3X,M2 = F12.5,3X,M3 = F12.5/6X

10 FORMAT(5)X,MD = F7.5,3X,RM02 = F7.5,3X,RM03 = F7.5/6X

```

55 11 FORMAT(6X, CAPR01 = F7.5, 3X, CAPR02 = F7.5, 3X, RB02 = F7.5, 3X,
1 RB03 = F7.5 /)
12 FORMAT(6X, CAPR01 = F7.5, 3X, CAPR02 = F7.5, 3X, RB02 = F7.5, 3X,
1 RB03 = F7.5 /)
13 FORMAT(6X, RND = E10.3 / 6X, RANGE DIVISOR = I4 / /)

```

```

C
C CONVERSION TO RADIAN
C
2 = PI/180.
THETA1 = THETA1*Z
THETA2 = THETA2*Z

```

```

C
C DETERMINATION OF GEAR TRAIN CONSTANTS
C
RATIO = (CAPR02*CAPR01)/(RB2*RB3)
TEST1 = TAN(THETA1)
TEST2 = TAN(THETA2)
D1 = (CAPR01 * RB2)*TAN(THETA1)
D2 = (CAPR02 * RB3)*TAN(THETA2)
MTOT = 0.

```

```

C
C DETERMINATION OF INITIAL AND FINAL VALUES OF ALPHAS
C
CALL ALPHA(CAPR01, RB2, THETA1, CAPR01, RB2, ALIIN, ALIFIN)
CALL ALPHA(CAPR02, RB3, THETA2, CAPR02, RB3, AL2IN, AL2FIN)
DELAL2 = (AL2FIN - AL2IN)/K
DELAL1 = DELAL2*RB2/CAPR01

```

```

C
C INITIALIZATION OF ALPHAS
C
ALPHA1 = ALIIN
ALPHA2 = AL2IN

```

```

C
C CENTRIFUGAL FORCES
C
T1 = W1*RI*OM2
T2 = W2*R2*OM2
T3 = W3*R3*OM2

```

```

C
C DEMON = 1. * WJ*RU
C
C UPRATE VALUES OF ALPHAS

```

```

C
14 IF (ALPHA2 .GT. AL2FIN) ALPHA2 = AL2IN
C
C TEST TO DETERMINE IF CONTACT POINT IS IN APPROACH OR RECESS
C
IF APPROACH, S = 1.
IF RECESS, S = -1.
AT PITCH POINT, S = 0.
C
IF (ALPHA1 .LT. TEST1) S = 1.
IF (ALPHA2 .LT. TEST2) S = 1.

```

```

IF (ALPHA1 .GT. TEST1) S1 = -1.
IF (ALPHA2 .GT. TEST2) S2 = -1.
IF (ALPHA1 .EQ. TEST1) S1 = 0.
IF (ALPHA2 .EQ. TEST2) S2 = 0.

```

110

```

C
C DETERMINATION OF INPUT FOR MOMENT EXPRESSIONS
C

```

```

A1 = ALPHA1 * CAPPR1
A2 = ALPHA2 * CAPPR2
AA1 = ABS((1.-MU*WU*S2)*COS(BETA2-THETA2) + MU*(S2-1.)*
      SIN(BETA2-THETA2))/DENOM
AA2 = ABS((S1*SIN(GAMMA3) + MU*COS(GAMMA3))/DENOM)
AA3 = ABS((1.-MU*WU*S2)*SIN(BETA2-THETA2) + MU*(1.-S2)*COS(BETA2
      -THETA2))/DENOM

```

124

```

AA4 = ABS((MU*SIN(GAMMA3) - COS(GAMMA3))/DENOM)
AA5 = ABS((MU*(1.-S1)*SIN(BETA1-THETA1) - (1.-S1)*MU*WU)*
      COS(BETA1-THETA1))/DENOM
AA6 = ABS((S1*SIN(GAMMA2) - MU*COS(GAMMA2))/DENOM)
AA7 = ABS((MU*(1.-S2)*SIN(BETA2-THETA2) + (1.-MU*WU*S2)*
      COS(BETA2-THETA2))/DENOM)
AA8 = ABS((MU*(1.-S1)*COS(BETA1-THETA1) - (1.-MU*WU*S1)*
      SIN(BETA1-THETA1))/DENOM)

```

125

```

AA9 = ABS((MU*SIN(GAMMA2) + COS(GAMMA2))/DENOM)
AA10 = ABS((1.-MU*WU*S2)*SIN(BETA2-THETA2) - MU*(1.-S2)*
      COS(BETA2-THETA2))/DENOM
AA11 = ABS((1.-MU*WU*S1)*SIN(BETA1-THETA1) + MU*(1.-S1)*
      COS(BETA1-THETA1))/DENOM
AA12 = 1./DENOM

```

130

```

AA13 = ABS((MU*(1.-S1)*SIN(BETA1-THETA1) - (1.-MU*WU*S1)*
      COS(BETA1-THETA1))/DENOM)
AA14 = MU/DENOM

```

135

```

CC1 = MU*RHO3*(AA2-AA4)
CC2 = AF*RB2 - MU*(S2*A2-P*Q2*(AA7-AA10))
CC3 = MU*RHO2*(AA6-AA9)
CC4 = MU*RHO1*(AA12-AA14)
DO1 = RB3 - MU*(S2*(R2-A2)+RHO3*(AA1-AA3))
DO2 = RB2 - MU*(S1*(R1-A1)+RHO2*(AA5-AA8))
DO3 = CAPPR1 - MU*(S1*A1-RHO1*(AA11-AA13))
ALPHID = ALPHA1/2

```

140

```

C
C OUTPUT MOMENT
C

```

145

```

M03 = (DO1+DO2)/(CC2+DO3)*(MIN-TI*CC4) - I2*CC3*Q0/CC2 - I3*CC1
POINTEE = P*TI*Q0/J*MIN
WRITE(6,15)ALPHID,S1,S2,POINTEE
15 FORMAT(6E10,ALPHAI =,F6.2,3E10,SI =,F5.1,3E10,S2 =,F5.1,3E10,
      1*POINT EFFICIENCY =,F7.5)
MTOT = MTOT + M03

```

150

```

C
C ADVANCE GEAR TRAIN TO NEXT POSITION
C

```

155

```

ALPHAI = ALPHA1 + DELTA1
IF (ALPHAI .GT. ALFIN) GO TO 16

```

160

```
160 ALPHA2 = ALPHA2 * DELAL1*CAPRB1/R52  
GO TO 14  
16 CYCLEFF = (RATIO*DELAL1*MTOT)/(MIN*(ALJFIN-ALJIN))  
WRITE(6,17)CYCLEFF  
17 FORMAT(9F6.1)CYCLE EFFICIENCY =*F5.3)  
IF(J .NE. 0)GO TO 100  
STOP  
END
```

SUBROUTINE ALPHA

7476 OP1=1

FIN 4.6428

09/05/78 16.49.21

PAGE

1

```
1 SUBROUTINE ALPHA(CAPRB, RB, THETA, CAPRO, RB, ALIN, ALFIN)
C
C THIS SUBROUTINE COMPUTES THE INITIAL AND FINAL VALUES OF ALPHAS
C
5 ALIN = ((CAPRB * RB) * TAN(THETA)) - SQRT((RO*RO - RB*RB))/CAPRB
ALFIN = SQRT((CAPRO*CAPRO - CAPRB*CAPRB)/CAERR)
RETURN
END
```

MIN = .12440E+08 NU = .288 CORR = 1888.

CAPR01 = .64636 CAPR02 = .43077

RP2 = .89901 RP3 = .96154

TETA1 = 28.838 TETA2 = 28.888

R1 = .75888 R2 = .75888 R3 = .75888

R4 = .51870E+04 R5 = .17413E+04 R6 = .69780E+05

R701 = .86888 R702 = .83888 R703 = .62588

CAPR81 = .59799 CAPR82 = .48478 R83 = .88543 R83 = .65783

CAPR01 = .54788 CAPR02 = .43797 R02 = .18978 R03 = .87428

W0 = .158E-04

RANGE DIVISION = 29

ALPHA1 = 17.24	S1 = 1.0	S2 = 1.0	POINT EFFICIENCY = .41895
ALPHA1 = 17.24	S1 = 1.0	S2 = 1.0	POINT EFFICIENCY = .41634
ALPHA1 = 17.31	S1 = 1.0	S2 = 1.0	POINT EFFICIENCY = .42267
ALPHA1 = 17.35	S1 = 1.0	S2 = 1.0	POINT EFFICIENCY = .42784
ALPHA1 = 17.39	S1 = 1.0	S2 = 1.0	POINT EFFICIENCY = .43300
ALPHA1 = 17.42	S1 = 1.0	S2 = 1.0	POINT EFFICIENCY = .43816
ALPHA1 = 17.46	S1 = 1.0	S2 = 1.0	POINT EFFICIENCY = .44332
ALPHA1 = 17.50	S1 = 1.0	S2 = 1.0	POINT EFFICIENCY = .44848
ALPHA1 = 17.53	S1 = 1.0	S2 = 1.0	POINT EFFICIENCY = .45364
ALPHA1 = 17.57	S1 = 1.0	S2 = 1.0	POINT EFFICIENCY = .45880
ALPHA1 = 17.61	S1 = 1.0	S2 = 1.0	POINT EFFICIENCY = .46396
ALPHA1 = 17.64	S1 = 1.0	S2 = 1.0	POINT EFFICIENCY = .46912
ALPHA1 = 17.68	S1 = 1.0	S2 = 1.0	POINT EFFICIENCY = .47428
ALPHA1 = 17.72	S1 = 1.0	S2 = 1.0	POINT EFFICIENCY = .47944
ALPHA1 = 17.75	S1 = 1.0	S2 = 1.0	POINT EFFICIENCY = .48460
ALPHA1 = 17.79	S1 = 1.0	S2 = 1.0	POINT EFFICIENCY = .48976
ALPHA1 = 17.83	S1 = 1.0	S2 = 1.0	POINT EFFICIENCY = .49492
ALPHA1 = 17.86	S1 = 1.0	S2 = 1.0	POINT EFFICIENCY = .50008
ALPHA1 = 17.90	S1 = 1.0	S2 = 1.0	POINT EFFICIENCY = .50524
ALPHA1 = 17.94	S1 = 1.0	S2 = 1.0	POINT EFFICIENCY = .51040
ALPHA1 = 17.97	S1 = 1.0	S2 = 1.0	POINT EFFICIENCY = .51556
ALPHA1 = 18.01	S1 = 1.0	S2 = 1.0	POINT EFFICIENCY = .52072
ALPHA1 = 18.05	S1 = 1.0	S2 = 1.0	POINT EFFICIENCY = .52588
ALPHA1 = 18.09	S1 = 1.0	S2 = 1.0	POINT EFFICIENCY = .53104
ALPHA1 = 18.12	S1 = 1.0	S2 = 1.0	POINT EFFICIENCY = .53620
ALPHA1 = 18.16	S1 = 1.0	S2 = 1.0	POINT EFFICIENCY = .54136
ALPHA1 = 18.19	S1 = 1.0	S2 = 1.0	POINT EFFICIENCY = .54652
ALPHA1 = 18.23	S1 = 1.0	S2 = 1.0	POINT EFFICIENCY = .55168
ALPHA1 = 18.27	S1 = 1.0	S2 = 1.0	POINT EFFICIENCY = .55684
ALPHA1 = 18.31	S1 = 1.0	S2 = 1.0	POINT EFFICIENCY = .56200
ALPHA1 = 18.34	S1 = 1.0	S2 = 1.0	POINT EFFICIENCY = .56716
ALPHA1 = 18.38	S1 = 1.0	S2 = 1.0	POINT EFFICIENCY = .57232
ALPHA1 = 18.42	S1 = 1.0	S2 = 1.0	POINT EFFICIENCY = .57748
ALPHA1 = 18.45	S1 = 1.0	S2 = 1.0	POINT EFFICIENCY = .58264
ALPHA1 = 18.49	S1 = 1.0	S2 = 1.0	POINT EFFICIENCY = .58780
ALPHA1 = 18.53	S1 = 1.0	S2 = 1.0	POINT EFFICIENCY = .59296
ALPHA1 = 18.56	S1 = 1.0	S2 = 1.0	POINT EFFICIENCY = .59812
ALPHA1 = 18.60	S1 = 1.0	S2 = 1.0	POINT EFFICIENCY = .60328
ALPHA1 = 18.64	S1 = 1.0	S2 = 1.0	POINT EFFICIENCY = .60844
ALPHA1 = 18.67	S1 = 1.0	S2 = 1.0	POINT EFFICIENCY = .61360
ALPHA1 = 18.71	S1 = 1.0	S2 = 1.0	POINT EFFICIENCY = .61876

ALPHA1 = 18.78	51	1.0	52	1.0	POINT EFFICIENCY = 53565
ALPHA1 = 18.82	51	1.0	52	1.0	POINT EFFICIENCY = 53161
ALPHA1 = 18.86	51	1.0	52	1.0	POINT EFFICIENCY = 52777
ALPHA1 = 18.89	51	1.0	52	1.0	POINT EFFICIENCY = 52392
ALPHA1 = 18.93	51	1.0	52	1.0	POINT EFFICIENCY = 52007
ALPHA1 = 18.97	51	1.0	52	1.0	POINT EFFICIENCY = 51621
ALPHA1 = 19.00	51	1.0	52	1.0	POINT EFFICIENCY = 51234
ALPHA1 = 19.04	51	1.0	52	1.0	POINT EFFICIENCY = 50847
ALPHA1 = 19.07	51	1.0	52	1.0	POINT EFFICIENCY = 50460
ALPHA1 = 19.11	51	1.0	52	1.0	POINT EFFICIENCY = 50072
ALPHA1 = 19.14	51	1.0	52	1.0	POINT EFFICIENCY = 49685
ALPHA1 = 19.18	51	1.0	52	1.0	POINT EFFICIENCY = 49297
ALPHA1 = 19.22	51	1.0	52	1.0	POINT EFFICIENCY = 48910
ALPHA1 = 19.26	51	1.0	52	1.0	POINT EFFICIENCY = 48523
ALPHA1 = 19.30	51	1.0	52	1.0	POINT EFFICIENCY = 48135
ALPHA1 = 19.33	51	1.0	52	1.0	POINT EFFICIENCY = 47748
ALPHA1 = 19.37	51	1.0	52	1.0	POINT EFFICIENCY = 47360
ALPHA1 = 19.41	51	1.0	52	1.0	POINT EFFICIENCY = 46973
ALPHA1 = 19.44	51	1.0	52	1.0	POINT EFFICIENCY = 46585
ALPHA1 = 19.48	51	1.0	52	1.0	POINT EFFICIENCY = 46198
ALPHA1 = 19.52	51	1.0	52	1.0	POINT EFFICIENCY = 45810
ALPHA1 = 19.56	51	1.0	52	1.0	POINT EFFICIENCY = 45423
ALPHA1 = 19.59	51	1.0	52	1.0	POINT EFFICIENCY = 45035
ALPHA1 = 19.63	51	1.0	52	1.0	POINT EFFICIENCY = 44648
ALPHA1 = 19.66	51	1.0	52	1.0	POINT EFFICIENCY = 44260
ALPHA1 = 19.70	51	1.0	52	1.0	POINT EFFICIENCY = 43873
ALPHA1 = 19.74	51	1.0	52	1.0	POINT EFFICIENCY = 43485
ALPHA1 = 19.77	51	1.0	52	1.0	POINT EFFICIENCY = 43098
ALPHA1 = 19.81	51	1.0	52	1.0	POINT EFFICIENCY = 42710
ALPHA1 = 19.85	51	1.0	52	1.0	POINT EFFICIENCY = 42323
ALPHA1 = 19.89	51	1.0	52	1.0	POINT EFFICIENCY = 41935
ALPHA1 = 19.92	51	1.0	52	1.0	POINT EFFICIENCY = 41548
ALPHA1 = 19.96	51	1.0	52	1.0	POINT EFFICIENCY = 41160
ALPHA1 = 20.00	51	1.0	52	1.0	POINT EFFICIENCY = 40773
ALPHA1 = 20.04	51	1.0	52	1.0	POINT EFFICIENCY = 40385
ALPHA1 = 20.07	51	1.0	52	1.0	POINT EFFICIENCY = 39998
ALPHA1 = 20.11	51	1.0	52	1.0	POINT EFFICIENCY = 39610
ALPHA1 = 20.14	51	1.0	52	1.0	POINT EFFICIENCY = 39223
ALPHA1 = 20.18	51	1.0	52	1.0	POINT EFFICIENCY = 38835
ALPHA1 = 20.22	51	1.0	52	1.0	POINT EFFICIENCY = 38448
ALPHA1 = 20.25	51	1.0	52	1.0	POINT EFFICIENCY = 38060
ALPHA1 = 20.29	51	1.0	52	1.0	POINT EFFICIENCY = 37673
ALPHA1 = 20.33	51	1.0	52	1.0	POINT EFFICIENCY = 37285
ALPHA1 = 20.36	51	1.0	52	1.0	POINT EFFICIENCY = 36898
ALPHA1 = 20.40	51	1.0	52	1.0	POINT EFFICIENCY = 36510
ALPHA1 = 20.44	51	1.0	52	1.0	POINT EFFICIENCY = 36123
ALPHA1 = 20.47	51	1.0	52	1.0	POINT EFFICIENCY = 35735
ALPHA1 = 20.51	51	1.0	52	1.0	POINT EFFICIENCY = 35348
ALPHA1 = 20.55	51	1.0	52	1.0	POINT EFFICIENCY = 34960
ALPHA1 = 20.58	51	1.0	52	1.0	POINT EFFICIENCY = 34573
ALPHA1 = 20.62	51	1.0	52	1.0	POINT EFFICIENCY = 34185
ALPHA1 = 20.66	51	1.0	52	1.0	POINT EFFICIENCY = 33798
ALPHA1 = 20.69	51	1.0	52	1.0	POINT EFFICIENCY = 33410
ALPHA1 = 20.73	51	1.0	52	1.0	POINT EFFICIENCY = 33023
ALPHA1 = 20.77	51	1.0	52	1.0	POINT EFFICIENCY = 32635
ALPHA1 = 20.80	51	1.0	52	1.0	POINT EFFICIENCY = 32248
ALPHA1 = 20.84	51	1.0	52	1.0	POINT EFFICIENCY = 31860
ALPHA1 = 20.88	51	1.0	52	1.0	POINT EFFICIENCY = 31473
ALPHA1 = 20.91	51	1.0	52	1.0	POINT EFFICIENCY = 31085
ALPHA1 = 20.95	51	1.0	52	1.0	POINT EFFICIENCY = 30698
ALPHA1 = 20.99	51	1.0	52	1.0	POINT EFFICIENCY = 30310
ALPHA1 = 21.02	51	1.0	52	1.0	POINT EFFICIENCY = 29923
ALPHA1 = 21.06	51	1.0	52	1.0	POINT EFFICIENCY = 29535
ALPHA1 = 21.10	51	1.0	52	1.0	POINT EFFICIENCY = 29148
ALPHA1 = 21.14	51	1.0	52	1.0	POINT EFFICIENCY = 28760

018



ALPHA1 = 23.00 S1 = -1.0 DC = -1.0 POINT EFFICIENCY = .53423  
ALPHA2 = 23.03 S2 = -1.0 POINT EFFICIENCY = .53423  
CYCLE EFFICIENCY = .513

APPENDIX D  
GEOMETRY OF GENERAL CLOCK GEAR TOOTH

The general ogival tooth of thickness  $t$  and outside radius  $r_o$  consists of a circular arc of radius  $\rho$  which blends tangentially into a radial tooth flank, as shown in Figure D-1 (only one center of curvature is indicated). The center of curvature,  $C$ , is located at a distance  $a$  from the center of the gear or pinion. Frequently this distance  $a$  equals the pitch radius  $r_p$ . The tooth geometry may either be described with the help of the parameters  $t$ ,  $\rho$  and  $a$ , or with the combination  $t$ ,  $\rho$  and  $r_o$ . Both approaches are shown below.

1. TOOTH GEOMETRY WITH HELP OF PARAMETERS  $t$ ,  $\rho$  AND  $a$

$C_x$  and  $C_y$  represent the coordinates of the center of curvature

C.  $C_x$  is defined by

$$C_x = \rho - \frac{t}{2} \quad (D-1)$$

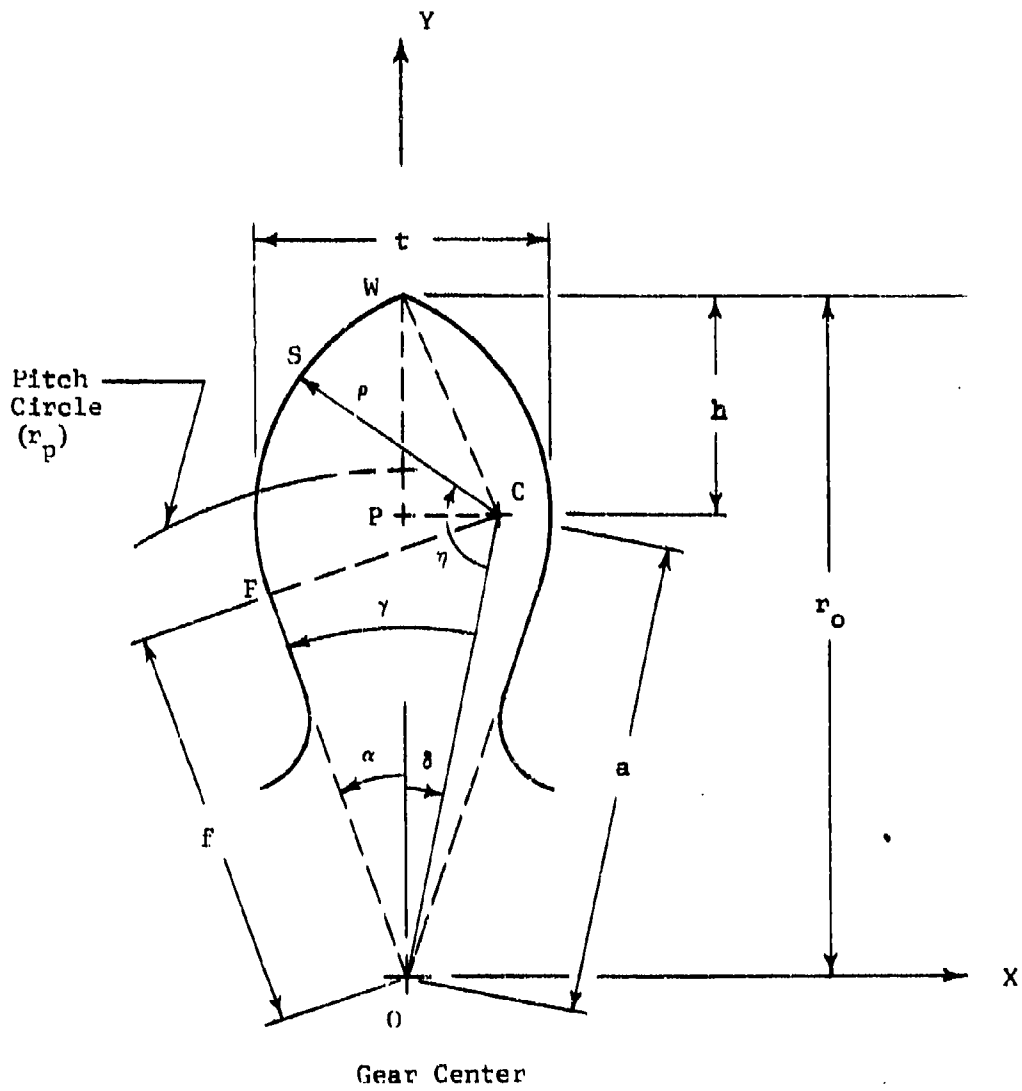


FIGURE D-1

GEOMETRY OF OGIVAL TOOTH (ONLY ONE CENTER OF CURVATURE SHOWN)

The angle  $\delta$  is given by

$$\delta = \sin^{-1} \frac{C_x}{a} \quad (D-2)$$

With the above,

$$C_y = a \cos \delta \quad (D-3)$$

Further, the outside radius  $r_o$  may be computed from

$$r_o = C_y + \sqrt{\rho^2 - C_x^2} \quad (D-4)$$

The angle  $\gamma$  is obtained from

$$\gamma = \sin^{-1} \frac{\rho}{a}, \quad (D-5)$$

and the flank angle  $\alpha$  from

$$\alpha = \gamma - \delta \quad (D-6)$$

The distance,  $f$ , from the center of rotation,  $O$ , to the blend point,  $F$ , of the flank of the tooth, is given by

$$f = a \cos \gamma \quad (D-7)$$

The angle  $\eta$  defines the tooth contact point  $S$  on the ogival, i.e., circular, portion of the tooth with the lines  $OC$  and  $CS$ . The minimum and maximum angles  $\eta_{\min}$  and  $\eta_{\max}$  are, respectively,

$$\eta_{\min} = \frac{\pi}{2} - \gamma \quad (D-8)$$

and

$$\eta_{\max} = \sin^{-1} \frac{r_o \sin \delta}{\rho} \quad (D-9)$$

(This angle extends into the second quadrant)

## 2. TOOTH GEOMETRY FROM PARAMETERS $\rho$ , $t$ AND $r_o$

If the outside radius,  $r_o$ , is given, distance  $a$  must be computed. The length,  $C_x$ , is still given by Equation (D-1), while

$$a = \sqrt{(r_o - h)^2 + C_x^2} \quad (D-10)$$

where, according to Figure D-1,

$$h = \sqrt{\rho^2 - C_x^2} \quad (D-11)$$

All other quantities of interest remain as before, i.e.,

$$\delta = \sin^{-1} \frac{C_x}{a} \quad \text{See Equation (D-2)}$$

$$\gamma = \sin^{-1} \frac{\rho}{a} \quad \text{See Equation (D-5)}$$

$$\alpha = \gamma - \delta \quad \text{See Equation (D-6)}$$

$$f = a \cos \gamma \quad \text{See Equation (D-7)}$$

$$\eta_{\min} = \frac{\pi}{2} - \gamma \quad \text{See Equation (D-8)}$$

$$\eta_{\max} = \sin^{-1} \frac{r_o \sin \delta}{\rho} \quad \text{See Equation (D-9)}$$

## APPENDIX E

### KINEMATICS AND MOMENT INPUT-OUTPUT RELATIONSHIP FOR SINGLE STEP-UP GEAR MESH WITH CLOCK TEETH

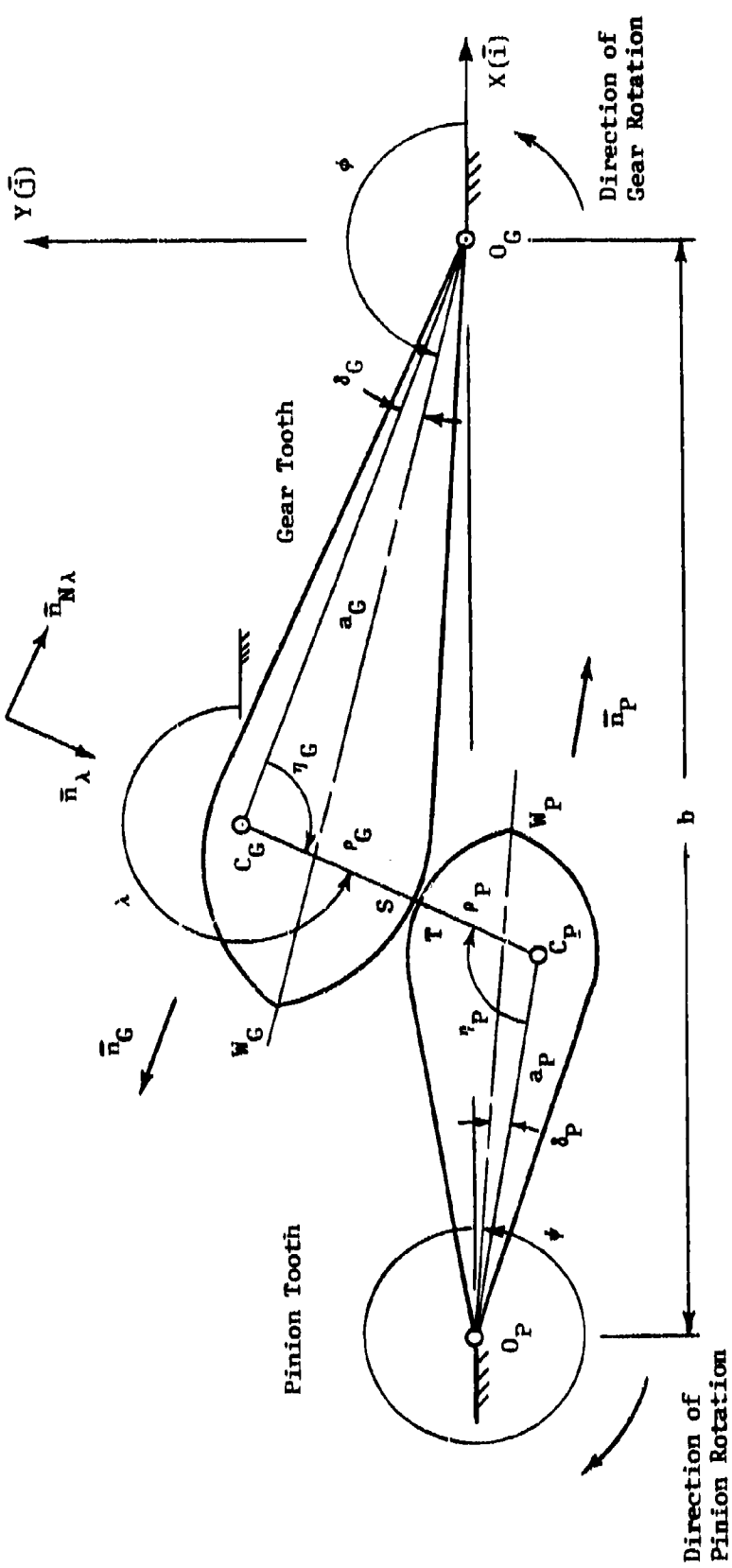
This appendix shows the kinematics of a single step-up gear mesh with ogival teeth and derives the moment input-output relationship. Both contact and pivot friction are included.

#### 1. KINEMATICS OF AN OGIVE MESH

Figure E-1 indicates the condition of initial contact in ogival meshes when the circular arc portion of the gear tooth drives the circular arc portion of the pinion tooth.<sup>1</sup> This type of direct contact will be called "round on round". As the motion progresses, the circular arc of the gear tooth moves into contact with the straight flank of the pinion tooth (Figure E-2). During this "round on flat" phase, distance  $g$  at first decreases and then increases again. Before round on round contact can again occur for a given mesh, i.e.,  $g$  has become equal to  $f_p$  again, the subsequent mesh comes into engagement with round on round contact. (See below.)

---

<sup>1</sup>See section b-VII of this appendix for a check that indicates whether the initial contact is round on round or whether possibly the round portion of the pinion touches the flat portion of the gear.



E-2

FIGURE E-1

ROUND ON ROUND PHASE OF CONTACT (GEAR DRIVES PINION)

The kinematics of both round on round and round on flat phases will be given first. Further it will be shown how to determine those gear angles,  $\phi$ , at which the regime changes from round on round to round on flat, and at which contact is taken over by the subsequent set of teeth. Since the ratio of angular velocities between gear and pinion varies with contact point, and the pinion moves faster for a given gear speed for round on round than for round on flat, the original set of teeth disengages as soon as the subsequent one makes contact. Thus, the contact ratio is unity for this type of gearing.

The gear tooth nomenclature given in Appendix D is used throughout. The additional subscripts G and P refer to gear and pinion, respectively.

#### a. ROUND ON ROUND PHASE OF MOTION

Figure E-1 shows the input angle  $\phi$  as the angle between the x-axis and the center line,  $O_G W_G$ , of the gear tooth. The output angle,  $\psi$ , is the angle between the x-axis and the centerline  $O_P W_P$ . During this phase of motion, the line connecting the centers of curvature  $C_G$  and  $C_P$  is of constant length  $L = r_G + r_P$  and passes

through the instantaneous contact points S on the gear and T on the pinion. Because of this constant length one may obtain both the output angle  $\psi$  and the "coupler" angle  $\lambda$  from the equivalent four-bar linkage  $O_G-C_G-C_P-O_P$ , with ground pivot distance  $b$ .

### I. UNIT VECTORS AND ANGLES $\eta_G$ AND $\eta_P$

The unit vectors associated with round on round phase are given now.

In direction  $O_G-C_G$

$$\bar{n}_G = \cos(\phi - \delta_G)\bar{I} + \sin(\phi - \delta_G)\bar{J} \quad (E-1)$$

In direction  $C_G-C_P$

$$\bar{n}_\lambda = \cos\lambda\bar{I} + \sin\lambda\bar{J} \quad (E-2)$$

The unit vector normal to  $\bar{n}_\lambda$  (in the right hand sense) becomes

$$\bar{n}_{N\lambda} = -\sin\lambda\bar{I} + \cos\lambda\bar{J} \quad (E-3)$$

In direction  $O_P-C_P$ .

$$\bar{n}_P = \cos(\psi - \delta_P)\bar{I} + \sin(\psi - \delta_P)\bar{J} \quad (E-4)$$

Since  $\lambda - (\phi - \delta_G) = \pi - \eta_G$

$$\eta_G = \pi + \phi - \lambda - \delta_G \quad (E-5)$$

The angle  $\eta_P$  is obtained from

$$\eta_P = (\psi - \delta_P) - \lambda \quad \text{for } \psi - \delta_P > 90^\circ \quad (E-6a)$$

and

$$\eta_P = 2\pi + (\psi - \delta_P) - \lambda \quad \text{for } \psi - \delta_P < 90^\circ \quad (E-6b)$$

The above values for  $\eta_G$  and  $\eta_P$  are only good for the round on round phase of the motion. For the round on flat phase the angle  $\eta_{GF}$  of the gear, may be of interest. (See Figure E-2).

This angle is given by:

$$\eta_{GF} = (\phi - \delta_G) - (\psi + \alpha_P) + \frac{3\pi}{2} \quad \text{for } \psi + \alpha_P > 90^\circ \quad (E-6c)$$

and

$$\eta_{GF} = (\phi - \delta_G) - (\psi + \alpha_P) - \frac{\pi}{2} \quad \text{for } \psi + \alpha_P < 90^\circ \quad (E-6d)$$

[Pinion flank in 4th quadrant]

[Pinion flank in first quadrant]

## II. DETERMINATION OF OUTPUT ANGLE $\psi$ AND "COUPLER" ANGLE $\lambda$

The loop equation of the equivalent four-bar linkage is given by

$$a_G \bar{n}_G + (\rho_G + \rho_P) \bar{n}_\lambda - a_P \bar{n}_P + b \bar{i} = 0 \quad (E-7)$$

With appropriate substitutions for the unit vectors, according to Equations (E-1), (E-2), and (E-4), one obtains the following component equation

$$a_G \cos(\phi - \delta_G) + L \cos \lambda + b - a_P \cos(\psi - \delta_P) = 0 \quad (E-8)$$

$$a_G \sin(\phi - \delta_G) + L \sin \lambda - a_P \sin(\psi - \delta_P) = 0 \quad (E-9)$$

where

$$L = \rho_G + \rho_P \quad (E-10)$$

To eliminate  $\lambda$ , let

$$\sin^2 \lambda + \cos^2 \lambda = 1 \quad (E-11)$$

Substitution of expressions for  $\sin\lambda$  and  $\cos\lambda$  from Equations (E-9) and (E-8), respectively, leads to

$$A_R \sin\psi + B_R \cos\psi = C_R \quad (E-12)$$

where

$$A_R = \sin(\phi - \delta_G) + \cos(\phi - \delta_G) \tan\delta_P + \frac{b}{a_G} \tan\delta_P$$

$$B_R = \cos(\phi - \delta_G) + \frac{b}{a_G} - \sin(\phi - \delta_G) \tan\delta_P$$

$$C_R = \frac{a_P^2 + a_G^2 + b^2 - L^2}{2a_P a_G \cos\delta_P} + \frac{b \cos(\phi - \delta_G)}{a_P \cos\delta_P}$$

Equation(E-12) is solved for  $\psi$  by a method similar to the one given on pg. 296 of R. S. Hartenberg and J. Denavit; Kinematic Synthesis of Linkages, McGraw-Hill Book Co., New York, 1964. Thus,

$$\psi = 2 \tan^{-1} \frac{A_R \pm \sqrt{A_R^2 + B_R^2 - C_R^2}}{B_R + C_R} \quad (E-13)$$

The correct sign in Equation (E-13) must be found from the geometric conditions of the equivalent four-bar linkage.

The "coupler" angle  $\lambda$  may now be determined either from Equation (E-8) or from Equation (E-9), i.e.,

$$\lambda = \cos^{-1} \left[ \frac{a_p \cos(\psi - \delta_p) - a_g \cos(\phi - \delta_g) - b}{L} \right] \quad (\text{E-14})$$

or

$$\lambda = \sin^{-1} \left[ \frac{a_p \sin(\psi - \delta_p) - a_g \sin(\phi - \delta_g)}{L} \right] \quad (\text{E-15})$$

### III. DETERMINATION OF OUTPUT PINION ANGULAR VELOCITY $\dot{\psi}$

Differentiation of Equation (E-12) with respect to time leads to

$$\dot{\psi} = \dot{\phi} \left[ \frac{A_{RD} \sin \psi + B_{RD} \cos \psi - C_{RD}}{A_R \cos \psi - B_R \sin \psi} \right] \quad (\text{E-16})$$

where  $A_R$  and  $B_R$  are given with Equation (E-12), and where

$$A_{RD} = \tan \delta_p \sin(\phi - \delta_g) - \cos(\phi - \delta_g)$$

$$B_{RD} = \sin(\phi - \delta_g) + \tan \delta_p \cos(\phi - \delta_g)$$

$$C_{RD} = \frac{b}{a_p \cos \delta_p} \sin(\phi - \delta_g)$$

E-8

#### IV. RELATIVE VELOCITY AT CONTACT POINT BETWEEN GEAR AND PINION

With point S on the gear and point T on the pinion, as shown by Figure E-1, the relative velocity between gear and pinion at the contact point is given by

$$\mathbf{V}_{S/T} = \mathbf{V}_{S/O_G} - \mathbf{V}_{T/O_P} \quad (\text{E-17})$$

This relative velocity is tangent to the contacting surfaces and can therefore be expressed in terms of the unit vector  $\bar{n}_{NA}$  (see Figure E-1). Then, the above becomes

$$\mathbf{V}_{S/T} = \left[ (\mathbf{V}_{S/O_G} \cdot \bar{n}_{NA}) - (\mathbf{V}_{T/O_P} \cdot \bar{n}_{NA}) \right] \bar{n}_{NA} \quad (\text{E-18})$$

or

$$\mathbf{V}_{S/T} = \left\{ \left[ \dot{\psi} \bar{k} \times (a_G \bar{n}_G + \rho_G \bar{n}_\lambda) \right] \cdot \bar{n}_{NA} - \left[ \dot{\psi} \bar{k} \times (a_P \bar{n}_P - \rho_P \bar{n}_\lambda) \right] \cdot \bar{n}_{NA} \right\} \bar{n}_{NA} \quad (\text{E-19})$$

Appropriate substitution of unit vectors and simplification results in

$$\mathbf{V}_{S/T} = \left\{ \dot{\psi} \left[ a_G \cos(\phi - \delta_G - \lambda) + \rho_G \right] - \dot{\psi} \left[ a_P \cos(\psi - \delta_P - \lambda) - \rho_P \right] \right\} \bar{n}_{NA} \quad (\text{E-20})$$

## b. ROUND ON FLAT PHASE OF MOTION

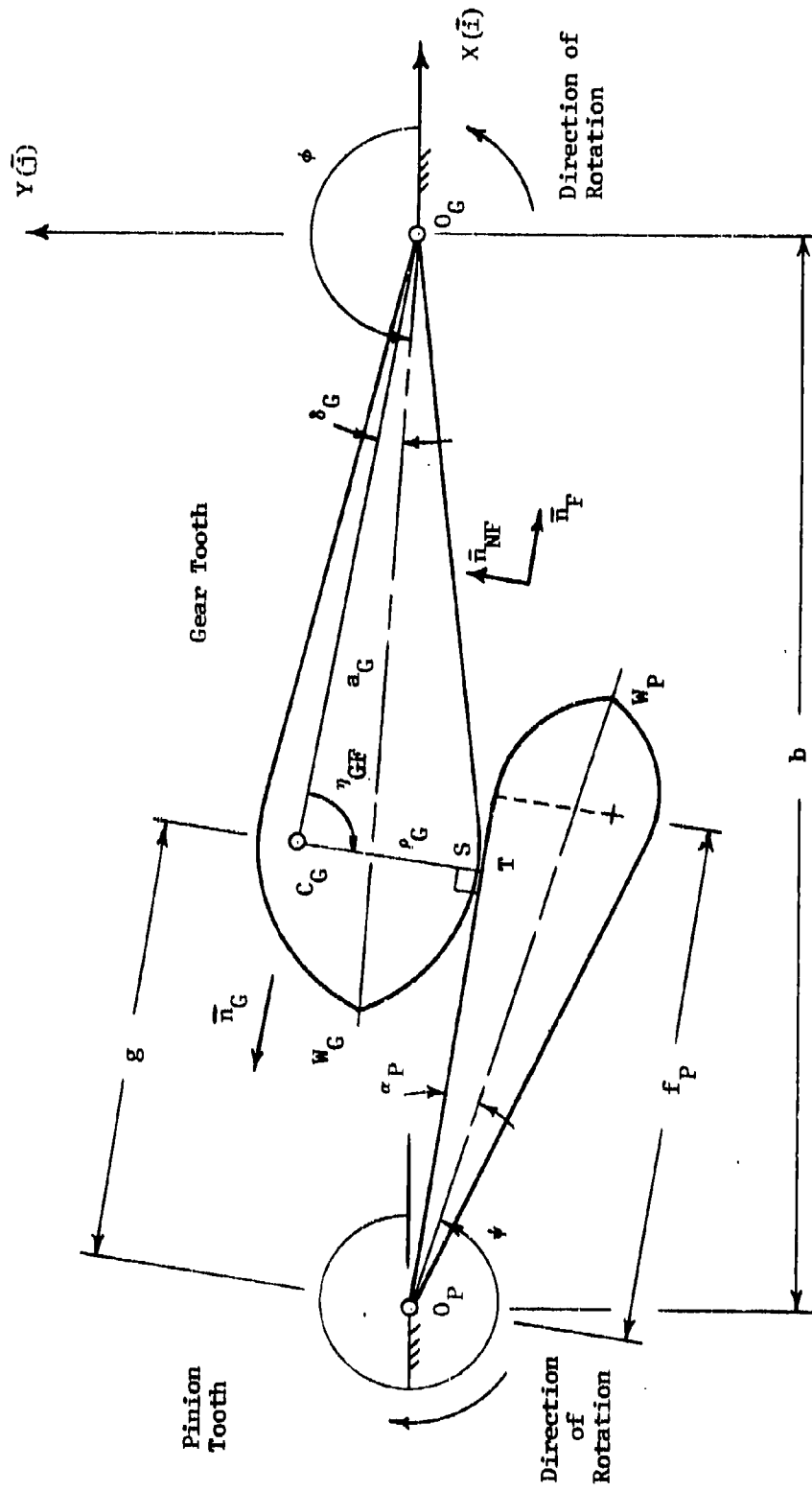
Figure E-2 gives the details of the round on flat contact between the driving gear and the driven pinion. The input angle  $\phi$  and the output angle  $\psi$  are again defined counter-clockwise between the x-axis and the respective tooth center lines  $O_G W_G$  and  $O_P W_P$ . Since contact is always made on the straight radial flank of the pinion, the line  $SC_G$  of the gear is always normal to the flank of the pinion. The contact point is at a distance  $g$  from the pinion center,  $O_P$ , and this distance is always smaller than, or equal to the distance  $f_P$  (which is defined by Equation (D-7) in Appendix D). Again, the subscripts G and P are used for gear and pinion tooth parameters, respectively.

### I. UNIT VECTORS

As before, the unit vector in direction  $O_G C_G$  is given by

$$\bar{n}_G = \cos(\phi - \delta_G)\bar{i} + \sin(\phi - \delta_G)\bar{j} \quad (E-21)$$

The unit vector in direction  $O_P T$ , along the flank of the pinion is given by



E-11

FIGURE E-2

ROUND ON FLAT PHASE OF CONTACT (GEAR DRIVES PINION)

$$\bar{n}_F = \cos(\psi + \alpha_P)\bar{i} + \sin(\psi + \alpha_P)\bar{j} \quad (E-22)$$

The unit vector in direction  $SC_G$  is normal to  $\bar{n}_F$  in the right hand sense

$$\bar{n}_{NF} = -\sin(\psi + \alpha_P)\bar{i} + \cos(\psi + \alpha_P)\bar{j} \quad (E-23)$$

## II. DETERMINATION OF OUTPUT ANGLE $\psi$ AND DISTANCE $g$

The vector equation for the mechanism loop  $O_G-C_G-S-T-O_P$ , which forms the basis of the desired solution, has the following form:

$$a_G\bar{n}_G - \rho_G\bar{n}_{NF} - g\bar{n}_F + b\bar{i} = 0 \quad (E-24)$$

Substitution of Equations (E-21) to (E-23) furnishes the component equations

$$a_G \cos(\phi - \delta_G) + \rho_G \sin(\psi + \alpha_P) - g \cos(\psi + \alpha_P) + b = 0 \quad (E25)$$

$$a_G \sin(\phi - \delta_G) - \rho_G \cos(\psi + \alpha_P) - g \sin(\psi + \alpha_P) = 0 \quad (E26)$$

From Equation (E-26) one obtains for  $g$

$$g = \frac{a_G \sin(\phi - \delta_G) - r_G \cos(\psi + \alpha_P)}{\sin(\psi + \alpha_P)} \quad (\text{E-27})$$

This expression for  $g$  is now substituted into Equation (E-25).

Rearrangement and simplification lead to

$$A_F \sin \psi + B_F \cos \psi = C_F \quad (\text{E-28})$$

where

$$A_F = b \cos \alpha_P + a_G \cos(\phi - \delta_G - \alpha_P)$$

$$B_F = b \sin \alpha_P - a_G \sin(\phi - \delta_G - \alpha_P)$$

$$C_F = -r_G$$

The solution of Equation (E-28) for  $\psi$  is obtained in the same way as that of Equation (E-13), i.e.,

$$\psi = 2 \tan^{-1} \frac{A_F \pm \sqrt{A_F^2 + B_F^2 - C_F^2}}{B_F + C_F} \quad (\text{E-29})$$

The correct sign in Equation (E-29) depends on the geometric conditions of the mechanism position as in all four-bar linkage solutions of this type.

### III. DETERMINATION OF PINION ANGULAR VELOCITY $\dot{\psi}$

Differentiation of Equation (E-28) with respect to time gives

$$\dot{\psi} = \dot{\phi} \left[ \frac{A_{FD} \sin \psi + B_{FD} \cos \psi}{A_F \cos \psi - B_F \sin \psi} \right] \quad (E-30)$$

where  $A_F$  and  $B_F$  are given with Equation (E-28) and where

$$A_{FD} = a_G \sin(\phi - \delta_G - \alpha_P)$$

$$B_{FD} = a_G \cos(\phi - \delta_G - \alpha_P)$$

### IV. RELATIVE VELOCITY AT CONTACT POINT BETWEEN GEAR AND PINION

As for round on round contact, the relative velocity between point S on the gear tooth and point T on the pinion tooth is tangent to the contacting surfaces. In this case it will have the direction of unit vector  $\mathbf{K}_F$  (see Figure E-2).

Then,

$$\bar{V}_{S/T} = \bar{V}_{S/O_G} - \bar{V}_{T/O_P} = \left[ (\bar{V}_{S/O_G} \cdot \bar{n}_F) - (\bar{V}_{T/O_P} \cdot \bar{n}_F) \right] \bar{n}_F \quad (E-31)$$

Since, because of the radial flank of the pinion, the velocity of the contact point T is normal to unit vector  $\bar{n}_F$ .

$$\bar{V}_{T/O_P} \cdot \bar{n}_F = 0 \quad (E-32)$$

Therefore,

$$\bar{V}_{S/T} = \left[ \bar{V}_{S/O_G} \cdot \bar{n}_F \right] \bar{n}_F \quad (E-33)$$

or

$$\bar{V}_{S/T} = \left\{ \left[ \dot{\phi} \bar{k} \times (a_G \bar{n}_P - \rho_G \bar{n}_{NF}) \right] \cdot \bar{n}_F \right\} \bar{n}_F \quad (E-34)$$

Appropriate substitution of unit vectors gives:

$$\bar{V}_{S/T} = \dot{\phi} \left[ \rho_G + a_G \sin(\psi - \phi + \alpha_P + \delta_G) \right] \bar{n}_F \quad (E-35)$$

V. DETERMINATION OF TRANSITION ANGLES FROM ROUND ON ROUND TO  
ROUND ON FLAT MOTION

The transition angles  $\phi_T$  and  $\psi_T$ , which occur when the round on flat phase follows the round on round one, may be determined with the help of the modified component equations (E-25) and (E-26), i.e., one lets  $\phi = \phi_T$ ,  $\psi = \psi_T$  and  $g = f_P$ . This results in

$$a_G \cos(\phi_T - \delta_G) + r_G \sin(\psi_T + \alpha_P) - f_P \cos(\psi_T + \alpha_P) + b = 0 \quad (E-36)$$

and

$$a_G \sin(\phi_T - \delta_G) - r_G \cos(\psi_T + \alpha_P) - f_P \sin(\psi_T + \alpha_P) = 0 \quad (E-37)$$

From the above,

$$\cos(\phi_T - \delta_G) = \frac{1}{a_G} [f_P \cos(\psi_T + \alpha_P) - b - r_G \sin(\psi_T + \alpha_P)] \quad (E-38)$$

and

$$\sin(\phi_T - \delta_G) = \frac{1}{a_G} [f_P \sin(\psi_T + \alpha_P) + r_G \cos(\psi_T + \alpha_P)] \quad (E-39)$$

The angle  $\psi_T$  may now be obtained by first eliminating  $\phi_T$  from Equations (E-38) and (E-39). This is accomplished with

$$\sin^2(\phi_T - \delta_G) + \cos^2(\phi_T - \delta_G) = 1 \quad (\text{E-40})$$

Substitution into the above leads to the following expression in  $\psi_T$ :

$$A_T \sin \psi_T + B_T \cos \psi_T = C_T \quad (\text{E-41})$$

where

$$A_T = r_G \cos \alpha_P + f_P \sin \alpha_P$$

$$B_T = r_G \sin \alpha_P - f_P \cos \alpha_P$$

$$C_T = \frac{a_G^2 - f_P^2 - b^2 - r_G^2}{2b}$$

Equation (E-41) is again solved in the manner of Equation (E-13)

$$\psi_T = 2 \tan^{-1} \frac{A_T \pm \sqrt{A_T^2 + B_T^2 - C_T^2}}{B_T + C_T} \quad (\text{E-42})$$

The correct sign must again be determined from the geometric conditions.

The associated transition angle  $\phi_T$  can now be obtained either with the help of Equation (E-38) or Equation (E-39):

$$\phi_T = \cos^{-1} \left[ \frac{f_P \cos(\psi_T + \alpha_P) - r_G \sin(\psi_T + \alpha_P) - b}{a_G} \right] + \delta_G$$

(E-43)

or

$$\phi_T = \sin^{-1} \left[ \frac{f_P \sin(\psi_T + \alpha_P) + r_G \cos(\psi_T + \alpha_P)}{a_G} \right] + \delta_G$$

(E-44)

VI. SENSING GEOMETRY FOR THE DETERMINATION OF CONTACT OF  
SUBSEQUENT TOOTH MESH

The following derives a computer sensing equation which indicates when contact is transferred from one tooth mesh to the succeeding one. Figure E-3 illustrates the case. The active mesh is in the round on flat mode and the subsequent mesh will make its initial contact in the round on round mode. This

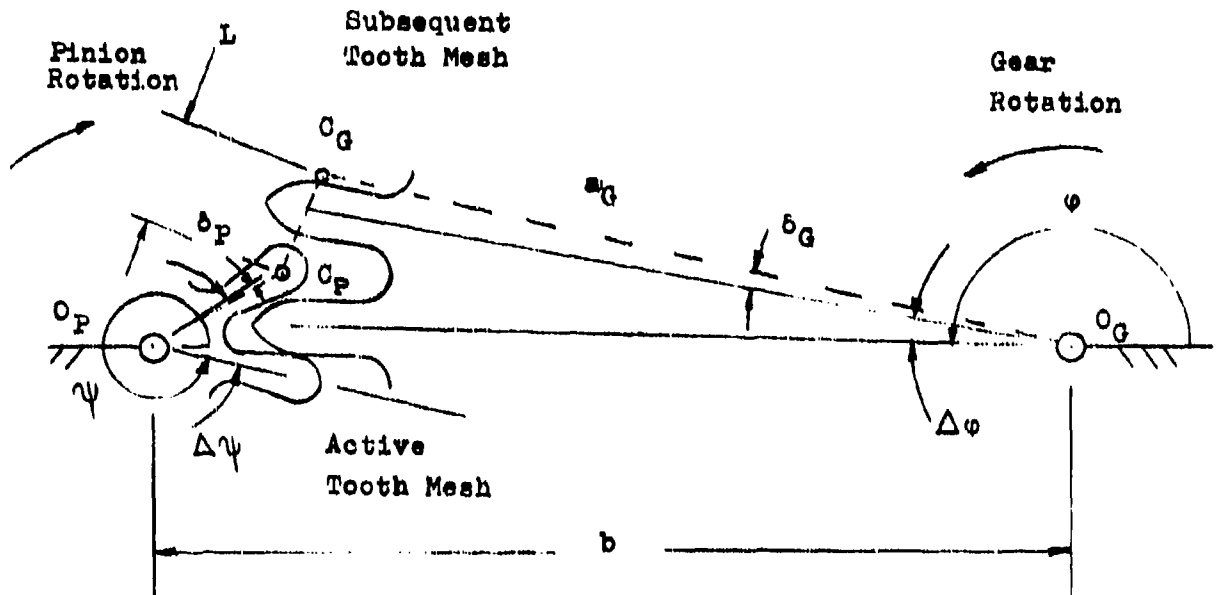


Figure E3  
Sensing Geometry for Contact of  
Subsequent Tooth Mesh

assertion is based on experience with the three gear and pinion combinations of the M125A1 booster. In each of these instances, the subsequent mesh makes contact before the round of the gear has left the flat of the pinion in the active mesh, i.e.,  $g < f_p$ . (See work in section V.) It has also been found that initial contact of the subsequent mesh is always in the round on round mode. Generally, contact between the flat of the gear and the round of the pinion does not occur, and it has not been considered in this report. Section VII gives a criterion for the existence of this inverted round on flat mode of contact.

Once contact has been made by the subsequent mesh it becomes the new active mesh. This can be proven by the fact that, for a given angular velocity  $\dot{\phi}$  of the gear, the angular velocity of the pinion is always larger in the initial stages of the round on round mode than in the final stages of the round on flat one. Thus, once the new mesh has made contact, the old one separates rapidly and the "contact ratio" is always unity.

The above may be shown theoretically by the position of the instant center of rotation between the gear and the pinion on line  $O_G O_P$ .

If  $\Delta\phi$  and  $\Delta\psi$  represent the angles between the individual tooth center lines of the gear and pinion, respectively, (see Figure E-3), the

closure equation for the subsequent mesh may be written in terms of the active mesh as follows:

$$\begin{aligned}
 a_p [\cos(\psi - \delta_p + \Delta\psi)\bar{i} + \sin(\psi - \delta_p + \Delta\psi)\bar{j}] + L_x\bar{i} + L_y\bar{j} \\
 = b\bar{i} + a_g [\cos(\phi - \delta_g - \Delta\phi)\bar{i} + \sin(\phi - \delta_g - \Delta\phi)\bar{j}]
 \end{aligned}
 \tag{E-45}$$

where  $L_x, L_y =$  components of the distance  $L = C_p C_g$

$\psi =$  pinion angle determined from round on flat mode according to Equation (E-29)

The components  $L_x$  and  $L_y$  may be obtained from Equation (E-45):

$$L_x = b + a_g \cos(\phi - \delta_g - \Delta\phi) - a_p \cos(\psi - \delta_p + \Delta\psi)
 \tag{E-46}$$

and

$$L_y = a_g \sin(\phi - \delta_g - \Delta\phi) - a_p \sin(\psi - \delta_p + \Delta\psi)
 \tag{E-47}$$

Contact will have occurred when the distance  $L$  becomes equal to, or slightly smaller than, the sum of the two radii of curvature  $\rho_G$  and  $\rho_P$ . Thus, the criterion of contact becomes:

$$\sqrt{L_x^2 + L_y^2} \leq \rho_G + \rho_P \quad (\text{E-48})$$

VII. POSSIBILITY OF FLAT OF GEAR MAKING CONTACT WITH THE  
ROUND PORTION OF THE PINION

Figure E-4 shows a transition configuration in which the flat part of the gear tooth makes contact with the circular arc of the pinion, i.e.,  $\overline{O_G S} = f_G$ . The radius of curvature  $\rho_P$  of the pinion will only then be normal to the flat of the gear

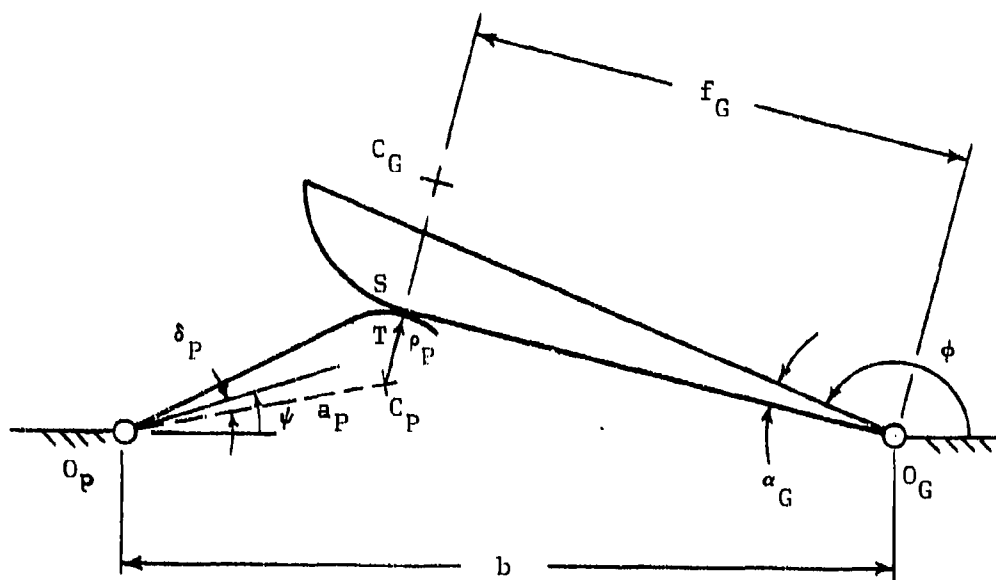


FIGURE E-4

FLAT OF GEAR CONTACTS ROUND OF PINION

when  $\overline{O_G S} \leq f_G$ . Accordingly, in order to avoid this type of contact, the following criterion must be met:

$$b > \left[ a_p + \sqrt{f_G^2 + p_p^2} \right] \quad (E-49)$$

The three gear meshes of the M125A1 booster always satisfy equation (E-49), and therefore the initial contact is made in the round on round mode.

## 2. MOMENT INPUT-OUTPUT RELATIONSHIP FOR SINGLE STEP-UP GEAR MESH WITH OGIVAL TEETH

The present section concerns itself with the determination of the equilibrant moment  $M_o$  acting on the output pinion of a single ogival mesh, when the input moment  $M_{in}$ , which acts on the gear, is given. This relationship must be derived both for the round on round and for the round on flat phases of the motion. The directions of the pivot friction forces are again chosen such that the resulting moments oppose the motion of the respective component. (See Appendix A.) The magnitude of these friction moments is expressed in the manner of equation (A-2) of the aforementioned appendix. The direction of the friction force of the gear on the pinion is the same as the direction of the relative velocity  $V_{S/T}$ , of the gear contact point S with respect to the pinion contact point T. This will be expressed by the appropriate signum convention. It must also be remembered that the kinematic expressions must conform to the motion phase under consideration.

a. INPUT-OUTPUT RELATIONSHIP FOR THE ROUND ON ROUND PHASE OF MOTION

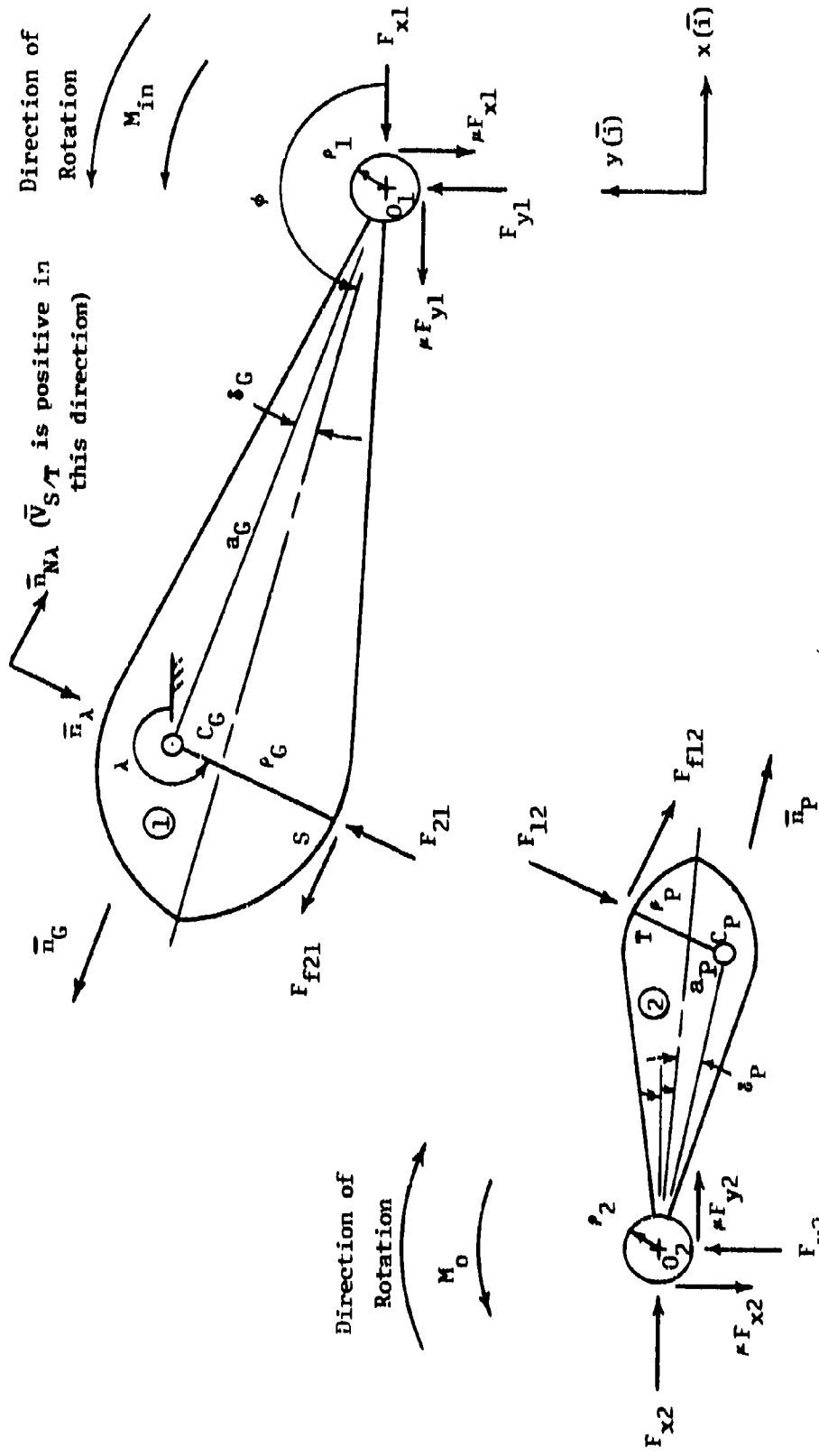
Figure E-5 shows the free body diagrams for the round on round phase of motion with the gear considered to be component no. 1 and the pinion defined as component no. 2. The contact forces  $F_{12}$  and  $F_{21}$  are expressed with the help of the unit vector  $\bar{n}_\lambda$  [see equation (E-2)]. This unit vector is always normal to both contacting surfaces at points S and T. The unit vector  $\bar{n}_{N\lambda}$  is used to describe the direction of the friction forces at the contact point. The sense of these friction forces is determined with the help of

$$s = \frac{v_{S/T}}{|v_{S/T}|} \quad (E-50)$$

(See equation (E-20) for  $\bar{v}_{S/T}$ .) Since the friction force  $F_{f12}$  of the gear on the pinion has the same direction as the relative velocity  $v_{S/T}$ , one may write

$$\bar{F}_{f12} = \mu s F_{12} \bar{n}_{N\lambda} \quad (E-51)$$

where  $\mu$  represents the coefficient of friction at the contact point.



E-27

FIGURE E-5

FREE BODY DIAGRAM FOR ROUND ON ROUND PHASE

Since

$$\bar{F}_{21} = -F_{12}\bar{n}_\lambda \quad (E-52)$$

the friction force of the pinion on the gear becomes

$$\bar{F}_{f21} = -\mu_s F_{12}\bar{n}_{N\lambda} \quad (E-53)$$

### I. FORCE AND MOMENT EQUILIBRIUM OF THE GEAR

The force equilibrium of the gear is assured when

$$-F_{12}\bar{n}_\lambda - \mu_s F_{12}\bar{n}_{N\lambda} - F_{x1}\bar{i} + F_{y1}\bar{j} - \mu F_{y1}\bar{i} - \mu F_{x1}\bar{j} = 0 \quad (E-54)$$

In the above  $\mu$  also stands for the pivot coefficient of friction.

Moment equilibrium is given by

$$M_{in}\bar{k} - \mu\rho_1\sqrt{F_{x1}^2 + F_{y1}^2}\bar{k} + [a_G\bar{n}_G + \rho_G\bar{n}_\lambda] \times [-F_{12}\bar{n}_\lambda - \mu_s F_{12}\bar{n}_{N\lambda}] = 0 \quad (E-55)$$

The unit vector  $\bar{n}_G$  is defined by equation (E-1).

The following component equations may be obtained from equation (E-54):

$$-F_{12}\cos\lambda + \mu s F_{12}\sin\lambda - F_{x1} - \mu F_{y1} = 0 \quad (E-56)$$

and

$$-F_{12}\sin\lambda - \mu s F_{12}\cos\lambda + F_{y1} - \mu F_{x1} = 0 \quad (E-57)$$

After substitution and cross-multiplication, one obtains the moment expression, equation (E-55), in scalar form:

$$M_{in} - \mu \rho_1 \sqrt{F_{x1}^2 + F_{y1}^2} + F_{12} \left[ -\mu s \rho_G + a_G \sin(\phi - \delta_G - \lambda) - \mu s a_G \cos(\phi - \delta_G - \lambda) \right] = 0 \quad (E-58)$$

Simultaneous solution of equations (E-56) and (E-57) for  $F_{x1}$  and  $F_{y1}$  results in

$$F_{x1} = -F_{12} \left[ \frac{(1 + \mu^2 s)\cos\lambda + \mu(1 - s)\sin\lambda}{1 + \mu^2} \right] \quad (E-59)$$

and

$$F_{y1} = F_{12} \left[ \frac{(1 + \mu^2 s)\sin\lambda - \mu(1 - s)\cos\lambda}{1 + \mu^2} \right] \quad (E-60)$$

These results are now substituted in equation (E-58). Since  $s^2$  is unity and always positive, the resulting expression for  $F_{12}$  has the following form:

$$F_{12} = \frac{M_{in}}{\mu(\rho_1 + s\rho_G) + a_G[\mu s \cos(\phi - \delta_G - \lambda) - \sin(\phi - \delta_G - \lambda)]}$$

(E-61)

## II. FORCE AND MOMENT EQUILIBRIUM OF THE PINION

Force equilibrium of the pinion is assured by

$$F_{12}\bar{n}_\lambda + \mu s F_{12}\bar{n}_{N\lambda} + F_{x2}\bar{i} + F_{y2}\bar{j} + \mu F_{y2}\bar{i} - \mu F_{x2}\bar{j} = 0$$

(E-62)

Moment equilibrium must satisfy

$$M_o\bar{k} + \mu r_2 \sqrt{F_{x2}^2 + F_{y2}^2} \bar{k} + [a_p\bar{n}_p - r_p\bar{n}_\lambda] \times [F_{12}\bar{n}_\lambda + \mu s F_{12}\bar{n}_{N\lambda}] = 0$$

(E-63)

The unit vector  $\bar{n}_p$  is defined by equation (E-4).

Equation (E-62) gives rise to the following component equations:

$$F_{12} \cos \lambda - \mu s F_{12} \sin \lambda + F_{x2} + \mu F_{y2} = 0 \quad (E-64)$$

and

$$F_{12} \sin \lambda + \mu s F_{12} \cos \lambda + F_{y2} - \mu F_{x2} = 0 \quad (E-65)$$

The moment equation (E-63) becomes, in scalar form,

$$M_o + \mu r_2 \sqrt{F_{x2}^2 + F_{y2}^2} + F_{12} \left[ -\mu s r_p - a_p \sin(\psi - \delta_p - \lambda) + \mu s a_p \cos(\psi - \delta_p - \lambda) \right] = 0 \quad (E-66)$$

Simultaneous solution of equations (E-64) and (E-65) for  $F_{x2}$  and  $F_{y2}$  results in

$$F_{x2} = F_{12} \left[ \frac{\mu(1+s)\sin\lambda - (1-\mu^2s)\cos\lambda}{1+\mu^2} \right] \quad (E-67)$$

and

$$F_{y2} = -F_{12} \left[ \frac{\mu(1+s)\cos\lambda + (1+\mu^2s)\sin\lambda}{1+\mu^2} \right] \quad (E-68)$$

The above expressions are now substituted into equation (E-66). Again,  $s^2$  is unity and always positive, and the following expression may be obtained for the contact force  $F_{12}$  in terms of the equilibrant moment  $M_o$

$$F_{12} = \frac{M_o}{\mu(s_P r_2 - r_2) - s_P [\mu s \cos(\psi - \delta_P - \lambda) - \sin(\psi - \delta_P - \lambda)]} \quad (E-69)$$

### III. MOMENT INPUT-OUTPUT RELATIONSHIP

When equations (E-61) and (E-69) are set equal to each other, one obtains the following input-output relationship:

$$M_o = M_{in} \left[ \frac{\mu(s_R r_P - r_2) - s_P [\mu s_R \cos(\psi - \delta_P - \lambda) - \sin(\psi - \delta_P - \lambda)]}{\mu(r_1 + s_R r_G) + s_G [\mu s_R \cos(\phi - \delta_G - \lambda) - \sin(\phi - \delta_G - \lambda)]} \right] \quad (E-70)$$

To account for the fact that equ.(E-70) is only valid for the round on round phase of motion, the signum symbol has now been changed to  $s_R$ .

b. INPUT-OUTPUT RELATIONSHIP FOR ROUND ON FLAT PHASE OF MOTION

Figure E-6 gives the free body diagrams for the round on flat phase of the motion. Again, the gear is considered to be component no. 1, while the pinion is component no. 2. Using the unit vector  $\bar{n}_{NF}$ , of equation (E-22), which is normal to the flat side of the pinion to express the force  $\bar{F}_{12}$  of the gear on the pinion, one obtains

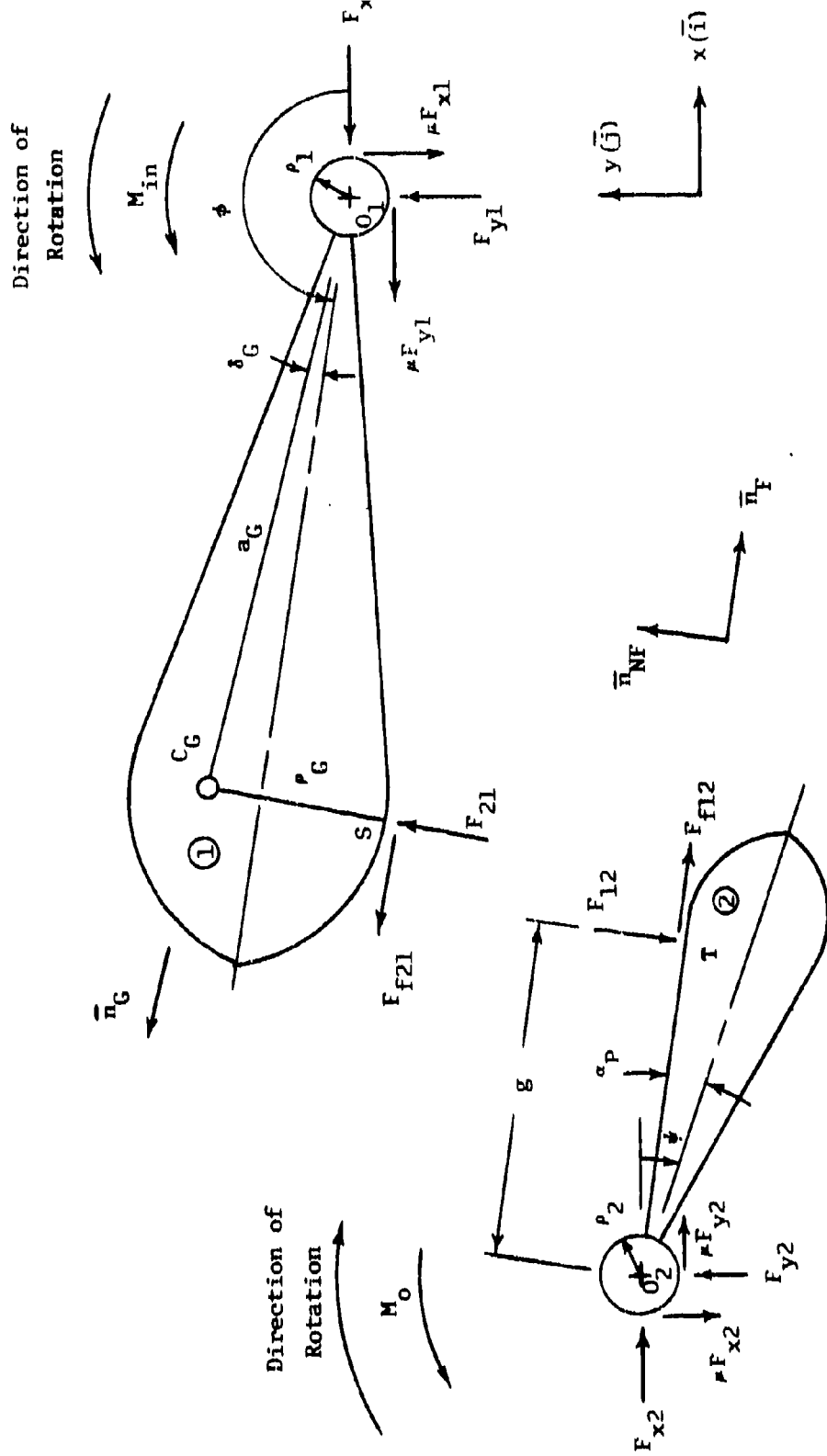
$$\bar{F}_{12} = -F_{12}\bar{n}_{NF} \quad (E-71)$$

The friction force of the gear on the pinion again has the same direction as the now applicable relative velocity  $\bar{v}_{S/T}$  of equation (E-35). With

$$s = \frac{v_{S/T}}{|v_{S/T}|} \quad (E-72)$$

as the applicable signum convention, the friction force  $\bar{F}_{f12}$  becomes

$$\bar{F}_{f12} = \mu s F_{12} \bar{n}_{NF} \quad (E-73)$$



E-34

Note:  $\psi$  is positive in  
ccw direction

FIGURE E-6

FREE BODY DIAGRAM FOR ROUND ON FLAT PHASE

The contact force  $\bar{F}_{21}$  of the pinion on the gear and the associated friction force are equal and opposite to the forces given by equations (E-71) and (E-73) respectively. Thus,

$$\bar{F}_{21} = F_{12} \bar{n}_{NF} \quad (E-74)$$

and

$$\bar{F}_{f21} = -\mu_s F_{12} \bar{n}_F \quad (E-75)$$

Note that the kinematics of the round on flat phase must now be used.

### I. FORCE AND MOMENT EQUILIBRIUM OF THE GEAR

Force equilibrium of the gear is given by

$$F_{12} \bar{n}_{NF} - \mu_s F_{12} \bar{n}_F - F_{x1} \bar{i} + F_{y1} \bar{j} - \mu F_{y1} \bar{i} - \mu F_{x1} \bar{j} = 0 \quad (E-76)$$

Moment equilibrium requires

$$M_{in} \bar{k} - \mu \rho_1 \sqrt{F_{x1}^2 + F_{y1}^2} \bar{k} + [a_G \bar{n}_G - \rho_G \bar{n}_{NF}] \times [F_{12} \bar{n}_{NF} - \mu_s F_{12} \bar{n}_F] = 0 \quad (E-77)$$

Equation (E-76) furnishes the following component expressions

$$-F_{12}\sin(\psi + \alpha_P) - \mu s F_{12}\cos(\psi + \alpha_P) - F_{x1} - \mu F_{y1} = 0 \quad (\text{E-78})$$

and

$$F_{12}\cos(\psi + \alpha_P) - \mu s F_{12}\sin(\psi + \alpha_P) + F_{y1} - \mu F_{x1} = 0 \quad (\text{E-79})$$

The scalar form of equation (E-77) is given by

$$M_{in} - \mu r_1 \sqrt{F_{x1}^2 + F_{y1}^2} + F_{12} \left[ -\mu s r_G + a_G \cos(\phi - \delta_G - \psi - \alpha_P) + \mu s a_G \sin(\phi - \delta_G - \psi - \alpha_P) \right] = 0 \quad (\text{E-80})$$

Simultaneous solution of equations (E-78) and (E-79) for  $F_{x1}$  and  $F_{y1}$  furnishes

$$F_{x1} = F_{12} \left[ \frac{\mu(1 - s)\cos(\psi + \alpha_P) - (1 + \mu^2 s)\sin(\psi + \alpha_P)}{1 + \mu^2} \right] \quad (\text{E-81})$$

and

$$F_{y1} = -F_{12} \left[ \frac{\mu(1 - s)\sin(\psi + \alpha_P) + (1 + \mu^2 s)\cos(\psi + \alpha_P)}{1 + \mu^2} \right] \quad (\text{E-82})$$

The above results are now substituted into equation (E-80).

Since  $s^2$  is again unity and positive at all times, the resulting expression for  $F_{12}$  becomes, in terms of  $M_{in}$ ,

$$F_{12} = \frac{M_{in}}{\mu(\rho_1 + s\rho_G) - a_G[\cos(\phi - \delta_G - \psi - \alpha_P) + \mu s \sin(\phi - \delta_G - \psi - \alpha_P)]}$$

(E-83)

## II . FORCE AND MOMENT EQUILIBRIUM OF THE PINION

Force equilibrium of the pinion is expressed by

$$-F_{12}\bar{n}_{NF} + \mu s F_{12}\bar{n}_F + F_{x2}\bar{i} + F_{y2}\bar{j} + \mu F_{y2}\bar{i} - \mu F_{x2}\bar{j} = 0$$

(E-84)

Moment equilibrium requires that

$$M_o\bar{k} + \mu\rho_2\sqrt{F_{x2}^2 + F_{y2}^2}\bar{k} + g\bar{n}_F \times (-F_{12}\bar{n}_{NF}) = 0$$

(E-85)

Equation (E-84) furnishes the following component equations

$$F_{12}\sin(\psi + \alpha_p) + \mu s F_{12}\cos(\psi + \alpha_p) + F_{x2} + \mu F_{y2} = 0$$

(E-86)

and

$$-F_{12}\cos(\psi + \alpha_p) + \mu s F_{12}\sin(\psi + \alpha_p) + F_{y2} - \mu F_{x2} = 0$$

(E-87)

The scalar form of the moment equation (E-85) becomes

$$M_0 + \mu p_2 \sqrt{F_{x2}^2 + F_{y2}^2} - s F_{12} = 0$$

(E-88)

Simultaneous solution of equations (E-86) and (E-87) for  $F_{x2}$

and  $F_{y2}$  leads to

$$F_{x2} = -F_{12} \left[ \frac{(1 - \mu^2 s)\sin(\psi + \alpha_p) + \mu(1 + s)\cos(\psi + \alpha_p)}{1 + \mu^2} \right]$$

(E-89)

and

$$F_{y2} = F_{12} \left[ \frac{(1 - \mu^2 s)\cos(\psi + \alpha_p) - \mu(1 + s)\sin(\psi + \alpha_p)}{1 + \mu^2} \right]$$

(E-90)

The above expressions are now substituted into equation (E-88). Again,  $s^2$  is unity and positive. The following expression for  $F_{12}$  is now obtained

$$F_{12} = \frac{M_0}{\mathcal{E} - \mu^2} \quad (\text{E-91})$$

### III. MOMENT INPUT-OUTPUT RELATIONSHIP

When equations (E-83) and (E-91) are set equal to each other, one obtains the following input-output relationship:

$$M_0 = M_{in} \left[ \frac{\mathcal{E} - \mu^2}{\mu(\rho_1 + s_F \rho_G) - s_G [\cos(\phi - \delta_G - \psi - \alpha_P) + \mu s_F \sin(\phi - \delta_G - \psi - \alpha_P)]} \right] \quad (\text{E-92})$$

Note that the signum symbol has been changed to  $s_F$  in the above expression to account for the fact that the expression is only valid in the round on flat phase of motion.

APPENDIX F  
COMPUTER MODELS FOR A SINGLE  
STEP-UP GEAR MESH WITH CLOCK TEETH

The present appendix contains descriptions, listings and sample outputs of the following computer models relating to single step-up gear meshes containing clock (ogival) teeth

1. Program CLOCK 1: Kinematics of single pass step-up gear mesh with clock (ogival) teeth
2. Program CLOCK 2: Point and cycle efficiencies for single pass step-up gear mesh with clock (ogival) teeth

The relevant background, the input parameters, the manner of the computations, and the form of the output of each program are discussed in detail. The program proper forms the last part of each section.

1. Program CLOCK 1: Kinematics of Single Pass Step-Up Gear  
Mesh With Clock (Ogival) Teeth

The program CLOCK 1 is based upon that portion of Appendix E which deals with the kinematics of single mesh step-up clock gearing. It may be used to check on the geometric performance of clock type meshes.

The nomenclature of the program is chosen to coincide as much as possible with that of Appendix D as well as that of Appendix E.

a. Input Parameters (see Program CLOCK 1, below)

The following parameters represent the input data for the program:

CAPRP =  $R_p$ , the pitch radius of the gear

RP =  $r_p$ , the pitch radius of the pinion

AG =  $a_G$ , the distance from the center of rotation of the gear to the center of curvature of the circular arc portion of the gear tooth

AP =  $a_p$ , the distance from the center of rotation of the pinion to the center of curvature of the circular arc portion of the pinion tooth

RHOG =  $\rho_G$ , the radius of curvature of the circular arc portion of the gear tooth

RHOP =  $\rho_p$ , the radius of curvature of the circular arc portion of the pinion tooth

TG =  $t_G$ , the maximum thickness of the gear tooth

TP =  $t_p$ , the maximum thickness of the pinion tooth

NG =  $n_G$ , the number of teeth of the gear

NP =  $n_p$ , the number of teeth of the pinion

K = range divisor

PHIDOT =  $\dot{\phi} = 1$ , all velocity computations are based on this value

b. Computations (see also COMMENT cards in program)

I. Computation of Gear Tooth Parameters

The following tooth parameters of the gear as well as of the pinion are first computed:

For the gear

CXG =  $c_{xG}$  (see eq. (D-1))

DELG =  $\delta_G$  (see eq. (D-2))

CYG =  $c_{yG}$  (see eq. (D-3))

ROG =  $r_{oG}$  (see eq. (D-4))

GAMMG =  $\gamma_G$  (see eq. (D-5))

ETMING =  $v_{minG}$  (see eq. (D-8))

ETMAXG =  $v_{maxG}$  (see eq. (D-9))

For the pinion

CXP =  $c_{xP}$  (see eq. (D-1))

DELP =  $\delta_p$  (see eq. (D-2))

CYP =  $c_{yP}$  (see eq. (D-3))

ROP =  $r_{oP}$  (see eq. (D-4))

GAMMP =  $\gamma_p$  (see eq. (D-5))

ALPHP =  $\alpha_p$  (see eq. (D-6))

ETMINP =  $v_{\min p}$  (see eq. (D-8))

ETMAXP =  $v_{\max p}$  (see eq. (D-9))

FP =  $f_p$  (see eq. (D-7))

### In general

B = b, the center distance between the gear and the pinion

DPHI =  $\Delta\phi$ , the angle between the center lines of adjacent gear teeth

DPSI =  $\Delta\psi$ , the angle between the center lines of adjacent pinion teeth

L (see eq. (E-10))

## II. Determination of Transition Angle

In order to define the ranges for the round on round and the round on flat phases of motion, it is first necessary to locate the transition angles  $\phi_T$  and  $\psi_T$ . This is accomplished with the help of the expression contained in section 1b-V, Appendix E. The transition angle  $\psi_T$  is first solved according to eq. (E-42). Since the solution furnishes two answers, i.e., the angles  $\psi_{T1}$  and  $\psi_{T2}$ , it is necessary to decide which of these is the desired one. The principal criterion for selecting the correct value of  $\psi_T$  is based on the motion of the contact point T with respect to the pinion. The first transition angles  $\psi_{T1}$  and  $\phi_{T1}$  occur as the contact point moves from the round portion of the pinion to the flat one (for increasing values of  $\phi$ ). As this motion is continued, the distance g becomes smaller than the transition parameter  $f_p$ . Once g has reached its minimum, the contact point moves outward on the

pinion flat until  $g$  theoretically equals  $f_p$  once again. This part of the motion is never completed in actuality since the subsequent set of teeth takes over before  $g$  reaches this transition value. It is this second transition situation which corresponds to the transition angles  $\psi_{T2}$  and  $\varphi_{T2}$ . Since the round on flat equation does not recognize any limitation on the length of the pinion flat, an increase of  $\varphi$  over the value of  $\varphi_{T2}$  will have associated with it a theoretical value for  $g$  which is larger than  $f_p$ . Thus, one may identify the correct value of  $\varphi_T$  and  $\psi_T$  by noting that an increase in the angle  $\varphi$  must lead to an associated value of  $g$  which is smaller than  $f_p$ .

The program uses this criterion in the following manner after  $\psi_{T1}$  and  $\psi_{T2}$  are known:

A. Subroutine TRANS is called and the angle  $\varphi_{T1}$ , which is associated with  $\psi_{T1}$ , is computed with the help of eqs. (E-43) and (E-44).

B. The angle  $\varphi$  is made slightly larger than  $\varphi_{T1}$  to produce PHINEXT, and eq. (E-29) is used to find the associated angle PSINEX. Since there are two such angles, the subroutine selects the one which is closest to the value of transition angle  $\psi_{T1}$ . Subsequently, the associated value of  $g_1$  is computed according to eq. (E-27).

C. Steps A and B are then repeated identically for the second transition angle  $\psi_{T2}$ . This results in the determination of  $g_2$ .

D. Control remains with the main program, and that value of  $\psi_T$  is chosen for which the associated value of  $g$  is smaller

than  $f_p$ .

For checking purposes, a subsidiary test for the determination of the transition angle was added to the program. It is based on the idea that, for the correct transition angle  $\psi_T$ , the line representing the flat portion of the pinion will make a smaller angle with the center line  $O_G O_P$  than will be the case for the incorrect one. To this end, TEST1 and TEST2 find both angles with the help of

$$\text{TEST} = 360^\circ - (\psi_T + \alpha_P) \quad (\text{F-1})$$

### III. Determination of Correct Sign for Round on Flat Regime

The sign preceding the square root in eq. (E-29), for the round on flat regime, is determined with the help of the angle  $\psi_T$ . The condition which yields that angle  $\psi$  which is closest to  $\psi_T$  governs. The variable SIGNF is used for the sign under consideration.

### IV. Computation of Final and Initial Values of $\varphi$ and $\psi$

The final and initial values of the gear and pinion angles are found by continuously evaluating the round on flat equation (E-29), using the previously determined value of SIGNF, and simultaneously checking the contact condition for the subsequent set of teeth, as given by eq. (E-48). This loop is initiated at the transition angle and terminated once the condition of eq. (E-48) is met. This allows the simultaneous determination

of both the angles at which the first set of teeth loses contact and at which the second set of teeth comes into engagement. The latter is accomplished by subtracting  $\Delta\varphi$  from the "loss of contact" angle  $\varphi_F$  and adding  $\Delta\psi$  to the "loss of contact" angle  $\psi_F$  (see computations following statement label no. 70). PHIF and PSIFF represent the angles when contact is lost for a given mesh, while PHII and PSII stand for the angles when initial contact is made.

#### V. Determination of Correct Sign for Round on Round Regime

Eq. (E-13) is used to determine the angle  $\psi$  while the gear and pinion are in the round on round regime. The correct sign in eq. (E-13) is obtained by comparing the value of the angle  $\psi$ , as computed with PHII, with the value of PSII. SIGNR is the variable which furnishes this sign.

#### VI. Kinematics

Since the limits as well as the correct signs for both the round on round and the round on flat regimes are known, the various kinematic properties of interest may now be computed.

The angular increment DDPHI of the input angle is found by dividing the range from PHII to PHIF into K parts. (K is the range divisor.) The computational loop begins with statement label no. 110 and ends with the third card from the end of the main program. The computation is terminated when the angle  $\varphi$  exceeds PHIF.

### A. Round on Round Regime

As long as PHI is smaller than the transition angle PHIT, the kinematics of the round on round phase of motion is computed. This results in the following:

$$\text{PSI} = \psi \text{ (see eq. (E-13))}$$

$$\text{LAMDA} = \lambda \text{ (see eqs. (E-14) and (E-15))}$$

$$\text{PSIDOT} = \dot{\psi} \text{ (see eq. (E-16))}$$

$$\text{VSTR} = \bar{v}_g/T \text{ for round on round (see eq. (E-20))}$$

$$\text{SR} = s \text{ (see eq. (E-50) for later use)}$$

$$\text{ETAPR} = \eta_p \text{ (see eqs. (E-6a) and (E-6b))}$$

$$\text{ETAGR} = \eta_G \text{ (see eq. (E-5)). For discussion of the usefulness of } \eta_p \text{ and } \eta_G, \text{ see output in section c below.)}$$

### B. Round on Flat Regime

When PHI is larger than the transition angle PHIT, the kinematics of the round on flat phase is computed. This computation includes the following:

$$\text{PSI} = \psi \text{ (see eq. (E-29))}$$

$$G = g \text{ (see eq. (E-27))}$$

$$\text{PSIDOT} = \dot{\psi} \text{ (see eq. (E-30))}$$

$$\text{VSTF} = \bar{v}_g/T \text{ for round on flat (see eq. (E-35))}$$

$$\text{SF} = s \text{ (see eq. (E-72) for later use)}$$

$$\text{ETAGF} = \eta_{GF} \text{ (see eqs. (E-6c) and (E-6d))}$$

c. Output (see Program CLOCK 1, below)

As previously, the output of the program is best explained with the help of the sample problem at the end of the program. It contains the following:

I. Input Parameters

CAPRP =  $R_p$  = .47725 in. (1.212 cm)  
RP =  $r_p$  = .09085 in. (0.231 cm)  
AG =  $a_G$  = .47725 in. (1.212 cm)  
AP =  $a_p$  = .09085 in. (0.231 cm)  
RHOG =  $r_G$  = .03870 in. (0.098 cm)  
RHOP =  $r_p$  = .01740 in. (0.044 cm)  
TG =  $t_G$  = .03480 in. (0.088 cm)  
TP =  $t_p$  = .02800 in. (0.071 cm)  
NG =  $n_G$  = 42  
NP =  $n_p$  = 8  
K = 50

II. Computed Values

The following parameters are printed out:

DELGD =  $\delta_G$  = 2.5880°  
DELPD =  $\delta_p$  = 2.1448°  
GAMMPD =  $\gamma_p$  = 11.0418°  
ALPHPD =  $\alpha_p$  = 8.8970°  
ETMINGD =  $\gamma_{\min G}$  = 85.3488°  
ETMAXGD =  $\gamma_{\max G}$  = 144.0484°

ETMINPD =  $\gamma_{\min P} = 78.9582^\circ$   
ETMAXPD =  $\gamma_{\max P} = 166.5870^\circ$   
FP =  $f_p = .08917$  in. (0.226 cm)

The printout concerning the transition angles consists of two lines. While the program automatically picks that transition configuration which leads to a decreasing value of  $g$  as  $\varphi$  is increased, both transition angles are printed out for checking purposes. Thus, one finds

$\varphi_{T1} = 186.36^\circ$      $\psi_{T1} = 308.63^\circ$      $g_1 = .0895$  in. (0.227 cm) TRST1 =  $42.47^\circ$   
 $\varphi_{T2} = 178.75^\circ$      $\psi_{T2} = 346.65^\circ$      $g_2 = .0888$  in. (0.226 cm) TRST2 =  $4.45^\circ$

Clearly, the second line represents the solution since  $g_2 = .0888$  for a slight increase in the angle  $\varphi$  over  $\varphi_T$ . This is less than the value of  $f_p = .08917$ . In addition, TRST2 furnishes the smaller number of degrees. Recall that TRST represents the angle between the flat of the pinion and the line connecting the pivots.

Furthermore, the program shows the initial and final angles of contact:

PHIID = the angle  $\varphi$  at initial contact  
PSIID = the angle  $\psi$  at initial contact  
PHIFD = the angle  $\varphi$  at final contact  
PSIFD = the angle  $\psi$  at final contact

Note that angle  $\phi$  increases while the angle  $\psi$  decreases from the beginning to the end of the contact.

The computational loop begins with PHIID and ends with PHIFD. Further, when PHID reaches the approximate value of PHITD, the output shifts from round on round parameters to round on flat ones. The purpose of the multiple output throughout the motion of the mesh is to gain insight concerning the behavior of the mesh as well as to be able to check geometric values.

The following conclusions may be drawn for either of the phases as well as in general for the gears under consideration.

A. Round on Round Phase ( $176.2623^\circ < \phi < 178.6623^\circ$ )

PSIDOT, the angular velocity of the pinion, is negative, and at all times near the "gear ratio" of  $42/8 = 5.25$ .

SR is printed here only for checking purposes. It becomes important in the moment input-output analyses of program CLOCK 2.

The angles ETAGRD and ETAPRD are of interest because one needs to make sure that the contact between gear and pinion does not occur too close to the respective tooth tips. This is necessary since the present mathematical model has a pointed tip while in a real situation the tips are rounded. Thus, if contact is sufficiently far from the tips of the teeth, the present model will give valid answers.

The range of ETAGRD is approximately between  $86^\circ$  and  $90^\circ$ . This is considerably smaller than the ETMAXGD of approximately  $144^\circ$  and larger than the ETMINGD of approximately  $85^\circ$ . (The

latter shows that the round of the pinion tooth does not touch the flat of the gear tooth.)

The angle ETAPRD of the pinion tooth is always considerably smaller than ETMAXPD. Since contact is transferred to the flat portion of the pinion at the end of this phase of motion, ETAPRD almost equals ETMINPD at that point.

LAMDAD is given for general checking purposes only.

B. Round on Flat Phase ( $178.6623^\circ < \varphi < 184.834^\circ$ )

The angular velocity  $\dot{\psi}$  continues relatively smoothly after the transition. The distance  $g$  remains smaller than  $f_p$ , as expected, and it reaches a minimum of .0822 in. at  $\varphi \approx 182.5^\circ$ . It is further to be noted that  $g$  never reaches the value of  $f_p$  again since the subsequent set of teeth takes over when  $g = .08439$  in. (0.214 cm). For the present program to be valid, it is necessary that contact ends before the round on flat phase is completed.

As before,  $s_F$  is given for checking purposes only, and its value has been confirmed, just as was done for  $s_R$ , by graphical analysis (not shown).

The angle ETAGFD of the gear reaches a maximum of approximately  $130^\circ$  at the end of this phase. Since this is well below the maximum value  $ETMAXGD = 144^\circ$ , there is enough margin for a tip radius on the gear tooth.

### C. General Considerations

As expected for a direct contact mechanism of this type, the angular velocity ratio, as represented by PSIDOT, is not constant and has a greater absolute value at initial contact than at final contact. This indicates that the pinion will speed up somewhat as the subsequent set of teeth comes into contact, and that therefore, the original set of teeth loses contact at that instant. This means that the "effective contact ratio" is unity.

Program CLOCK 1

F-14

C PROGRAM CLOCK I (INPUT, OUTPUT, TAPES=INPUT, TAP=OUTPUT)

C KINEMATICS OF SINGLE PASS STEP-UP GEAR MESH WITH CLOCK (OGIVAL) TEETH

5 REAL NP,NG,LX,LY,K,LAMDA,LANDAD

1 FORMAT(2F10.5)

READ(5,1)CAPR,RP

READ(5,1)AG,AP

READ(5,1)HOG,RHOP

READ(5,1)TG,TP

READ(5,2)NG,NP

2 FORMAT(2F10.0)

READ(5,3)K

3 FORMAT(F10.0)

PI = 3.14159

2 = PI/180.

PHIDOT = 1.

4 WRITE(6,\*)CAPR,RP,AG,AP

5 FORMAT(1E5,3E10,\*)

WRITE(6,\*)F7.5,3\*NP = F7.5,3\*RP = F7.5,3\*AG = F7.5,3\*AP

6 FORMAT(1E5,3E10,\*)

WRITE(6,\*)TG,TP

7 FORMAT(1E5,3E10,\*)

WRITE(6,\*)NG,NP = F7.5/

8 FORMAT(1E5,3E10,\*)

WRITE(6,\*)K

9 FORMAT(1E5,3E10,\*)

WRITE(6,\*)PHIDOT = F5.1/

10 FORMAT(1E5,3E10,\*)

WRITE(6,\*)K = F5.1/

11 C COMPUTATION OF GEAR LOGIN PARAMETERS

C CRG = RHOG - LG/LZ

DELG = ASIN(CRG/RG)

DELGD = DELG/2

CYG = AG\*COS(DELG)

RUG = CYG - SORT(HOG-RHOG - CRG\*CRG)

GAMMG = ASIN(RUG/AG)

GAMMGD = GAMMG/2

ELMNGD = 90. - GAMMGD

ELMNG = 180. - ASIN(RUG/SIN(DELG/RHOG))/2

CRP = RHOP - TP/LZ

DELP = DELP/2

CYP = AP\*COS(DELAP)

RUP = CYP - SORT(RHOP-RHOP - CRP\*CRP)

GAMMP = ASIN(RUP/AP)

GAMMPD = GAMMP/2

ALPHPD = ALPHP/2

ELMPO = 40. - GAMMPD

ELMXP0 = 180. - ASIN(RUP/SIN(DELPP/RHOP))/2

```

55 FP = AP*COS(GAMP)
   B = CAP*P
   DPMI = 360./NG*Z
   DPSI = 360./NP*Z
   L = RMDS + RMDP
   WRITE(6,10)DELGD,DELDP,GAMPD,ALPHAD,ETMINGD,ETMAIGD,ETMIND,
10 LETMAXDP,FP
   I = 1
   DO 100 FORMATTING,DELGZ,FP,ALPHAD,ETMINGD,ETMAIGD,ETMIND,
   CMPD,FP,ALPHAD,ETMINGD,ETMAIGD,ETMIND,ETMIND,
   C

```

```

55 C DETERMINATION OF TRANSITION ANGLE
   C

```

```

   AT = RMDS*COS(DELDP) - FP*SIN(GAMP)
   BT = RMDS*SIN(DELDP) + FP*COS(GAMP)
   CT = (AG*AG + FB*FB - AB*AB - RMDS*RMDS)/(2.*AB)
70 RDOTI = AT*AT + BT*BT - CT*CT
   Y1 = AT + SQR(RDOTI)
   Y2 = AT - SQR(RDOTI)
   XT = BT + CT

```

```

   PSII = 2.*ATAN2(Y1,XT)
   PSI2 = 2.*ATAN2(Y2,XT)
75 IF(PSII.LT.0.)PSII = PSII + 2.*PI
   IF(PSI2.LT.0.)PSI2 = PSI2 + 2.*PI
   IF(PSI2.GT.2.*PI)PSI2 = PSI2 - 2.*PI

```

```

90 CALL TRANS(RMDS,ALPHAD,FP,AG,AB,DELG,7,PSII,PHI1,EL1)
   CALL TRANS(RMDS,ALPHAD,FP,AG,AB,DELG,7,PSI2,PHI2,EL2)
   PHIID = PHI1/2
   PHI2D = PHI2/2

```

```

   TEST1 = 360. - (PSIID + ALPHAD)
   TEST2 = 360. - (PSI2D + ALPHAD)
   WRITE(6,11)PHIID,PSIID,EL1,TEST1
   WRITE(6,12)PHI2D,PSI2D,EL2,TEST2

```

```

11 FORMAT(5A,10F1.2)
   I = 1
12 FORMAT(5A,10F1.2)
   I = 2

```

```

IF(EL1.LT.FPIGO TO 24
PHI1 = PHI2
PSI1 = PSI2

```

```

95 GO TO 30
20 PHIT = PHI1
   PSI1 = PSI1
30 PHID = PHIT/2
   PSID = PSI1/2

```

```

100 C DETERMINATION OF CORRECT SIGN FOR ROUND ON FLAT REGIME
   C

```

```

   BF = B*COS(ALPHAD) - AG*COS(PHI1-DELG-ALPHAD)
   CF = B*SIN(ALPHAD) - AG*SIN(PHI1-DELG-ALPHAD)
   HOUTF = AF*AF + BF*BF + CF*CF
105

```

```

110 7F1 = AF * SORT(MODIFF)
    7F2 = BF * SORT(MODIFF)

```

```

    AF = BF * CF
    PSIF1 = 2.*ATAN2(Y1,X1)
    PSIF2 = 2.*ATAN2(Y2,X2)

```

```

    IF(PSIF1.LT. 0.)PSIF1 = PSIF1 + 2.*PI
    IF(PSIF2.LT. 0.)PSIF2 = PSIF2 + 2.*PI

```

```

    IF(ABS(PSIF1-PSIF2).LT. .000001)PSIF1=PSIF2

```

```

    SIGN = -1.

```

```

    GO TO 50

```

```

    40 SIGN = 1.

```

```

    C COMPUTATION OF FINAL AND INITIAL VALUES OF PHI AND PSI

```

```

    C

```

```

    50 DO 60 I=1,1000

```

```

    PHID = PHID + (1-I.)/100.
    PHI = PHID*Z

```

```

    AF = B*CDSTALPHA + AG*COS(PHI-DELG-ALPHA)
    BF = B*SIN(ALPHA) - AG*SIN(PHI-DELG-ALPHA)

```

```

    CF = -B*ROD

```

```

    AOOTF = AF*AF + BF*BF + CF*CF

```

```

    Y1 = AF * SIGN(SORT(AOOTF))
    Y2 = BF * CF

```

```

    PSIF = 2.*ATAN2(Y1,Y2)

```

```

    IF(PSIF.LT. 0.)PSIF = PSIF + 2.*PI

```

```

    LX = B * AG*COS(PHI-DELG-DMPI) - AP*COS(PSIF-DPSI-DELPH)

```

```

    LY = AG*SIN(PHI-DELG-DMPI) - AP*SIN(PSIF-DELPH-DPSI)

```

```

    IF(SORT(LX**2+LY**2).LT. .000001)GOTO 100-10-70

```

```

    60 CONTINUE

```

```

    PHIF = PHI
    PSIF = PSIF

```

```

    PHII = PHIF * DMPI
    PSII = PSIF * DPSI

```

```

    IF(PSII.GT. 2.*PI)PHII=PHII-2.*PI
    PHID = PHII/Z

```

```

    PSID = PSII/Z

```

```

    PSIF = PSIF/Z

```

```

    PHIF = PSIF/Z

```

```

    PSIF = PSIF/Z

```

```

    WRITE(6,88)PHID,PSID,PHIF,PSIF

```

```

    88 FORMATTED WRITE(6,9)PHID,PSID,PHIF,PSIF

```

```

    100 PSIFD = .0F9.4//11

```

```

    C

```

```

    C DETERMINATION OF CORRECT SIGN FOR ROUND ON ROUND REGIME

```

```

    C

```

```

    AR = SIN(PHII-DELG) * COS(PHII-DELG) * TAN(DELPH) + ROTAN(DELPH)/AG

```

```

    BR = COS(PHII-DELG) * B/AG - SIN(PHII-DELG) * LAM(DELPH)

```

```

    CR = (AP*AP + AG*AG + B*B - L*L)/(2.*AP*AG*COS(DELPH))

```

```

    150 COS(PHII-DELG)/AP=COS(DELPH)

```

```

    POOR = AR*AR + BR*BR - CR*CR

```

```

    PH1 = BR * SIGN(POOR)

```

```

    PH2 = AR - SORT(MODTR)

```

```

    PH = PH1 - CR

```

```

    PSIR = 2.*ATAN2(Y1,X1)

```

```

146 PSIM2 = 2.0*AIAP2(1+2,AG)
   IF(PSIM1.GT.0.0)PSI1 = PSI1 + 2.0*PI
   IF(PSIM2.LT.0.0)PSI2 = PSI2 - 2.0*PI
   IF(LAMB(SPSI) .GT. ABS(PSI) .LI. ABS(PSI) .PSIM2)GO TO 90
   SIGMA = -1.
165 GO TO 100
   90 SIGMA = 1.

```

C KINEMATICS

```

170 IUG DOPHI = 1.0*IF .PHI1/K
   PHI = PHI + DOPHI
110 PHI = PHI + DOPHI
   PHID = PHID + DOPHI
   IF(ABS(DEL.PHI) .GT. 120)
     AM = SIN(PHI) .DEL.G) + COS(PHI) .DEL.G)TAN(DEL.P) + N*TAN(DEL.P)/AG
     CM = COS(PHI) .DEL.G) + TAN(DEL.P) .SIN(PHI) .DEL.G)
     CH = (AP*AP + AG*AG + BG + L*P)/12.0*AP*AG*CUS(DEL.P)
     T = 1.0/COS(PHI) .DEL.G)TAN(DEL.P)
149 00014 = AM*AG + BM*BG + CM*CM
     T4 = AM*SIGMA + BM*BM + CM*CM
     AM = BM + CM

```

```

145 PSI = 2.0*ATAN2(T4,T3)
   IF(PSI .LT. 0.0)PSI = PSI + 2.0*PI
   PSIG = PSI
   SLAM = (AP*PSI .DEL.P) - AG*PSI(PHI) .DEL.G) //
   CLAM = (AP*COS(PSI) .DEL.P) - AG*COS(PHI) .DEL.G) //
   LAMDA = ATAN2(SLAM,CLAM)
   IF(LAMDA .GT. 0.0)LAMDA = LAMDA - 2.0*PI
   LAMDA0 = LAMDA //
   AMP = TAN(DEL.P) .DEL.G)TAN(PHI) .DEL.G) - COS(PHI) .DEL.G)
   AG0 = SIN(PHI) .DEL.G) + TAN(DEL.P) .COS(PHI) .DEL.G)
   BMO = 1.0/SIN(PHI) .DEL.G)TAN(DEL.P) - COS(PHI) .DEL.G)
   PSIDOT = (AP*PSI .DEL.P) + BMO*COS(PSI) - CM0 // (AP*COS(PSI) - BM0
   SIF(ABS(PSIDOT)
     VSTW = PSIDOT/AG*COS(PHI) .DEL.G)LAMBDA + BM05) - PSIDOT/AGP
     LUS = SIF*DEL.P*LAMDA //
     SW = VSTW/ABS(SIF)

```

```

200 IF(PSID0 .DEL.P0 .LT. 90)ETAP00 = 12.0*PI + PSI - LAMDA - DEL.P //
   IF(PSID0 .DEL.P0 .GT. 90)ETAP00 = (PSI - LAMDA - DEL.P) //
   ETAP00 = 180 - PHI - LAMDA - DEL.P //
   MATE(6,11)PHI0 = PSI0 + PSIDOT * SIF //
   IF(ABS(MATE(6,11) .DEL.G) .GT. 1.0)ETAP00 = 180 - PSI - LAMDA0 +
     1.0*SW * SIF * 3.1415926535897932384626433832795 //
     2.0*PI
   GO TO 110

```

```

210 100 AF = AG*CUS(ALMP) - AG*COS(PHI) .DEL.G)ALMP //
     BF = BSIN(ALMP) - AG*SIN(PHI) .DEL.G)ALMP //
     CF = BM*AG
     D00TF = AF*AF + BF*BF + CF*CF
     TF = AF + BF + CF

```



```

215 PSI = 2.*ATAN2(YF,XF)
      LEIPSI = LI. *ALIPSA = PSI * 2.*PI
      PSID = PSI/7
      G = (AG*SIN(PHI-DELG) - AH*G*2COS(PSI*ALPHA))/SIN(PSI*ALPHA)
      AFD = AG*SIN(PHI-DELG-ALPHA)
      AFD = AG*2COS(PHI-DELG-ALPHA)
      PSIDOT = PHIDOT*(AFD*SIN(PSI) + AFD*2COS(PSI))/(AF*2COS(PSI) - BF*
      1*SIN(PSI))
      VSTF = PHIDOT*(AH*H* + AG*SIN(PSI-2PHI-ALPHA-DELG))
      SF = VSTF/ABS(VSTF)
      IF (PSID-ALPHA) .GE. 90.1E16 AFD = (PHI-DELG-PSI-ALPHA)*3.*PI/2./Z
      IF (PSID-ALPHA) .LT. 90.1E16 AFD = (PHI-DELG-PSI-ALPHA)*3.*PI/2./Z
      WRITE(6,13) PHID, PSID, PSIDOT, SF, ETAGFU
      13) FORMATT(13) PHID = F9.4, PSID = F9.4, PSIDOT = F9.4, SF = F9.4, Z =
      106 = F7.5, 31 = SF = F4.1, 31 = ETAGFU = F9.4)
      GO TO 110
      STOP
      END
210

```

```

1  SUM(CU:INE TRANS(INOG*ALPH*FP*AG*DEL6*PSII,PHII*G)
   VI = 2*VI5V
5  SI = (FP*SI(PSII*ALPH) + INOG*COS(PSII*ALPH))/AG
   CI = (FP*CS(PSII*ALPH) - INOG*SI(PSII*ALPH)) - B/AG
   PHII = ATAN2(SI,CI) * DELG
   IF (PHII .LT. 0) PHII = PHII + 2*PI
   PSINE1 = PHII * .10Z
10  AF = B*CCOS(CPHI) - B*CCOS(PHINE1) - DELG - ALPH*P
   HF = B*OSIN(ALPH) - AG*SI(PHINE1 - DELG - ALPH)
   CF = INOG
   MOOIF = AF*HF + W*HF - CF*CF
   YF1 = AF - SQR(MOOIF)
   YF2 = AF - SQR(MOOIF)
   AF = BF + CF
15  PSINE1 = 2*ATAN2(YF1,BF)
   PSINE2 = 2*ATAN2(YF2,BF)
   IF (PSINE1 .LT. 0) PSINE1 = PSINE1 + 2*PI
   IF (PSINE2 .LT. 0) PSINE2 = PSINE2 + 2*PI
   IF (ABS(PSINE1-PSII) .LT. ABS(PSINE2-PSII)) GO TO 1
20  PSINE1 = PSINE2
   GO TO 2
   I PSINE1 = PSINE1
   C G = TAG*SI(PHINE1-DELG) - RHOG*COS(PSINE1*ALPH))/SI(PSINE1
   L ALPH)
   DEL6 =
   END

```

CONFIDENTIAL - SECURITY INFORMATION



PMID = 181.4822	PSID = 332.6464	PSID00T = -5.4823	6 = .08286	SF = 1.0	ETAGFD = 107.8542
PMID = 181.5766	PSID = 331.1581	PSID00T = -5.4591	6 = .08268	SF = 1.0	ETAGFD = 109.8635
PMID = 181.7488	PSID = 330.2245	PSID00T = -5.4328	6 = .08252	SF = 1.0	ETAGFD = 110.8695
PMID = 181.9194	PSID = 329.2959	PSID00T = -5.4011	6 = .08248	SF = 1.0	ETAGFD = 111.1695
PMID = 182.0993	PSID = 328.3729	PSID00T = -5.3663	6 = .08238	SF = 1.0	ETAGFD = 112.2629
PMID = 182.2823	PSID = 327.4562	PSID00T = -5.3278	6 = .08224	SF = 1.0	ETAGFD = 113.3511
PMID = 182.4337	PSID = 326.5464	PSID00T = -5.2859	6 = .08220	SF = 1.0	ETAGFD = 114.4323
PMID = 182.6852	PSID = 325.6441	PSID00T = -5.2403	6 = .08228	SF = 1.0	ETAGFD = 115.5068
PMID = 182.7766	PSID = 324.7499	PSID00T = -5.1915	6 = .08222	SF = 1.0	ETAGFD = 116.5717
PMID = 182.9498	PSID = 323.8644	PSID00T = -5.1394	6 = .08227	SF = 1.0	ETAGFD = 117.6284
PMID = 183.1194	PSID = 322.9886	PSID00T = -5.0843	6 = .08235	SF = 1.0	ETAGFD = 118.6794
PMID = 183.2939	PSID = 322.1213	PSID00T = -5.0263	6 = .08244	SF = 1.0	ETAGFD = 119.7195
PMID = 183.4623	PSID = 321.2648	PSID00T = -4.9656	6 = .08268	SF = 1.0	ETAGFD = 120.7425
PMID = 183.5337	PSID = 320.4198	PSID00T = -4.9023	6 = .08277	SF = 1.0	ETAGFD = 121.7597
PMID = 183.8952	PSID = 319.5842	PSID00T = -4.8367	6 = .08297	SF = 1.0	ETAGFD = 122.7668
PMID = 183.9766	PSID = 318.7688	PSID00T = -4.7689	6 = .08328	SF = 1.0	ETAGFD = 123.7698
PMID = 184.1488	PSID = 317.9492	PSID00T = -4.6998	6 = .08346	SF = 1.0	ETAGFD = 124.7438
PMID = 184.3194	PSID = 317.1484	PSID00T = -4.6274	6 = .08374	SF = 1.0	ETAGFD = 125.7164
PMID = 184.4993	PSID = 316.3628	PSID00T = -4.5542	6 = .08405	SF = 1.0	ETAGFD = 126.6731
PMID = 184.6623	PSID = 315.5885	PSID00T = -4.4795	6 = .08439	SF = 1.0	ETAGFD = 127.6188
PMID = 184.8337	PSID = 314.8270	PSID00T = -4.4036	6 = .08476	SF = 1.0	ETAGFD = 128.5517

2. Program Clock 2: Point and Cycle Efficiencies for Single  
Pass Step-Up Gear Mesh With Clock  
(Ogival) Teeth

The program CLOCK 2 furnishes the moment input-output relationship for a single step-up gear mesh with clock (ogival) teeth as derived in section 2 of Appendix E. This program uses the same kinematics as program CLOCK 1, and it differs from that program only in that it also determines both point and cycle efficiencies. Because of the above, sections a to c below will only contain discussions on those portions of the program which are different from CLOCK 1. The last section shows the complete program CLOCK 2.

a. Input Parameters (see Program CLOCK 2, below)

In addition to the input parameters of CLOCK 1, the following data must be supplied to the program:

MU =  $\mu$ , the coefficient of friction at the gear and pinion pivots as well as at the contact point between the gear and the pinion

RHO1 =  $r_1$ , the pivot radius of the gear

RHO2 =  $r_2$ , the pivot radius of the pinion

b. Computations (See also COMMENT cards in program)

I. Computation of Gear Tooth Parameters

The computation of the gear tooth parameters is identical

with that given in program CLOCK 1.

## II. Determination of Transition Angle

The transition angle is determined in the same manner as described in program CLOCK 1.

## III. Determination of Correct Sign for Round on Flat Regime

This computation is also identical with that given in program CLOCK 1.

## IV. Computation of Final and Initial Values of $\varphi$ and $\psi$

This computation is also identical with that given in program CLOCK 1.

## V. Determination of Correct Sign for Round on Round Regime

This computation is also identical with that given in program CLOCK 1.

## VI. Kinematics, Point and Cycle Efficiencies

The angular increment DDPHI of the input angle is found in the same manner as shown in program CLOCK 1. While the initial, transition and final angles of the mesh are obtained in the same manner as shown in CLOCK 1, the computational loop of the program ranges from the initial angle PHII to one increment before the final angle PHIF. This is necessary in

order to accommodate the numerical integration for the cycle efficiency.

#### A. Round on Round Regime

As before for CLOCK 1, as long as PHI is smaller than the transition angle PHIT, the kinematics of the round on round phase of the motion is computed for each increment. These kinematic computations are identical with those given in CLOCK 1. The point efficiency in this phase of motion is obtained with the help of eq. (E-70) and takes the form of eq. (3), i.e.,

$$\epsilon_P = K_{\text{ratio}} \frac{M_0}{M_{\text{in}}} \quad (\text{F-2})$$

Since the transmission ratio depends on the angular velocity ratio, and the input angular velocity is unity, eq. (F-2) becomes

$$\epsilon_P = \frac{M_0}{M_{\text{in}}} |\dot{\psi}| \quad (\text{POINTEF}) \quad (\text{F-3})$$

#### B. Round on Flat Regime

When PHI is larger than the transition angle PHIT, the kinematics of the round on flat phase becomes applicable. While the computed kinematic quantities are identical with those of CLOCK 1, the present program contains an expression for the point efficiency for the round on flat phase of the motion. This expression is obtained with the help of eq. (E-92), and it

is computed in the manner of eq. (F-3) with the now current values of the output angular velocity PSIDOT.

C. Computation of Cycle Efficiency

Once the computational loop is terminated, the cycle efficiency is computed in the manner of eq. (C-10) of Appendix C, i.e.,

$$\epsilon_C = \frac{\Delta\phi \Sigma r_p}{(\phi_{FIN} - \phi_{IN})} \quad (\text{CYCLEFF}) \quad (\text{F-4})$$

The summation was accomplished inside the loop in terms of

$$\text{MTOT} = \text{MTOT} + \text{POINTEP} \quad (\text{F-5})$$

Further,

$\Delta\phi = \text{DDPHI}$  in the program, and similarly

$\phi_{FIN} = \text{PHIF}$  and

$\phi_{IN} = \text{PHII}$

c. Output (See sectiond below)

The output of CLOCK 2 is identical with that of CLOCK 1 with the exception that the point and cycle efficiencies are printed out. The identical geometric parameters are used, and therefore, the same kinematic output is obtained.

Program CLOCK 2

F-27

PROGRAM CLOCK 2 (INPUT, OUTPUT, TAPES=INPUT, TAPE6=OUTPUT)

C POINT AND CYCLE EFFICIENCIES FOR SINGLE PASS STEP-UP

C GEAR-MESH WITH CLOCK (OGIVAL)-FELM

REAL NP,NG,L,L1,L2,K,M,NTOT,LAMBDA

HEAD(5):CAPMP,MP

FORMAT(2F10.4)

HEAD(5):AC,AP

READ(5:1)RHOG,RHOP

READ(5:1)IG\*TP

READ(5:2)PMG\*MP

FORMAT(2F10.3)

HEAD(5:3)RHOG

HEAD(5:3)K

FORMAT(10.8)

HEAD(5:3)M1

PI=3.14159

Z=PI/180.

PHID01=1.

WRITE(6:6)CAPMP,MP\*AG\*AP

FORMAT(10.5X,2CAPMP=,F7.5,3X,RP=,F7.5,3X,2G=,F7.5,3X,

LOAD=,F7.5/)

WRITE(6:5)PMG\*MP

FORMAT(10.5X,3X,PMG=,F7.5,3X,3X,PMG=,F7.5/)

WRITE(6:6)IG\*TP

FORMAT(10.5X,2IG\*TP=,F7.5/)

WRITE(6:7)PMG\*MP

FORMAT(10.5X,3X,PMG=,F4.0,3X,MP=,F4.0/)

WRITE(6:8)RHOG1\*RHOG

FORMAT(10.5X,2RHOG1=,F6.3X,2RHOG=,F6.4/)

WRITE(6:9)PHID01\*PHID01

FORMAT(10.5X,2PHID01=,F5.1/6X,2X=,F5.8/6X,2MU=,F5.2/1/)

PHID01=0.

PHID01=0.

C COMPUTATION OF GEAR TOOTH PARAMETERS

CXG=NM06-IG\*Z

DELG=ASIN(CXG/AG)

CYG=AG\*COS(DELG)

ROE=CYG\*SORT(NM06\*RHOG-CXG\*CIG)

DELG0=DELG/Z

GAMMG=ASIN(RHOG/AG)

GAMMG0=GAMMG/Z

EIMNGD=08.-GAMMGSD

EIMNGD=180.-ASIN(ROE/SIN(DELG1/RHOG1/Z

CAP=RHOP-TP/Z

DELP=ASIN(ES\*AP)

CTP=AP\*CTS(DELPL)

ROE=CYP-SORT(NM06\*MP-CAP\*CAP)

DELPD=DELP/Z

GAMMPD=ASIN(ROE/MP)

GAMMPD=GAMMP/Z

P-28

```

55 ALPHD = GAMDP - DELP
   ALPHD = ALPHD - 2
   EIMPD = 98 - GAMPD
   EIMPD = 188 - ASIN(0P+SIN(DEL P)/AMDP) / Z
   FP = AP * COS(GAMP)
   B = CAPPP - BP
   DPMI = 360. / MG * Z
   DPMI = 360. / MG * Z
   L = 4006 + RMOP
   WRITE(6,10) DELG0, DELP0, GAMPD0, ALPHD0, EIMPD0, EIMAXG0,
10 EIMINP0, EIMAXP0, FP
   FORMAT(6X,DELG0 = F9.4,3X,DELP0 = F9.4//6X,GAMP0 = F9.4,3X,
15 ALPHD0 = F9.4//6X,EIMING0 = F9.4//6X,EIMAXG0 = F9.4
   Z776X,EIMINP0 = F9.4,3X,EIMAXP0 = F9.4//6X,EP = F9.4//6X,EP = F9.4//6X)

C DETERMINATION OF TRANSITION ANGLE
70 C
   AT = RMG * COS(ALPHD) + FP * SIN(ALPHD)
   BT = RMG * SIN(ALPHD) - FP * COS(ALPHD)
   CT = (AG * AS - FP * EP) / (AG - FP * RMG * RMG) / (Z * 90)
   RDOTI = AT * AT + BT * BT + CT * CT
   YII = AT + SORT(MDOTI)
   YI2 = AT - SORT(MDOTI)
   AT = BT + CT
   PSII1 = 2 * AT * AM2(YII,AT)
   PSII2 = 2 * AT * AM2(YI2,AT)
   IF(PSII1 .LT. 0) PSII1 = PSII1 + 2 * PI
   IF(PSII2 .LT. 0) PSII2 = PSII2 + 2 * PI
   PSIII = PSII1 / Z
   PSII2 = PSII2 / Z
   CALL TRANS(06,ALPHD,FP,AG,B,DELG,7,PSIII,PSII1,61)
   CALL TRANS(06,ALPHD,FP,AG,B,DELG,7,PSII2,PSII2,62)
   PHII1 = PHII1 / Z
   PHII2 = PHII2 / Z
   IE511 = 360. - (PSIII + ALPHD)
   IE512 = 360. - (PSII2 + ALPHD)
   WRITE(6,11) PHII1,PSIII,GI,IE511
10 WRITE(6,12) PHII2,PSII2,GI,IE512
   I1 FORMAT(6X,PHII1 = F9.4,3X,PSIII = F9.4,3X,IE511 = F9.4,3X,
15 IE511 = F9.4,3X)
   I2 FORMAT(6X,PHII2 = F9.4,3X,PSII2 = F9.4,3X,IE512 = F9.4,3X,
20 IE512 = F9.4,3X)
   IF(GI .LT. FPI60) I1 20
   PHII = PHII1
   PSII = PSII2
   GO TO 30
80 I1 20 PHII = PHII1
   PSII = PSII1
30 PHII = PHII / Z
   PSII = PSII / Z
105 C DETERMINATION OF CORRECT SIGN FOR ROUND-OFF FLAT-NEIGNE
   C

```

PROGRAM UUCAL2 7/2/76 (M=1)

```

110 AF = B*CDOS(ALPWP) + AG*COS(PHI1-DELG-ALPWP)
    BF = B*SIN(ALPWP) - AG*SIN(PHI1-DELG-ALPWP)
    CF = -MMOG
    WUOIF = AF*AF + BF*BF - CF*CF
    YF1 = AF + SORT(MOUIF)
    YF2 = AF - SORT(MOUIF)
    AF = BF + CF
    PSIF1 = 2.*ATAN2(YF1,RF)
    PSIF2 = 2.*ATAN2(YF2,RF)
    IF PSIF1 .LT. 0.1PSIF1 = PSIF1 + 2.*PI
    IF PSIF2 .LT. 0.1PSIF2 = PSIF2 + 2.*PI
    IF ABS(PSIF1-PSIF2) .LT. ABS(PSIF2-PSIF1) GO TO 10
    SIGNF = -1.
    GO TO 50
115
120

```

```

    SU SIGNF = 1.
C
C COMPUTATION OF FINAL AND INITIAL VALUES OF PHI AND PSI
C

```

```

125 50 DO 60 I=1,1000
    PHI0 = PHI0 + (.1-2.77186.
    PHI = PHI0*Z
    AF = B*CDOS(ALPWP) - AG*COS(PHI-DELG-ALPWP)
    BF = B*SIN(ALPWP) - AG*SIN(PHI-DELG-ALPWP)
    CF = -MMOG
    WUOIF = AF*AF + BF*BF - CF*CF
    IF -WUOIF .SIGN. SORT(WUOIF)
    RF = BF + CF
    PSIF = 2.*ATAN2(YF,RF)
    IF (PSIF .LT. 0.1)PSIF = PSIF + 2.*PI
    LA = B + AG*COS(PHI-DELG-APHI) - AP*CDOS(PSIF+DPSI-DELP)
    LY = AG*SIN(PHI-DELG-APHI) - AP*SIN(PSIF+DPSI)
    IF SORT(LA) .LT. SORT(LY) .AND. LY .GT. 0.
    CONTINUE
    PHIF = PHIF + PHI
    PSIFF = PSIF
    PSII = PSIFF + PSI
    IF (PSII .GT. 2.*PI)PSII = PSII - 2.*PI
    PHI0 = PHIF/Z
    PSII0 = PSII/Z
    PHIFD = PSIFF/Z
    PSIFD = PSIF/Z
    WRITE(6,86)PHI0,PSII0,PHIFD,PSIFD
    PSII0 = PSII0 + 2.*PI
    PSII0 = PSII0 - 2.*PI
    L*PSIFD = 0.09,0.11/

```

```

C
C DETERMINATION OF CORRECT SIGN FOR ROUND ON ROUND REGIME
C

```

```

130 86 PSII0 = PSII0 + COS(PHI-DELG)TAN(DELP) + B*TAN(DELP)/AG
    BF = COS(PHI-DELG) + B/AG - S14(PHI-DELG)TAN(DELP)
    CN = LAPWP + 20*AG + 200 - L*YF2 - AP*AG*CDOS(DELP)
    L*AP*CDOS(PHI-DELG)/(AP*CDOS(DELP))
    MOUIF = AN*AR + BR*BR - CR*CR
    YM1 = AR + SORT(MOUIF)

```



```

60 TO 150
210 AF = B*COS(ALPHA) + A*ACOS(PHI-DELTA-ALPHA)
    BF = B*SIN(ALPHA) - A*OSIN(PHI-DELTA-ALPHA)
    CF = -R*06
    WOOTF = AF*AF + BF*BF - CF*CF
    YF = AF + SIGN(SQRT(WOOTF))
    AF = BF + CF
    PSI = 2.0*ATAN2(YE,FE)
    IF(PSI .LT. 0) PSI = PSI + 2.0*PI
    PSIO = PSI/2
    G = (A*OSIN(PHI-DELTA) - R*06*COS(PSI*ALPHA))/SIN(PSI*ALPHA)
    AFU = A*OSIN(PHI-DELTA-ALPHA)
    BFU = A*COS(PHI-DELTA-ALPHA)
    PSINDI = PRINTO*(B*OSIN(PSI) + B*FCOS(PSI))/A*FCOS(PSI) + B*FO
    SIN(PSI)
    YST = PHIDOT*(R*06 + A*OSIN(PSI-PI*ALPHA*DELTA))
    BF = YST/ABS(YSTF)
    IF(PSIO*ALPHA*0.6<Y9) IETAGF=(PHI-DELTA-PSI-ALPHA*0.3*PI/2)/Z
    IF(PSIO*ALPHA*0.1<Y9) IETAGF=(PHI-DELTA-PSI-ALPHA*0.5*PI)/Z
    EEN = G - W*06
    EFFU = WU*(R*01 + SF*06) - A*0*(COS(PHI-DELTA-PSI-ALPHA)
    1. W*SE*OSIN(PHI-DELTA-PSI-ALPHA)
    POINTF = EFFU/EST*0.05*(PSINDI)
    WRITE(6,130) PHIO,PSIO,SINDI,SF,IETAGF,POINTF
130 FORMAT(10E10,10E10,10E10,10E10,10E10,10E10)
106 STOP 7.5,3,0,5F 2E14.1,3,0,IETAGF 2E19,4,3,0,POINTF 2E18,3)
190 WUJ = WUJ + POINTF
    GO TO 110
200 CYCLEFF = WUJ*0.001/(PHI*PI)
    WRITE(6,210) CYCLEFF
210 FORMAT(10E10,5X,CYCLE EFFICIENCY 2E18,3)
    STOP
    END
205

```

```

1      SUBROUTINE TRANS(RHOG,ALPH,P,FP,SG,B,DELS,Z,PSIIT,PHIT,G)
      PI = 3.14159
      SI = (FP*SIN(PSIIT*ALPH)) + RHOG*COS(PSIIT*ALPH))/AG
      CI = (FP*COS(PSIIT*ALPH)) - RHOG*SIN(PSIIT*ALPH) - G)/AG
      PHIT = ATAN2(SI,CI) + 5E6
      IF (PHIT .LT. 0.) PHIT = PHIT + 2.*PI
      PSINEXT = PHIT + .107
      RF = B*COSTRCPMP) - AG*COS(PHINEXT) - DELG - ALPH
      CF = (RF - B*SIN(ALPH)) - AG*SIN(PHINEXT) - DELG - ALPH
      ROOTF = AF*RF + RF*RF - CF*CF
      YF1 = AF + SQRT(ROOTF)
      YF2 = AF - SQRT(ROOTF)
      XF = RF + CF
      PSINEX1 = 2.*ATAN2(YF1,XF)
      PSINEX2 = 2.*ATAN2(YF2,RF)
      IF (PSINEX1 .LT. 0.) PSINEX1 = PSINEX1 + 2.*PI
      IF (PSINEX2 .LT. 0.) PSINEX2 = PSINEX2 + 2.*PI
      IF (ABS(PSINEX1-PSIIT) .LT. ABS(PSINEX2-PSIIT)) GO TO 1
      PSINEXT = PSINEX1
      GO TO 2
1      PSINEXT = PSINEXT
      Z G = (AG*SIN(PHINEXT-DELG) - RHOG*COS(PSINEXT*ALPH))/SIN(PSINEXT)
      RETURN
      END
  
```

CAADP = .0172 ED = .0125 AE = .0175 AP = .0905

PAIC = .03079 RCP = .01748

TA = .03308 TP = .02483

WS = .02, WP = 6.

WVI = .0003 WVC2 = .0309

PHIDOT = 1.0

K = 50.

C = .20

NELEB = 2.5508 DELPO = 2.1004

CAADPO = 11.0018 CALMPO = 8.0078

ETAGD = 0.0000 ETAGD = 100.0000

ETAGD = 70.0502 ETAGDPO = 140.5070

CP = .00017

PSI10 = 100.3023 PSI10 = 300.0704 G1 = .0005 TEST1 = 42.07

PSI20 = 170.7537 PSI20 = 340.0000 G2 = .0000 TEST2 = 0.05

PSI30 = 170.2023 PSI30 = 350.0270 PSI30 = 100.0337 PSI30 = 310.0270

PSI0 = 170.2023	PSI0 = 350.0195	PSI00T = -0.2450	PSI = 1.0	ETAGD = 04.7219	ETAGD = 03.0923	POINTEF = .075
PSI0 = 170.4337	PSI0 = 350.2204	PSI00T = -0.2451	PSI = 1.0	ETAGD = 04.0859	ETAGD = 03.7053	POINTEF = .074
PSI0 = 170.4802	PSI0 = 350.0211	PSI00T = -0.2400	PSI = 1.0	ETAGD = 04.0172	ETAGD = 00.7004	POINTEF = .003
PSI0 = 170.7705	PSI0 = 357.1214	PSI00T = -0.0501	PSI = 1.0	ETAGD = 07.0957	ETAGD = 07.0137	POINTEF = .000
PSI0 = 170.9403	PSI0 = 356.0218	PSI00T = -0.2506	PSI = 1.0	ETAGD = 07.2214	ETAGD = 00.0077	POINTEF = .000
PSI0 = 177.1106	PSI0 = 355.0159	PSI00T = -0.0005	PSI = 1.0	ETAGD = 07.0105	ETAGD = 00.0201	POINTEF = .003
PSI0 = 177.0904	PSI0 = 350.0174	PSI00T = -0.0074	PSI = 1.0	ETAGD = 07.0251	ETAGD = 02.0108	POINTEF = .077
PSI0 = 177.0023	PSI0 = 353.0130	PSI00T = -0.0752	PSI = 1.0	ETAGD = 07.0031	ETAGD = 00.0070	POINTEF = .000
PSI0 = 177.0737	PSI0 = 352.0087	PSI00T = -0.0399	PSI = 1.0	ETAGD = 00.1507	ETAGD = 03.0000	POINTEF = .000
PSI0 = 177.0002	PSI0 = 351.7521	PSI00T = -0.0000	PSI = 1.0	ETAGD = 00.0000	ETAGD = 02.7722	POINTEF = .007
PSI0 = 177.0700	PSI0 = 350.7030	PSI00T = -0.0000	PSI = 1.0	ETAGD = 00.7931	ETAGD = 02.0235	POINTEF = .007
PSI0 = 170.1000	PSI0 = 349.0030	PSI00T = -0.0000	PSI = 1.0	ETAGD = 00.1521	ETAGD = 01.0000	POINTEF = .007
PSI0 = 170.3100	PSI0 = 348.0000	PSI00T = -0.0000	PSI = 1.0	ETAGD = 00.5370	ETAGD = 00.0000	POINTEF = .003
PSI0 = 170.0000	PSI0 = 347.1000	PSI00T = -0.0000	PSI = 1.0	ETAGD = 00.0000	ETAGD = 00.0000	POINTEF = .000
PSI0 = 170.0000	PSI0 = 346.2000	PSI00T = -0.0000	PSI = 1.0	ETAGD = 00.0000	ETAGD = 00.0000	POINTEF = .000
PSI0 = 170.0000	PSI0 = 345.0000	PSI00T = -0.0000	PSI = 1.0	ETAGD = 00.0000	ETAGD = 00.0000	POINTEF = .000
PSI0 = 170.1700	PSI0 = 344.0000	PSI00T = -0.0000	PSI = 1.0	ETAGD = 01.1534	ETAGD = 00.0000	POINTEF = .000
PSI0 = 170.3000	PSI0 = 343.0000	PSI00T = -0.0000	PSI = 1.0	ETAGD = 02.2000	ETAGD = 00.0000	POINTEF = .000
PSI0 = 170.5100	PSI0 = 342.0000	PSI00T = -0.0000	PSI = 1.0	ETAGD = 03.3000	ETAGD = 00.0000	POINTEF = .000
PSI0 = 170.0000	PSI0 = 341.0000	PSI00T = -0.0000	PSI = 1.0	ETAGD = 04.4000	ETAGD = 00.0000	POINTEF = .000
PSI0 = 170.0000	PSI0 = 340.0000	PSI00T = -0.0000	PSI = 1.0	ETAGD = 05.5000	ETAGD = 00.0000	POINTEF = .000
PSI0 = 170.0000	PSI0 = 339.0000	PSI00T = -0.0000	PSI = 1.0	ETAGD = 06.6000	ETAGD = 00.0000	POINTEF = .000
PSI0 = 170.0000	PSI0 = 338.0000	PSI00T = -0.0000	PSI = 1.0	ETAGD = 07.7000	ETAGD = 00.0000	POINTEF = .000
PSI0 = 170.0000	PSI0 = 337.0000	PSI00T = -0.0000	PSI = 1.0	ETAGD = 08.8000	ETAGD = 00.0000	POINTEF = .000

PM10 = 181.5400	PS10 = 336.8703	PS100T = -5.5366	6 = .0820	SF = 1.0	ETAGFD = 102.2407	POINTEF = .055
PM10 = 181.7194	PS10 = 335.8771	PS100T = -5.5353	6 = .08300	SF = 1.0	ETAGFD = 103.3074	POINTEF = .052
PM10 = 181.8944	PS10 = 334.9707	PS100T = -5.5286	6 = .08350	SF = 1.0	ETAGFD = 104.5071	POINTEF = .048
PM10 = 181.6623	PS10 = 333.9426	PS100T = -5.5168	6 = .08331	SF = 1.0	ETAGFD = 105.6253	POINTEF = .044
PM10 = 181.2317	PS10 = 333.0375	PS100T = -5.5015	6 = .08307	SF = 1.0	ETAGFD = 106.7412	POINTEF = .041
PM10 = 181.4852	PS10 = 332.8903	PS100T = -5.4923	6 = .08286	SF = 1.0	ETAGFD = 107.8542	POINTEF = .037
PM10 = 181.5760	PS10 = 331.1501	PS100T = -5.4591	6 = .08268	SF = 1.0	ETAGFD = 108.9635	POINTEF = .034
PM10 = 181.7408	PS10 = 330.2245	PS100T = -5.4320	6 = .08252	SF = 1.0	ETAGFD = 110.0665	POINTEF = .030
PM10 = 181.9194	PS10 = 329.2959	PS100T = -5.4011	6 = .08240	SF = 1.0	ETAGFD = 111.1605	POINTEF = .027
PM10 = 182.0909	PS10 = 328.3729	PS100T = -5.3663	6 = .08230	SF = 1.0	ETAGFD = 112.2629	POINTEF = .023
PM10 = 182.2623	PS10 = 327.4552	PS100T = -5.3279	6 = .08224	SF = 1.0	ETAGFD = 113.3511	POINTEF = .019
PM10 = 182.4317	PS10 = 326.5464	PS100T = -5.2859	6 = .08220	SF = 1.0	ETAGFD = 114.4323	POINTEF = .016
PM10 = 182.6052	PS10 = 325.6441	PS100T = -5.2403	6 = .08220	SF = 1.0	ETAGFD = 115.5008	POINTEF = .012
PM10 = 182.7766	PS10 = 324.7496	PS100T = -5.1915	6 = .08222	SF = 1.0	ETAGFD = 116.5717	POINTEF = .009
PM10 = 182.9400	PS10 = 323.8644	PS100T = -5.1394	6 = .08227	SF = 1.0	ETAGFD = 117.6206	POINTEF = .005
PM10 = 183.1194	PS10 = 322.9880	PS100T = -5.0843	6 = .08235	SF = 1.0	ETAGFD = 118.6764	POINTEF = .002
PM10 = 183.2904	PS10 = 322.1213	PS100T = -5.0263	6 = .08246	SF = 1.0	ETAGFD = 119.7145	POINTEF = .000
PM10 = 183.4623	PS10 = 321.2648	PS100T = -4.9656	6 = .08260	SF = 1.0	ETAGFD = 120.7425	POINTEF = .000
PM10 = 183.6337	PS10 = 320.4190	PS100T = -4.9023	6 = .08277	SF = 1.0	ETAGFD = 121.7597	POINTEF = .000
PM10 = 183.8052	PS10 = 319.5842	PS100T = -4.8367	6 = .08297	SF = 1.0	ETAGFD = 122.7608	POINTEF = .000
PM10 = 183.9766	PS10 = 318.7600	PS100T = -4.7689	6 = .08320	SF = 1.0	ETAGFD = 123.7608	POINTEF = .000
PM10 = 184.1480	PS10 = 317.9432	PS100T = -4.6998	6 = .08346	SF = 1.0	ETAGFD = 124.7438	POINTEF = .000
PM10 = 184.3194	PS10 = 317.1450	PS100T = -4.6274	6 = .08374	SF = 1.0	ETAGFD = 125.7146	POINTEF = .000
PM10 = 184.4909	PS10 = 316.3628	PS100T = -4.5542	6 = .08405	SF = 1.0	ETAGFD = 126.6731	POINTEF = .000
PM10 = 184.6623	PS10 = 315.5885	PS100T = -4.4795	6 = .08439	SF = 1.0	ETAGFD = 127.6180	POINTEF = .000

CYCLE EFFICIENCY = .050

APPENDIX G  
KINEMATICS OF TWO AND THREE STEP-UP GEAR TRAINS WITH CLOCK TEETH

Figure G-1 shows the basic configuration of a three step-up gear train used in certain fuze applications. The general layout is identical to that shown in Figure A-5 of Appendix A. Now, ogival type gear teeth are used instead of involute type ones. Again, it is required to find the equilibrant moment  $M_{o4}$ , acting on pinion no. 4 which holds the input moment,  $M_{in}$ , acting on gear no. 1, in equilibrium when both pivot and contact friction are taken into account, and when the fuze body spins. Appendix H gives the force and moment analyses for the determination of this moment input-output relationship. The same appendix also shows the derivation of such an input-output relationship for a two step-up gear train with ogival gear teeth which must operate in a spin environment. (Figure A-10 of Appendix A shows this type of configuration with involute teeth.) The present appendix lays the groundwork for the moment relationships of Appendix H by providing the kinematics of the three ogival gear meshes involved.

In each case both round on round and round on flat phases

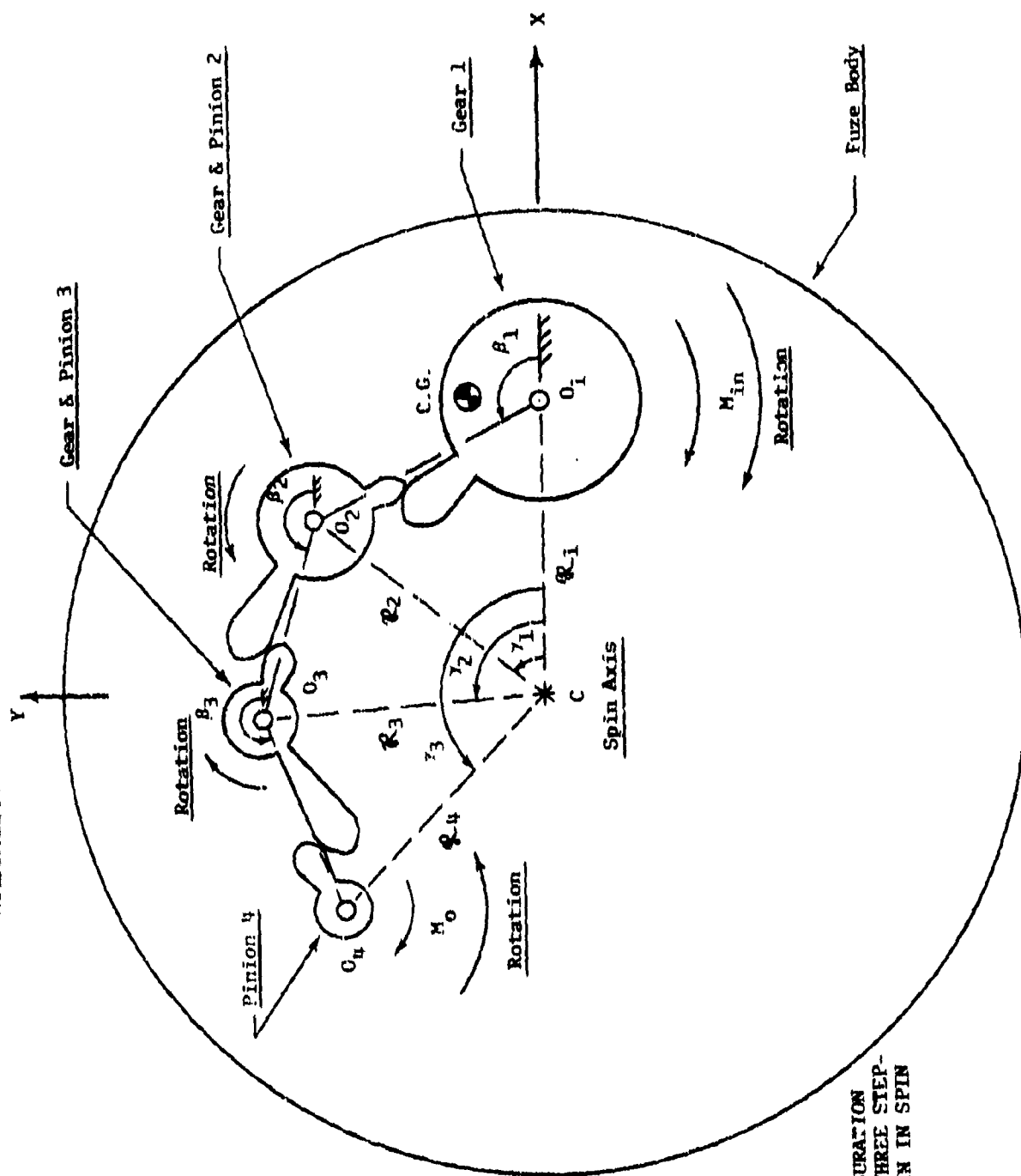


FIGURE G-1  
 BASIC CONFIGURATION  
 FOR OCIVAL THREE STEP-  
 UP GEAR TRAIN IN SPIN  
 ENVIRONMENT

of motion have to be considered. All derivations follow the pattern set in Section 1 of Appendix E. The derivations must take into account that the driving gears of meshes no. 1 and no. 3, i.e., between gear no. 1 and pinion no. 2 and between gear no. 3 and pinion no. 4, respectively, have clockwise rotations. The driving gear of mesh no. 2, i.e., between gear no. 2 and pinion no. 3, has counterclockwise rotation.

Finally, the inclinations of the various pivot to pivot centerlines with respect to the body-fixed X-axes, as represented by the angles  $\beta_1$ ,  $\beta_2$  and  $\beta_3$ , must be considered.

For the sake of simplicity, the notation will in most cases not differentiate between round on round and round on flat phases of motion. For example, the output angle,  $\psi_1$ , and its derivatives will have the same symbol for both phases.

For definitions of angles  $\beta_1$  and  $\gamma_1$  as well as the distances  $Q_1$ , see Appendix A-6.

## 1. KINEMATICS OF MESH NO. 1 (GEAR NO. 1 AND PINION NO. 2)

### a. ROUND ON ROUND PHASE OF MOTION

Figure G-2 shows the round on round phase of the motion of mesh no. 1 in a schematic manner. Only the contacting faces of the gear and the pinion are indicated.

#### I. UNIT VECTORS

The unit vector in the direction  $O_1C_{G1}$  of the gear is given by

$$\bar{n}_{G1} = \cos(\phi_1 + \delta_{G1})\bar{i} + \sin(\phi_1 + \delta_{G1})\bar{j} \quad (G-1)$$

The unit vector in the direction  $C_{G1}C_{P1}$  is given by

$$\bar{n}_{\lambda 1} = \cos\lambda_1\bar{i} + \sin\lambda_1\bar{j} \quad (G-2)$$

The unit vector normal to  $\bar{n}_{\lambda 1}$  (in the right hand sense) becomes

$$\bar{n}_{N\lambda 1} = -\sin\lambda_1\bar{i} + \cos\lambda_1\bar{j} \quad (G-3)$$

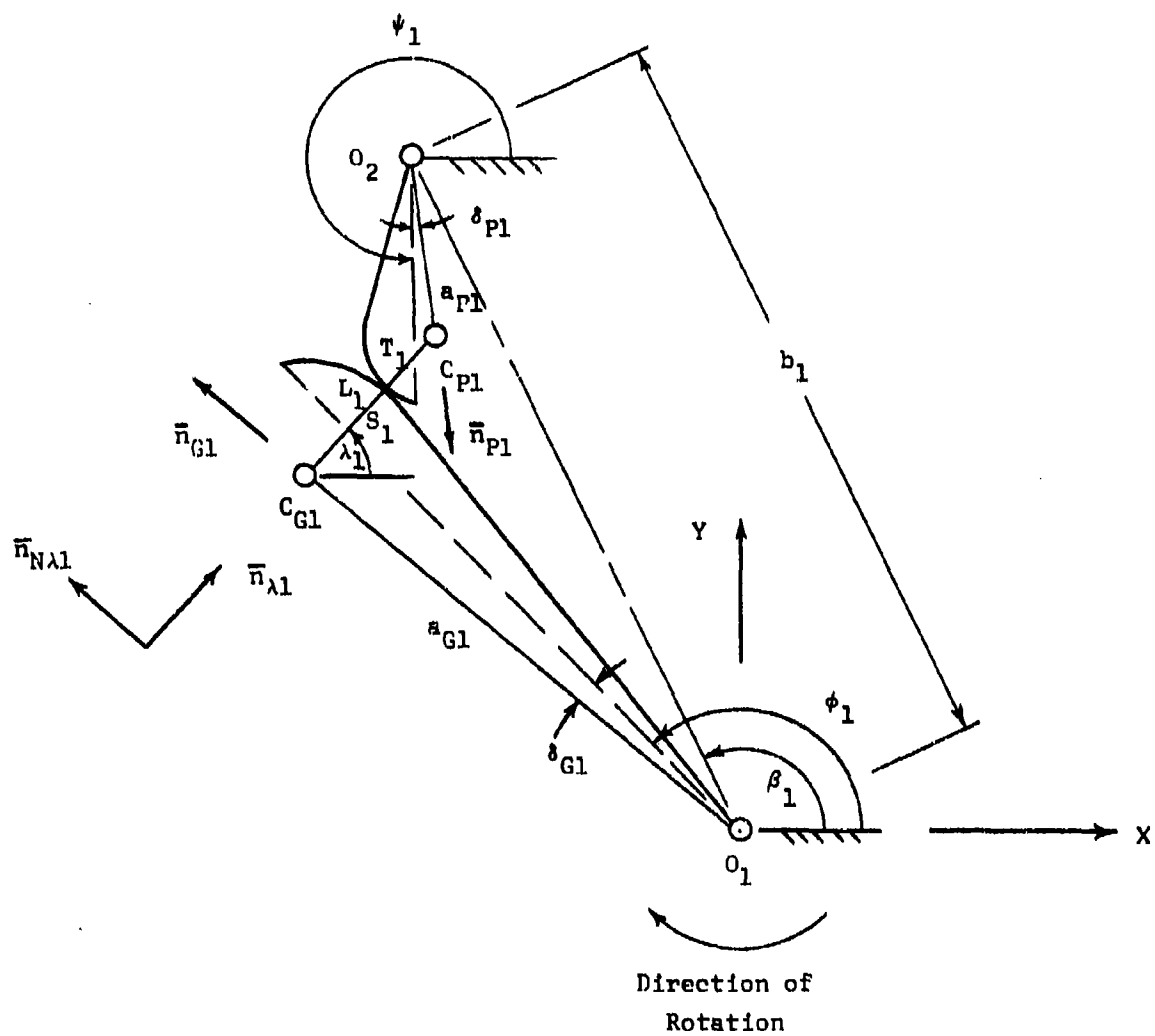


FIGURE G-2  
 ROUND ON ROUND PHASE FOR MESH NO. 1

The unit vector in the direction  $O_2C_{P1}$  is given by

$$\bar{n}_{P1} = \cos(\psi_1 + \delta_{P1})\bar{i} + \sin(\psi_1 + \delta_{P1})\bar{j} \quad (G-4)$$

Finally, the unit vector along the centerline,  $O_1O_2$ , is given by

$$\bar{n}_{\beta_1} = \cos\beta_1\bar{i} + \sin\beta_1\bar{j} \quad (G-5)$$

## II. DETERMINATION OF OUTPUT ANGLE $\psi_1$ AND "COUPLER" ANGLE $\lambda_1$

The loop equation of the equivalent four-bar linkage is given by

$$a_{G1}\bar{n}_{G1} + L_1\bar{n}_{\lambda_1} - a_{P1}\bar{n}_{P1} - b_1\bar{n}_{\beta_1} = 0 \quad (G-6)$$

$$\text{where } L_1 = \rho_{G1} + \rho_{P1} \quad (G-7)$$

With the appropriate substitution for the unit vectors, one obtains the following component equations:

$$a_{G1} \cos(\phi_1 + \delta_{G1}) + L_1 \cos \lambda_1 - b_1 \cos \beta_1 - a_{P1} \cos(\psi_1 + \delta_{P1}) = 0 \quad (G-8)$$

and

$$a_{G1} \sin(\phi_1 + \delta_{G1}) + L_1 \sin \lambda_1 - b_1 \sin \beta_1 - a_{P1} \sin(\psi_1 + \delta_{P1}) = 0 \quad (G-9)$$

To eliminate  $\lambda_1$ , let

$$\sin^2 \lambda_1 + \cos^2 \lambda_1 = 1 \quad (G-10)$$

The above trigonometric functions are obtained from equations (G-8) and (G-9), respectively. Substitution into equation (G-10) furnishes

$$A_{1R} \sin \psi_1 + B_{1R} \cos \psi_1 = C_{1R} \quad (G-11)$$

where

$$A_{1R} = a_{G1} \sin(\phi_1 + \delta_{G1} - \delta_{P1}) - b_1 \sin(\beta_1 - \delta_{P1})$$

$$B_{1R} = a_{G1} \cos(\phi_1 + \delta_{G1} - \delta_{P1}) - b_1 \cos(\beta_1 - \delta_{P1})$$

$$C_{1R} = \frac{a_{P1}^2 + a_{G1}^2 + b_1^2 - L_1^2 - 2a_{G1} b_1 \cos(\phi_1 + \delta_{G1} - \beta_1)}{2a_{P1}}$$

Equation (G-11) is now solved for  $\psi_1$  in the manner described in Appendix E in connection with equation (E-12), i.e.,

$$\psi_1 = 2 \tan^{-1} \frac{A_{1R} \pm \sqrt{A_{1R}^2 + B_{1R}^2 - C_{1R}^2}}{B_{1R} + C_{1R}} \quad (G-12)$$

The correct sign on equation (G-12) must be found from geometric considerations.

The coupler angle  $\lambda_1$  may now be determined either from equation (G-8) or from equation (G-9). Thus,

$$\lambda_1 = \cos^{-1} \left[ \frac{b_1 \cos \beta_1 + a_{p1} \cos(\psi_1 + \delta_{p1}) - a_{g1} \cos(\phi_1 + \delta_{g1})}{L_1} \right] \quad (G-13)$$

or

$$\lambda_1 = \sin^{-1} \left[ \frac{b_1 \sin \beta_1 + a_{p1} \sin(\psi_1 + \delta_{p1}) - a_{g1} \sin(\phi_1 + \delta_{g1})}{L_1} \right] \quad (G-14)$$

### III. DETERMINATION OF ANGULAR VELOCITY $\dot{\psi}_1$ OF PINION NO. 2

Differentiation of equation (G-11) with respect to time gives

$$\dot{\psi}_1 = \dot{\phi}_1 \left[ \frac{B_{1RD} \cos \psi_1 - A_{1RD} \sin \psi_1 + C_{1RD}}{A_{1R} \cos \psi_1 - B_{1R} \sin \psi_1} \right] \quad (G-15)$$

where

$$A_{1RD} = a_{G1} \cos(\phi_1 + \delta_{G1} - \delta_{P1})$$

$$B_{1RD} = a_{G1} \sin(\phi_1 + \delta_{G1} - \delta_{P1})$$

$$C_{1RD} = \frac{a_{G1} b_1 \sin(\phi_1 + \delta_{G1} - \beta_1)}{a_{P1}}$$

#### IV. RELATIVE VELOCITY AT THE CONTACT POINT

The relative velocity  $\bar{V}_{S_1/T_1R}$  of the contact point  $S_1$  on gear no. 1 with respect to point  $T_1$  on pinion no. 2, represents the vectorial difference between the absolute velocities of these points. Thus,

$$\bar{V}_{S_1/T_1R} = \bar{V}_{S_1/C} - \bar{V}_{T_1/C} \quad (G-16)$$

where C represents the spin center of the fuze body. If  $\bar{\omega}$  stands for the angular velocity of the fuze body, then appropriate substitution into equation (G-16) gives (See also Figures G-1 and G-2)

$$\begin{aligned} \bar{V}_{S_1/T_1R} = & \left[ \bar{\omega} \times \bar{r}_1 + (\bar{\omega} + \bar{\phi}_1) \times (\bar{a}_{G1} + \bar{p}_{G1}) \right] \\ & - \left[ \bar{\omega} \times \bar{r}_2 + (\bar{\omega} + \bar{\psi}_1) \times (\bar{a}_{P1} + \bar{p}_{P1}) \right] \end{aligned} \quad (G-17)$$

Since

$$\bar{\omega} \times [\bar{r}_1 + \bar{a}_{G1} + \bar{p}_{G1}] = \bar{\omega} \times [\bar{r}_2 + \bar{a}_{P1} + \bar{p}_{P1}] \quad (G-18)$$

because the position vectors in brackets are equal, equation (G-17) may be written

$$\begin{aligned}\bar{V}_{S1/T1_R} &= \bar{V}_{S1/O_1} - \bar{V}_{T1/O_2} \\ &= \dot{\bar{\phi}}_1 \times (\bar{a}_{G1} + \bar{r}_{G1}) - \dot{\bar{\psi}}_1 \times (\bar{a}_{P1} + \bar{r}_{P1})\end{aligned}\quad (G-19)$$

Note that  $\bar{V}_{S1/T1_R}$  becomes the vectorial difference of the contact point velocities with respect to the fuze body.

Since this relative velocity is tangent to the contacting surfaces, it may be written as the vectorial difference of the velocity components along these surfaces. Accordingly, equation (G-19) becomes, with the help of the unit vector  $\bar{n}_{N\lambda 1}$ ,

$$\begin{aligned}\bar{V}_{S1/T1_R} &= \left\{ \left[ \dot{\bar{\phi}}_1 \bar{k} \times (\bar{a}_{G1} \bar{n}_{G1} + \bar{r}_{G1} \bar{n}_{\lambda 1}) \right] \cdot \bar{n}_{N\lambda 1} \right. \\ &\quad \left. - \left[ \dot{\bar{\psi}}_1 \bar{k} \times (\bar{a}_{P1} \bar{n}_{P1} + \bar{r}_{P1} \bar{n}_{\lambda 1}) \right] \cdot \bar{n}_{N\lambda 1} \right\} \bar{n}_{N\lambda 1}\end{aligned}\quad (G-20)$$

Appropriate substitution of unit vectors given earlier in Section I and simplification results in

$$\begin{aligned}
 \mathbf{V}_{S_1/T_1R} = & \left\{ \dot{\psi}_1 [a_{G1} \cos(\psi_1 + \delta_{G1} - \lambda_1) + r_{G1}] \right. \\
 & \left. - \dot{\psi}_1 [a_{P1} \cos(\psi_1 + \delta_{P1} - \lambda_1) - r_{P1}] \right\} \mathbf{E}_{N\lambda 1}
 \end{aligned}
 \tag{G-21}$$

b. ROUND ON FLAT PHASE OF MOTION

Figure G-3 shows a schematic view of mesh no. 1 in the round on flat phase of the motion.

I. UNIT VECTORS

The unit vector in the direction  $O_2T_1$  is given by

$$\bar{n}_{F1} = \cos(\psi_1 - \alpha_{P1})\bar{i} + \sin(\psi_1 - \alpha_{P1})\bar{j}
 \tag{G-22}$$

The unit vector  $\bar{n}_{NF1}$ , in the direction  $C_{G1}S_1$ , is always normal to  $\bar{n}_{F1}$

$$\bar{n}_{NF1} = -\sin(\psi_1 - \alpha_{P1})\bar{i} + \cos(\psi_1 - \alpha_{P1})\bar{j}
 \tag{G-23}$$

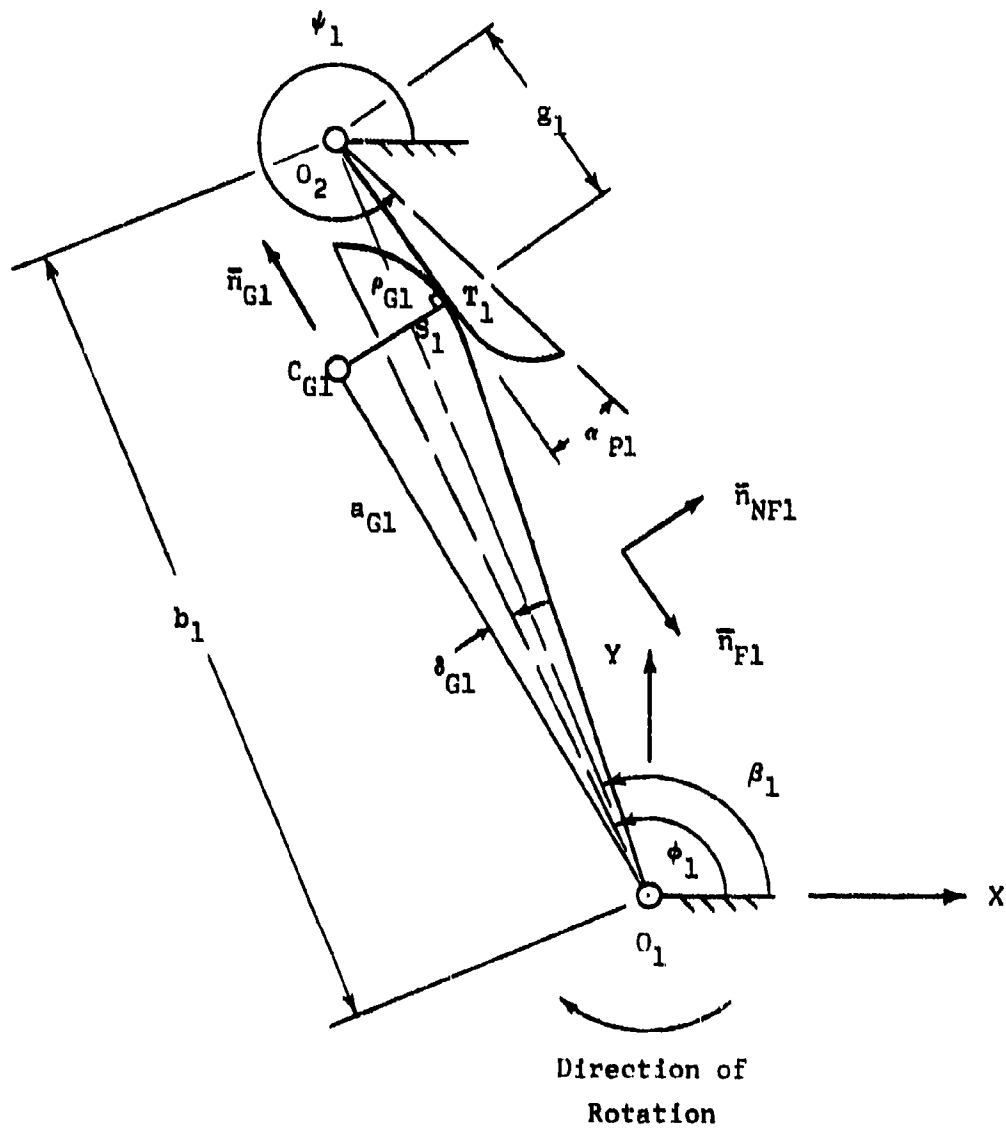


FIGURE G-3  
 ROUND ON FLAT PHASE FOR MESH NO. 1

## II. DETERMINATION OF OUTPUT ANGLE $\psi_1$ AND DISTANCE $s_1$

The vector equation for the mechanism loop  $O_1-C_{G1}-S_1-T_1-O_2$  has the form:

$$a_{G1}\bar{n}_{G1} + r_{G1}\bar{n}_{NF1} - s_1\bar{n}_{P1} - b_1\bar{n}_{\beta_1} = 0 \quad (G-24)$$

Substitution of equations (G-1), (G-5), (G-22) and (G-23) leads to the following component equations.

$$\begin{aligned} a_{G1}\cos(\phi_1 + \theta_{G1}) - r_{G1}\sin(\psi_1 - \alpha_{P1}) - b_1\cos\beta_1 - s_1\cos(\psi_1 - \alpha_{P1}) \\ = 0 \end{aligned} \quad (G-25)$$

and

$$\begin{aligned} a_{G1}\sin(\phi_1 + \theta_{G1}) + r_{G1}\cos(\psi_1 - \alpha_{P1}) - b_1\sin\beta_1 - s_1\sin(\psi_1 - \alpha_{P1}) \\ = 0 \end{aligned} \quad (G-26)$$

From equation (G-26) one obtains for the quantity  $s_1$

$$s_1 = \frac{a_{G1}\sin(\phi_1 + \theta_{G1}) + r_{G1}\cos(\psi_1 - \alpha_{P1}) - b_1\sin\beta_1}{\sin(\psi_1 - \alpha_{P1})} \quad (G-27)$$

This expression is now substituted in equation (G-25). This leads to the following:

$$A_{1F} \sin \psi_1 + B_{1F} \cos \psi_1 = C_{1F} \quad (G-28)$$

where

$$A_{1F} = a_{G1} \cos(\phi_1 + \delta_{G1} + \alpha_{P1}) - b_1 \cos(\beta_1 + \alpha_{P1})$$

$$B_{1F} = -a_{G1} \sin(\phi_1 + \delta_{G1} + \alpha_{P1}) + b_1 \sin(\beta_1 + \alpha_{P1})$$

$$C_{1F} = r_{G1}$$

Equation (G-28) is solved for  $\psi_1$  in the now customary manner:

$$\psi_1 = 2 \tan^{-1} \frac{A_{1F} \pm \sqrt{A_{1F}^2 + B_{1F}^2 - C_{1F}^2}}{B_{1F} + C_{1F}} \quad (G-29)$$

The appropriate sign is again found from geometric considerations.

III. DETERMINATION OF ANGULAR VELOCITY  $\dot{\psi}_1$  DURING ROUND ON FLAT  
PHASE OF MOTION

Implicit differentiation of equation (G-28) with respect to time gives, for  $\dot{\psi}_1$ :

$$\dot{\psi}_1 = \dot{\phi}_1 \left[ \frac{A_{1FD} \sin \psi_1 + B_{1FD} \cos \psi_1}{A_{1F} \cos \psi_1 - B_{1F} \sin \psi_1} \right] \quad (G-30)$$

where

$$A_{1FD} = a_{G1} \sin(\phi_1 + \delta_{G1} + \alpha_{P1})$$

$$B_{1FD} = a_{G1} \cos(\phi_1 + \delta_{G1} + \alpha_{P1})$$

IV. RELATIVE VELOCITY  $\bar{V}_{S1/T1_F}$  AT CONTACT POINT DURING ROUND  
ON FLAT PHASE OF MOTION

For the round on flat phase, the relative velocity  $\bar{V}_{S1/T1_F}$  may be expressed by

$$\bar{V}_{S1/T1_F} = \bar{V}_{S1/O_1} - \bar{V}_{T1/O_2} \quad (G-31)$$

Now, this velocity has the direction of the unit vector  $\pm \bar{n}_{F1}$ . Since there is no velocity component along the pinion flank, equation (G-31) becomes

$$\begin{aligned} \bar{V}_{S1/T1_F} &= \bar{V}_{S1/O_1} \cdot \bar{n}_{F1} \\ &= \left\{ \left[ \dot{\phi}_1 \times (a_{G1} \bar{n}_{G1} + r_{G1} \bar{n}_{NF1}) \right] \cdot \bar{n}_{F1} \right\} \bar{n}_{F1} \end{aligned} \quad (G-32)$$

Appropriate substitution of unit vectors furnishes

$$\bar{V}_{S1/T1_F} = \dot{\phi}_1 \left[ a_{G1} \sin(\psi_1 - \alpha_{P1} - \phi_1 - \delta_{G1}) - r_{G1} \right] \bar{n}_{F1} \quad (G-33)$$

## V. DETERMINATION OF TRANSITION ANGLES

The transition angle,  $\phi_{1T}$ , and the corresponding angle,  $\psi_{1T}$ , are reached when the round or round phase is followed by the round on flat one. They are obtained by letting  $g_1 = f_{p1}$  in the component equations (G-25) and (G-26). This gives

$$\begin{aligned} a_{G1} \cos(\phi_{1T} + \delta_{G1}) - p_{G1} \sin(\psi_{1T} - \alpha_{P1}) - b_1 \cos \beta_1 - f_{P1} \cos(\psi_{1T} - \alpha_{P1}) \\ = 0 \end{aligned} \quad (G-34)$$

and

$$\begin{aligned} a_{G1} \sin(\phi_{1T} + \delta_{G1}) + p_{G1} \cos(\psi_{1T} - \alpha_{P1}) - b_1 \sin \beta_1 - f_{P1} \sin(\psi_{1T} - \alpha_{P1}) \\ = 0 \end{aligned} \quad (G-35)$$

From the above, one obtains

$$\cos(\phi_{1T} + \delta_{G1}) = \frac{1}{a_{G1}} \left[ p_{G1} \sin(\psi_{1T} - \alpha_{P1}) + b_1 \cos \beta_1 + f_{P1} \cos(\psi_{1T} - \alpha_{P1}) \right] \quad (G-36)$$

$$\sin(\phi_{1T} + \delta_{G1}) = \frac{1}{a_{G1}} \left[ -p_{G1} \cos(\psi_{1T} - \alpha_{P1}) + b_1 \sin \beta_1 + f_{P1} \sin(\psi_{1T} - \alpha_{P1}) \right] \quad (G-37)$$

The angle  $\psi_{1T}$  is now obtained by letting

$$\sin^2(\phi_{1T} + \delta_{G1}) + \cos^2(\phi_{1T} + \delta_{G1}) = 1$$

This results in

$$A_{1T} \sin \psi_{1T} + B_{1T} \cos \psi_{1T} = C_{1T} \quad (G-38)$$

where

$$A_{1T} = \rho_{G1} \cos(\beta_1 + \alpha_{P1}) + f_{P1} \sin(\beta_1 + \alpha_{P1})$$

$$B_{1T} = -\rho_{G1} \sin(\beta_1 + \alpha_{P1}) + f_{P1} \cos(\beta_1 + \alpha_{P1})$$

$$C_{1T} = \frac{a_{G1}^2 - \rho_{G1}^2 - b_1^2 - f_{P1}^2}{2b_1}$$

Finally,

$$\psi_{1T} = 2 \tan^{-1} \frac{A_{1T} \pm \sqrt{A_{1T}^2 + B_{1T}^2 - C_{1T}^2}}{B_{1T} + C_{1T}} \quad (G-39)$$

The appropriate sign must be found from geometric considerations.

The associated angle  $\phi_{1T}$  may be found with the help of either equation (G-36) or equation (G-37):

$$\phi_{1T} = \cos^{-1} \left[ \frac{\rho_{G1} \sin(\psi_{1T} - \alpha_{P1}) + f_{P1} \cos(\psi_{1T} - \alpha_{P1}) + b_1 \cos \beta_1}{a_{G1}} \right]$$

-  $\delta_{G1}$  (G-40)

or

$$\phi_{1T} = \sin^{-1} \left[ \frac{-\rho_{G1} \cos(\psi_{1T} - \alpha_{P1}) + f_{P1} \sin(\psi_{1T} - \alpha_{P1}) + b_1 \sin \beta_1}{a_{G1}} \right]$$

-  $\delta_{G1}$  (G-41)

#### VI. SENSING EQUATION FOR THE DETERMINATION OF CONTACT ON SUBSEQUENT TOOTH MESH

The following contact sensing equation is derived with the assumption that subsequent contact is made in the round on round phase of the motion, in the manner shown in Section VI of Appendix E. Now, the configuration is that of Figure G-2 where gear no. 1 rotates in a clockwise direction.

Before contact is made, the distance between the centers of curvature  $C_{G1}$  and  $C_{P1}$  is given by

$$\overline{C_{G1}C_{P1}} = L_{x1}\bar{i} + L_{y1}\bar{j} \quad (G-42)$$

If  $\Delta\phi_1$  and  $\Delta\psi_1$  represent the tooth spacing angles of gear no. 1 and pinion no. 2, respectively, the associated loop equation becomes (see Figures E-3 and G-2).

$$\begin{aligned} & a_{G1} [\cos(\phi_1 + \Delta\phi_1 + \delta_{G1})\bar{i} + \sin(\phi_1 + \Delta\phi_1 + \delta_{G1})\bar{j}] + L_{x1}\bar{i} + L_{y1}\bar{j} \\ & = b_1 (\cos\beta_1\bar{i} + \sin\beta_1\bar{j}) + a_{P1} [\cos(\psi_1 - \Delta\psi_1 + \delta_{P1})\bar{i} + \sin(\psi_1 - \Delta\psi_1 + \delta_{P1})\bar{j}] \end{aligned} \quad (G-43)$$

where

$\psi_1$  = angle of pinion no. 2 as determined for the round on flat mode with equation (G-29)

The magnitudes of  $L_{x1}$  and  $L_{y1}$  are determined from the component form of equation (G-43), i.e.,

$$L_{x1} = b_1 \cos\beta_1 + a_{P1} \cos(\psi_1 - \Delta\psi_1 + \delta_{P1}) - a_{G1} \cos(\phi_1 + \Delta\phi_1 + \delta_{G1}) \quad (G-44)$$

and

$$L_{y1} = b_1 \sin\beta_1 + a_{P1} \sin(\psi_1 - \Delta\psi_1 + \delta_{P1}) - a_{G1} \sin(\phi_1 + \Delta\phi_1 + \delta_{G1}) \quad (G-45)$$

Contact will have occurred as soon as

$$\sqrt{L_{x1}^2 + L_{y1}^2} \leq P_{G1} + P_{P1}$$

(G-46)

## 2. KINEMATICS OF MESH NO. 2 (GEAR NO. 2 AND PINION NO. 3)

### a. ROUND ON ROUND PHASE OF MOTION

Figure G-4 gives a schematic representation of the round on round phase of the motion. Only the contacting faces of the gear and the pinion are shown. It is to be noted that the input gear rotates in the counter-clockwise direction, and that the output angle  $\psi_1$  of mesh no. 1 is identical to the input angle  $\phi_2$  of mesh no. 2.

#### I. UNIT VECTORS

The unit vector in the direction  $O_2C_{G2}$  of the gear is given by

$$\bar{n}_{G2} = \cos(\phi_2 - \delta_{G2})\bar{i} + \sin(\phi_2 - \delta_{G2})\bar{j} \quad (G-47)$$

The unit vector in the direction  $C_{G2}C_{P2}$  is given by

$$\bar{n}_{\lambda 2} = \cos\lambda_2\bar{i} + \sin\lambda_2\bar{j} \quad (G-48)$$

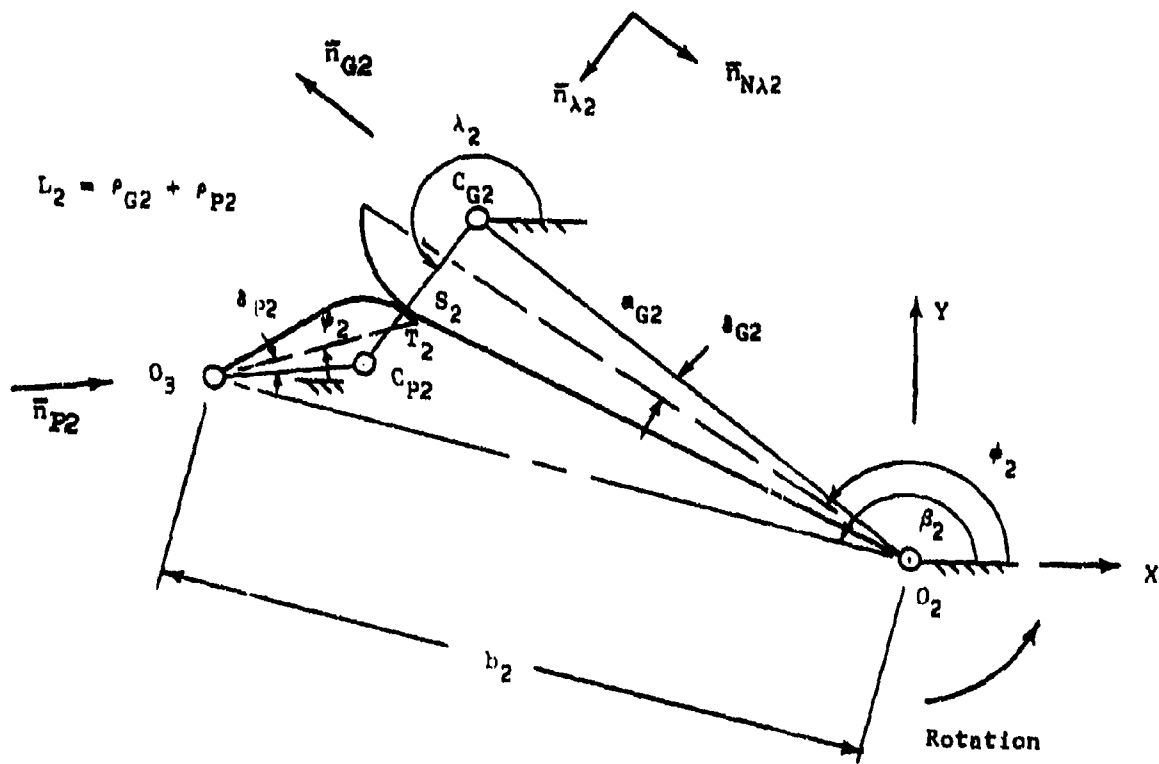


FIGURE G-4  
 ROUND ON ROUND PHASE FOR MESH NO. 2

The unit vector normal to  $\bar{n}_{\lambda_2}$  in the right hand sense becomes

$$\bar{n}_{N\lambda_2} = -\sin\lambda_2\bar{i} + \cos\lambda_2\bar{j} \quad (G-49)$$

The pinion unit vector  $\bar{n}_{p_2}$ , in the direction  $O_3C_{p_2}$ , is represented by

$$\bar{n}_{p_2} = \cos(\psi_2 - \delta_{p_2})\bar{i} + \sin(\psi_2 - \delta_{p_2})\bar{j} \quad (G-50)$$

Finally, the unit vector along the centerline  $O_2O_3$  is given by

$$\bar{n}_{\beta_2} = \cos\beta_2\bar{i} + \sin\beta_2\bar{j} \quad (G-51)$$

## II. DETERMINATION OF OUTPUT ANGLE $\psi_2$ AND "COUPLER" ANGLE $\lambda_2$

The loop equation of the equivalent four-bar linkage is given by

$$a_{G_2}\bar{n}_{G_2} + L_2\bar{n}_{\lambda_2} - a_{p_2}\bar{n}_{p_2} - b_2\bar{n}_{\beta_2} = 0 \quad (G-52)$$

where

$$L_2 = \rho_{G2} + \rho_{P2} \quad (G-53)$$

After substitution of the unit vector, as given earlier, one obtains the following component equations

$$a_{G2} \cos(\phi_2 - \delta_{G2}) + L_2 \cos \lambda_2 - a_{P2} \cos(\psi_2 - \delta_{P2}) - b_2 \cos \beta_2 = 0 \quad (G-54)$$

and

$$a_{G2} \sin(\phi_2 - \delta_{G2}) + L_2 \sin \lambda_2 - a_{P2} \sin(\psi_2 - \delta_{P2}) - b_2 \sin \beta_2 = 0 \quad (G-55)$$

To solve for the output angle  $\psi_2$  in terms of the input angle  $\phi_2$ , substitute the expressions for  $\sin \lambda_2$  and  $\cos \lambda_2$ , as obtained from the component equations (G-54) and (G-55), into

$$\sin^2 \lambda_2 + \cos^2 \lambda_2 = 1 \quad (G-56)$$

This leads to

$$A_{2R} \sin \psi_2 + B_{2R} \cos \psi_2 = C_{2R} \quad (G-57)$$

where

$$A_{2R} = b_2 \sin(\beta_2 + \delta_{p2}) - a_{G2} \sin(\phi_2 - \delta_{G2} + \delta_{p2})$$

$$B_{2R} = b_2 \cos(\beta_2 + \delta_{p2}) - a_{G2} \cos(\phi_2 - \delta_{G2} + \delta_{p2})$$

$$C_{2R} = \frac{L_2^2 - b_2^2 - a_{G2}^2 - a_{p2}^2 + 2a_{G2}b_2 \cos(\phi_2 - \delta_{G2} - \beta_2)}{2a_{p2}}$$

Equation (G-57) is then solved for  $\psi_2$  in the manner discussed in Appendix E

$$\psi_2 = 2 \tan^{-1} \frac{A_{2R} \pm \sqrt{A_{2R}^2 + B_{2R}^2 - C_{2R}^2}}{B_{2R} + C_{2R}} \quad (G-58)$$

The correct sign must again be determined from geometric considerations

The angle  $\lambda_2$  may now be determined either from equation (G-54) or equation (G-55)

$$\lambda_2 = \cos^{-1} \left[ \frac{b_2 \cos \beta_2 + a_{p2} \cos(\psi_2 - \delta_{p2}) - a_{G2} \cos(\phi_2 - \delta_{G2})}{L_2} \right] \quad (G-59)$$

or

$$\lambda_2 = \sin^{-1} \left[ \frac{b_2 \sin \beta_2 + a_{p2} \sin(\psi_2 - \delta_{p2}) - a_{G2} \sin(\phi_2 - \delta_{G2})}{L_2} \right] \quad (G-60)$$

### III. DETERMINATION OF OUTPUT ANGULAR VELOCITY $\dot{\psi}_2$

Implicit differentiation of equation (G-57) with respect to time leads to

$$\dot{\psi}_2 = \dot{\phi}_2 \left[ \frac{A_{2RD} \sin \psi_2 - B_{2RD} \cos \psi_2 - C_{2RD}}{A_{2R} \cos \psi_2 - B_{2R} \sin \psi_2} \right] \quad (G-61)$$

where

$$A_{2RD} = a_{G2} \cos(\phi_2 - \delta_{G2} + \delta_{p2})$$

$$B_{2RD} = a_{G2} \sin(\phi_2 - \delta_{G2} + \delta_{p2})$$

$$C_{2RD} = \frac{a_{G2} b_2 \sin(\phi_2 - \delta_{G2} - \beta_2)}{a_{p2}}$$

#### IV. RELATIVE VELOCITY AT THE CONTACT POINT

The relative velocity  $\bar{V}_{S_2/T_2R}$ , of point  $S_2$  on gear no. 2 with respect to point  $T_2$  on pinion no. 3 has the direction of the unit vector  $\bar{n}_{N\lambda 2}$ . Thus, in the manner of equation (G-20).

$$\bar{V}_{S_2/T_2R} = \left\{ \begin{aligned} & [\dot{\phi}_2 \bar{k} \times (a_{G2} \bar{n}_{G2} + r_{G2} \bar{n}_{\lambda 2})] \cdot \bar{n}_{N\lambda 2} \\ & - [\dot{\psi}_2 \bar{k} \times (a_{P2} \bar{n}_{P2} - r_{P2} \bar{n}_{\lambda 2})] \cdot \bar{n}_{N\lambda 2} \end{aligned} \right\} \bar{n}_{N\lambda 2} \quad (G-62)$$

Substitution of unit vectors yields

$$\bar{V}_{S_2/T_2R} = \left\{ \begin{aligned} & \dot{\phi}_2 [a_{G2} \cos(\phi_2 - \delta_{G2} - \lambda_2) + r_{G2}] \\ & - \dot{\psi}_2 [a_{P2} \cos(\psi_2 - \delta_{P2} - \lambda_2) - r_{P2}] \end{aligned} \right\} \bar{n}_{N\lambda 2} \quad (G-63)$$

## b. ROUND ON FLAT PHASE OF MOTION

Figure G-5 shows a schematic view of mesh no. 2 in the round on flat phase of the motion. Again, only the contacting sides of the gear teeth are indicated.

### I. UNIT VECTORS

The unit vector in the direction  $O_3T_2$ , along the flank of pinion no. 3, is given by

$$\bar{n}_{F2} = \cos(\psi_2 + \alpha_{p2})\bar{i} + \sin(\psi_2 + \alpha_{p2})\bar{j} \quad (G-64)$$

The unit vector  $\bar{n}_{NF2}$ , in the direction  $S_2C_{G2}$ , is normal to  $\bar{n}_{F2}$  in the right hand sense

$$\bar{n}_{NF2} = -\sin(\psi_2 + \alpha_{p2})\bar{i} + \cos(\psi_2 + \alpha_{p2})\bar{j} \quad (G-65)$$

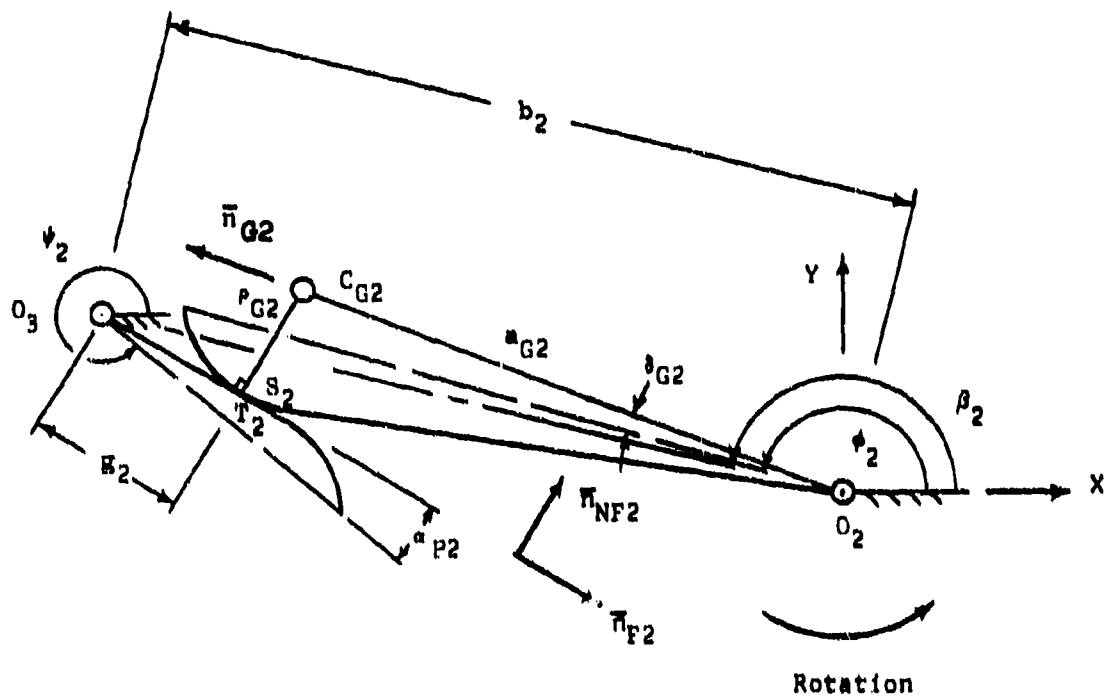


FIGURE G-5

ROUND ON FLAT PHASE OF MOTION OF MESH NO. 2

## II. DETERMINATION OF OUTPUT ANGLE $\psi_2$ AND DISTANCE $g_2$

The vector equation for the mechanism loop  $O_2-C_{G2}-S_2-T_2-O_3$  has the form

$$a_{G2}\bar{n}_{G2} - r_{G2}\bar{n}_{NF2} - g_2\bar{n}_{F2} - b_2\bar{n}_{\beta 2} = 0 \quad (G-66)$$

Appropriate substitutions for the unit vectors furnish the following component equations.

$$a_{G2}\cos(\phi_2 - \delta_{G2}) + r_{G2}\sin(\psi_2 + \alpha_{P2}) - b_2\cos\beta_2 - g_2\cos(\psi_2 + \alpha_{P2}) = 0 \quad (G-67)$$

and

$$a_{G2}\sin(\phi_2 - \delta_{G2}) - r_{G2}\cos(\psi_2 + \alpha_{P2}) - b_2\sin\beta_2 - g_2\sin(\psi_2 + \alpha_{P2}) = 0 \quad (G-68)$$

From equation (G-68) one obtains the following expression for  $g_2$

$$g_2 = \frac{a_{G2}\sin(\phi_2 - \delta_{G2}) - r_{G2}\cos(\psi_2 + \alpha_{P2}) - b_2\sin\beta_2}{\sin(\psi_2 + \alpha_{P2})} \quad (G-69)$$

This expression is now substituted into equation (G-67), and one obtains the following:

$$A_{2F} \sin \psi_2 + B_{2F} \cos \psi_2 = C_{2F} \quad (G-70)$$

where

$$A_{2F} = a_{G2} \cos(\phi_2 - \delta_{G2} - \alpha_{P2}) - b_2 \cos(\beta_2 - \alpha_{P2})$$

$$B_{2F} = -a_{G2} \sin(\phi_2 - \delta_{G2} - \alpha_{P2}) + b_2 \sin(\beta_2 - \alpha_{P2})$$

$$C_{2F} = -r_{G2}$$

Equation (G-70) is solved in the customary manner:

$$\psi_2 = 2 \tan^{-1} \frac{A_{2F} \pm \sqrt{A_{2F}^2 + B_{2F}^2 - C_{2F}^2}}{B_{2F} + C_{2F}} \quad (G-71)$$

The appropriate sign is again found from geometric considerations.

III. DETERMINATION OF ANGULAR VELOCITY  $\dot{\psi}_2$  DURING ROUND ON FLAT  
PHASE OF MOTION

Implicit differentiation of equation (G-70) with respect to time gives the following expression for  $\dot{\psi}_2$ :

$$\dot{\psi}_2 = \dot{\phi}_2 \left[ \frac{A_{2FD} \sin \psi_2 + B_{2FD} \cos \psi_2}{A_{2F} \cos \psi_2 - B_{2F} \sin \psi_2} \right] \quad (G-72)$$

where

$$A_{2FD} = a_{G2} \sin(\phi_2 - \delta_{G2} - \alpha_{P2})$$

$$B_{2FD} = a_{G2} \cos(\phi_2 - \delta_{G2} - \alpha_{P2})$$

IV. RELATIVE VELOCITY  $\bar{V}_{S2/T2_F}$  AT CONTACT POINT DURING ROUND  
ON FLAT PHASE OF MOTION

Again, the relative velocity  $\bar{V}_{S2/T2_F}$  consists only of that component of  $\bar{V}_{S2/O_2}$  which is directed along the pinion flank.

Thus,

$$\begin{aligned} \bar{v}_{S2/T2_F} &= [\bar{v}_{S2/O2} \cdot \bar{n}_{F2}] \bar{n}_{F2} \\ &= \left\{ \left[ \dot{\phi}_2 \bar{k} \times (a_{G2} \bar{n}_{G2} - r_{G2} \bar{n}_{NF2}) \right] \cdot \bar{n}_{F2} \right\} \bar{n}_{F2} \end{aligned} \quad (G-73)$$

Appropriate substitution of unit vectors gives

$$\bar{v}_{S2/T2_F} = \dot{\phi}_2 \left[ a_{G2} \sin(\psi_2 + \alpha_{P2} - \phi_2 + \delta_{G2}) + r_{G2} \right] \bar{n}_{F2} \quad (G-74)$$

#### V. DETERMINATION OF TRANSITION ANGLES

The transition angle  $\phi_{2T}$  and the angle  $\psi_{2T}$ , which correspond to the transition from the round on round to the round on flat phase of motion, are obtained by letting  $s_2 = f_{P2}$  in the component equations (G-67) and (G-68). From this one finds the following with  $\phi_2 = \phi_{2T}$  and  $\psi_2 = \psi_{2T}$ :

$$\cos(\phi_{2T} - \delta_{G2}) = \frac{1}{a_{G2}} \left[ -r_{G2} \sin(\psi_{2T} + \alpha_{P2}) + b_2 \cos \beta_2 + f_{P2} \cos(\psi_{2T} + \alpha_{P2}) \right] \quad (G-75)$$

and

$$\sin(\phi_{2T} - \delta_{G2}) = \frac{1}{a_{G2}} \left[ p_{G2} \cos(\psi_{2T} + \alpha_{P2}) + b_2 \sin \beta_2 + f_{P2} \sin(\psi_{2T} + \alpha_{P2}) \right] \quad (G-76)$$

The angle  $\psi_{2T}$  is now found by substituting the above expressions into

$$\sin^2(\phi_{2T} - \delta_{G2}) + \cos^2(\phi_{2T} - \delta_{G2}) = 1 \quad (G-77)$$

This results in

$$A_{2T} \sin \psi_{2T} + B_{2T} \cos \psi_{2T} = C_{2T} \quad (G-78)$$

where

$$A_{2T} = -p_{G2} \cos(\beta_2 - \alpha_{P2}) + f_{P2} \sin(\beta_2 - \alpha_{P2})$$

$$B_{2T} = p_{G2} \sin(\beta_2 - \alpha_{P2}) + f_{P2} \cos(\beta_2 - \alpha_{P2})$$

$$C_{2T} = \frac{a_{G2}^2 - p_{G2}^2 - b_2^2 - f_{P2}^2}{2 b_2}$$

Finally, in the usual way

$$\psi_{2T} = 2 \tan^{-1} \frac{A_{2T} \pm \sqrt{A_{2T}^2 + B_{2T}^2 - C_{2T}^2}}{B_{2T} + C_{2T}} \quad (G-79)$$

Again, the sign must be decided from geometric considerations.

The associated angle  $\phi_{2T}$  may be found with the help of either equation (G-75) or equation (G-76), i.e.,

$$\phi_{2T} = \cos^{-1} \left[ \frac{-r_{G2} \sin(\psi_{2T} + \alpha_{P2}) + b_2 \cos \beta_2 + f_{P2} \cos(\psi_{2T} + \alpha_{P2})}{a_{G2}} \right] + \delta_{G2} \quad (G-80)$$

or

$$\phi_{2T} = \sin^{-1} \left[ \frac{r_{G2} \cos(\psi_{2T} + \alpha_{P2}) + b_2 \sin \beta_2 + f_{P2} \sin(\psi_{2T} + \alpha_{P2})}{a_{G2}} \right] + \delta_{G2} \quad (G-81)$$

VI. SENSING EQUATION FOR THE DETERMINATION OF CONTACT ON  
SUBSEQUENT TOOTH MESH

The contact sensing equation for mesh no. 2 is derived similarly to that for mesh no. 1 before contact is made in the round on round mode. The distance between the centers of curvature  $C_{G2}$  and  $C_{P2}$  is given by

$$\overline{C_{G2}C_{P2}} = L_{x2}\bar{i} + L_{y2}\bar{j} \quad (G-82)$$

If  $\Delta\phi_2$  and  $\Delta\psi_2$  represent the tooth spacing angles of gear no. 2 and pinion no. 3 respectively, the associated loop equation becomes (see Figures E-3 and G-4)

$$\begin{aligned} & a_{G2} [\cos(\phi_2 - \Delta\phi_2 - \delta_{G2})\bar{i} + \sin(\phi_2 - \Delta\phi_2 - \delta_{G2})\bar{j}] + L_{x2}\bar{i} + L_{y2}\bar{j} \\ & - a_{P2} [\cos(\psi_2 + \Delta\psi_2 - \delta_{P2})\bar{i} + \sin(\psi_2 + \Delta\psi_2 - \delta_{P2})\bar{j}] \\ & - b_2 [\cos\beta_2\bar{i} + \sin\beta_2\bar{j}] = 0 \end{aligned} \quad (G-83)$$

Note that for mesh no. 2, the angular increment  $\Delta\phi_2$  is negative while  $\Delta\psi_2$  is positive. Further, as before, the angle  $\psi_2$  must be

determined for the round on flat phase of the motion.

The magnitudes of  $L_{x2}$  and  $L_{y2}$  are determined from the components of equation (G-83), i.e.,

$$L_{x2} = b_2 \cos \beta_2 + a_{p2} \cos(\psi_2 + \Delta\psi_2 - \delta_{p2}) - a_{g2} \cos(\phi_2 - \Delta\phi_2 - \delta_{g2}) \quad (G-84)$$

while

$$L_{y2} = b_2 \sin \beta_2 + a_{p2} \sin(\psi_2 + \Delta\psi_2 - \delta_{p2}) - a_{g2} \sin(\phi_2 - \Delta\phi_2 - \delta_{g2}) \quad (G-85)$$

Contact will occur as soon as

$$\sqrt{L_{x2}^2 + L_{y2}^2} \leq r_{g2} + r_{p2} \quad (G-86)$$

### 3. KINEMATICS OF MESH NO. 3 (GEAR NO. 3 AND PINION NO. 4)

Since mesh no. 3 is kinematically equivalent to mesh no. 1, the kinematic equations for mesh no. 3 may be obtained from those for mesh no. 1. The angle  $\beta_3$  must replace the angle  $\beta_1$  and the center distance  $b_3$  is used instead of  $b_1$ . All parameters of gear no. 1 are replaced by those of gear no. 3 and the pinion parameters of pinion no. 4 are substituted for those of pinion no. 2.

It is to be noted that the input angle  $\phi_3$  of mesh no. 3 is identical to the output angle  $\psi_2$  of mesh no. 2.

#### a. ROUND ON ROUND PHASE OF MOTION

The output angle  $\psi_3$  is obtained with the help of equation (G-12)

$$\psi_3 = 2 \tan^{-1} \frac{A_{3R} \pm \sqrt{A_{3R}^2 + B_{3R}^2 - C_{3R}^2}}{B_{3R} + C_{3R}} \quad (G-87)$$

where

$$A_{3R} = a_{G3} \sin(\phi_3 + \delta_{G3} - \delta_{P3}) - b_3 \sin(\beta_3 - \delta_{P3})$$

$$B_{3R} = a_{G3} \cos(\phi_3 + \delta_{G3} - \delta_{P3}) - b_3 \cos(\beta_3 - \delta_{P3})$$

$$C_{3R} = \frac{a_{P3}^2 + a_{G3}^2 + b_3^2 - L_3^2 - 2a_{G3}b_3 \cos(\phi_3 + \delta_{G3} - \beta_3)}{2 a_{P3}}$$

and

$$L_3 = r_{G3} + r_{P3} \quad (G-88)$$

The angle  $\lambda_3$  may be found with the help of equation (G-13) or equation (G-14)

$$\lambda_3 = \cos^{-1} \left[ \frac{b_3 \cos \beta_3 + a_{P3} \cos(\psi_3 + \delta_{P3}) - a_{G3} \cos(\phi_3 + \delta_{G3})}{L_3} \right] \quad (G-89)$$

or

$$\lambda_3 = \sin^{-1} \left[ \frac{b_3 \sin \beta_3 + a_{P3} \sin(\psi_3 + \delta_{P3}) - a_{G3} \sin(\phi_3 + \delta_{G3})}{L_3} \right] \quad (G-90)$$

The angular velocity  $\dot{\psi}_3$  is obtained from equation (G-15)

$$\dot{\psi}_3 = \dot{\phi}_3 \left[ \frac{B_{3RD} \cos \psi_3 - A_{3RD} \sin \psi_3 + C_{3RD}}{A_{3R} \cos \psi_3 - B_{3R} \sin \psi_3} \right] \quad (G-91)$$

where

$$A_{3RD} = a_{G3} \cos(\phi_3 + \delta_{G3} - \delta_{P3})$$

$$B_{3RD} = a_{G3} \sin(\phi_3 + \delta_{G3} - \delta_{P3})$$

$$C_{3RD} = \frac{a_{G3} b_3 \sin(\phi_3 + \delta_{G3} - \beta_3)}{a_{P3}}$$

The relative velocity  $\bar{v}_{S3/T3R}$  becomes, according to Equation (G-21),

$$\bar{v}_{S3/T3R} = \left\{ \begin{array}{l} \dot{\phi}_3 [a_{G3} \cos(\phi_3 + \delta_{G3} - \lambda_3) + r_{G3}] \\ - \dot{\psi}_3 [a_{P3} \cos(\psi_3 + \delta_{P3} - \lambda_3) - r_{P3}] \end{array} \right\} \bar{n}_{N\lambda_3}$$

(G-92)

where, according to equation (G-3),

$$\bar{n}_{N\lambda_3} = -\sin \lambda_3 \bar{i} + \cos \lambda_3 \bar{j}$$

(G-93)

b. ROUND ON FLAT PHASE OF MOTION

The output angle  $\psi_3$  is obtained from equation (G-29)

$$\psi_3 = 2 \tan^{-1} \frac{A_{3F} \pm \sqrt{A_{3F}^2 + B_{3F}^2 - C_{3F}^2}}{B_{3F} + C_{3F}} \quad (G-94)$$

where

$$A_{3F} = a_{G3} \cos(\phi_3 + \delta_{G3} + \alpha_{P3}) - b_3 \cos(\beta_3 + \alpha_{P3})$$

$$B_{3F} = -a_{G3} \sin(\phi_3 + \delta_{G3} + \alpha_{P3}) + b_3 \sin(\beta_3 + \alpha_{P3})$$

$$C_{3F} = r_{G3}$$

The distance  $g_3$  becomes, according to equation (G-27),

$$g_3 = \frac{a_{G3} \sin(\phi_3 + \delta_{G3}) + r_{G3} \cos(\psi_3 - \alpha_{P3}) - b_3 \sin \beta_3}{\sin(\psi_3 - \alpha_{P3})} \quad (G-95)$$

The angular velocity  $\dot{\psi}_3$  for the round on flat phase of the motion is found from equation (G-30)

$$\dot{\psi}_3 = \dot{\phi}_3 \left[ \frac{A_{3FD} \sin \psi_3 + B_{3FD} \cos \psi_3}{A_{3F} \cos \psi_3 - B_{3F} \sin \psi_3} \right] \quad (G-96)$$

where

$$A_{3FD} = a_{G3} \sin(\phi_3 + \delta_{G3} + \alpha_{P3})$$

$$B_{3FD} = a_{G3} \cos(\phi_3 + \delta_{G3} + \alpha_{P3})$$

The relative velocity  $\bar{V}_{S3/T3F}$  for the round on flat phase comes from equation (G-33)

$$\bar{V}_{S3/T3F} = \dot{\phi}_3 \left[ a_{G3} \sin(\psi_3 - \alpha_{P3} - \phi_3 - \delta_{G3}) - \rho_{G3} \right] \bar{n}_{F3} \quad (G-97)$$

where

$$\bar{n}_{F3} = \cos(\psi_3 - \alpha_{P3}) \bar{i} + \sin(\psi_3 - \alpha_{P3}) \bar{j} \quad (G-98)$$

according to equation (G-22).

The transition angle  $\psi_{3T}$  is obtained by way of equation (G-39)

$$\psi_{3T} = 2 \tan^{-1} \frac{A_{3T} \pm \sqrt{A_{3T}^2 + B_{3T}^2 - C_{3T}^2}}{B_{3T} + C_{3T}} \quad (G-99)$$

where

$$A_{3T} = \rho_{G3} \cos(\beta_3 + \alpha_{P3}) + f_{P3} \sin(\beta_3 + \alpha_{P3})$$

$$B_{3T} = -\rho_{G3} \sin(\beta_3 + \alpha_{P3}) + f_{P3} \cos(\beta_3 + \alpha_{P3})$$

$$C_{3T} = \frac{a_{G3}^2 - \rho_{G3}^2 - b_3^2 - f_{P3}^2}{2 b_3}$$

The associated angle  $\phi_{3T}$  may be obtained from equation (G-40)  
or from equation (G-41)

$$\phi_{3T} = \cos^{-1} \left[ \frac{\rho_{G3} \sin(\psi_{3T} - \alpha_{P3}) + f_{P3} \cos(\psi_{3T} - \alpha_{P3}) + b_3 \cos \beta_3}{a_{G3}} \right] - \delta_{G3} \quad (G-100)$$

or

$$\phi_{3T} = \sin^{-1} \left[ \frac{-\rho_{G3} \cos(\psi_{3T} - \alpha_{P3}) + f_{P3} \sin(\psi_{3T} - \alpha_{P3}) + b_3 \sin \beta_3}{a_{G3}} \right] - \delta_{G3} \quad (G-101)$$

Finally, the contact sensing equation is based on equations

(G-44) - (G-46). Contact will occur, when

$$\sqrt{L_{x3}^2 + L_{y3}^2} \leq r_{G3} + r_{P3} \quad (G-102)$$

where with the tooth spacing angles  $\Delta\phi_3$  and  $\Delta\psi_3$ ,

$$L_{x3} = b_3 \cos \beta_3 + a_{P3} \cos(\psi_3 - \Delta\psi_3 + \delta_{P3}) - a_{G3} \cos(\phi_3 + \Delta\phi_3 + \delta_{G3}) \quad (G-103)$$

and

$$L_{y3} = b_3 \sin \beta_3 + a_{P3} \sin(\psi_3 - \Delta\psi_3 + \delta_{P3}) - a_{G3} \sin(\phi_3 + \Delta\phi_3 + \delta_{G3}) \quad (G-104)$$

APPENDIX H  
MOMENT INPUT-OUTPUT RELATIONSHIPS FOR TWO AND THREE STEP-UP  
GEAR TRAINS WITH TEETH OPERATING IN A SPIN ENVIRONMENT

The following gives the derivations for the moment input-output relationships of two and three step-up gear trains which operate in a spin environment.

Figure G-1 of Appendix G shows the basic configuration of a three step-up gear train. The input moment,  $M_{1n}$ , which acts on gear no. 1, is held in equilibrium by the moment,  $M_{o4}$ , which acts on pinion no. 4.

Since in all three meshes there may either be round on round or round on flat type of contact, the force and moment analyses must account for various contact combinations. Table H-1 shows the eight different phase combinations which may occur in a three step-up gear train, and for which input-output relationships must be found. The two step-up gear train, which is shown in Figure A-10 of Appendix A for involute gearing, does not contain pinion 4 and gear no. 3. Here, the input moment  $M_{1n}$ , which acts on gear no. 1, is held in equilibrium by moment  $M_{o3}$ , which acts on pinion no. 3.

Case no.	Mesh No. 3 (Gear 3 & Pinion 4)	Mesh No. 2 (Gear 2 & Pinion 3)	Mesh No. 1 (Gear 1 & Pinion 2)
1	R	R	R
2	R	R	F
3	R	F	F
4	R	F	R
5	F	F	F
6	F	F	R
7	F	R	R
8	F	R	F

TABLE H-1

POSSIBLE COMBINATIONS OF PHASES FOR THREE STEP-UP GEAR TRAIN AS SHOWN IN FIGURE G-1

R = Round on Round

F = Round on Flat

When ogival teeth are involved, there are four possible phase combinations of the two remaining meshes. These are shown in Table H-2. Again input-output relationships must be obtained for each of them.

Case No.	Mesh No. 2 (Gear 2 & Pinion 3)	Mesh No. 1 (Gear 1 & Pinion 2)
1	R	R
2	R	F
3	F	F
4	F	R

TABLE H-2

POSSIBLE COMBINATIONS OF PHASES FOR TWO STEP-UP GEAR TRAIN AS SHOWN IN FIGURE A-10

R = Round on Round

F = Round on Flat

The unit vectors, mechanism angles and kinematic terms necessary for the following analyses were derived in Appendix G. (See also Appendix D for a description of the geometry of ogival teeth.) Certain terms used in connection with mesh no. 3 may be obtained from expressions derived for mesh no. 1 in Appendix G by the replacement of the appropriate subscript numbers, since the kinematics of these meshes are identical. The following additional nomenclature is used:

- $R_i$  = distance from spin axis C to pivot points  $O_i$  of individual gears. ( $i = 1, 2, 3, 4$  as applicable)
- $\gamma_i$  = angle of lines  $R_i = CO_i$  with respect to the body-fixed X-axis
- $\omega$  = spin velocity of fuze body
- $m_i$  = mass of various gears, pinions and gear-pinion combinations
- $Q_i$  =  $m_i R_i \omega^2$ , centrifugal force acting on individual gear components. (Now called  $Q_i$  to differentiate it from the pinion contact point  $T_i$ .)
- $r_i$  = pivot radius
- $r_{pi}$  = radius of curvature of pinion tooth (ogival)
- $r_{Gi}$  = radius of curvature of gear tooth (ogival)
- $\mu$  = coefficient of friction at pivots as well as at contact point between gears and pinions

The pivot friction moments are obtained according to equation (A-3b) of Appendix A. They always oppose motion regardless of the assumption of direction of the pivot reactions  $F_{xi}$  and  $F_{yi}$ . To this end the pivot forces  $\tilde{F}_{xi}$  and  $\tilde{F}_{yi}$ , which represent the sums of the absolute values of their component parts, are added

algebraically. The algebraic addition of such modified reactions provides a conservative, i.e., a somewhat overstated friction moment.

The directions of the friction forces of the gears on the pinions are always those of the relative velocities  $\bar{V}_{S_1/T_1}$ , where points  $S_1$  and  $T_1$  are located at the contact points of the gears and pinions, respectively. This allows the introduction of a signum convention. For the round on round phases,

$$s_{1R} = \frac{V_{S_1/T_1R}}{|V_{S_1/T_1R}|} \quad (H-1)$$

For the round on flat phase, the convention becomes

$$s_{1F} = \frac{V_{S_1/T_1F}}{|V_{S_1/T_1F}|} \quad (H-2)$$

The expressions for the above relative velocities, which are different for round on round and for round on flat, are given in Appendix G.

## 1. INPUT-OUTPUT ANALYSIS OF THREE STEP-UP GEAR TRAIN

### a. CASE NO. 1: RRR

#### I. FORCE AND MOMENT EQUILIBRIA OF PINION NO. 4

Figure H-1 shows a schematic free body diagram of pinion no. 4 in the round on round mode of contact. The equivalent four-bar linkage associated with mesh no. 3 is also indicated. The pinion is acted upon by the equilibrant moment  $M_{o4}$  in the direction opposite to its counterclockwise rotation. The contact force of gear no. 3 on the pinion is given by

$$\vec{F}_{34} = F_{34} \bar{n}_{\lambda 3} \quad (H-3)$$

The associated friction force exerted by the gear on the pinion has the direction of the relative velocity  $\bar{v}_{s3/T3R}$ , as given by equation (G-92). With the use of the signum convention of equation (H-1) the friction force  $\vec{F}_{f34}$  becomes

$$\vec{F}_{f34} = \mu_{34} F_{34} \bar{n}_{\lambda 3} \quad (H-4)$$

Note:  $\psi$  is positive in ccw direction

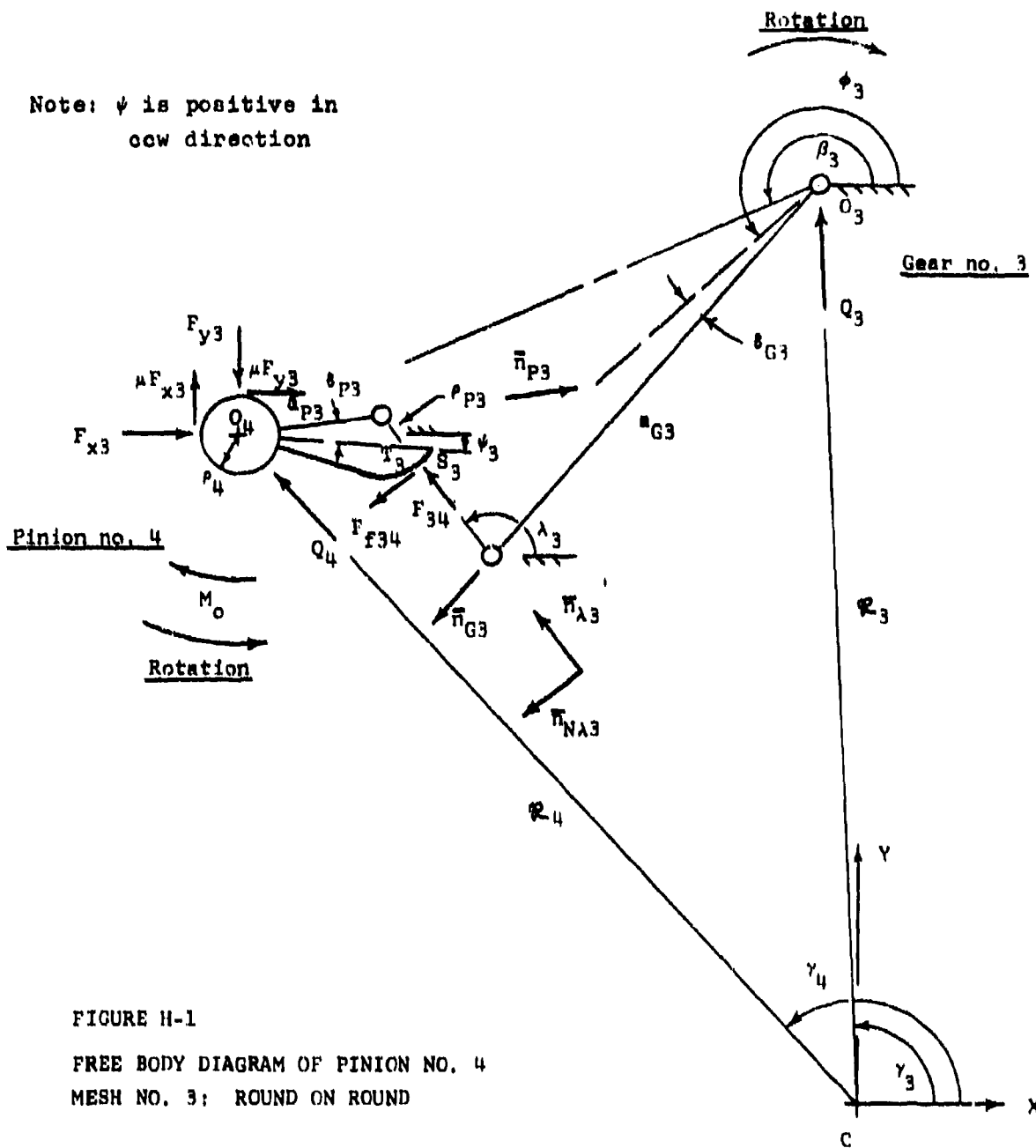


FIGURE H-1  
FREE BODY DIAGRAM OF PINION NO. 4  
MESH NO. 3; ROUND ON ROUND

The centrifugal force, due to the pinion mass, is given by

$$\bar{Q}_4 = Q_4(\cos\gamma_4\bar{i} + \sin\gamma_4\bar{j}) \quad (H-5)$$

where

$$Q_4 = R_4 m_4 \omega^2 \quad (H-6)$$

Force equilibrium is given by

$$F_{34}\bar{n}_{\lambda 3} + \mu_{3R}F_{34}\bar{n}_{N\lambda 3} + F_{x4}\bar{i} + \mu F_{y4}\bar{i} - F_{y4}\bar{j} + \mu F_{x4}\bar{j} + \bar{Q}_4 = 0 \quad (H-7)$$

Moment equilibrium requires the following:

$$-M_{o4}\bar{k} - \mu\rho_4(\bar{F}_{x4} + \bar{F}_{y4})\bar{k} + (a_{p3}\bar{n}_{p3} - r_{p3}\bar{n}_{\lambda 3}) \times (F_{34}\bar{n}_{\lambda 3} + \mu_{3R}F_{34}\bar{n}_{N\lambda 3}) = 0 \quad (H-8)$$

Equation (H-7) furnishes the following component equations:

$$F_{34}\cos\lambda_3 - \mu_{3R}F_{34}\sin\lambda_3 + F_{x4} + \mu F_{y4} + Q_4\cos\gamma_4 = 0 \quad (H-9)$$

and

$$F_{34}\sin\lambda_3 + \mu_{3R}F_{34}\cos\lambda_3 - F_{y4} + \mu F_{x4} + Q_4\sin\gamma_4 = 0 \quad (H-10)$$

The scalar form of the moment equation becomes

$$-M_{o4} - \mu \rho_4 (\tilde{F}_{x4} + \tilde{F}_{y4}) - F_{34} \left\{ \mu_{3R} \left[ \sin(\psi_3 + \delta_{P3} - \lambda_3) - \mu_{3R} \cos(\psi_3 + \delta_{P3} - \lambda_3) \right] + \mu_{3R} \rho_{P3} \right\} = 0 \quad (H-11)$$

Simultaneous solution of equations (H-9) and (H-10) for  $F_{x4}$  and  $F_{y4}$  gives

$$F_{x4} = \frac{F_{34} [\mu(\mu_{3R} - 1) \sin \lambda_3 - (1 + \mu^2 \mu_{3R}) \cos \lambda_3] - Q_4 (\mu \sin \gamma_4 + \cos \gamma_4)}{1 + \mu^2} \quad (H-12)$$

and

$$F_{y4} = \frac{F_{34} [(1 + \mu^2 \mu_{3R}) \sin \lambda_3 + \mu(\mu_{3R} - 1) \cos \lambda_3] + Q_4 (\sin \gamma_4 - \mu \cos \gamma_4)}{1 + \mu^2} \quad (H-13)$$

The sum  $\tilde{F}_{x4} + \tilde{F}_{y4}$  of equation (H-11) is now made up of equations (H-12) and (H-13) in the sense of equation (A-3b) of Appendix A

$$\tilde{F}_{x4} + \tilde{F}_{y4} = Q_4 A_1 + F_{34} A_2 + Q_4 A_3 + F_{34} A_4 \quad (H-14)$$

$$A_1 = \left| \frac{\mu \sin \gamma_4 + \cos \gamma_4}{1 + \mu^2} \right| \quad (\text{H-15})$$

$$A_2 = \left| \frac{\mu (s_{3R} - 1) \sin \lambda_3 - (1 + \mu^2 s_{3R}) \cos \lambda_3}{1 + \mu^2} \right| \quad (\text{H-16})$$

$$A_3 = \left| \frac{\sin \gamma_4 - \mu \cos \gamma_4}{1 + \mu^2} \right| \quad (\text{H-17})$$

$$A_4 = \left| \frac{(1 + \mu^2 s_{3R}) \sin \lambda_3 + \mu (s_{3R} - 1) \cos \lambda_3}{1 + \mu^2} \right| \quad (\text{H-18})$$

Equation (H-14) is now substituted into the moment equation (H-11) and the latter is solved for the contact force  $F_{34}$

$$F_{34} = \frac{M_{o4}}{C_2} + \frac{Q_4 C_1}{C_2} \quad (\text{H-19})$$

where

$$C_1 = \mu \rho_4 (A_1 + A_3)$$

$$C_2 = a_{P3} \left[ \mu s_{3R} \cos(\psi_3 + \delta_{P3} - \lambda_3) - \sin(\psi_3 + \delta_{P3} - \lambda_3) \right] \\ - \mu \left[ \rho_{P3} s_{3R} + \rho_4 (A_2 + A_4) \right]$$

## II. FORCE AND MOMENT EQUILIBRIA OF GEAR AND PINION SET NO. 3

Figure H-2 gives a schematic free body diagram of the gear and pinion combination no. 3. Mesh no. 2 is also indicated to obtain the directions of the forces of gear no. 2 on pinion no. 3. The forces of pinion no. 4 on gear no. 3 are opposite to those given by equations (H-3) and (H-4) respectively. Thus, the contact force becomes

$$\bar{F}_{43} = -\bar{F}_{34} = -F_{34}\bar{n}_{\lambda 3} \quad (\text{H-20})$$

The friction force of pinion no. 4 on gear no. 3 becomes:

$$\bar{F}_{f43} = -\bar{F}_{f34} = -\mu_{s3} F_{34} \bar{n}_{\lambda 3} \quad (\text{H-21})$$

The contact force of gear no. 2 on pinion no. 3 is given by

$$\bar{F}_{23} = F_{23}\bar{n}_{\lambda 2} \quad (\text{H-22})$$

while the associated friction force of gear no. 2 on pinion no. 3 becomes

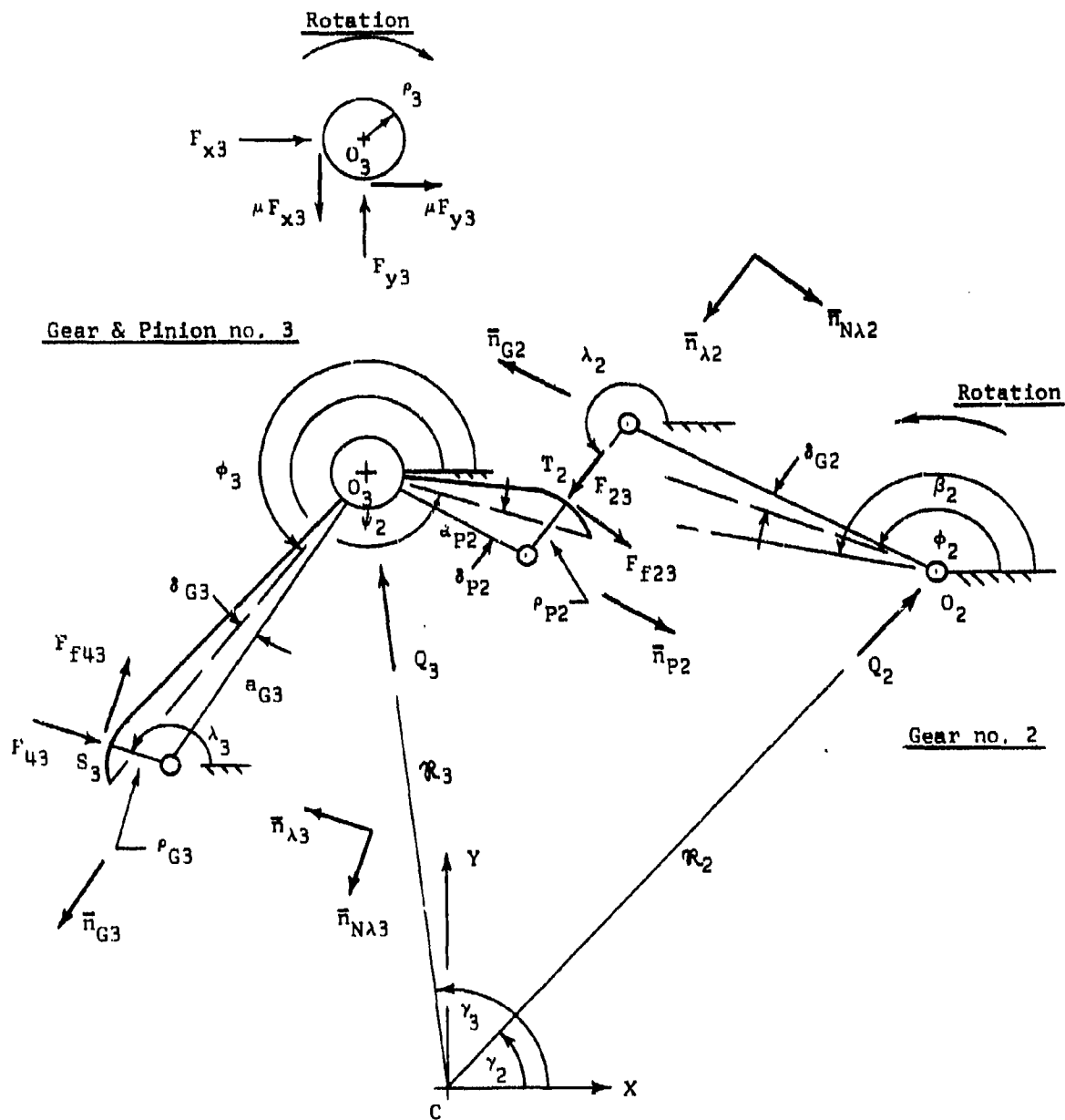


FIGURE H-2  
 FREE BODY DIAGRAM OF GEAR & PINION NO. 3  
 MESH NO. 3: ROUND ON ROUND  
 MESH NO. 2: ROUND ON ROUND

$$\bar{F}_{f23} = \mu_{s2R} F_{23} \bar{n}_{N\lambda 2} \quad (H-23)$$

The pivot reactions  $F_{x3}$  and  $F_{y3}$  as well as the associated friction forces are drawn in a separate diagram in Figure H-2. As was the case earlier, the friction moment due to the friction forces again opposes rotation.

The centrifugal force, due to the mass of the combined gear and pinion no. 3, is given by

$$\bar{Q}_3 = Q_3 (\cos \gamma_3 \bar{i} + \sin \gamma_3 \bar{j}) \quad (H-24)$$

where

$$Q_3 = \omega_3 m_3 \omega^2 \quad (H-25)$$

The force equilibrium of the combination is given by

$$\begin{aligned} -F_{34} \bar{n}_{\lambda 3} - \mu_{s3R} F_{34} \bar{n}_{N\lambda 3} + F_{23} \bar{n}_{\lambda 2} + \mu_{s2R} F_{23} \bar{n}_{N\lambda 2} + F_{x3} \bar{i} + \mu F_{y3} \bar{i} \\ + F_{y3} \bar{j} - \mu F_{x3} \bar{j} + \bar{Q}_3 = 0 \end{aligned} \quad (H-26)$$

The moment equation is given by

$$\begin{aligned} & \mu \rho_3 (\tilde{F}_{x3} + \tilde{F}_{y3}) \bar{k} + [a_{G3} \bar{n}_{G3} + \rho_{G3} \bar{n}_{\lambda 3}] \times [-F_{34} \bar{n}_{\lambda 3} - \mu_{S3R} F_{34} \bar{n}_{N\lambda 3}] \\ & + [a_{P2} \bar{n}_{P2} - \rho_{P2} \bar{n}_{\lambda 2}] \times [F_{23} \bar{n}_{\lambda 2} + \mu_{S2R} F_{23} \bar{n}_{N\lambda 2}] = 0 \quad (H-27) \end{aligned}$$

Equation (H-26) gives the following component expressions:

$$\begin{aligned} -F_{34} \cos \lambda_3 + \mu_{S3R} F_{34} \sin \lambda_3 + Q_3 \cos \gamma_3 + F_{x3} + \mu F_{y3} + F_{23} \cos \lambda_2 \\ - \mu_{S2R} F_{23} \sin \lambda_2 = 0 \quad (H-28) \end{aligned}$$

and

$$\begin{aligned} -F_{34} \sin \lambda_3 - \mu_{S3R} F_{34} \cos \lambda_3 + Q_3 \sin \gamma_3 + F_{y3} - \mu F_{x3} + F_{23} \sin \lambda_2 \\ + \mu_{S2R} F_{23} \cos \lambda_2 = 0 \quad (H-29) \end{aligned}$$

The scalar form of the moment equation (H-27) becomes

$$\begin{aligned} & \mu \rho_3 (\tilde{F}_{x3} + \tilde{F}_{y3}) - \mu_{S3R} \rho_{G3} F_{34} - \mu_{S2R} \rho_{P2} F_{23} + a_{G3} F_{34} [\sin(\phi_3 + \delta_{G3} - \lambda_3) \\ & - \mu_{S3R} \cos(\phi_3 + \delta_{G3} - \lambda_3)] + a_{P2} F_{23} [-\sin(\psi_2 - \delta_{P2} - \lambda_2) \\ & + \mu_{S2R} \cos(\psi_2 - \delta_{P2} - \lambda_2)] = 0 \quad (H-30) \end{aligned}$$

Simultaneous solution of equations (H-28) and (H-29) for the pivot reactions  $F_{x3}$  and  $F_{y3}$  gives

$$F_{x3} = \frac{1}{1 + \mu^2} \left\{ F_{34} [(1 - \mu^2 s_{3R}) \cos \lambda_3 - \mu(1 + s_{3R}) \sin \lambda_3] + \right. \\ F_{23} [\mu(1 + s_{2R}) \sin \lambda_2 - (1 - \mu^2 s_{2R}) \cos \lambda_2] + \\ \left. Q_3 [\mu \sin \gamma_3 - \cos \gamma_3] \right\} \quad (H-31)$$

and

$$F_{y3} = \frac{1}{1 + \mu^2} \left\{ F_{34} [(1 - \mu^2 s_{3R}) \sin \lambda_3 + \mu(1 + s_{3R}) \cos \lambda_3] + \right. \\ F_{23} [(\mu^2 s_{2R} - 1) \sin \lambda_2 - \mu(1 + s_{2R}) \cos \lambda_2] - \\ \left. Q_3 [\sin \gamma_3 + \mu \cos \gamma_3] \right\} \quad (H-32)$$

The sum  $\tilde{F}_{x3} + \tilde{F}_{y3}$  of equation (H-30) is now made up of equations (H-31) and (H-32) in the sense of equation (A-3b).

$$\tilde{F}_{x3} + \tilde{F}_{y3} = F_{34} A_5 + F_{23} A_6 + Q_3 A_7 + F_{34} A_8 + F_{23} A_9 + Q_3 A_{10} \quad (H-33)$$

where

$$A_5 = \left| \frac{(1 - \mu^2 s_{3R}) \cos \lambda_3 - \mu(1 + s_{3R}) \sin \lambda_3}{1 + \mu^2} \right| \quad (H-34)$$

$$A_6 = \left| \frac{\mu(1 + s_{2R}) \sin \lambda_2 - (1 - \mu^2 s_{2R}) \cos \lambda_2}{1 + \mu^2} \right| \quad (H-35)$$

$$A_7 = \left| \frac{\mu \sin \gamma_3 - \cos \gamma_3}{1 + \mu^2} \right| \quad (H-36)$$

$$A_8 = \left| \frac{(1 - \mu^2 s_{3R}) \sin \lambda_3 + \mu(1 + s_{3R}) \cos \lambda_3}{1 + \mu^2} \right| \quad (H-37)$$

$$A_9 = \left| \frac{(\mu^2 s_{2R} - 1) \sin \lambda_2 - \mu(1 + s_{2R}) \cos \lambda_2}{1 + \mu^2} \right| \quad (H-38)$$

$$A_{10} = \left| \frac{\sin \gamma_3 + \mu \cos \gamma_3}{1 + \mu^2} \right| \quad (H-39)$$

Equation (H-33) is now substituted into equation (H-30) and the resulting expression is solved for the contact force  $F_{23}$ . Thus,

$$F_{23} = \frac{-F_{34} C_3 - Q_3 C_4}{C_5} \quad (H-40)$$

where

$$C_3 = \mu_{P3}(A_5 + A_8) - \mu_{S3R}^S \rho_{G3} + a_{G3} [\sin(\phi_3 + \delta_{G3} - \lambda_3) - \mu_{S3R}^S \cos(\phi_3 + \delta_{G3} - \lambda_3)]$$

$$C_4 = \mu_{P3}(A_7 + A_{10})$$

$$C_5 = \mu_{P3}(A_6 + A_9) - \mu_{S2R}^S \rho_{P2} + a_{P2} [\mu_{S2R}^S \cos(\psi_2 - \delta_{P2} - \lambda_2) - \sin(\psi_2 - \delta_{P2} - \lambda_2)]$$

### III. FORCE AND MOMENT EQUILIBRIA OF GEAR AND PINION SET NO. 2

Figure H-3 gives the free body diagram of the gear and pinion combination no. 2. In addition, mesh no. 1 is indicated to obtain the directions of the forces of gear no. 1 on pinion no. 2.

The forces of pinion no. 3 on gear no. 2 have directions opposite to those given by equation (H-22) and (H-23) respectively. Thus, the normal force is given by

$$\bar{F}_{32} = -F_{23}\bar{n}_{\lambda 2} \quad (H-41)$$

The friction force of pinion no. 3 on gear no. 2 becomes

$$\bar{F}_{f32} = -\mu_{s2} F_{23} \bar{n}_{\lambda 2} \quad (H-42)$$

The contact force of gear no. 1 on pinion no. 2 is given by

$$\bar{F}_{12} = F_{12}\bar{n}_{\lambda 1} \quad (H-43)$$

while the associated friction force of gear no. 1 on pinion no. 2 becomes

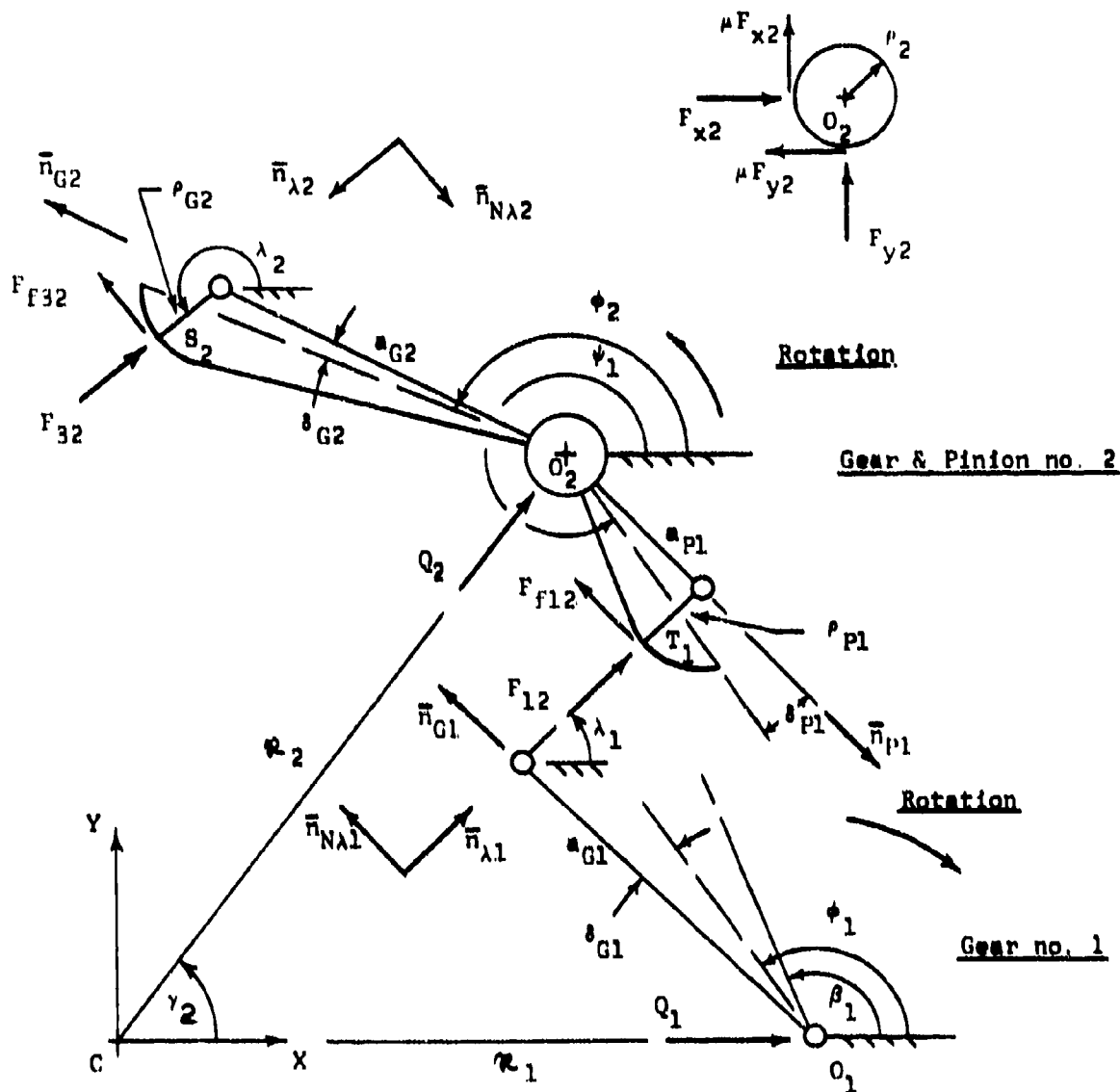


FIGURE H-3

FREE BODY DIAGRAM OF GEAR & PINION NO. 2

MESH NO. 2: ROUND ON ROUND

MESH NO. 1: ROUND ON ROUND

$$\bar{F}_{f12} = \mu_{1R} F_{12} \bar{n}_{N\lambda 1} \quad (H-44)$$

The pivot reactions, of the fuse body on the pivot shaft, together with the pivot friction forces, are shown in a separate diagram in Figure H-3. The centrifugal force, due to the mass of gear and pinion assembly no. 2, is given by

$$\bar{Q}_2 = Q_2 (\cos \gamma_2 \bar{i} + \sin \gamma_2 \bar{j}) \quad (H-45)$$

where

$$Q_2 = R_2 m_2 \omega^2 \quad (H-46)$$

Force equilibrium is assured by

$$\begin{aligned} -F_{23} \bar{n}_{\lambda 2} - \mu_{2R} F_{23} \bar{n}_{N\lambda 2} + F_{12} \bar{n}_{\lambda 1} + \mu_{1R} F_{12} \bar{n}_{N\lambda 1} + \bar{Q}_2 \\ + F_{x2} \bar{i} - \mu F_{y2} \bar{i} + F_{y2} \bar{j} + \mu F_{x2} \bar{j} = 0 \end{aligned} \quad (H-47)$$

Moment equilibrium must satisfy

$$\begin{aligned}
 & -\mu_2(\tilde{F}_{x2} + \tilde{F}_{y2})\bar{k} + [a_{G2}\bar{n}_{G2} + \rho_{G2}\bar{n}_{\lambda 2}] \times [-F_{23}\bar{n}_{\lambda 2} - \mu_{2R}F_{23}\bar{n}_{N\lambda 2}] \\
 & + [a_{P1}\bar{n}_{P1} - \rho_{P1}\bar{n}_{\lambda 1}] \times [F_{12}\bar{n}_{\lambda 1} + \mu_{1R}F_{12}\bar{n}_{N\lambda 1}] = 0 \quad (H-48)
 \end{aligned}$$

Equation (H-47) gives the following component expressions

$$\begin{aligned}
 & -F_{23}\cos\lambda_2 + \mu_{2R}F_{23}\sin\lambda_2 + F_{12}\cos\lambda_1 - \mu_{1R}F_{12}\sin\lambda_1 \\
 & + Q_2\cos\gamma_2 + F_{x2} - \mu F_{y2} = 0 \quad (H-49)
 \end{aligned}$$

and

$$\begin{aligned}
 & -F_{23}\sin\lambda_2 - \mu_{2R}F_{23}\cos\lambda_2 + F_{12}\sin\lambda_1 + \mu_{1R}F_{12}\cos\lambda_1 \\
 & + Q_2\sin\gamma_2 + F_{y2} + \mu F_{x2} = 0 \quad (H-50)
 \end{aligned}$$

The scalar form of the moment equation (H-48) becomes

$$\begin{aligned}
 & -\mu^2(\tilde{F}_{x2} + \tilde{F}_{y2}) + s_{G2}F_{23}[\sin(\phi_2 - \delta_{G2} - \lambda_2) - \mu s_{2R}\cos(\phi_2 - \delta_{G2} - \lambda_2)] \\
 & - \mu s_{2R}s_{G2}F_{23} + s_{P1}F_{12}[-\sin(\psi_1 + \delta_{P1} - \lambda_1) + \mu s_{1R}\cos(\psi_1 + \delta_{P1} - \lambda_1)] \\
 & - \mu s_{1R}s_{P1}F_{12} = 0 \qquad \qquad \qquad (H-51)
 \end{aligned}$$

Simultaneous solution of equations (H-49) and (H-50) for  $F_{x2}$  and  $F_{y2}$  leads to

$$\begin{aligned}
 F_{x2} = \frac{1}{1 + \mu^2} \left\{ F_{23} [(1 + \mu^2 s_{2R})\cos\lambda_2 - \mu(s_{2R} - 1)\sin\lambda_2] \right. \\
 + F_{12} [\mu(s_{1R} - 1)\sin\lambda_1 - (1 + \mu^2 s_{1R})\cos\lambda_1] \\
 \left. + Q_2 [-\cos\gamma_2 - \mu\sin\gamma_2] \right\} \qquad \qquad \qquad (H-52)
 \end{aligned}$$

and

$$\begin{aligned}
 F_{y2} = \frac{1}{1 + \mu^2} \left\{ F_{23} [(1 + \mu^2 s_{2R})\sin\lambda_2 - \mu(1 - s_{2R})\cos\lambda_2] \right. \\
 + F_{12} [\mu(1 - s_{1R})\cos\lambda_1 - (1 + \mu^2 s_{1R})\sin\lambda_1] \\
 \left. + Q_2 [\mu\cos\gamma_2 - \sin\gamma_2] \right\} \qquad \qquad \qquad (H-53)
 \end{aligned}$$

The sum of  $\tilde{F}_{x2}$  and  $\tilde{F}_{y2}$  of equation (H-51) is now made up of equations (H-52) and (H-53) in the sense of equation (A-3b) of Appendix A

$$\begin{aligned} \tilde{F}_{x2} + \tilde{F}_{y2} = & F_{23}A_{11} + F_{12}A_{12} + Q_2A_{13} + F_{23}A_{14} + F_{12}A_{15} \\ & + Q_2A_{16} \end{aligned} \quad (H-54)$$

where

$$A_{11} = \left| \frac{(1 + \mu^2 s_{2R}) \cos \lambda_2 - \mu (s_{2R} - 1) \sin \lambda_2}{1 + \mu^2} \right| \quad (H-55)$$

$$A_{12} = \left| \frac{\mu (s_{1R} - 1) \sin \lambda_1 - (1 + \mu^2 s_{1R}) \cos \lambda_1}{1 + \mu^2} \right| \quad (H-56)$$

$$A_{13} = \left| \frac{-\cos \gamma_2 - \mu \sin \gamma_2}{1 + \mu^2} \right| \quad (H-57)$$

$$A_{14} = \left| \frac{(1 + \mu^2 s_{2R}) \sin \lambda_2 - \mu (1 - s_{2R}) \cos \lambda_2}{1 + \mu^2} \right| \quad (H-58)$$

$$A_{15} = \left| \frac{\mu (1 - s_{1R}) \cos \lambda_1 - (1 + \mu^2 s_{1R}) \sin \lambda_1}{1 + \mu^2} \right| \quad (H-59)$$

$$A_{16} = \left| \frac{\mu \cos \gamma_2 - \sin \gamma_2}{1 + \mu^2} \right| \quad (\text{H-60})$$

Equation (H-54) is now substituted into the moment equation (H-51).

The resulting expression is then solved for the contact force  $F_{12}$

$$F_{12} = \frac{-F_{23}C_6 + Q_2C_7}{C_8} \quad (\text{H-61})$$

where

$$C_6 = a_{g2} [\sin(\phi_2 - \delta_{g2} - \lambda_2) - \mu_{2R} \cos(\phi_2 - \delta_{g2} - \lambda_2)] \\ - \mu_{P2}(A_{11} + A_{14}) - \mu_{2R}^P Q_2$$

$$C_7 = \mu_{P2}(A_{13} + A_{16})$$

$$C_8 = - \left\{ a_{P1} [\sin(\psi_1 + \delta_{P1} - \lambda_1) - \mu_{1R} \cos(\psi_1 + \delta_{P1} - \lambda_1)] \right. \\ \left. + \mu_{P2}(A_{12} + A_{15}) + \mu_{1R}^P P_1 \right\}$$

#### IV. FORCE AND MOMENT EQUILIBRIA OF INPUT GEAR NO. 1

Figure H-4 represents the free body diagram of the input gear no. 1 which has the input moment  $M_{in}$  acting on it.

The forces of pinion no. 2 on gear no. 1 are given according to equations (H-43) and (H-44),

$$\bar{F}_{21} = -F_{12}\bar{n}_{\lambda 1} \quad (H-62)$$

and

$$\bar{F}_{f21} = -\mu_{s1}R^F_{12}\bar{n}_{N\lambda 1} \quad (H-63)$$

The moments due to the friction forces on the pivot oppose rotation as indicated.

The centrifugal force, due to the mass of gear no. 1, is given by

$$\bar{Q}_1 = Q_1\bar{i} \quad (H-64)$$

where

$$Q_1 = \mathcal{R}_1 m_1 \omega^2 \quad (H-65)$$

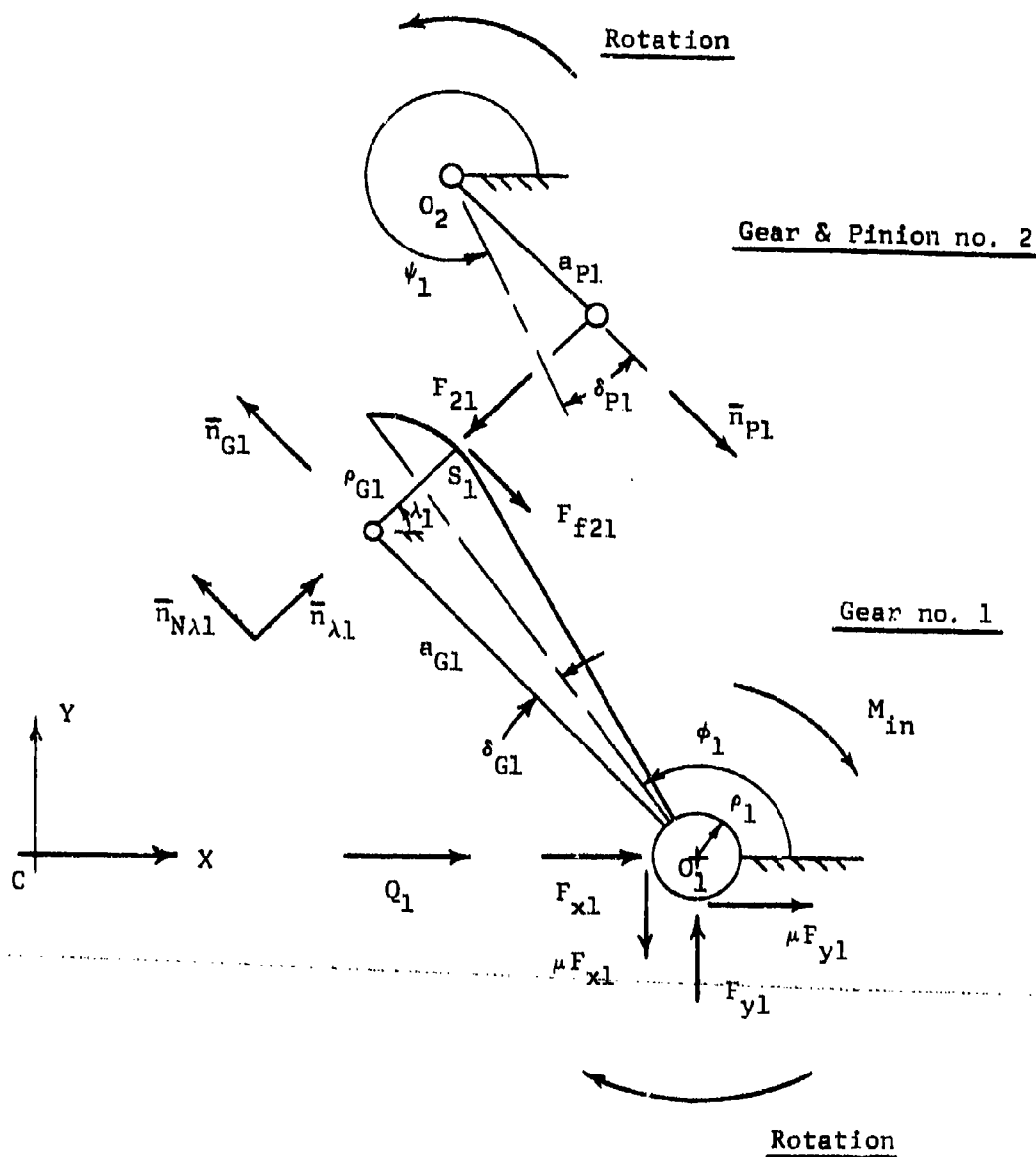


FIGURE H-4

FREE BODY DIAGRAM OF GEAR NO. 1

MESH NO. 1: ROUND ON ROUND

Force equilibrium requires, that

$$\begin{aligned}
 -F_{12}\bar{n}_{\lambda 1} - \mu s_{1R}F_{12}\bar{n}_{N\lambda 1} + Q_1 + F_{x1}\bar{i} + \mu F_{y1}\bar{i} + F_{y1}\bar{j} \\
 - \mu F_{x1}\bar{j} = 0
 \end{aligned}
 \tag{H-66}$$

Moment equilibrium is given by.

$$\begin{aligned}
 \mu p_1(\tilde{F}_{x1} + \tilde{F}_{y1})\bar{k} - M_{in}\bar{k} + [a_{G1}\bar{n}_{G1} + p_{G1}\bar{n}_{\lambda 1}] \times \\
 [-F_{12}\bar{n}_{\lambda 1} - \mu s_{1R}F_{12}\bar{n}_{N\lambda 1}] = 0
 \end{aligned}
 \tag{H-67}$$

Equation (H-66) furnishes the following component equations:

$$-F_{12}\cos\lambda_1 + \mu s_{1R}F_{12}\sin\lambda_1 + Q_1 + F_{x1} + \mu F_{y1} = 0 \tag{H-68}$$

and

$$-F_{12}\sin\lambda_1 - \mu s_{1R}F_{12}\cos\lambda_1 + F_{y1} - \mu F_{x1} = 0 \tag{H-69}$$

The scalar form of equation (H-67) becomes

$$\begin{aligned}
 \mu p_1(\tilde{F}_{x1} + \tilde{F}_{y1}) - M_{in} + a_{G1}F_{12}[\sin(\phi_1 + \delta_{G1} - \lambda_1) \\
 - \mu s_{1R}\cos(\phi_1 + \delta_{G1} - \lambda_1)] - \mu s_{1R}p_{G1}F_{12} = 0
 \end{aligned}
 \tag{H-70}$$

The simultaneous solution of equations (H-68) and (H-69)

furnishes

$$F_{x1} = \frac{1}{1 + \mu^2} \left\{ F_{12} [(1 - \mu^2 s_{1R}) \cos \lambda_1 - \mu(1 + s_{1R}) \sin \lambda_1] - Q_1 \right\} \quad (H-71)$$

and

$$F_{y1} = \frac{1}{1 + \mu^2} \left\{ F_{12} [(1 - \mu^2 s_{1R}) \sin \lambda_1 + \mu(1 + s_{1R}) \cos \lambda_1] - \mu Q_1 \right\} \quad (H-72)$$

Then, with the same reasoning as before,

$$\tilde{F}_{x1} + \tilde{F}_{y1} = F_{12} A_{17} + Q_1 A_{18} + F_{12} A_{19} + Q_1 A_{20} \quad (H-73)$$

where

$$A_{17} = \left| \frac{(1 - \mu^2 s_{1R}) \cos \lambda_1 - \mu(1 + s_{1R}) \sin \lambda_1}{1 + \mu^2} \right| \quad (H-74)$$

$$A_{18} = \left| \frac{1}{1 + \mu^2} \right| \quad (H-75)$$

$$A_{19} = \left| \frac{(1 - \mu^2 s_{1R}) \sin \lambda_1 + \mu(1 + s_{1R}) \cos \lambda_1}{1 + \mu^2} \right| \quad (\text{H-76})$$

$$A_{20} = \left| \frac{\mu}{1 + \mu^2} \right| \quad (\text{H-77})$$

Equation (H-73) is now substituted into equation (H-70) and the result is solved for the contact force  $F_{12}$

$$F_{12} = \frac{M_{1n} - Q_1 C_9}{C_{10}} \quad (\text{H-78})$$

where

$$C_9 = \mu P_1 (A_{18} + A_{20})$$

$$C_{10} = \mu P_1 (A_{17} + A_{19}) + s_{G1} [\sin(\phi_1 + \delta_{G1} - \lambda_1) - \mu s_{1R} \cos(\phi_1 + \delta_{G1} - \lambda_1)] - \mu s_{1R} P_{G1}$$

## V. MOMENT INPUT-OUTPUT RELATIONSHIP

Equations (H-61) and (H-78), which are both expressions in  $F_{12}$ , are now set equal to each other and the result is solved for  $F_{23}$

$$F_{23} = \frac{-c_8}{c_6 c_{10}} (M_{1n} - Q_1 c_9) + \frac{c_7}{c_6} Q_2 \quad (\text{H-79})$$

The above is now equated to equation (H-40) and the result is solved for  $F_{34}$

$$F_{34} = \frac{c_5 c_8 (M_{1n} - Q_1 c_9) - c_5 c_{10} c_7 Q_2 - c_4 c_6 c_{10} Q_3}{c_3 c_6 c_{10}} \quad (\text{H-80})$$

Finally equation (H-80) is equated to equation (H-19). This permits the determination of the equilibrant moment  $M_{o41}$  (for case no. 1: RRR)

$$M_{o41} = M_{1n} \frac{c_2 c_5 c_8}{c_3 c_6 c_{10}} - Q_1 \frac{c_2 c_5 c_8 c_9}{c_3 c_6 c_{10}} - Q_2 \frac{c_2 c_5 c_7}{c_3 c_6} - Q_3 \frac{c_2 c_4}{c_3} - Q_4 c_1 \quad (\text{H-81})$$

b. CASE NO. 2: RRF

Since only mesh 1 is now assumed to be in the round on flat phase of motion, the forces  $F_{34}$  and  $F_{23}$  remain as given by equations (H-19) and (H-40), respectively.

I. FORCE AND MOMENT EQUILIBRIA OF GEAR AND PINION SET NO. 2

Figure H-5 shows the free body diagram of the gear and pinion set with the necessary portions of mesh no. 1.

The forces of pinion no. 3 on gear no. 2 are given by equations (H-41) and (H-42), i.e.,

$$\vec{F}_{32} = -F_{23}\vec{H}_{\lambda 2} \quad (\text{H-82})$$

and

$$\vec{F}_{f32} = -\mu_s 2R F_{23} \vec{H}_{N\lambda 2} \quad (\text{H-83})$$

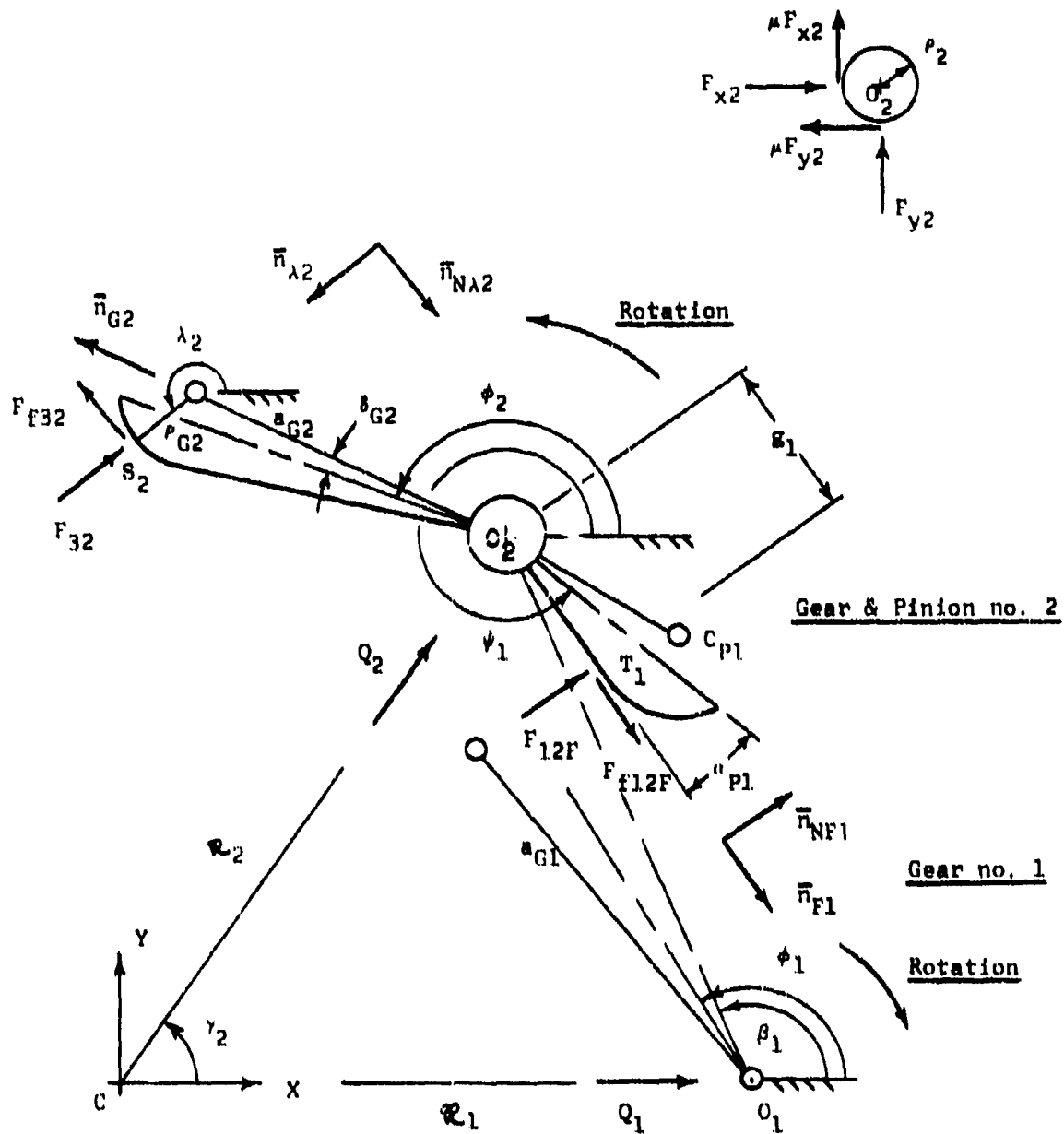


FIGURE H-5

FREE BODY DIAGRAM OF GEAR & PINION NO. 2

MESH NO. 2: ROUND ON ROUND

MESH NO. 1: ROUND ON FLAT

The contact force of gear no. 1 on pinion no. 2 is now given by

$$\bar{F}_{12F} = F_{12F} \bar{n}_{NF1} \quad (H-84)$$

(Note that the additional subscript F is introduced to distinguish round on flat from round on round contact.)

The associated friction force is given by

$$\bar{F}_{f12F} = \mu_{s1F} F_{12F} \bar{n}_{F1} \quad (H-85)$$

(See equation (H-2) for  $s_{1F}$ .)

The pivot reactions, together with the pivot friction forces, are shown in a separate diagram in Figure H-5. As before, the pivot friction moments oppose rotation.

The centrifugal force  $\bar{Q}_2$  is again given by equations (H-45) and (H-46).

Force equilibrium is given by

$$\begin{aligned} -F_{23} \bar{n}_{\lambda 2} - \mu_{s2R} F_{23} \bar{n}_{N\lambda 2} + F_{12F} \bar{n}_{NF1} + \mu_{s1F} F_{12F} \bar{n}_{F1} + \bar{Q}_2 \\ + F_{x2} \bar{i} - \mu F_{y2} \bar{i} + F_{y2} \bar{j} + \mu F_{x2} \bar{j} = 0 \end{aligned} \quad (H-86)$$

Moment equilibrium about point  $O_2$  requires

$$\begin{aligned}
 & -\mu P_2(\bar{F}_{x2} + \bar{F}_{y2})\bar{k} + [a_{O2}\bar{e}_{O2} + r_{O2}\bar{e}_{\lambda 2}] \times [-F_{23}\bar{e}_{\lambda 2} - \mu_{2R}F_{23}\bar{e}_{N\lambda 2}] \\
 & + S_1\bar{e}_{F1} \times F_{12F}\bar{e}_{NF1} = 0 \quad (H-87)
 \end{aligned}$$

Note that since the line of action of the friction force  $F_{f12F}$  passes through point  $O_2$ , this friction force exerts no moment about point  $O_2$ .

Equation (H-86) furnishes the following component equations:

$$\begin{aligned}
 & -F_{23}\cos\lambda_2 + \mu_{2R}F_{23}\sin\lambda_2 - F_{12F}\sin(\psi_1 - \alpha_{P1}) + \mu_{1F}F_{12F}\cos(\psi_1 - \alpha_{P1}) \\
 & + F_{x2} - \mu F_{y2} + Q_2\cos\gamma_2 = 0 \quad (H-88)
 \end{aligned}$$

and

$$\begin{aligned}
 & -F_{23}\sin\lambda_2 - \mu_{2R}F_{23}\cos\lambda_2 + F_{12F}\cos(\psi_1 - \alpha_{P1}) + \mu_{1F}F_{12F}\sin(\psi_1 - \alpha_{P1}) \\
 & + F_{y2} + \mu F_{x2} + Q_2\sin\gamma_2 = 0 \quad (H-89)
 \end{aligned}$$

The scalar form of the moment equation (H-87) becomes

$$\begin{aligned}
 -\mu P_2(\bar{F}_{x2} + \bar{F}_{y2}) + a_{Q2} F_{23} [\sin(\phi_2 - \theta_{Q2} - \lambda_2) - \mu a_{2R} \cos(\phi_2 - \theta_{Q2} - \lambda_2)] \\
 - \mu a_{2R} \theta_{Q2} F_{23} + F_{12} \epsilon_1 = 0
 \end{aligned}
 \tag{H-90}$$

Simultaneous solution of these component equations for  $F_{x2}$  and  $F_{y2}$  leads to

$$\begin{aligned}
 F_{x2} = \frac{1}{1 + \mu^2} \left\{ F_{23} [\mu(1 - a_{2R}) \sin \lambda_2 + (1 + \mu^2 a_{2R}) \cos \lambda_2] \right. \\
 + F_{12} [(1 - \mu^2 a_{1F}) \sin(\psi_1 - \alpha_{P1}) - \mu(1 + a_{1F}) \cos(\psi_1 - \alpha_{P1})] \\
 \left. - Q_2 [\mu \sin \gamma_2 + \cos \gamma_2] \right\}
 \end{aligned}
 \tag{H-91}$$

and

$$\begin{aligned}
 F_{y2} = \frac{1}{1 + \mu^2} \left\{ F_{23} [(1 + \mu^2 a_{2R}) \sin \lambda_2 - \mu(1 - a_{2R}) \cos \lambda_2] \right. \\
 + F_{12} [-\mu(1 + a_{1F}) \sin(\psi_1 - \alpha_{P1}) + (\mu^2 a_{1F} - 1) \cos(\psi_1 - \alpha_{P1})] \\
 \left. + Q_2 [-\sin \gamma_2 + \mu \cos \gamma_2] \right\}
 \end{aligned}
 \tag{H-92}$$

The sum ( $\tilde{F}_{x2} + \tilde{F}_{y2}$ ) of equation (H-90) is now made up of equations (H-91) and (H-92) in the sense of equation (A-3b) of Appendix A

$$\tilde{F}_{x2} + \tilde{F}_{y2} = F_{23}A_{21} + F_{12}A_{22} + Q_2A_{23} + F_{23}A_{24} + F_{12}A_{25} + Q_2A_{26} \quad (\text{H-93})$$

where

$$A_{21} = \left| \frac{\mu(1 - s_{2R})\sin\lambda_2 + (1 + \mu^2 s_{2R})\cos\lambda_2}{1 + \mu^2} \right| \quad (\text{H-94})$$

$$A_{22} = \left| \frac{(1 - \mu^2 s_{1R})\sin(\psi_1 - \alpha_{P1}) - \mu(1 + s_{1R})\cos(\psi_1 - \alpha_{P1})}{1 + \mu^2} \right| \quad (\text{H-95})$$

$$A_{23} = \left| \frac{\mu\sin\gamma_2 + \cos\gamma_2}{1 + \mu^2} \right| \quad (\text{H-96})$$

$$A_{24} = \left| \frac{(1 + \mu^2 s_{2R})\sin\lambda_2 - \mu(1 - s_{2R})\cos\lambda_2}{1 + \mu^2} \right| \quad (\text{H-97})$$

$$A_{25} = \left| \frac{-\mu(1 + s_{1R})\sin(\psi_1 - \alpha_{P1}) + (\mu^2 s_{1R} - 1)\cos(\psi_1 - \alpha_{P1})}{1 + \mu^2} \right| \quad (\text{H-98})$$

$$A_{26} = \left| \frac{-\sin\gamma_2 + \mu\cos\gamma_2}{1 + \mu^2} \right| \quad (\text{H-99})$$

Equation (H-93) is now substituted into equation (H-90), and the resulting expression is solved for the contact force  $F_{12F}$

$$F_{12F} = \frac{-F_{23}C_{11} + Q_2C_{12}}{C_{13}} \quad (\text{H-100})$$

where

$$C_{11} = A_{g2} [\sin(\phi_2 - \delta_{g2} - \lambda_2) - \mu_{2R} \cos(\phi_2 - \delta_{g2} - \lambda_2)] \\ - \mu P_2 (A_{21} + A_{24}) - \mu_{2R} P_{g2}$$

$$C_{12} = \mu P_2 (A_{23} + A_{26})$$

$$C_{13} = \delta_1 - \mu P_2 (A_{22} + A_{25})$$

## II. FORCE AND MOMENT EQUILIBRIA OF INPUT GEAR NO. 1

Figure H-6 represents the free body diagram of input gear no. 1.

The forces of pinion no. 2 on this gear are given according to equations (H-84) (H-85) ,

$$\bar{F}_{21F} = -F_{12F}\bar{n}_{NF1} \quad (H-101)$$

and

$$\bar{F}_{f21F} = -\mu_{s1F}F_{12F}\bar{n}_{F1} \quad (H-102)$$

The moments due to the pivot friction forces oppose the indicated rotation due to the moment  $M_{1n}$ .

The centrifugal force  $\bar{Q}_1$  has been defined by equations (H-64) and (H-65).

The force equilibrium equation is given by

$$\begin{aligned} -F_{12F}\bar{n}_{NF1} - \mu_{s1F}F_{12F}\bar{n}_{F1} + Q_1\bar{i} + F_{x1}\bar{i} + \mu F_{y1}\bar{i} + F_{y1}\bar{j} - \mu F_{x1}\bar{j} \\ = 0 \end{aligned} \quad (H-103)$$

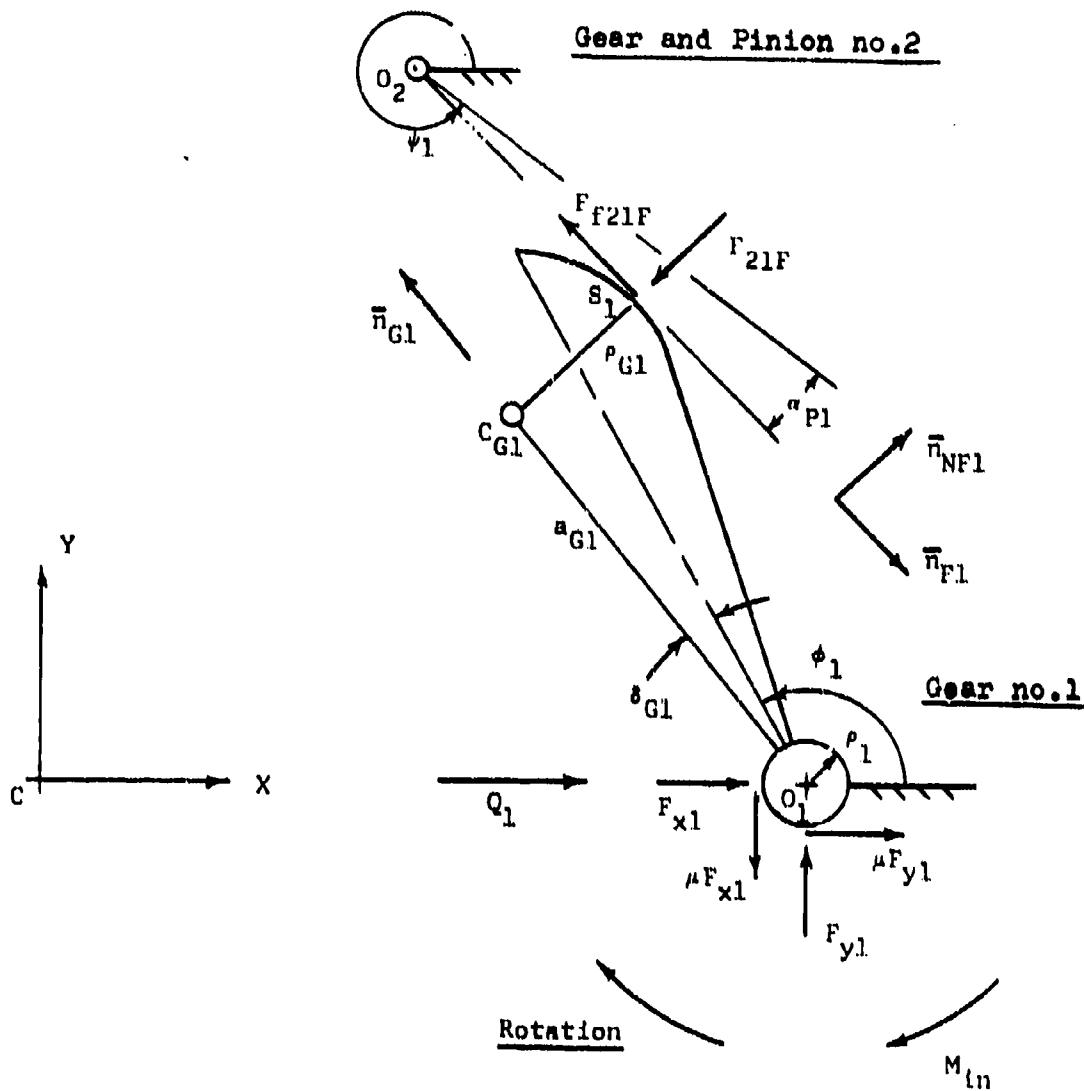


FIGURE H-6  
 FREE BODY DIAGRAM OF GEAR NO. 1  
 MECH NO. 1: ROUND ON FLAT

The moment equilibrium equation becomes

$$-M_{1N} \bar{k} + \mu \rho_1 (\tilde{F}_{x1} + \tilde{F}_{y1}) \bar{k} + [a_{G1} \bar{n}_{G1} + \rho_{G1} \bar{n}_{NF1}] \times [-F_{12F} \bar{n}_{NF1} - \mu s_{1F} F_{12F} \bar{n}_{F1}] = 0 \quad (H-104)$$

Equation (H-103) furnishes the following component expressions

$$F_{12F} \sin(\psi_1 - \alpha_{P1}) - \mu s_{1F} F_{12F} \cos(\psi_1 - \alpha_{P1}) + Q_1 + F_{x1} + \mu F_{y1} = 0 \quad (H-105)$$

and

$$-F_{12F} \cos(\psi_1 - \alpha_{P1}) - \mu s_{1F} F_{12F} \sin(\psi_1 - \alpha_{P1}) + F_{y1} - \mu F_{x1} = 0 \quad (H-106)$$

The scalar form of the moment equation (H-104) becomes

$$-M_{1N} + \mu \rho_1 (\tilde{F}_{x1} + \tilde{F}_{y1}) + \mu s_{1F} \rho_{G1} F_{12F} + a_{G1} F_{12F} [-\cos(\phi_1 + \delta_{G1} - \psi_1 + \alpha_{P1}) + \mu s_{1F} \sin(\phi_1 + \delta_{G1} - \psi_1 + \alpha_{P1})] = 0 \quad (H-107)$$

Simultaneous solution of equations (H-105) and (H-106) for  $F_{x1}$  and  $F_{y1}$  furnishes

$$F_{x1} = \frac{F_{12F} [-(1 + \mu^2 s_{1F}) \sin(\psi_1 - \alpha_{P1}) + \mu (s_{1F} - 1) \cos(\psi_1 - \alpha_{P1})] - Q_1}{1 + \mu^2} \quad (H-108)$$

and

$$F_{y1} = \frac{F_{12F} [(1 + \mu^2 s_{1F}) \cos(\psi_1 - \alpha_{P1}) + \mu(s_{1F} - 1) \sin(\psi_1 - \alpha_{P1})] - \mu Q_1}{1 + \mu^2} \quad (\text{H-109})$$

Now let

$$\tilde{F}_{x1} + \tilde{F}_{y1} = F_{12F} A_{27} + Q_1 A_{28} + F_{12F} A_{29} + Q_1 A_{30} \quad (\text{H-110})$$

where

$$A_{27} = \left| \frac{-(1 + \mu^2 s_{1F}) \sin(\psi_1 - \alpha_{P1}) + \mu(s_{1F} - 1) \cos(\psi_1 - \alpha_{P1})}{1 + \mu^2} \right| \quad (\text{H-111})$$

$$A_{28} = \left| \frac{1}{1 + \mu^2} \right| \quad (\text{H-112})$$

$$A_{29} = \left| \frac{\mu(s_{1F} - 1) \sin(\psi_1 - \alpha_{P1}) + (1 + \mu^2 s_{1F}) \cos(\psi_1 - \alpha_{P1})}{1 + \mu^2} \right| \quad (\text{H-113})$$

$$A_{30} = \left| \frac{\mu}{1 + \mu^2} \right| \quad (\text{H-114})$$

Equation (H-110) is now substituted into the moment equation (H-107).

This furnishes

$$F_{12F} = \frac{M_{1n} - Q_1 C_{14}}{C_{15}} \quad (H-115)$$

where

$$C_{14} = \mu p_1 (A_{28} + A_{30})$$

$$C_{15} = \mu p_1 (A_{27} + A_{29}) + \mu s_{1F} p_{G1}$$

$$+ a_{G1} [\mu s_{1F} \sin(\phi_1 + \delta_{G1} - \psi_1 + \alpha_{P1}) - \cos(\phi_1 + \delta_{G1} - \psi_1 + \alpha_{P1})]$$

### III. MOMENT INPUT-OUTPUT RELATIONSHIP

Equations (H-100) and (H-115), which are both expressions in  $F_{12}$ , are now set equal to each other and the result is solved for  $F_{23}$

$$F_{23} = \frac{-c_{13}}{c_{11}c_{15}} (M_{1n} - Q_1 c_{14}) + Q_2 \frac{c_{12}}{c_{11}} \quad (\text{H-116})$$

The above expression is now equated to equation (H-40) and solved for  $F_{34}$

$$F_{34} = \frac{c_5 c_{13}}{c_3 c_{11} c_{15}} (M_{1n} - Q_1 c_{14}) - Q_2 \frac{c_5 c_{12}}{c_3 c_{11}} - Q_3 \frac{c_4}{c_3} \quad (\text{H-117})$$

Finally, this expression is set equal to equation (H-19) and the result is solved for the equilibrant moment  $M_{o42}$  (for case 2: RRF)

$$M_{o42} = M_{1n} \frac{c_2 c_5 c_{13}}{c_3 c_{11} c_{15}} - Q_1 \frac{c_2 c_5 c_{13} c_{14}}{c_3 c_{11} c_{15}} - Q_2 \frac{c_2 c_5 c_{12}}{c_3 c_{11}} - Q_3 \frac{c_2 c_4}{c_3} - Q_4 c_1 \quad (\text{H-118})$$

c. CASE NO. 3: RFF

With both meshes no. 1 and no. 2 in the round on flat phase of motion, only force  $F_{34}$  of the round on round phase can be incorporated for the present case. The equilibrium equations for gear and pinion set no. 3, gear and pinion set no. 2 and the input gear no. 1 must be newly derived.

I. FORCE AND MOMENT EQUILIBRIA OF GEAR AND PINION SET NO. 3

Figure H-7 shows the free body diagram of gear and pinion set no. 3, together with the necessary outline of mesh no. 2.

The forces of pinion no. 4 on gear no. 3 are given by equations (H-20) and (H-21)

$$\bar{F}_{43} = -F_{34} \bar{n}_{\lambda 3} \quad (\text{H-119})$$

and

$$\bar{F}_{f43} = -\mu_{3R} F_{34} \bar{n}_{N\lambda 3} \quad (\text{H-120})$$

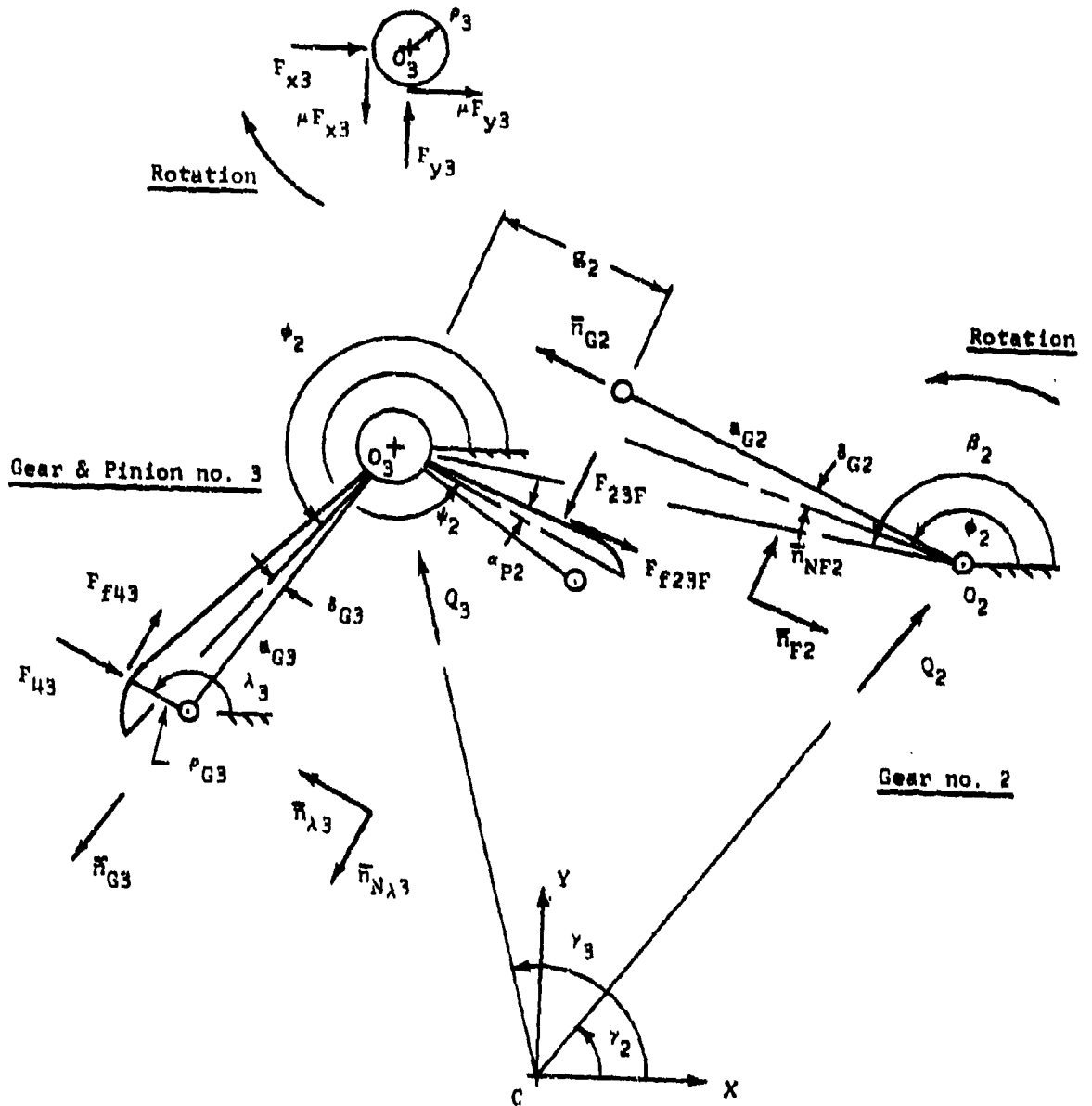


FIGURE H-7  
 FREE BODY DIAGRAM OF GEAR & PINION NO. 3  
 MESH NO. 3: ROUND ON ROUND  
 MESH NO. 2: ROUND ON FLAT

The normal contact force of gear no. 2 on pinion no. 3 is given by

$$\bar{F}_{23F} = -F_{23F} \bar{n}_{NF2} \quad (H-121)$$

The associated friction force is given by

$$\bar{F}_{f23F} = \mu_{s2F} F_{23F} \bar{n}_{NF2} \quad (H-122)$$

The pivot friction forces are chosen so that the resulting friction moments oppose the indicated rotation. The centrifugal force  $\bar{Q}_3$  is that of equations (H-24) and (H-25).

Force equilibrium is given by

$$\begin{aligned} -F_{34} \bar{n}_{\lambda 3} - \mu_{s3R} F_{34} \bar{n}_{N\lambda 3} - F_{23F} \bar{n}_{NF2} + \mu_{s2F} F_{23F} \bar{n}_{NF2} + \bar{Q}_3 \\ + F_{x3} \bar{i} + \mu_{Fy3} \bar{i} + F_{y3} \bar{j} - \mu_{Fx3} \bar{j} = 0 \end{aligned} \quad (H-123)$$

Moment equilibrium about point  $O_3$  is given by

$$\begin{aligned} \mu_{F3} (\bar{F}_{x3} + \bar{F}_{y3}) \bar{k} + [a_{O3} \bar{n}_{O3} + r_{O3} \bar{n}_{\lambda 3}] \times [-F_{34} \bar{n}_{\lambda 3} - \mu_{s3R} F_{34} \bar{n}_{N\lambda 3}] \\ + \epsilon_2 \bar{n}_{F2} \times \bar{F}_{23F} = 0 \end{aligned} \quad (H-124)$$

Note that the friction force  $F_{f23}$  exerts no moment about point  $O_3$ .

Equation (H-123) furnishes the following component equations:

$$\begin{aligned}
 -F_{34} \cos \lambda_3 + \mu_{3R} F_{34} \sin \lambda_3 + Q_3 \cos \gamma_3 + F_{x3} + \mu F_{y3} + F_{23} \sin(\psi_2 + \alpha_{p2}) \\
 + \mu_{2F} F_{23} \cos(\psi_2 + \alpha_{p2}) = 0 \quad (H-125)
 \end{aligned}$$

and

$$\begin{aligned}
 -F_{34} \sin \lambda_3 - \mu_{3R} F_{34} \cos \lambda_3 + Q_3 \sin \gamma_3 + F_{y3} - \mu F_{x3} - F_{23} \cos(\psi_2 + \alpha_{p2}) \\
 + \mu_{2F} F_{23} \sin(\psi_2 + \alpha_{p2}) = 0 \quad (H-126)
 \end{aligned}$$

The scalar form of the moment equation (H-124) becomes

$$\begin{aligned}
 \mu_{p3} (\tilde{F}_{x3} + \tilde{F}_{y3}) + a_{03} F_{34} [\sin(\phi_3 + \delta_{03} - \lambda_3) - \mu_{3R} \cos(\phi_3 + \delta_{03} - \lambda_3)] \\
 - \mu_{3R} a_{03} F_{34} - \delta_2 F_{23} = 0 \quad (H-127)
 \end{aligned}$$

Simultaneous solution of equations (H-125) and (H-126) for  $F_{x3}$  and  $F_{y3}$  leads to

$$F_{x3} = \frac{1}{1 + \mu^2} \left\{ F_{34} [(1 - \mu^2 a_{3R}) \cos \lambda_3 - \mu(1 + a_{3R}) \sin \lambda_3] \right. \\ \left. + F_{23F} [-\mu(1 + a_{2F}) \cos(\psi_2 + \alpha_{P2}) - (1 - \mu^2 a_{2F}) \sin(\psi_2 + \alpha_{P2})] \right. \\ \left. + Q_3 [\mu \sin \gamma_3 - \cos \gamma_3] \right\} \quad (H-128)$$

and

$$F_{y3} = \frac{1}{1 + \mu^2} \left\{ F_{34} [(1 - \mu^2 a_{3R}) \sin \lambda_3 + \mu(1 + a_{3R}) \cos \lambda_3] \right. \\ \left. + F_{23F} [(1 - \mu^2 a_{2F}) \cos(\psi_2 + \alpha_{P2}) - \mu(1 + a_{2F}) \sin(\psi_2 + \alpha_{P2})] \right. \\ \left. - Q_3 [\sin \gamma_3 + \mu \cos \gamma_3] \right\} \quad (H-129)$$

The sum  $\bar{F}_{x3} + \bar{F}_{y3}$  of equation (H-127) is now made up of equations (H-128) and (H-129) in the sense of equation (A-5b)

$$\bar{F}_{x3} + \bar{F}_{y3} = F_{34} A_{31} + F_{23F} A_{32} + Q_3 A_{33} + F_{34} A_{34} + F_{23F} A_{35} + Q_3 A_{36} \quad (H-130)$$

where

$$A_{31} = \left| \frac{(1 - \mu^2 \epsilon_{3R}) \cos \lambda_3 - \mu(1 + \epsilon_{3R}) \sin \lambda_3}{1 + \mu^2} \right| \quad (\text{H-131})$$

$$A_{32} = \left| \frac{-\mu(1 + \epsilon_{2R}) \cos(\psi_2 + \alpha_{P2}) - (1 - \mu^2 \epsilon_{2R}) \sin(\psi_2 + \alpha_{P2})}{1 + \mu^2} \right| \quad (\text{H-132})$$

$$A_{33} = \left| \frac{\mu \sin \gamma_3 - \cos \gamma_3}{1 + \mu^2} \right| \quad (\text{H-133})$$

$$A_{34} = \left| \frac{(1 - \mu^2 \epsilon_{3R}) \sin \lambda_3 + \mu(1 + \epsilon_{3R}) \cos \lambda_3}{1 + \mu^2} \right| \quad (\text{H-134})$$

$$A_{35} = \left| \frac{(1 - \mu^2 \epsilon_{2R}) \cos(\psi_2 + \alpha_{P2}) - \mu(1 + \epsilon_{2R}) \sin(\psi_2 + \alpha_{P2})}{1 + \mu^2} \right| \quad (\text{H-135})$$

$$A_{36} = \left| \frac{\sin \gamma_3 + \mu \cos \gamma_3}{1 + \mu^2} \right| \quad (\text{H-136})$$

Equation (H-130) is now substituted into equation (H-127) and the result is solved for  $F_{23F}$

$$F_{23R} = \frac{-F_{34}C_{16} - Q_3C_{17}}{C_{18}}$$

(H-137)

where

$$C_{16} = \mu P_3(A_{31} + A_{34}) + a_{Q3} [\sin(\phi_3 + \delta_{Q3} - \lambda_3) - \mu_{3R}^{Q3}(\phi_3 + \delta_{Q3} - \lambda_3)] - \mu_{3R}^Q Q_3$$

$$C_{17} = \mu P_3(A_{33} + A_{36})$$

$$C_{18} = \mu P_3(A_{32} + A_{35}) - \delta_2$$

## II. FORCE AND MOMENT EQUILIBRIA OF GEAR AND PINION SET NO. 2

Figure H-8 shows the free body diagram of the gear and pinion set no. 2.

The forces of pinion no. 3 on gear no. 2 are equal and opposite to those given by equations (H-121) and (H-122), i.e.,

$$\bar{F}_{32F} = F_{23F} \bar{n}_{NF2} \quad (H-138)$$

and

$$\bar{F}_{f32F} = -\mu_{2F} F_{23F} \bar{n}_{NF2} \quad (H-139)$$

The forces of gear no. 1 on pinion no. 2 are those of equations (H-84) and (H-85).

The pivot friction is accounted for in the usual manner and the centrifugal force  $\bar{Q}_2$  is given by equation (H-45).

Force equilibrium is given by

$$\begin{aligned} F_{23F} \bar{n}_{NF2} - \mu_{2F} F_{23F} \bar{n}_{NF2} + F_{12F} \bar{n}_{NF1} + \mu_{1F} F_{12F} \bar{n}_{NF1} + \bar{Q}_2 + F_{x2} \bar{i} - \mu F_{y2} \bar{i} \\ + F_{y2} \bar{j} + \mu F_{x2} \bar{j} = 0 \end{aligned} \quad (H-140)$$

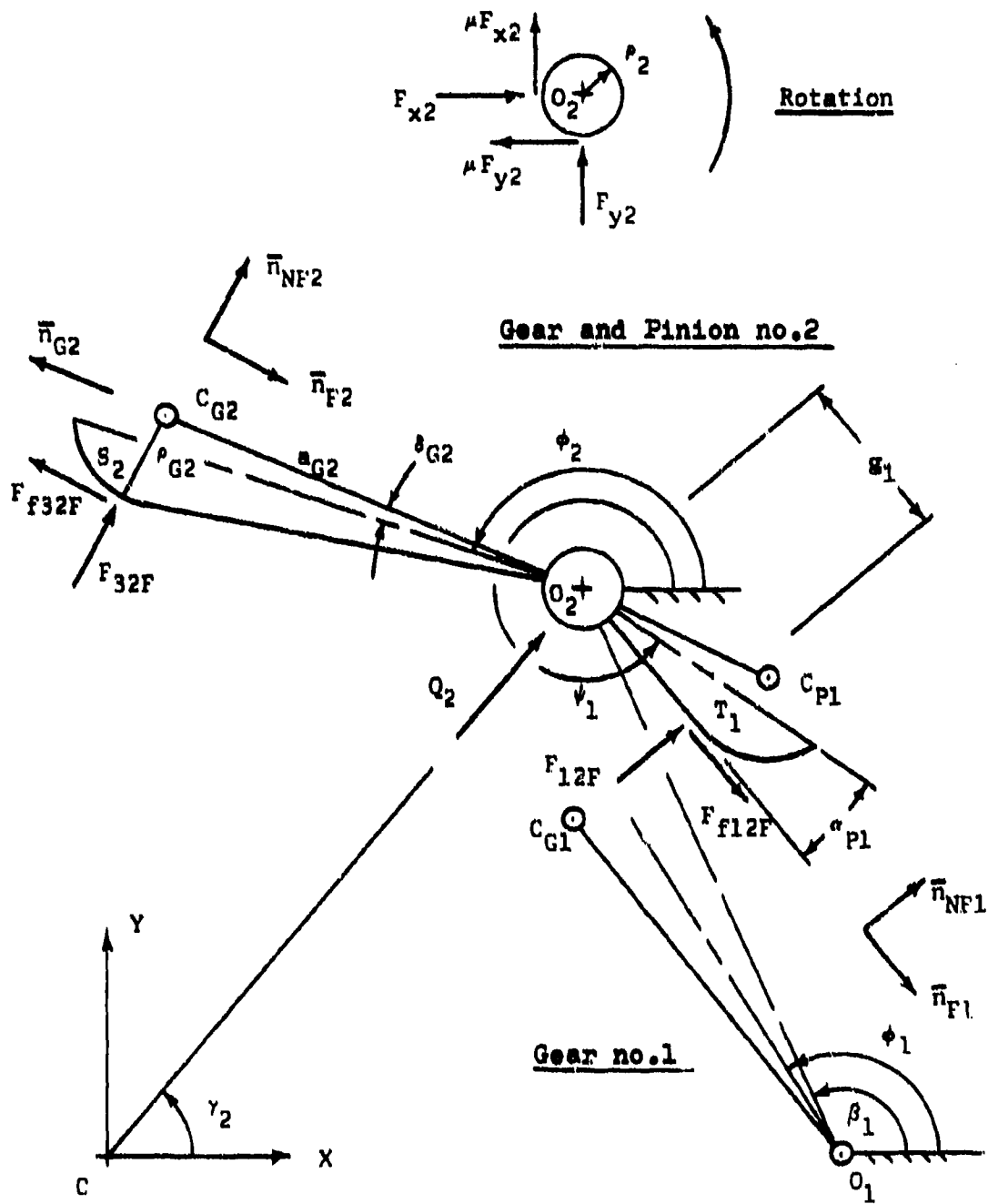


FIGURE H-8

FREE BODY DIAGRAM OF GEAR & PINION NO. 2

MESH NO. 2: ROUND ON FLAT

MESH NO. 1: ROUND ON FLAT

Moment equilibrium about point  $O_2$  requires

$$\begin{aligned}
 -\mu^2(\tilde{F}_{x2} + \tilde{F}_{y2})\bar{k} + [\rho_{G2}\bar{n}_{G2} - \rho_{G2}\bar{n}_{NF2}] \times [F_{23F}\bar{n}_{NF2} - \mu^2_{2F}F_{23F}\bar{n}_{F2}] \\
 + s_1\bar{n}_{F1} \times F_{12F}\bar{n}_{NF1} = 0
 \end{aligned}
 \tag{H-141}$$

Equation (H-140) gives the component equations

$$\begin{aligned}
 -F_{23F}\sin(\psi_2 + \alpha_{P2}) - \mu^2_{2F}F_{23F}\cos(\psi_2 + \alpha_{P2}) + Q_2\cos\gamma_2 + F_{x2} - \mu F_{y2} \\
 - F_{12F}\sin(\psi_1 - \alpha_{P1}) + \mu^2_{1F}F_{12F}\cos(\psi_1 - \alpha_{P1}) = 0
 \end{aligned}
 \tag{H-142}$$

and

$$\begin{aligned}
 F_{23F}\cos(\psi_2 + \alpha_{P2}) - \mu^2_{2F}F_{23F}\sin(\psi_2 + \alpha_{P2}) + Q_2\sin\gamma_2 + F_{y2} + \mu F_{x2} \\
 + F_{12F}\cos(\psi_1 - \alpha_{P1}) + \mu^2_{1F}F_{12F}\sin(\psi_1 - \alpha_{P1}) = 0
 \end{aligned}
 \tag{H-143}$$

The scalar form of the moment equation (H-141) becomes

$$\begin{aligned}
 & -\mu p_2(\tilde{F}_{x2} + \tilde{F}_{y2}) + a_{G2} F_{23F} [\cos(\psi_2 - \delta_{G2} - \psi_2 - \alpha_{P2}) \\
 & + \mu s_{2F} \sin(\psi_2 - \delta_{G2} - \psi_2 - \alpha_{P2})] - \mu s_{2F} p_{G2} F_{23F} + \delta_1 F_{12F} = 0
 \end{aligned}
 \tag{H-144}$$

Simultaneous solution of the component equations (H-142) and (H-143) for  $F_{x2}$  and  $F_{y2}$  leads to

$$\begin{aligned}
 F_{x2} = \frac{1}{1 + \mu^2} \left\{ F_{23F} [(1 + \mu^2 s_{2F}) \sin(\psi_2 + \alpha_{P2}) + \mu (s_{2F} - 1) \cos(\psi_2 + \alpha_{P2})] \right. \\
 + F_{12F} [(1 - \mu^2 s_{1F}) \sin(\psi_1 - \alpha_{P1}) - \mu (1 + s_{1F}) \cos(\psi_1 - \alpha_{P1})] \\
 \left. - Q_2 [\mu \sin \gamma_2 + \cos \gamma_2] \right\}
 \end{aligned}
 \tag{H-145}$$

and

$$\begin{aligned}
 F_{y2} = \frac{1}{1 + \mu^2} \left\{ F_{23F} [\mu (s_{2F} - 1) \sin(\psi_2 + \alpha_{P2}) - (1 + \mu^2 s_{2F}) \cos(\psi_2 + \alpha_{P2})] \right. \\
 - F_{12F} [\mu (1 + s_{1F}) \sin(\psi_1 - \alpha_{P1}) + (1 - \mu^2 s_{1F}) \cos(\psi_1 - \alpha_{P1})] \\
 \left. + Q_2 [\mu \cos \gamma_2 - \sin \gamma_2] \right\}
 \end{aligned}
 \tag{H-146}$$

The sum  $\tilde{F}_{x2} + \tilde{F}_{y2}$  of equation (H-144) is now made up of equations (H-145) and (H-146) in the sense of equation (A-3b)

$$\tilde{F}_{x2} + \tilde{F}_{y2} = F_{23F}A_{37} + F_{12F}A_{38} + Q_2A_{39} + F_{23F}A_{40} + F_{12F}A_{41} + Q_2A_{42} \quad (\text{H-147})$$

where

$$A_{37} = \left| \frac{(1 + \mu^2 s_{2F}) \sin(\psi_2 + \alpha_{P2}) + \mu(s_{2F} - 1) \cos(\psi_2 + \alpha_{P2})}{1 + \mu^2} \right| \quad (\text{H-148})$$

$$A_{38} = \left| \frac{(1 - \mu^2 s_{1F}) \sin(\psi_1 - \alpha_{P1}) - \mu(1 + s_{1F}) \cos(\psi_1 - \alpha_{P1})}{1 + \mu^2} \right| \quad (\text{H-149})$$

$$A_{39} = \left| \frac{\mu \sin \gamma_2 + \cos \gamma_2}{1 + \mu^2} \right| \quad (\text{H-150})$$

$$A_{40} = \left| \frac{\mu(s_{2F} - 1) \sin(\psi_2 + \alpha_{P2}) - (1 + \mu^2 s_{2F}) \cos(\psi_2 + \alpha_{P2})}{1 + \mu^2} \right| \quad (\text{H-151})$$

$$A_{41} = \left| \frac{\mu(1 + s_{1F}) \sin(\psi_1 - \alpha_{P1}) + (1 - \mu^2 s_{1F}) \cos(\psi_1 - \alpha_{P1})}{1 + \mu^2} \right| \quad (\text{H-152})$$

$$A_{42} = \left| \frac{\mu \cos \gamma_2 - \sin \gamma_2}{1 + \mu^2} \right| \quad (\text{H-153})$$

Equation (H-147) is now substituted into equation (H-144) and the result is solved for  $F_{12F}$

$$F_{12F} = \frac{-F_{23F}C_{19} + Q_2C_{20}}{C_{21}} \quad (H-154)$$

where

$$C_{19} = -\mu P_2(A_{37} + A_{40}) + s_{G2}[\cos(\phi_2 - \delta_{G2} - \psi_2 - \alpha_{P2}) + \mu s_{2F} \sin(\phi_2 - \delta_{G2} - \psi_2 - \alpha_{P2})] - \mu s_{2F} P_{G2}$$

$$C_{20} = \mu P_2(A_{39} + A_{42})$$

$$C_{21} = -\mu P_2(A_{38} + A_{41}) + S_1$$

### III. FORCE AND MOMENT EQUILIBRIA OF INPUT GEAR NO. 1

While the numerical values of the force  $F_{21F}$  and its associated friction force  $F_{f12F}$ , both acting on gear no. 1, are peculiar to the present combination of contact phases, its functional relationship to the input moment  $M_{1n}$  and the centrifugal force  $Q_1$  is identical to that derived in section 1b-II of this appendix. (See also Figure H-6.)

According to equation (H-115), one obtains for  $F_{12F}$

$$F_{12F} = \frac{M_{1n} - Q_1 C_{14}}{C_{15}} \quad (H-155)$$

#### IV. MOMENT INPUT-OUTPUT RELATIONSHIP

Equations (H-154) and (H-155), both in  $F_{12F}$ , are set equal to each other and the result is solved for  $F_{23F}$

$$F_{23F} = \frac{-c_{21}}{c_{15}c_{19}} (M_{1n} - Q_1 c_{14}) + Q_2 \frac{c_{20}}{c_{19}} \quad (\text{H-156})$$

The above is now equated to equation (H-137) and the result is solved for  $F_{34}$

$$F_{34} = \frac{c_{18}c_{21}}{c_{15}c_{16}c_{19}} (M_{1n} - Q_1 c_{14}) - Q_2 \frac{c_{18}c_{20}}{c_{16}c_{19}} - Q_3 \frac{c_{17}}{c_{16}} \quad (\text{H-157})$$

Finally, equation (H-157) is equated to equation (H-19), which corresponds to the round on round phase of mesh no. 3. The result is solved for the equilibrant moment  $M_{043}$  (for case 3: RFF)

$$M_{043} = M_{1n} \frac{c_2 c_{18} c_{21}}{c_{15} c_{16} c_{19}} - Q_1 \frac{c_2 c_{14} c_{18} c_{21}}{c_{15} c_{16} c_{19}} - Q_2 \frac{c_2 c_{18} c_{20}}{c_{16} c_{19}} - Q_3 \frac{c_2 c_{17}}{c_{16}} - Q_4 c_1 \quad (\text{H-158})$$

d. CASE NO. 4: RFR

For this contact combination force  $F_{34}$  may be taken from the results of case no. 1 [see equation (H-19)], since mesh no. 3 is in the round on round phase of motion. The force  $F_{23F}$  of case no. 3, i.e., equation (H-137), also is incorporated.

The input-output relationship of the gear and pinion combination no. 2 must be newly derived, i.e., the force  $F_{12}$  must be expressed in terms of the contact force  $F_{32F}$  and the centrifugal force  $Q_2$ . Finally, the results of the equilibrium equations for the input gear no. 1 of case no. 1 are used. For this case of contact, the force  $F_{12}$  is given by equation (H-78).

I. FORCE AND MOMENT EQUILIBRIA OF GEAR AND PINION SET NO. 2

Figure H-9 shows the free body diagram of gear and pinion set no. 2 with the necessary portions of mesh no. 1.

The forces of pinion no. 3 on gear no. 2 were given by equations (H-138) and (H-139)

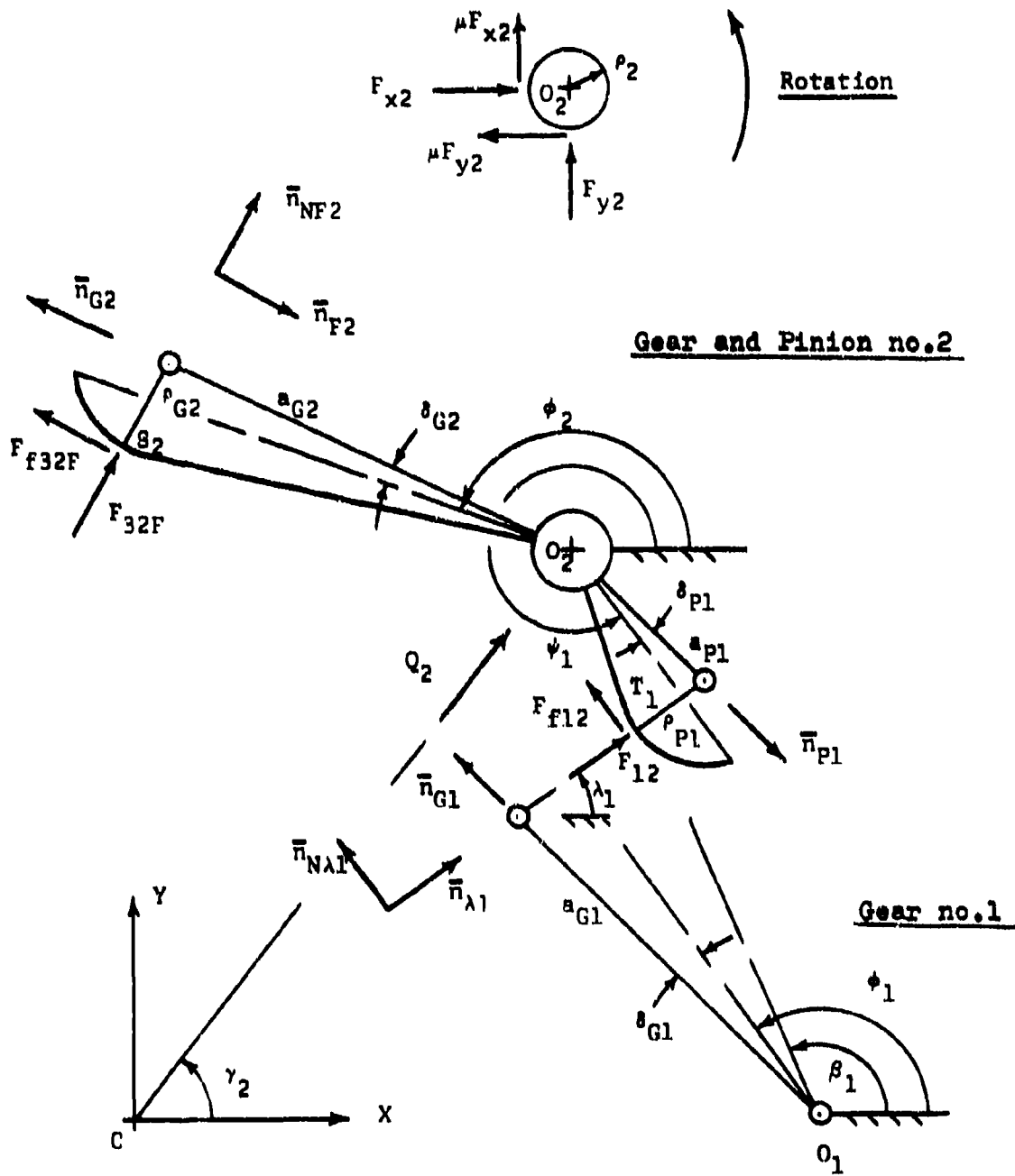


FIGURE H-9

FREE BODY DIAGRAM OF GEAR & PINION NO. 2

MESH NO. 2: ROUND ON FLAT

MESH NO. 1: ROUND ON ROUND

$$\bar{F}_{32F} = F_{23F} \bar{n}_{NF2} \quad (H-159)$$

and

$$\bar{F}_{f32F} = -\mu_{2F} F_{23F} \bar{n}_{NF2} \quad (H-160)$$

The forces of gear no. 1 on pinion no. 2 are given by equations (H-43) and (H-44)

$$\bar{F}_{12} = F_{12} \bar{n}_{\lambda 1} \quad (H-161)$$

and

$$\bar{F}_{f12} = \mu_{1R} F_{12} \bar{n}_{N\lambda 1} \quad (H-162)$$

The centrifugal force  $\bar{Q}_2$  is given by equation (H-45). The pivot reactions and friction forces are handled as before.

Force equilibrium is given by

$$\begin{aligned} F_{23F} \bar{n}_{NF2} - \mu_{2F} F_{23F} \bar{n}_{NF2} + F_{12} \bar{n}_{\lambda 1} + \mu_{1R} F_{12} \bar{n}_{N\lambda 1} + \bar{Q}_2 + F_{x2} \bar{i} - \mu F_{y2} \bar{i} \\ + F_{y2} \bar{j} + \mu F_{x2} \bar{j} = 0 \end{aligned} \quad (H-163)$$

Moment equilibrium about point  $O_2$  is given by

$$\begin{aligned}
 & -\mu^p_2(\tilde{F}_{x2} + \tilde{F}_{y2}) + [a_{G2}\bar{H}_{G2} - r_{G2}\bar{H}_{NF2}] \times [F_{23F}\bar{n}_{NF2} - \mu^s_{2F}F_{23F}\bar{n}_{F2}] \\
 & + [a_{P1}\bar{n}_{P1} - r_{P1}\bar{n}_{\lambda 1}] \times [F_{12}\bar{n}_{\lambda 1} + \mu^s_{1R}F_{12}\bar{n}_{N\lambda 1}] = 0 \quad (H-164)
 \end{aligned}$$

Equation (H-163) gives the following component equations

$$\begin{aligned}
 & -F_{23F}\sin(\psi_2 + \alpha_{P2}) - \mu^s_{2F}F_{23F}\cos(\psi_2 + \alpha_{P2}) + F_{x2} - \mu F_{y2} + F_{12}\cos\lambda_1 \\
 & - \mu^s_{1R}F_{12}\sin\lambda_1 + Q_2\cos\gamma_2 = 0 \quad (H-165)
 \end{aligned}$$

and

$$\begin{aligned}
 & F_{23F}\cos(\psi_2 + \alpha_{P2}) - \mu^s_{2F}F_{23F}\sin(\psi_2 + \alpha_{P2}) + F_{y2} + \mu F_{x2} + F_{12}\sin\lambda_1 \\
 & + \mu^s_{1R}F_{12}\cos\lambda_1 + Q_2\sin\gamma_2 = 0 \quad (H-166)
 \end{aligned}$$

The scalar form of the moment equation (H-164) becomes

$$\begin{aligned}
 & - p_2(\tilde{F}_{x2} + \tilde{F}_{y2}) + a_{G2} F_{23F} [\cos(\phi_2 - \delta_{G2} - \psi_2 - \alpha_{P2}) \\
 & + \mu s_{2F} \sin(\phi_2 - \delta_{G2} - \psi_2 - \alpha_{P2})] - \mu s_{2F} a_{G2} F_{23F} - \mu s_{1R} p_1 F_{12} \\
 & + a_{P1} F_{12} [\mu s_{1R} \cos(\psi_1 + \delta_{P1} - \lambda_1) - \sin(\psi_1 + \delta_{P1} - \lambda_1)] = 0
 \end{aligned}
 \tag{H-167}$$

Simultaneous solution of the force component equations (H-165)

and (H-166) for  $F_{x2}$  and  $F_{y2}$  results in

$$\begin{aligned}
 F_{x2} = \frac{1}{1 + \mu^2} \left\{ F_{23F} [(1 + \mu^2 s_{2F}) \sin(\psi_2 + \alpha_{P2}) - \mu(1 - s_{2F}) \cos(\psi_2 + \alpha_{P2})] \right. \\
 + F_{12} [\mu(s_{1R} - 1) \sin \lambda_1 - (1 + \mu^2 s_{1R}) \cos \lambda_1] \\
 \left. - Q_2 [\mu \sin \gamma_2 + \cos \gamma_2] \right\}
 \end{aligned}
 \tag{H-168}$$

and

$$\begin{aligned}
 F_{y2} = \frac{1}{1 + \mu^2} \left\{ F_{23F} [\mu(s_{2F} - 1) \sin(\psi_2 + \alpha_{P2}) - (1 + \mu^2 s_{2F}) \cos(\psi_2 + \alpha_{P2})] \right. \\
 + F_{12} [-(1 + \mu^2 s_{1R}) \sin \lambda_1 + \mu(1 - s_{1R}) \cos \lambda_1] \\
 \left. + Q_2 [-\sin \gamma_2 + \mu \cos \gamma_2] \right\}
 \end{aligned}
 \tag{H-169}$$

The sum  $\tilde{F}_{x2} + \tilde{F}_{y2}$  of equation(H-167) is now made up of equations (H-168) and (H-169) in the usual manner

$$\tilde{F}_{x2} + \tilde{F}_{y2} = F_{23F}A_{43} + F_{12}A_{44} + Q_2A_{45} + F_{23F}A_{46} + F_{12}A_{47} + Q_2A_{48} \quad (H-170)$$

where

$$A_{43} = \left| \frac{(1 + \mu^2 s_{2F}) \sin(\psi_2 + \alpha_{P2}) - \mu(1 - s_{2F}) \cos(\psi_2 + \alpha_{P2})}{1 + \mu^2} \right| \quad (H-171)$$

$$A_{44} = \left| \frac{\mu(s_{1R} - 1) \sin \lambda_1 - (1 + \mu^2 s_{1R}) \cos \lambda_1}{1 + \mu^2} \right| \quad (H-172)$$

$$A_{45} = \left| \frac{\mu \sin \gamma_2 + \cos \gamma_2}{1 + \mu^2} \right| \quad (H-173)$$

$$A_{46} = \left| \frac{\mu(s_{2F} - 1) \sin(\psi_2 + \alpha_{P2}) - (1 + \mu^2 s_{2F}) \cos(\psi_2 + \alpha_{P2})}{1 + \mu^2} \right| \quad (H-174)$$

$$A_{47} = \left| \frac{-(1 + \mu^2 s_{1R}) \sin \lambda_1 + \mu(1 - s_{1R}) \cos \lambda_1}{1 + \mu^2} \right| \quad (H-175)$$

$$A_{48} = \left| \frac{-\sin \gamma_2 + \mu \cos \gamma_2}{1 + \mu^2} \right| \quad (H-176)$$

Equation (H-170) is now substituted into the moment equation (H-167) and the result is solved for  $F_{12}$

$$F_{12} = \frac{-F_{23}C_{22} + Q_2C_{23}}{C_{24}} \quad (H-177)$$

where

$$C_{22} = -\mu p_2(A_{43} + A_{46}) + a_{g2}[\cos(\phi_2 - \delta_{g2} - \psi_2 - \alpha_{p2}) + \mu a_{2F} \sin(\phi_2 - \delta_{g2} - \psi_2 - \alpha_{p2})] - \mu a_{2F} p_{g2}$$

$$C_{23} = \mu p_2(A_{45} + A_{48})$$

$$C_{24} = -\mu p_2(A_{44} + A_{47}) + a_{p1}[\mu a_{1R} \cos(\psi_1 + \delta_{p1} - \lambda_1) - \sin(\psi_1 + \delta_{p1} - \lambda_1)] - \mu a_{1R} p_{p1}$$

## II. MOMENT INPUT-OUTPUT RELATIONSHIP

Equations (H-177) and (H-78) are now set equal to each other and the result is solved for  $F_{23F}$

$$F_{23F} = \frac{-C_{24}}{C_{10}C_{22}} (M_{1n} - Q_1 C_9) + Q_2 \frac{C_{23}}{C_{22}} \quad (H-178)$$

The above is now equated to equation (H-137) to obtain  $F_{34}$

$$F_{34} = \frac{C_{18}C_{24}}{C_{10}C_{16}C_{22}} (M_{1n} - Q_1 C_9) - Q_2 \frac{C_{18}C_{23}}{C_{16}C_{22}} - Q_3 \frac{C_{17}}{C_{16}} \quad (H-179)$$

Finally equations (H-179) and (H-19) are set equal to each other and the equilibrant moment  $M_{o44}$  (For case 4: RFR) is determined

$$M_{o44} = M_{1n} \frac{C_2 C_{18} C_{24}}{C_{10} C_{16} C_{22}} - Q_1 \frac{C_2 C_9 C_{18} C_{24}}{C_{10} C_{16} C_{22}} - Q_2 \frac{C_2 C_{18} C_{23}}{C_{16} C_{22}} - Q_3 \frac{C_2 C_{17}}{C_{16}} - Q_4 C_1 \quad (H-180)$$

e. CASE NO. 5: FFF

For this contact combination it is necessary to determine new expressions for the force  $F_{34F}$  of gear no. 3 on pinion no. 4, and for force  $F_{23F}$  of gear no. 2 on pinion no. 3.

Equation (H-156), derived for case 3, and which relates force  $F_{23F}$  to the input moment  $M_{in}$ , may be used for the determination of the final input-output relationship.

I. FORCE AND MOMENT EQUILIBRIA OF PINION NO. 4

Figure H-10 gives the free body diagram of pinion no. 4 in the round on flat phase of motion with gear no. 3.

The equilibrant moment  $M_{o4}$  acts in a clockwise direction and opposes the counter-clockwise rotation of the pinion.

The normal contact force  $\bar{F}_{34F}$  is given by

$$\bar{F}_{34F} = F_{34F} \bar{H}_{NF3} \quad (H-181)$$

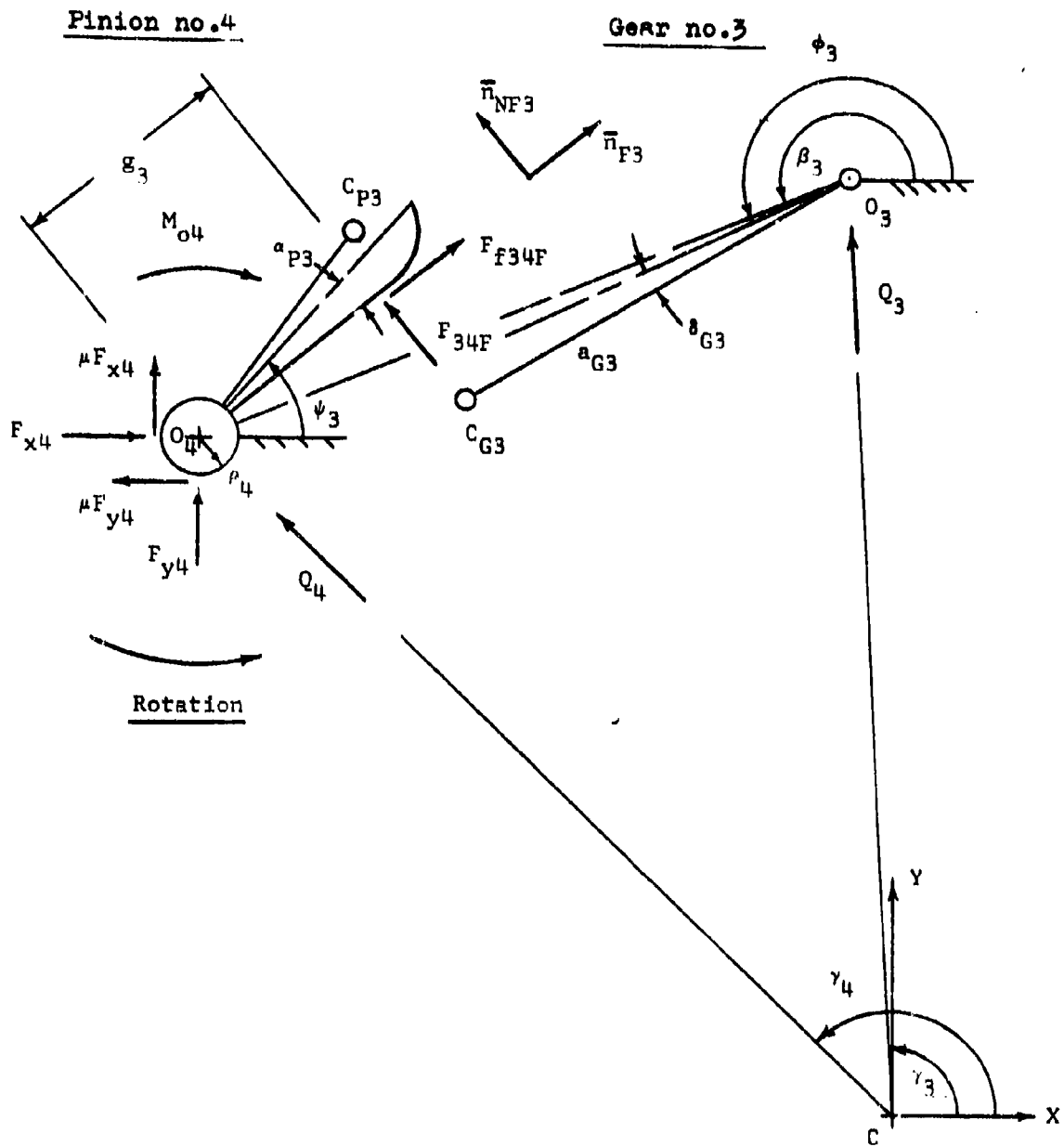


FIGURE H-10  
 FREE BODY DIAGRAM OF PINION NO. 4  
 MESH NO. 3: ROUND ON FLAT

The associated friction force becomes

$$\bar{F}_{f34F} = \mu s_3 F_{34F} \bar{n}_{F3} \quad (H-182)$$

The centrifugal force  $\bar{Q}_4$  is given by equation (H-5) and the pivot friction forces are chosen such that they oppose rotation.

Force equilibrium is given by

$$\begin{aligned} F_{34F} \bar{n}_{NF3} + \mu s_3 F_{34F} \bar{n}_{F3} + F_{x4} \bar{i} - \mu F_{y4} \bar{i} + F_{y4} \bar{j} + \mu F_{x4} \bar{j} \\ + Q_4 (\cos \gamma_4 \bar{i} + \sin \gamma_4 \bar{j}) = 0 \end{aligned} \quad (H-183)$$

Moment equilibrium about point  $O_4$  requires that

$$-M_{O_4} \bar{k} - \mu \rho_4 (\tilde{F}_{x4} + \tilde{F}_{y4}) \bar{k} + s_3 \bar{n}_{F3} \times F_{34F} \bar{n}_{NF3} = 0 \quad (H-184)$$

Note that the friction force  $F_{f34F}$  does not exert a moment about point  $O_4$ , since its line of action passes through it.

Equation (H-183) furnishes the following component equations

$$\begin{aligned} -F_{34F} \sin(\psi_3 - \alpha_{P3}) + \mu s_3 F_{34F} \cos(\psi_3 - \alpha_{P3}) + F_{x4} - \mu F_{y4} \\ + Q_4 \cos \gamma_4 = 0 \end{aligned} \quad (H-185)$$

and

$$F_{34F} \cos(\psi_3 - \alpha_{p3}) + \mu s_{3F} F_{34F} \sin(\psi_3 - \alpha_{p3}) + F_{y4} + \mu F_{x4} + Q_4 \sin \gamma_4 = 0 \quad (H-186)$$

The scalar form of the moment equation (H-184) becomes

$$-M_{o4} - \mu P_4 (\tilde{F}_{x4} + \tilde{F}_{y4}) + \epsilon_3 F_{34F} = 0 \quad (H-187)$$

Simultaneous solution of equations (H-185) and (H-186) for  $F_{x4}$  and  $F_{y4}$  results in

$$F_{x4} = \frac{1}{1 + \mu^2} \left\{ F_{34F} [(1 - \mu^2 s_{3F}) \sin(\psi_3 - \alpha_{p3}) - \mu(1 + s_{3F}) \cos(\psi_3 - \alpha_{p3})] + Q_4 [-\mu \sin \gamma_4 - \cos \gamma_4] \right\} \quad (H-188)$$

and

$$F_{y4} = \frac{1}{1 + \mu^2} \left\{ F_{34F} [-\mu(1 + s_{3F}) \sin(\psi_3 - \alpha_{p3}) - (1 - \mu^2 s_{3F}) \cos(\psi_3 - \alpha_{p3})] + Q_4 [-\sin \gamma_4 + \mu \cos \gamma_4] \right\} \quad (H-189)$$

The sum  $\tilde{F}_{x4} + \tilde{F}_{y4}$  of equation (H-187) is now made up of equations (H-188) and (H-189) in the sense of equation (A-3b)

$$\tilde{F}_{x4} + \tilde{F}_{y4} = F_{34F}A_{49} + Q_4A_{50} + F_{34F}A_{51} + Q_4A_{52} \quad (\text{H-190})$$

where

$$A_{49} = \left| \frac{(1 - \mu^2 s_{3F}) \sin(\psi_3 - \alpha_{P3}) - \mu(1 + s_{3F}) \cos(\psi_3 - \alpha_{P3})}{1 + \mu^2} \right| \quad (\text{H-191})$$

$$A_{50} = \left| \frac{-\mu \sin \gamma_4 - \cos \gamma_4}{1 + \mu^2} \right| \quad (\text{H-192})$$

$$A_{51} = \left| \frac{-\mu(1 + s_{3F}) \sin(\psi_3 - \alpha_{P3}) - (1 - \mu^2 s_{3F}) \cos(\psi_3 - \alpha_{P3})}{1 + \mu^2} \right| \quad (\text{H-193})$$

$$A_{52} = \left| \frac{-\sin \gamma_4 + \mu \cos \gamma_4}{1 + \mu^2} \right| \quad (\text{H-194})$$

Equation (H-190) is now substituted into equation (H-187) and the result is solved for  $F_{34F}$

$$F_{34F} = \frac{M_{04} + Q_4 C_{25}}{C_{26}} \quad (\text{H-195})$$

where

$$C_{25} = \mu p_4 (A_{50} + A_{52})$$

$$C_{26} = \delta_3 - \mu p_4 (A_{49} + A_{51})$$

## II. FORCE AND MOMENT EQUILIBRIA OF GEAR AND PINION SET NO. 3

Figure H-11 gives the free body diagram of gear and pinion combination no. 3. Both mesh 3 and mesh 2 are in their round on flat phase of contact.

The forces of pinion 4 on gear 3 are equal to, but opposite in direction to, those given by equations (H-181) and (H-182)

$$\bar{F}_{43F} = - F_{34F} \bar{n}_{NF3} \quad (H-196)$$

and

$$\bar{F}_{f43F} = - \mu_{s3F} F_{34F} \bar{n}_{F3} \quad (H-197)$$

The forces of gear 2 on pinion 3 are given by

$$\bar{F}_{23F} = - F_{23F} \bar{n}_{NF2} \quad (H-198)$$

and

$$\bar{F}_{f23F} = \mu_{s2F} F_{23F} \bar{n}_{F2} \quad (H-199)$$

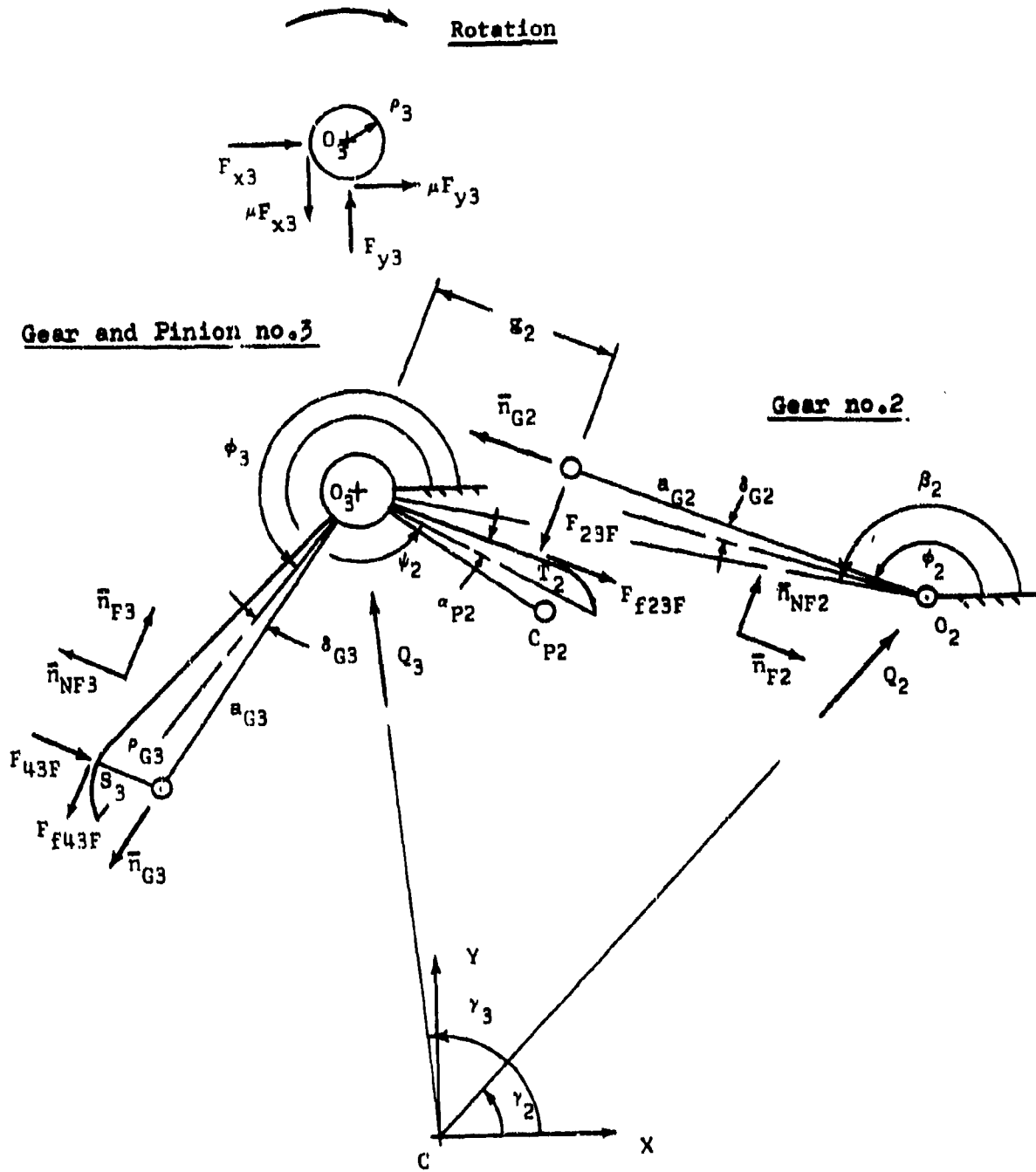


FIGURE H-11

FREE BODY DIAGRAM OF GEAR & PINION NO. 3  
 MESH NO. 3: ROUND ON FLAT  
 MESH NO. 2: ROUND ON FLAT

The pivot forces and moments are chosen in the usual manner and the centrifugal force  $\bar{Q}_3$  is defined by equation (H-24).

Force equilibrium is given by

$$\begin{aligned}
 & -F_{34}\bar{n}_{NF3} - \mu_{3F}F_{34}\bar{n}_{F3} - F_{23}\bar{n}_{NF2} + \mu_{2F}F_{23}\bar{n}_{F2} + \bar{Q}_3 + F_{x3}\bar{i} \\
 & + \mu_{Fy3}\bar{i} + F_{y3}\bar{j} - \mu_{Fx3}\bar{j} = 0 \quad (H-200)
 \end{aligned}$$

Moment equilibrium about point  $O_3$  requires that

$$\begin{aligned}
 & \mu_{F3}(\bar{F}_{x3} + \bar{F}_{y3})\bar{k} + [a_{G3}\bar{n}_{G3} + r_{G3}\bar{n}_{NF3}] \times [-F_{34}\bar{n}_{NF3} - \mu_{3F}F_{34}\bar{n}_{F3}] \\
 & + b_{2F}\bar{n}_{F2} \times (-)F_{23}\bar{n}_{NF2} = 0 \quad (H-201)
 \end{aligned}$$

Note that the friction force  $F_{f23F}$  does not exert a moment about point  $O_3$ .

Equation (H-200) furnishes, after all necessary substitutions, the following component equations:

$$\begin{aligned}
 & F_{34}\sin(\psi_3 - \alpha_{P3}) - \mu_{3F}F_{34}\cos(\psi_3 - \alpha_{P3}) + \bar{Q}_3\cos\gamma_3 + F_{x3} + \mu_{Fy3} \\
 & + F_{23}\sin(\psi_2 + \alpha_{P2}) + \mu_{2F}F_{23}\cos(\psi_2 + \alpha_{P2}) = 0 \quad (H-202)
 \end{aligned}$$

and

$$\begin{aligned}
 & -F_{34F} \cos(\psi_3 - \alpha_{P3}) - \mu s_{3F} F_{34F} \sin(\psi_3 - \alpha_{P3}) + Q_3 \sin \gamma_3 + F_{y3} - \mu F_{x3} \\
 & - F_{23F} \cos(\psi_2 + \alpha_{P2}) + \mu s_{2F} F_{23F} \sin(\psi_2 + \alpha_{P2}) = 0 \quad (H-203)
 \end{aligned}$$

The scalar form of the moment equation (H-201) becomes

$$\begin{aligned}
 & \mu P_3 (\tilde{F}_{x3} + \tilde{F}_{y3}) + s_{G3} F_{34F} [-\cos(\phi_3 + \delta_{G3} - \psi_3 + \alpha_{P3}) \\
 & + \mu s_{3F} \sin(\phi_3 + \delta_{G3} - \psi_3 + \alpha_{P3})] + \mu s_{3F} P_{G3} F_{34F} - s_{2F} F_{23F} = 0 \\
 & \quad \quad \quad (H-204)
 \end{aligned}$$

Simultaneous solution of the component equations (H-202) and (H-203)

for  $F_{x3}$  and  $F_{y3}$  gives

$$\begin{aligned}
 F_{x3} = \frac{1}{1 + \mu^2} \left\{ F_{34F} [-(1 + \mu^2 s_{3F}) \sin(\psi_3 - \alpha_{P3}) + \mu (s_{3F} - 1) \cos(\psi_3 - \alpha_{P3})] \right. \\
 + F_{23F} [(\mu^2 s_{2F} - 1) \sin(\psi_2 + \alpha_{P2}) - \mu (1 + s_{2F}) \cos(\psi_2 + \alpha_{P2})] \\
 \left. + Q_3 [\mu \sin \gamma_3 - \cos \gamma_3] \right\} \quad (H-205)
 \end{aligned}$$

and

$$\begin{aligned}
 F_{y3} = \frac{1}{1 + \mu^2} & \left\{ F_{34F} \left[ \mu(s_{3F} - 1) \sin(\psi_3 - \alpha_{P3}) + (1 + \mu^2 s_{3F}) \cos(\psi_3 - \alpha_{P3}) \right] \right. \\
 & + F_{23F} \left[ -\mu(1 + s_{2F}) \sin(\psi_2 + \alpha_{P2}) + (1 - \mu^2 s_{2F}) \cos(\psi_2 + \alpha_{P2}) \right] \\
 & \left. + Q_3 \left[ -\sin \gamma_3 - \mu \cos \gamma_3 \right] \right\} \quad (H-206)
 \end{aligned}$$

The sum  $\tilde{F}_{x3} + \tilde{F}_{y3}$  is now made up from equations (H-205) and (H-206)

$$\tilde{F}_{x3} + \tilde{F}_{y3} = F_{34F} A_{53} + F_{23F} A_{54} + Q_3 A_{55} + F_{34F} A_{56} + F_{23F} A_{57} + Q_3 A_{58} \quad (H-207)$$

where

$$A_{53} = \left| \frac{-(1 + \mu^2 s_{3F}) \sin(\psi_3 - \alpha_{P3}) + \mu(s_{3F} - 1) \cos(\psi_3 - \alpha_{P3})}{1 + \mu^2} \right| \quad (H-208)$$

$$A_{54} = \left| \frac{(\mu^2 s_{2F} - 1) \sin(\psi_2 + \alpha_{P2}) - \mu(1 + s_{2F}) \cos(\psi_2 + \alpha_{P2})}{1 + \mu^2} \right| \quad (H-209)$$

$$A_{55} = \left| \frac{\mu \sin \gamma_3 - \cos \gamma_3}{1 + \mu^2} \right| \quad (H-210)$$

$$A_{56} = \left| \frac{\mu(a_{3F} - 1)\sin(\psi_3 - \alpha_{P3}) + (1 + \mu^2 a_{3F})\cos(\psi_3 - \alpha_{P3})}{1 + \mu^2} \right| \quad (\text{H-211})$$

$$A_{57} = \left| \frac{-\mu(1 + a_{2F})\sin(\psi_2 + \alpha_{P2}) + (1 - \mu^2 a_{2F})\cos(\psi_2 + \alpha_{P2})}{1 + \mu^2} \right| \quad (\text{H-212})$$

$$A_{58} = \left| \frac{\sin\gamma_3 + \mu\cos\gamma_3}{1 + \mu^2} \right| \quad (\text{H-213})$$

Equation (H-207) is now substituted into equation (H-204).

The result is solved for  $F_{23F}$

$$F_{23F} = \frac{-F_{34F}C_{27} - Q_3C_{28}}{C_{29}} \quad (\text{H-214})$$

where

$$C_{27} = \mu^2 P_3(A_{53} + A_{56}) + a_{G3}[-\cos(\phi_3 + \delta_{G3} - \psi_3 + \alpha_{P3}) + \mu a_{3F}\sin(\phi_3 + \delta_{G3} - \psi_3 + \alpha_{P3})] + \mu a_{3F}P_3$$

$$C_{28} = \mu^2 P_3(A_{55} + A_{58})$$

$$C_{29} = \mu^2 P_3(A_{54} + A_{57}) - G_2$$

### III. MOMENT INPUT-OUTPUT RELATIONSHIP

Equation (H-156) is an expression for  $F_{23F}$  as a function of the moment  $M_{1n}$  and the centrifugal forces  $Q_1$  and  $Q_2$ , when both meshes no. 1 and no. 2 are in the round on flat phase of motion. This expression for  $F_{23F}$  is now equated to equation (H-214). The result is solved for  $F_{34F}$

$$F_{34F} = \frac{c_{21}c_{29}}{c_{15}c_{19}c_{27}} (M_{1n} - Q_1c_{14}) - Q_2 \frac{c_{20}c_{29}}{c_{19}c_{27}} - Q_3 \frac{c_{28}}{c_{27}} \quad (\text{H-215})$$

The above is now equated to equation (H-195) and the resulting expression is used to determine the equilibrant moment  $M_{o45}$   
(for Case 5: FFF)

$$M_{o45} = M_{1n} \frac{c_{21}c_{26}c_{29}}{c_{15}c_{19}c_{27}} - Q_1 \frac{c_{14}c_{21}c_{26}c_{29}}{c_{15}c_{19}c_{27}} - Q_2 \frac{c_{20}c_{26}c_{29}}{c_{19}c_{27}} - Q_3 \frac{c_{26}c_{28}}{c_{27}} - Q_4c_{25} \quad (\text{H-216})$$

f. CASE NO. 6: FFR

MOMENT INPUT-OUTPUT RELATIONSHIP

The moment input-output relationship for this contact combination can be assembled entirely from previously derived component relationships. As for case no. 4, mesh no. 1 is in the round on round phase while mesh no. 2 is in the round on flat phase. Therefore, equation (H-178), which relates the force  $F_{23F}$  to the input moment  $M_{in}$ , may be used. The input-output relationship of the gear and pinion set no. 3, i.e. the relationship between the forces  $F_{34F}$  and  $F_{23F}$ , is given by equation (H-214) of case no. 5. The force  $F_{34F}$  may be obtained from equation (H-195). This expression was also derived for a round on flat contact in case no. 5.

Thus, equation (H-178) is first set equal to equation (H-214) and the result is solved for the force  $F_{34F}$

$$F_{34F} = \frac{c_{24}c_{29}}{c_{10}c_{22}c_{27}} (M_{in} - Q_1c_9) - Q_2 \frac{c_{23}c_{29}}{c_{22}c_{27}} - Q_3 \frac{c_{28}}{c_{27}} \quad (H-217)$$

The above expression is now set equal to equation (H-195).

This then allows the determination of the equilibrant moment

$M_{046}$  for the present contact combination.

$$\begin{aligned} M_{046} = M_{1n} \frac{C_{24}C_{26}C_{29}}{C_{10}C_{22}C_{27}} - Q_1 \frac{C_9C_{24}C_{26}C_{29}}{C_{10}C_{22}C_{27}} - Q_2 \frac{C_{23}C_{26}C_{29}}{C_{22}C_{27}} \\ - Q_3 \frac{C_{26}C_{28}}{C_{27}} - Q_4 C_{25} \end{aligned} \quad (H-218)$$

E. CASE NO. 7: FRR

For the present contact combination the expression for force  $F_{34F}$  may be taken over from equation (H-195) of case no. 5. The input-output relationship of gear and pinion set no. 3, which relates the forces  $F_{34F}$  and  $F_{23}$ , must be newly derived. The relationship between force  $F_{23}$  and the input moment  $M_{in}$  is taken from case no. 1 in the form of equation (H-79).

I. FORCE AND MOMENT EQUILIBRIA OF GEAR AND PINION SET NO. 3

Figure H-12 gives the free body diagram of gear and pinion set no. 3. Mesh no. 3 is in the round on flat phase of contact, while mesh no. 2 is in the round on round one.

The forces of pinion no. 4 on gear no. 3 are equal to, but opposite in direction to those given by equations (H-181) and (H-182)

$$\bar{F}_{43F} = - F_{34F} \bar{n}_{NF3} \quad (H-219)$$

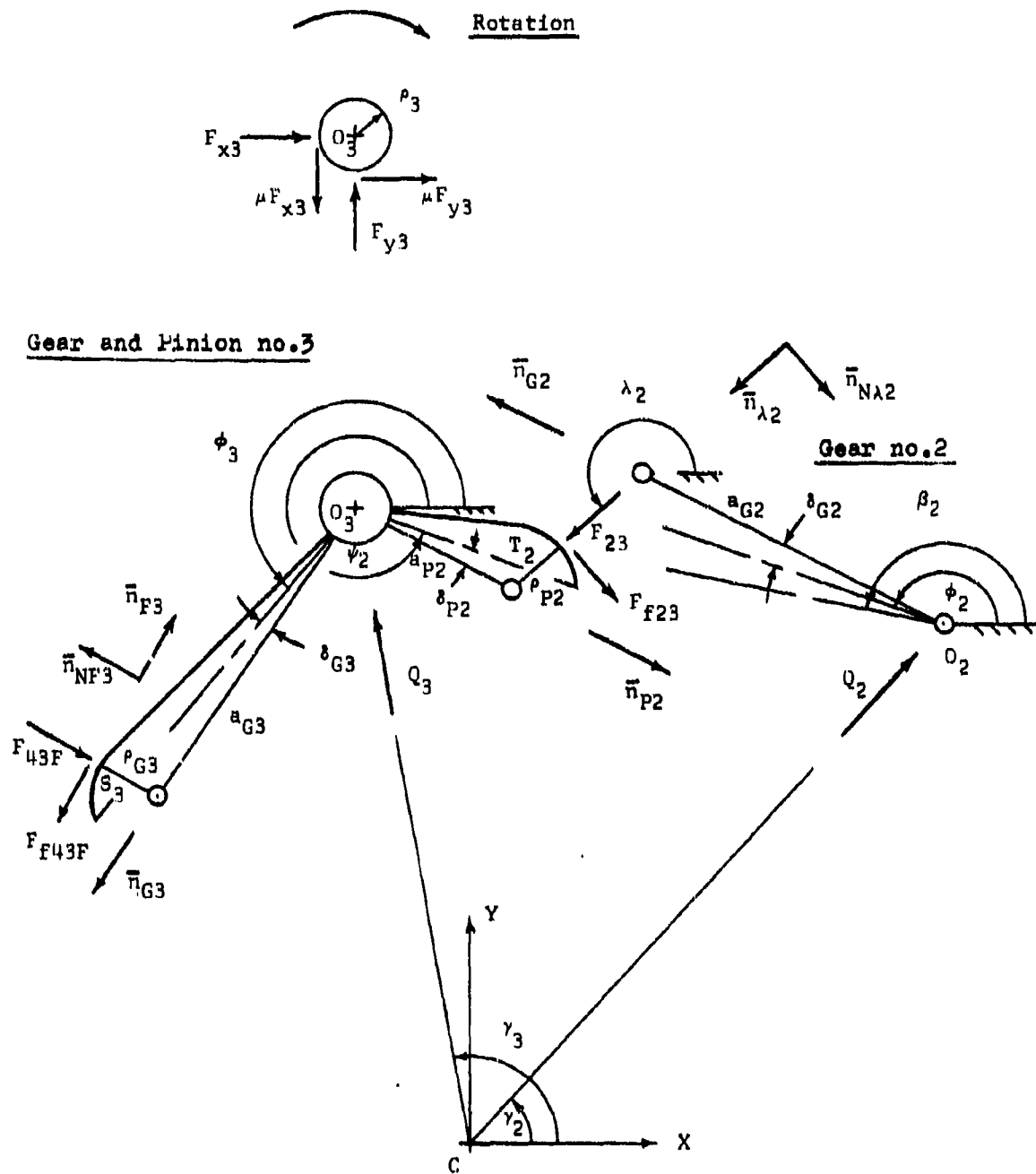


FIGURE H-12

FREE BODY DIAGRAM OF GEAR & PINION NO. 3

MESH NO. 3: ROUND ON FLAT

MESH NO. 2: ROUND ON ROUND

and

$$\bar{F}_{f43F} = -\mu_{3F} F_{34F} \bar{n}_{F3} \quad (H-220)$$

The forces of gear no. 2 on pinion no. 3 are given by

$$\bar{F}_{23} = F_{23} \bar{n}_{\lambda 2} \quad (H-221)$$

and

$$\bar{F}_{f23} = \mu_{2R} F_{23} \bar{n}_{N\lambda 2} \quad (H-222)$$

The pivot reactions are chosen in the same manner as before.

The centrifugal force  $\bar{Q}_3$  was defined by equation (H-24).

Force equilibrium of the gear set requires

$$\begin{aligned} -F_{34F} \bar{n}_{NF3} - \mu_{3F} F_{34F} \bar{n}_{F3} + F_{23} \bar{n}_{\lambda 2} + \mu_{2R} F_{23} \bar{n}_{N\lambda 2} + \bar{Q}_3 + F_{x3} \bar{i} \\ + \mu_{Fy3} \bar{i} + F_{y3} \bar{j} - \mu_{Fx3} \bar{j} = 0 \end{aligned} \quad (H-223)$$

Moment equilibrium about point  $O_3$  is given by

$$\begin{aligned} & \mu_{P3}(\tilde{F}_{x3} + \tilde{F}_{y3})\bar{k} + [a_{G3}\bar{n}_{G3} + \rho_{G3}\bar{n}_{NF3}] \times [-F_{34}\bar{n}_{NF3} - \mu_{S3}F_{34}\bar{n}_{F3}] \\ & + [a_{P2}\bar{n}_{P2} - \rho_{P2}\bar{n}_{\lambda 2}] \times [F_{23}\bar{n}_{\lambda 2} + \mu_{S2}F_{23}\bar{n}_{N\lambda 2}] = 0 \end{aligned} \quad (H-224)$$

Equation (H-223) gives the following component expressions

$$\begin{aligned} & F_{34}\sin(\psi_3 - \alpha_{P3}) - \mu_{S3}F_{34}\cos(\psi_3 - \alpha_{P3}) + Q_3\cos\gamma_3 + F_{x3} + \mu F_{y3} \\ & + F_{23}\cos\lambda_2 - \mu_{S2}F_{23}\sin\lambda_2 = 0 \end{aligned} \quad (H-225)$$

and

$$\begin{aligned} & -F_{34}\cos(\psi_3 - \alpha_{P3}) - \mu_{S3}F_{34}\sin(\psi_3 - \alpha_{P3}) + Q_3\sin\gamma_3 + F_{y3} - \mu F_{x3} \\ & + F_{23}\sin\lambda_2 + \mu_{S2}F_{23}\cos\lambda_2 = 0 \end{aligned} \quad (H-226)$$

The scalar form of the moment equation (H-224) becomes.

$$\begin{aligned}
 & \mu P_3(\tilde{F}_{x3} + \tilde{F}_{y3}) + a_{G3}F_{34F}[-\cos(\psi_3 + \delta_{G3} - \psi_3 + \alpha_{P3}) \\
 & + \mu s_{3F}\sin(\psi_3 + \delta_{G3} - \psi_3 + \alpha_{P3})] + \mu s_{3F}^2 a_{G3}F_{34F} \\
 & + a_{P2}F_{23}[-\sin(\psi_2 - \delta_{P2} - \lambda_2) + \mu s_{2R}\cos(\psi_2 - \delta_{P2} - \lambda_2)] \\
 & - \mu s_{2R}^2 a_{P2}F_{23} = 0 \qquad \qquad \qquad (H-227)
 \end{aligned}$$

Simultaneous solution of the component equations (H-225) and (H-226)

for  $F_{x3}$  and  $F_{y3}$  results in:

$$\begin{aligned}
 F_{x3} = \frac{1}{1 + \mu^2} \left\{ F_{34F} [-(1 + \mu^2 s_{3F})\sin(\psi_3 - \alpha_{P3}) + \mu(s_{3F} - 1)\cos(\psi_3 - \alpha_{P3})] \right. \\
 + F_{23} [\mu(1 + s_{2R})\sin\lambda_2 + (\mu^2 s_{2R} - 1)\cos\lambda_2] \\
 \left. + Q_3 [\mu\sin\gamma_3 - \cos\gamma_3] \right\} \qquad \qquad \qquad (H-228)
 \end{aligned}$$

and

$$\begin{aligned}
 F_{y3} = \frac{1}{1 + \mu^2} & \left\{ F_{34F} [\mu(s_{3F} - 1)\sin(\psi_3 - \alpha_{P3}) + (1 + \mu^2 s_{3F})\cos(\psi_3 - \alpha_{P3})] \right. \\
 & + F_{23} [(\mu^2 s_{2R} - 1)\sin\lambda_2 - \mu(1 + s_{2R})\cos\lambda_2] \\
 & \left. + Q_3 [-\sin\gamma_3 - \mu\cos\gamma_3] \right\} \quad (H-229)
 \end{aligned}$$

The sum  $\tilde{F}_{x3} + \tilde{F}_{y3}$  in equation (H-227) is now made up from equations (H-228) and (H-229) in the sense of equation (A-3b)

$$\tilde{F}_{x3} + \tilde{F}_{y3} = F_{34F}A_{59} + F_{23}A_{60} + Q_3A_{61} + F_{34F}A_{62} + F_{23}A_{63} + Q_3A_{64} \quad (H-230)$$

where

$$A_{59} = \left| \frac{-(1 + \mu^2 s_{3F})\sin(\psi_3 - \alpha_{P3}) + \mu(s_{3F} - 1)\cos(\psi_3 - \alpha_{P3})}{1 + \mu^2} \right| \quad (H-231)$$

$$A_{60} = \left| \frac{\mu(1 + s_{2R})\sin\lambda_2 + (\mu^2 s_{2R} - 1)\cos\lambda_2}{1 + \mu^2} \right| \quad (H-232)$$

$$A_{61} = \left| \frac{\mu\sin\gamma_3 - \cos\gamma_3}{1 + \mu^2} \right| \quad (H-233)$$

$$A_{62} = \left| \frac{\mu(a_{3F} - 1)\sin(\psi_3 - \alpha_{P3}) + (1 + \mu^2 a_{3F})\cos(\psi_3 - \alpha_{P3})}{1 + \mu^2} \right| \quad (H-234)$$

$$A_{63} = \left| \frac{(\mu^2 a_{2R} - 1)\sin\lambda_2 - \mu(1 + a_{2R})\cos\lambda_2}{1 + \mu^2} \right| \quad (H-235)$$

$$A_{64} = \left| \frac{-\sin\gamma_3 - \mu\cos\gamma_3}{1 + \mu^2} \right| \quad (H-236)$$

Equation (H-230) is now substituted into the moment equation (H-227)

and the resulting expression is solved for  $F_{23}$

$$F_{23} = \frac{-F_{34}C_{30} - Q_3 C_{31}}{C_{32}} \quad (H-237)$$

where

$$C_{30} = \mu p_3 (A_{59} + A_{62}) - a_{Q3} [\cos(\psi_3 + \delta_{Q3} - \psi_3 + \alpha_{P3}) - \mu a_{3F} \sin(\psi_3 + \delta_{Q3} - \psi_3 + \alpha_{P3})] + \mu a_{3F} p_{Q3}$$

$$C_{31} = \mu p_3 (A_{61} + A_{64})$$

$$C_{32} = \mu^P_3(A_{60} + A_{63}) - a_{P2}[\sin(\psi_2 - \delta_{P2} - \lambda_2) - \mu^B_{2R}\cos(\psi_2 - \delta_{P2} - \lambda_2)]$$

$$- \mu^B_{2R}P_2$$

## II. MOMENT INPUT-OUTPUT RELATIONSHIP

Equation (H-79), which gives the force  $F_{23}$  in terms of  $M_{in}$ ,  $Q_1$  and  $Q_2$  for the appropriate contact combinations, is now set equal to equation (H-237). Subsequently, one finds the following formulation for  $F_{34F}$ :

$$F_{34F} = \frac{C_8 C_{32}}{C_6 C_{10} C_{30}} (M_{in} - Q_1 C_9) - Q_2 \frac{C_7 C_{32}}{C_6 C_{30}} - Q_3 \frac{C_{31}}{C_{30}} \quad (H-238)$$

The above expression is now set equal to equation (H-195) which gives  $F_{34F}$  in terms of  $M_{O4}$  and  $Q_4$ . The determination of the equilibrant moment  $M_{O47}$  (for case 7: FRR) is now possible.

Thus,

$$M_{047} = M_{1n} \frac{C_8^C C_{26}^C C_{32}^C}{C_6^C C_{10}^C C_{30}^C} - Q_1 \frac{C_8^C C_9^C C_{26}^C C_{32}^C}{C_6^C C_{10}^C C_{30}^C} - Q_2 \frac{C_7^C C_{26}^C C_{32}^C}{C_6^C C_{30}^C}$$

$$- Q_3 \frac{C_{26}^C C_{31}^C}{C_{30}^C} - Q_4 C_{25}^C$$

(H-239)

h. CASE NO. 8: FRF

MOMENT INPUT-OUTPUT RELATIONSHIP

The input-output relationship for this contact combination can also be assembled entirely from existing expressions. With mesh no. 2 in the round on round phase of contact and mesh no. 1 in the round on flat one, the relationship between force  $F_{23}$  and the moment  $M_{1n}$  is that of case no. 2. Equation (H-116) is applicable. The input-output relationship of gear and pinion set no. 3, which relates  $F_{34F}$  to  $F_{23}$ , was derived for case no. 7 and is given by equation (H-237). Finally, with mesh no. 3 in the round on flat phase, one uses equation (H-195) for the relationship between force  $F_{34F}$  and moment  $M_{o4}$ . Thus, equation (H-116) is first set equal to equation (H-237) to obtain an expression for force  $F_{34F}$

$$F_{34F} = \frac{c_{13}c_{32}}{c_{11}c_{15}c_{30}} (M_{1n} - Q_1 c_{14}) - Q_2 \frac{c_{12}c_{32}}{c_{11}c_{30}} - Q_3 \frac{c_{31}}{c_{30}} \quad (H-240)$$

The above expression is now set equal to equation (H-195). This allows the determination of  $M_{048}$  (for case 8: FRF)

$$M_{048} = M_{1n} \frac{C_{13} C_{26} C_{32}}{C_{11} C_{15} C_{30}} - Q_1 \frac{C_{13} C_{14} C_{26} C_{32}}{C_{11} C_{15} C_{30}} - Q_2 \frac{C_{12} C_{26} C_{32}}{C_{11} C_{30}} - Q_3 \frac{C_{26} C_{31}}{C_{30}} - Q_4 C_{25} \quad (\text{H-241})$$

## 2. INPUT-OUTPUT ANALYSIS OF TWO STEP-UP GEAR TRAIN

The following gives derivations for the moment input-output relationships associated with the four possible contact combinations of a two step-up gear train. (See Table H-2).

### a. CASE NO. 1: RR

For this contact combination, the relationship between the equilibrant moment  $M_{o3}$  and force  $F_{23}$ , both acting on pinion no. 3, must first be newly obtained. The relationships between forces  $F_{23}$  and  $F_{12}$  of gear and pinion set no. 2, as well as between force  $F_{12}$  and input moment  $M_{1n}$  of gear no. 1, may be taken from case no. 1 of the three step-up gear train analysis. Equations (H-61) and (H-78), respectively, are applicable.

### I. FORCE AND MOMENT EQUILIBRIA OF PINION NO. 3

Figure H-13 shows a schematic free body diagram of pinion no. 3 in the round on round phase of contact. The equilibrant

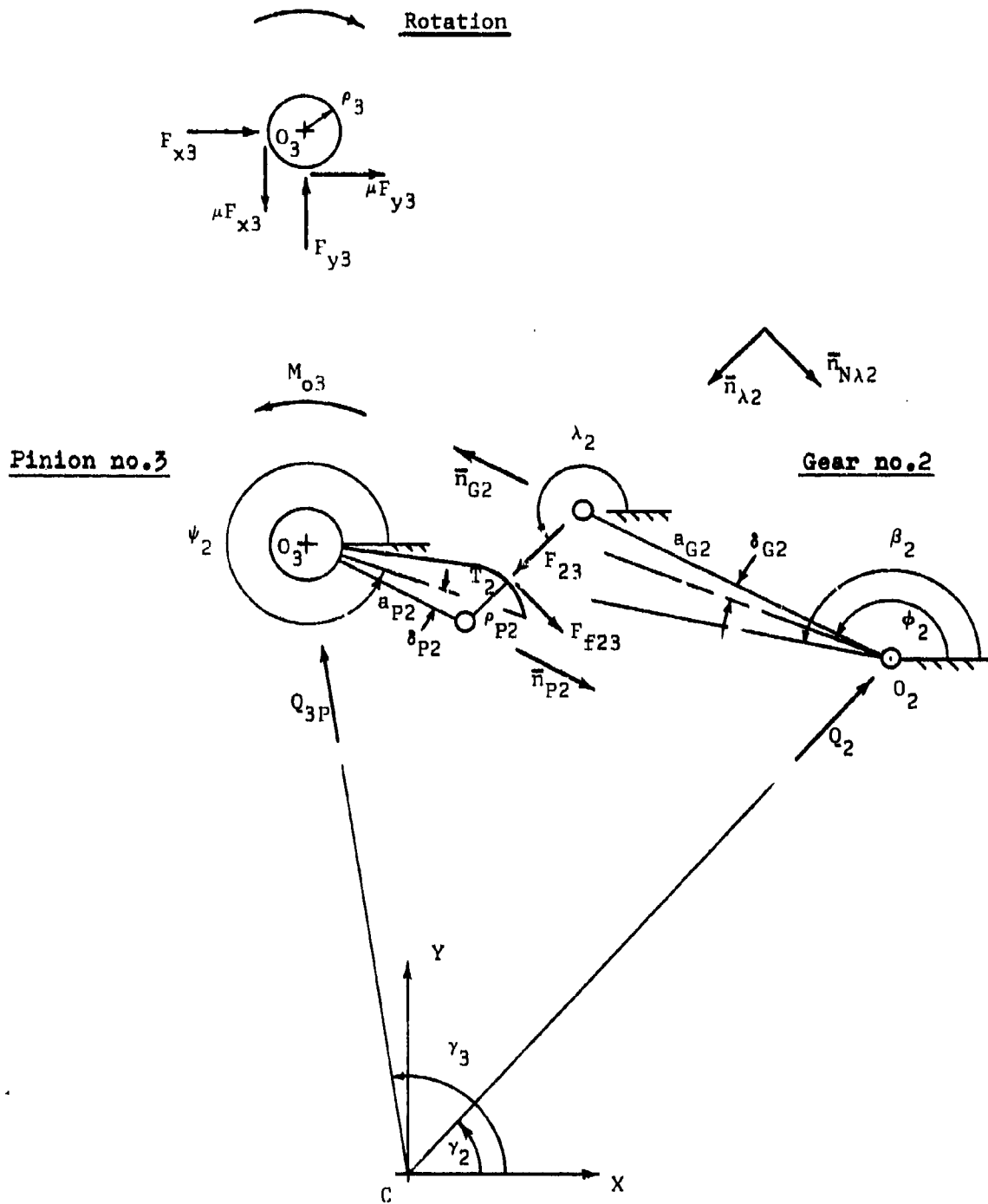


FIGURE H-13

FREE BODY DIAGRAM OF PINION NO. 3  
MESH NO. 2: ROUND ON ROUND

moment  $M_{o3}$  acts in the direction opposite to the clockwise rotation of the pinion. The normal contact force of gear no. 2 on pinion no. 3 is given by

$$\bar{F}_{23} = F_{23} \bar{n}_{\lambda 2} \quad (\text{H-242})$$

The associated friction force becomes

$$\bar{F}_{f23} = \mu_s 2R F_{23} \bar{n}_{\lambda 2} \quad (\text{H-243})$$

The pivot reactions are chosen in the usual manner.

The centrifugal force  $\bar{Q}_{3p}$  is now due to the mass  $m_{3p}$  of the pinion alone, i.e.,

$$\bar{Q}_{3p} = Q_{3p} (\cos \gamma_3 \bar{i} + \sin \gamma_3 \bar{j}) \quad (\text{H-244})$$

where

$$Q_{3p} = m_{3p} r_3 \omega^2 \quad (\text{H-245})$$

Force equilibrium of the pinion is assured by

$$F_{23}\bar{n}_{\lambda 2} + \mu s_{2R}F_{23}\bar{n}_{N\lambda 2} + F_{x3}\bar{i} + \mu F_{y3}\bar{i} + F_{y3}\bar{j} - \mu F_{x3}\bar{j} + \bar{Q}_{3P} = 0$$

(H-246)

Moment equilibrium about point  $O_3$  is given by

$$\mu \rho_3(\tilde{F}_{x3} + \tilde{F}_{y3})\bar{k} + M_{O3}\bar{k} + [a_{P2}\bar{n}_{P2} - \rho_{P2}\bar{n}_{\lambda 2}] \times [F_{23}\bar{n}_{\lambda 2} + \mu s_{2R}F_{23}\bar{n}_{N\lambda 2}]$$

= 0

(H-247)

Equation (H-246) gives the following component expressions

$$F_{23}\cos\lambda_2 - \mu s_{2R}F_{23}\sin\lambda_2 + F_{x3} + \mu F_{y3} + Q_{3P}\cos\gamma_3 = 0 \quad (H-248)$$

and

$$F_{23}\sin\lambda_2 + \mu s_{2R}F_{23}\cos\lambda_2 + F_{y3} - \mu F_{x3} + Q_{3P}\sin\gamma_3 = 0 \quad (H-249)$$

The scalar form of the moment equation (H-247) becomes

$$\begin{aligned} \mu^2(\tilde{F}_{x3} + \tilde{F}_{y3}) + M_{o3} - \mu s_{2R}^2 P_2 F_{23} + s_{P2} F_{23} [-\sin(\psi_2 - \delta_{P2} - \lambda_2)] \\ + \mu s_{2R} \cos(\psi_2 - \delta_{P2} - \lambda_2)] = 0 \end{aligned} \quad (H-250)$$

Simultaneous solution of equations (H-248) and (H-249) for the forces  $F_{x3}$  and  $F_{y3}$  gives

$$\begin{aligned} F_{x3} = \frac{1}{1 + \mu^2} \left\{ F_{23} [\mu(1 + s_{2R}) \sin \lambda_2 + (\mu^2 s_{2R} - 1) \cos \lambda_2] \right. \\ \left. + Q_{3P} [\mu \sin \gamma_3 - \cos \gamma_3] \right\} \end{aligned} \quad (H-251)$$

and

$$\begin{aligned} F_{y3} = \frac{1}{1 + \mu^2} \left\{ F_{23} [(\mu^2 s_{2R} - 1) \sin \lambda_2 - \mu(1 + s_{2R}) \cos \lambda_2] \right. \\ \left. + Q_{3P} [-\sin \gamma_3 - \mu \cos \gamma_3] \right\} \end{aligned} \quad (H-252)$$

The sum  $\tilde{F}_{x3} + \tilde{F}_{y3}$  of equation (H-250) is now made up from equations (H-251) and (H-252) in the sense of equation (A-3b)

$$\tilde{F}_{x3} + \tilde{F}_{y3} = F_{23}A_{65} + Q_{3P}A_{66} + F_{23}A_{67} + Q_{3P}A_{68} \quad (\text{H-253})$$

where

$$A_{65} = \left| \frac{\mu(1 + s_{2R})\sin\lambda_2 + (\mu^2 s_{2R} - 1)\cos\lambda_2}{1 + \mu^2} \right| \quad (\text{H-254})$$

$$A_{66} = \left| \frac{\mu\sin\gamma_3 - \cos\gamma_3}{1 + \mu^2} \right| \quad (\text{H-255})$$

$$A_{67} = \left| \frac{(\mu^2 s_{2R} - 1)\sin\lambda_2 - \mu(1 + s_{2R})\cos\lambda_2}{1 + \mu^2} \right| \quad (\text{H-256})$$

$$A_{68} = \left| \frac{-\sin\gamma_3 - \mu\cos\gamma_3}{1 + \mu^2} \right| \quad (\text{H-257})$$

Equation (H-253) is now substituted into the moment equation (H-250) and the result is solved for  $F_{23}$

$$F_{23} = \frac{-M_{03} - Q_{3P}C_{33}}{C_{34}} \quad (\text{H-258})$$

where

$$C_{33} = \mu_{P3}(A_{66} + A_{68})$$

$$C_{34} = \mu_{P3}(A_{65} + A_{67}) - \mu_{S2R}^o p_2$$

$$+ s_{P2} [\mu_{S2R} \cos(\psi_2 - \delta_{P2} - \lambda_2) - \sin(\psi_2 - \delta_{P2} - \lambda_2)]$$

## II. MOMENT INPUT-OUTPUT RELATIONSHIP

In the derivation for case 1 of the three step-up gear train it was shown that if one sets equations (H-61) and (H-78) equal to each other, one obtains the following relationship [i.e., equation (H-79)] between force  $F_{23}$  and the input moment  $M_{1n}$ :

$$F_{23} = \frac{-c_8}{c_6 c_{10}} (M_{1n} - q_1 c_9) + q_2 \frac{c_7}{c_6} \quad (\text{H-259})$$

The above expression is now set equal to equation (H-258), and the result is solved for the equilibrant moment  $M_{o31}$  (for case 1: RR)

$$M_{o31} = M_{1n} \frac{c_8 c_{34}}{c_6 c_{10}} - q_1 \frac{c_8 c_9 c_{34}}{c_6 c_{10}} - q_2 \frac{c_7 c_{34}}{c_6} - q_3 p c_{33} \quad (\text{H-260})$$

b. CASE NO. 2: RF

MOMENT INPUT-OUTPUT RELATIONSHIP

The moment equation for the present case, in which mesh no. 1 is in the round on flat phase and mesh no. 2 in the round on round one, may be derived entirely from existing relationships. Equation (H-116) gives an expression for the force  $F_{23}$  in terms of the input moment  $M_{1n}$  and the centrifugal forces  $Q_1$  and  $Q_2$  for the present combination of contacts in both meshes. When this expression, from case no. 2 of the three step-up gear train, is set equal to equation (H-259) of case no. 1 of the two step-up gear train, one obtains for  $M_{o32}$  (case no. 2: RF)

$$M_{o32} = M_{1n} \frac{c_{13}c_{34}}{c_{11}c_{15}} - Q_1 \frac{c_{13}c_{14}c_{34}}{c_{11}c_{15}} - Q_2 \frac{c_{12}c_{34}}{c_{11}} - Q_3Pc_{33}$$

(H-261)

c. CASE NO. 3: FF

For this contact combination, where both meshes no. 1 and no.2 are in the round on flat phase, the relationship between the equilibrant moment  $M_{o3}$  and the normal contact force  $F_{23F}$ , both acting on pinion no. 3, must first be determined. The resulting expression in  $F_{23F}$  can then be set equal to the relationship between  $F_{23F}$  and the input moment  $M_{in}$ , which is given by equation (H-156), and which was derived in conjunction with case no. 3 of the three step-up gear train.

I. FORCE AND MOMENT EQUILIBRIA OF PINION NO. 3

Figure H-14 shows the free body diagram of pinion no. 3 in the round on flat phase of contact. Again, the equilibrant moment  $M_{o3}$  acts in a counter-clockwise direction. The normal force  $F_{23F}$  of gear no. 2 on pinion no. 3 is given by

$$\bar{F}_{23F} = - F_{23F} \bar{n}_{NF2} \quad (H-262)$$



The associated friction force of gear no. 2 on pinion no. 3 becomes

$$\vec{F}_{f23F} = \mu_{s2F} F_{23F} \vec{n}_{F2} \quad (H-263)$$

The pivot reactions and pivot friction forces are chosen in the usual manner. The centrifugal force  $\vec{Q}_{3P}$  was given previously by equation (H-244).

The force equilibrium expression becomes

$$-F_{23F} \vec{n}_{NF2} + \mu_{s2F} F_{23F} \vec{n}_{F2} + F_{x3} \vec{i} + \mu_{Fy3} \vec{i} + F_{y3} \vec{j} - \mu_{Fx3} \vec{j} + \vec{Q}_{3P} = 0 \quad (H-264)$$

Moment equilibrium about point  $O_3$  is assured by

$$\mu_{P3} (\vec{F}_{x3} + \vec{F}_{y3}) \vec{k} + M_{O3} \vec{k} + r_2 \vec{n}_{F2} \times (-) F_{23F} \vec{n}_{NF2} = 0 \quad (H-265)$$

As always before, the friction force  $F_{f23F}$  exerts no moment about point  $O_3$ .

Equation (H-264) gives the following component expressions

$$F_{23F} \sin(\psi_2 + \alpha_{P2}) + \mu s_{2F} F_{23F} \cos(\psi_2 + \alpha_{P2}) + F_{x3} + \mu F_{y3} + Q_{3P} \cos \gamma_3 = 0 \quad (\text{H-266})$$

and

$$-F_{23F} \cos(\psi_2 + \alpha_{P2}) + \mu s_{2F} F_{23F} \sin(\psi_2 + \alpha_{P2}) + F_{y3} - \mu F_{x3} + Q_{3P} \sin \gamma_3 = 0 \quad (\text{H-267})$$

The scalar form of the moment equation (H-265) is given by

$$\mu p_3 (\tilde{F}_{x3} + \tilde{F}_{y3}) + M_{o3} - s_2 F_{23F} = 0 \quad (\text{H-268})$$

Simultaneous solution of equations (H-266) and (H-267) for  $F_{x3}$

and  $F_{y3}$  leads to

$$F_{x3} = \frac{1}{1 + \mu^2} \left\{ F_{23F} [(\mu^2 s_{2F} - 1) \sin(\psi_2 + \alpha_{P2}) - \mu(1 + s_{2F}) \cos(\psi_2 + \alpha_{P2})] + Q_{3P} [\mu \sin \gamma_3 - \cos \gamma_3] \right\} \quad (\text{H-269})$$

$$F_{y3} = \frac{1}{1 + \mu^2} \left\{ F_{23F} \left[ -\mu(1 + s_{2F}) \sin(\psi_2 + \alpha_{P2}) + (1 - \mu^2 s_{2F}) \cos(\psi_2 + \alpha_{P2}) \right] + Q_{3P} \left[ -\sin \gamma_3 - \mu \cos \gamma_3 \right] \right\} \quad (H-270)$$

The sum  $\tilde{F}_{x3} + \tilde{F}_{y3}$  of equation (H-268) is now made up of equations (H-269) and (H-270) in the sense of equation (A-3b)

$$\tilde{F}_{x3} + \tilde{F}_{y3} = F_{23F} A_{69} + Q_{3P} A_{70} + F_{23F} A_{71} + Q_{3P} A_{72} \quad (H-271)$$

where

$$A_{69} = \left| \frac{(\mu^2 s_{2F} - 1) \sin(\psi_2 + \alpha_{P2}) - \mu(1 + s_{2F}) \cos(\psi_2 + \alpha_{P2})}{1 + \mu^2} \right| \quad (H-272)$$

$$A_{70} = \left| \frac{\mu \sin \gamma_3 - \cos \gamma_3}{1 + \mu^2} \right| \quad (H-273)$$

$$A_{71} = \left| \frac{-\mu(1 + s_{2F}) \sin(\psi_2 + \alpha_{P2}) + (1 - \mu^2 s_{2F}) \cos(\psi_2 + \alpha_{P2})}{1 + \mu^2} \right| \quad (H-274)$$

$$A_{72} = \left| \frac{-\sin \gamma_3 - \mu \cos \gamma_3}{1 + \mu^2} \right| \quad (H-275)$$

Equation (H-271) is now substituted into the moment equation (H-268), and the result is solved for  $F_{23F}$

$$F_{23F} = \frac{-M_{03} - Q_{3P}C_{35}}{C_{36}} \quad (H-276)$$

where

$$C_{35} = \mu P_3(A_{70} + A_{72})$$

$$C_{36} = \mu P_3(A_{69} + A_{71}) - S_2$$

## II. MOMENT INPUT-OUTPUT RELATIONSHIP

The moment input-output relationship for the present case is obtained, as stated earlier, by setting equation (H-276) equal to equation (H-156) and solving the resulting expression for the equilibrant moment  $M_{033}$  (case no. 3: FF)

$$M_{033} = M_{1n} \frac{C_{21}C_{36}}{C_{15}C_{19}} - Q_1 \frac{C_{14}C_{21}C_{36}}{C_{15}C_{19}} - Q_2 \frac{C_{20}C_{36}}{C_{19}} - Q_{3P}C_{35} \quad (H-277)$$

d. CASE NO. 4: FR

MOMENT INPUT-OUTPUT RELATIONSHIP

The moment input-output relationship for this case, where mesh no. 1 is in round on round contact while mesh no. 2 is in the round on flat phase, may also be derived entirely by assembling existing relationships.

Equation (H-276), of the previous section, gives force  $F_{23F}$  in terms of the equilibrant moment  $M_{o3}$  when mesh no. 2 is in the round on flat phase. Equation (H-178), derived for case no. 4 (RFR) of the three step-up gear train, relates this force  $F_{23F}$  to the input moment  $M_{in}$ .

Thus, one first sets equations (H-178) and (H-276) equal to each other and then solves the result for  $M_{o34}$  (case 4: FR)

$$M_{o34} = M_{in} \frac{C_{24}C_{36}}{C_{10}C_{22}} - Q_1 \frac{C_9C_{24}C_{36}}{C_{10}C_{22}} - Q_2 \frac{C_{23}C_{36}}{C_{22}} - Q_{3P}C_{35}$$

(H-278)

APPENDIX I  
COMPUTER MODELS FOR THREE AND TWO STEP-UP GEAR TRAINS  
WITH CLOCK TEETH OPERATING IN A SPIN ENVIRONMENT

The following appendix contains descriptions, listings and sample outputs of the computer models relating to step-up gear trains containing clock (ogival) gear teeth:

1. Program CLOCK 3: Point and cycle efficiencies for three pass clock (ogival) step-up gear train in spin environment.
2. Program CLOCK 4: Point and cycle efficiencies for two pass clock (ogival) step-up gear train in spin environment.

The relevant background, the input parameters, the manner of the computations and the form of the output of each program are discussed in detail. The program proper forms the last part of each section.

1. Program CLOCK 3: Point and Cycle Efficiencies for Three  
Pass Clock (Ogival) Step-Up Gear Train  
in Spin Environment

The kinematics of program CLOCK 3 is based on the work in Appendix G, while the moment input-output relationships are derived in section 1 of Appendix H. The nomenclature of the program is chosen to coincide as much as possible with the above appendices. It is to be noted that, even though the fuze related geometry produces different expressions for the various meshes, the kinematic computations of the individual meshes are very similar to those shown in CLOCK 1 in Appendix F for the single mesh in the standard position. It is also assumed that all three meshes will have been tested by program CLOCK 1 for their geometric suitability, i.e. whether there is enough room for tip radii.

a. Input Parameters (see Program CLOCK 3, below)

The following parameters represent the input data for the program (for explanations and nomenclature, see sections 1 and 2 of Appendix F, as well as section 3 of Appendix C):

MU, coefficient of friction, as before

RPM, spin velocity

CAPRP1, CAPRP2, CAPRP3, RP2, RP3, RP4, pitch radii of gears and  
pinions with nomenclature  
of Fig. G-1

RHOG1, RHOG2, RHOG3, RHOP1, RHOP2, RHOP3, radii of curvature of circu-  
lar arc portion of gear and  
pinion teeth

ACG1, ACG2, ACG3\* =  $a_{CG_1}$ , distance from the center of rotation of the gear of the 1<sup>th</sup> mesh to the center of curvature of the circular arc portion of the gear tooth. (Unless otherwise noted, this and all following numbering schemes refer to those associated with the mesh mechanics as given in the text of Appendices G and H.)

ACP1, ACP2, ACP3 =  $a_{CP_1}$ , distance from the center of rotation of the pinion of the 1<sup>th</sup> mesh to the center of curvature of the circular arc portion of the pinion tooth

R1, R2, R3, R4 =  $R_1$  (nomenclature of Fig. G-1)

TG1, TG2, TG3, TP1, TP2, TP3, maximum thickness of gear and pinion teeth (mesh nomenclature)

NG1, NG2, NG3, NP2, NP3, NP4, numbers of teeth in various gears and pinions (nomenclature of Fig. G-1)

RHO1, RHO2, RHO3, RHO4, gear and/or pinion pivot radii (nomenclature of Fig. G-1)

M1, M2, M3, M4, masses of gear and/or pinion combinations

MD, see program INVOL 3

---

\*Since many parts of the computer program were written before the nomenclature for these distances was changed in the report from  $a_{CG_1}$  and  $a_{CP_1}$  to  $a_{G_1}$  and  $a_{P_1}$ , there is a certain discrepancy between the program and the report.

K. range divisor

PHDOT1 = -1, all velocity computations are based on this value.

The input motion in the fuze gearing model is negative (see Fig. (G-1)).

b. Computations (see also COMMENT cards in program)

I. Computation of Gear Tooth Parameters

The tooth parameters of the gears and pinions of all three meshes are first computed. These computations are essentially the same as those shown in program CLOCK 1 for a single mesh. Certain parameters are omitted because they have been checked separately by using CLOCK 1 and are not required for the kinematics of CLOCK 3.

In addition, the pivot to pivot distances B1, B2 and B3 are obtained.

II. Computation of MIN, GAMMAS and BETAS

To begin with, the program computes the input moment

$$\text{MIN} = M_{in} = md\omega^2 \quad (\text{I-1})$$

Subsequently, the angles  $\gamma_2$ ,  $\gamma_3$ ,  $\gamma_4$  and  $\beta_1$ ,  $\beta_2$ ,  $\beta_3$  are established according to the expressions of section 6b of Appendix A.

III. Computation of Other Parameters

The angles  $\Delta\phi_1$  and  $\Delta\psi_1$  between the centerlines of adjacent gear and pinion teeth, respectively, are determined in this

section of the computations. In addition, the lengths  $L_1$  are found (see eqs. (G-7), (G-53) and (G-88)). Finally, the centrifugal forces  $Q_1$ ,  $Q_2$ ,  $Q_3$  and  $Q_4$  are computed according to eqs. (H-65), (H-46), (H-25) and (H-6), respectively.

#### IV. Preliminary Computations for Mesh 1

##### A. Determination of Transition Angle

The primary consideration for determining the transition angles in the fuze related clock gear meshes is identical with that used in Appendix F. The transition angle  $\psi_T$  is established as that angle for which, depending upon whether the input angle  $\varphi$  has counterclockwise or clockwise motion, a small increase or decrease in  $\varphi$ , respectively, will cause the associated value of  $g$  to become smaller than its transition value  $f_p$ . Since the gear of mesh 1 turns in a clockwise direction, the above increment of  $\varphi$  will be negative.

The program uses this criterion in the following manner:

(a) Transition angles  $\psi_{1T1}$  and  $\psi_{1T2}$  are computed according to eq. (G-39).

(b) The subroutine TRANS1 (which is valid for meshes in which the input gear has clockwise rotation, as is the case also for mesh 3) is called, and the angle  $\varphi_{1T1}$  (PHIT), which is associated with  $\psi_{1T1}$ , is computed with the help of eqs. (G-40) and (G-41).

(c) The angle  $\varphi$  is made slightly smaller than  $\varphi_{1T1}$  to produce the angle PHINEXT, and eq. (G-29) is used to find the associated angle PSINEX. Since there are two such angles, the

subroutine selects the one which is closest in value to the transition angle  $\psi_{1T1}$ . Subsequently, the associated value of  $g_{11}$  is computed according to eq. (G-27).

(d) Steps (b) and (c) are then repeated identically for the second transition angle  $\psi_{1T2}$ . This results in the determination of  $g_{12}$ .

(e) Control returns to the main program, and that value of  $\psi_{1T}$  is chosen for which the associated value of  $g_1$  is smaller than  $f_{p1}$ .

For checking, a subsidiary test, which is similar to the one shown in Appendix F, is added to the program. It is based on the idea that, for the correct transition angle  $\psi_{1T}$ , the line representing the flat portion of the pinion will make a smaller angle with the centerline  $O_1O_2$  than will be the case for the incorrect one. TEST11 and TEST12 find these angles with the help of the expressions shown below. These expressions hold for all values of  $\beta_1$  and make use of a new variable  $\psi_{test}$ , which had to be introduced since the tests require that the transition angles be expressed in a range between  $-180^\circ$  and  $+180^\circ$ . Thus,

For  $0^\circ < \psi_{test} < 180^\circ$

$$\text{TEST11} = |\pi - \beta_1 + \psi_{test} - \alpha_{p1}| \quad (\text{I-2})$$

For  $-180^\circ < \psi_{test} < 0^\circ$

$$\text{TEST12} = |\pi + \beta_1 - (\psi_{test} + 2\pi - \alpha_{p1})| \quad (\text{I-3})$$

To determine the angle  $\psi_{\text{test}}$ , let

$$\psi_{\text{test}} = \psi_{1T} \text{ if } -180^\circ < \psi_{1T} < 180^\circ \quad (\text{I-4})$$

$$\psi_{\text{test}} = \psi_{1T} + 2\pi \text{ if } \psi_{1T} < -180^\circ \quad (\text{I-5})$$

$$\psi_{\text{test}} = \psi_{1T} - 2\pi \text{ if } \psi_{1T} > 180^\circ \quad (\text{I-6})$$

B. Determination of Correct Sign for Round on Flat Regime

The sign preceding the square root in eq. (G-29), for the round on flat regime, is determined with the help of  $\varphi_{1T}$ . The condition yielding that angle  $\psi_{1F}$  which is closest to the angle  $\psi_{1T}$  governs. The variable SIGNIF is used for the sign in question.

C. Computation of Final and Initial Values of  $\varphi_1$  and  $\psi_1$

The final and initial values of the gear and pinion angles  $\varphi_1$  and  $\psi_1$ , respectively, are found by continuously evaluating the round on flat regime eq. (G-29), using the previously determined value of SIGNIF, and simultaneously checking the contact condition for the subsequent set of teeth as given by eq. (G-46). This loop is initiated at the transition angle  $\varphi_{1T}$ , and it is terminated when the condition of eq. (G-46) is met. This allows the determination of the angles PHILF and PSILFF, at which the first set of teeth loses contact, as well as of the angles PHILI and PSILI at which the second set of teeth simultaneously comes into engagement. The initial engagement angles PHILI and PSILI are obtained by adding  $\varphi_1$  to the "loss of contact" angle PHILF

and by subtracting  $\Delta\psi_1$  from the "loss of contact" angle  $\text{PSI1FF}$ .

D. Determination of Correct Sign for Round on Round Regime

Eq. (G-12) is used to determine the angle  $\psi_1$ , while the gear and pinion are in the round on round regime. The correct sign for this expression is obtained by comparing the value  $\psi_1$ , as computed with  $\text{PHI1I}$ , with the value for  $\text{PSI1I}$ .  $\text{SIGN1R}$  is the variable used for the desired sign.

V. Preliminary Computations for Mesh 2

A. Determination of Transition Angle

The primary criterion for determining the transition angle is again similar to that used in Appendix F and described earlier for mesh 1.

(a) Transition angles  $\psi_{2T1}$  and  $\psi_{2T2}$  are computed according to eq. (G-79).

(b) The subroutine  $\text{TRANS2}$ , which is valid for meshes in which the input gear has counterclockwise rotation, is called, and the angle  $\varphi_{2T1}$ , which is associated with  $\psi_{2T1}$  is computed, with the help of eqs. (G-80) and (G-81).

(c) The angle  $\varphi_2$  is made slightly larger than  $\varphi_{2T1}$  to produce the angle  $\text{PHINEXT}$ , and eq. (G-71) is used to find the associated output angle  $\text{PSINEX}$ . Since there are two such angles, the subroutine selects the one which is closest to the transition value  $\psi_{2T1}$ . Subsequently, the associated value of  $\text{S21}$  is computed according to eq. (G-69).

(d) Steps (b) and (c) are then repeated identically for the second transition angle  $\psi_{2T2}$ . This results in the determination of  $g_{22}$ .

(e) Control returns to the main program, and that value of  $\psi_{2T}$  is chosen for which the associated value of  $g_2$  is smaller than  $f_{p2}$ .

The procedure for the associated subsidiary test for the transition angle is similar to that for mesh 1 and is given by

For  $0^\circ < \psi_{\text{test}} < 180^\circ$

$$\text{TEST21} = |\pi - \beta_2 + \psi_{\text{test}} + \alpha_{p2}| \quad (\text{I-7})$$

For  $-180^\circ < \psi_{\text{test}} < 0^\circ$

$$\text{TEST22} = |\beta_2 + \pi - (\psi_{\text{test}} + 2\pi + \alpha_{p2})| \quad (\text{I-8})$$

To determine the angle  $\psi_{\text{test}}$ , let

$$\psi_{\text{test}} = \psi_{2T} \quad \text{if} \quad -180^\circ < \psi_{2T} < 180^\circ \quad (\text{I-9})$$

$$\psi_{\text{test}} = \psi_{2T} + 2\pi \quad \text{if} \quad \psi_{2T} < -180^\circ \quad (\text{I-10})$$

$$\psi_{\text{test}} = \psi_{2T} - 2\pi \quad \text{if} \quad \psi_{2T} > 180^\circ \quad (\text{I-11})$$

#### B. Determination of Correct Sign for Round on Flat Regime

The sign preceding the square root in eq. (G-71), for the round on flat regime, is determined with the help of  $\psi_{2T}$ . The condition yielding that angle  $\psi_{2F}$  which is closest to the angle  $\psi_{2T}$  governs. The variable SIGN2F is used for the sign in question.

C. Computation of Final and Initial Values of  $\varphi_2$  and  $\psi_2$

The final and initial values of the gear and pinion angles  $\varphi_2$  and  $\psi_2$ , respectively, are found by continuously evaluating the round on flat eq. (G-71), using the previously determined value of SIGN2F, and simultaneously checking the contact condition for the subsequent set of teeth, as given by eq. (G-86). This loop is initiated at the transition angle  $\varphi_{2T}$  and is terminated when the condition of eq. (G-86) is met. (Recall that in meshes 1 and 3 the driving gear turns clockwise, while in mesh 2 it turns in a counterclockwise direction.) This allows the determination of the two angles PHI2F and PSI2FF at which the first set of teeth loses contact as well as of the angles PHI2I and PSI2I at which the second set of teeth simultaneously comes into contact. The initial engagement angles PHI2I and PSI2I are obtained by subtracting  $\Delta\varphi_2$  from the "loss of contact" angle PHI2F and by adding  $\Delta\psi_2$  to the "loss of contact" angle PSI2FF.

D. Determination of Correct Sign for Round on Round Regime

Eq. (G-58) is used to determine the angle  $\psi_2$  while the gear and pinion are in the round on round phase of motion. The correct sign for this expression is obtained by comparing the value of  $\psi_2$ , as computed with PHI2I, with the previously obtained value for PSI2I. SIGN2R is the variable used for the desired sign.

## VI. Preliminary Computations for Mesh 3

### A. Determination of Transition Angle

The determination of the transition angles for mesh 3 runs along parallel lines to the one shown for mesh 1 since the driving gear also rotates in a clockwise direction. In all cases, the parameters of section 3 of Appendix G are used.

(a) Transition angles  $\psi_{3T1}$  and  $\psi_{3T2}$  are computed with the help of eq. (G-99).

(b) The subroutine TRANS1 determines the angle  $\psi_{3T1}$ , associated with  $\psi_{3T1}$ , according to eqs. (G-100) and (G-101).

(c) PHINEXT, which is now obtained by a decrease of the angle  $\psi_3$  from  $\psi_{3T1}$ , serves as the input variable of eq. (G-94), and is used to determine PSINEX. Appropriate controls, as described before, determine the angle  $\psi_{3T1}$ . In addition, the associated value of  $g_{31}$  is computed with the help of eq. (G-95).

(d) Steps (b) and (c) are again repeated for the second transition angle  $\psi_{3T2}$  and  $g_{32}$  is determined.

(e) After control is returned to the main program, that value of  $\psi_{3T}$  is chosen for which the associated value of  $g_3$  is smaller than  $f_{p3}$ .

The subsidiary test for the transition angles runs parallel to that described for mesh 1, i.e.,

For  $0^\circ < \psi_{\text{test}} < 180^\circ$

$$\text{TEST31} = |\pi - \beta_3 + \psi_{\text{test}} - \alpha_{p3}| \quad (\text{I-12})$$

For  $-180^\circ < \psi_{\text{test}} < 0^\circ$

$$\text{TEST32} = |\pi + \beta_3 - (\psi_{\text{test}} + 2\pi - \alpha_{P3})| \quad (\text{I-13})$$

To determine the angle  $\psi_{\text{test}}$ , let

$$\psi_{\text{test}} = \psi_{3T} \quad \text{if} \quad -180^\circ < \psi_{3T} < 180^\circ \quad (\text{I-14})$$

$$\psi_{\text{test}} = \psi_{3T} + 2\pi \quad \text{if} \quad \psi_{3T} < -180^\circ \quad (\text{I-15})$$

$$\psi_{\text{test}} = \psi_{3T} - 2\pi \quad \text{if} \quad \psi_{3T} > 180^\circ \quad (\text{I-16})$$

#### B. Determination of Correct Sign for Round on Flat Regime

The sign preceding the square root in eq. (G-94), for the round on flat regime, is determined with the help of the angle  $\varphi_{3T}$ . The condition yielding that angle  $\psi_{3F}$  which is closest to the angle  $\psi_{3T}$  will govern. The variable SIGN3F is used for the sign in question.

#### C. Computation of Final and Initial Values of $\varphi_3$ and $\psi_3$

The final and initial values of the gear and pinion angles  $\varphi_3$  and  $\psi_3$ , respectively, are found by continuously evaluating the round on flat regime eq. (G-94), using the previously determined value of SIGN3F, and simultaneously checking the contact condition for the subsequent set of teeth, as given by eq. (G-102). This loop is initiated at the transition angle  $\varphi_{3T}$ , and it is terminated when the condition of eq. (G-102) is met. This allows the determination of the two angles PHI3F and PSI3FF at which the first set of teeth loses contact as well

as the angles  $\text{PHI3I}$  and  $\text{PSI3I}$  at which the second set of teeth simultaneously comes into contact. The initial engagement angles  $\text{PHI3I}$  and  $\text{PSI3I}$  are obtained by adding  $\Delta\psi_3$  to the "loss of contact" angle  $\text{PHI3F}$  and by subtracting  $\Delta\psi_3$  from the "loss of contact" angle  $\text{PSI3FF}$ .

D. Determination of Correct Sign for Round on Round Regime

Eq. (G-87) is used to determine the angle  $\psi_3$  while the gear and pinion are in the round on round phase of motion. The correct sign for this expression is obtained by comparing the value of  $\psi_3$ , as computed with  $\text{PHI3I}$ , with the previously obtained value for  $\text{PSI3I}$ .  $\text{SIGN3R}$  is the variable used for the desired sign.

VII. Gear Train Motion Model: Kinematics, Point and Cycle Efficiency

The simulation of the gear train model, which is necessary for the computation of both  $\text{POINTEF}$  and  $\text{CYCLEFF}$ , is found in a loop, starting with statement label no. 29 (card no. 458) and ending with card no. 812. The motions of the individual driving gears are initialized at their respective angles  $\text{PHI1I}$ ,  $\text{PHI2I}$  and  $\text{PHI3I}$ . (This again is arbitrary.) The meshes will be in round on round contact until they reach their respective transition angles  $\text{PHI1T}$ ,  $\text{PHI2T}$  and  $\text{PHI3T}$ . Once the transition angles are passed, the meshes will be in round on flat contact. These regimes continue until the final angles  $\text{PHI1F}$ ,  $\text{PHI2F}$  and  $\text{PHI3F}$  are reached.

The increment  $\text{DDPHI1}$  of the angle  $\text{PHI1}$  of the input gear 1

is obtained from an adaptation of eqs. (A-211) and (A-213), in which tooth numbers, rather than base circle radii, are used. The increment  $DDPHI2$  of gear 2 is related to the increment of the pinion angle  $PSI1$ . Similarly, the increment  $DDPHI3$  is obtained with the help of the pinion angle  $PSI2$ .

While the motion of gear 1 is terminated when the angle  $PHI1$  reaches the angle  $PHI1F$  (or rather  $PHI1F + DDPHI1$  for moment summation purposes), both gears 2 and 3 must be reset to their respective starting angles whenever their final angles  $PHI2F$  and  $PHI3F$  are reached.

The appropriate choice of moment equation depends upon which of the eight possible combinations of contact conditions, as indicated by Table H-1, is applicable.

The following discusses the kinematics of the individual meshes as well as the determination of the point and cycle efficiencies in greater detail.

#### A. Kinematics

##### (1) Mesh 1

Depending on whether  $PHI1$  is larger or smaller than  $PHI1T$ , the parameters of the round on round or the round on flat regime are computed. (Recall that gear 1 turns in a clockwise direction.)

For the round on round phase, the following calculations are made:

- $\psi_1$ , according to eq. (G-11), and with the help of the previously determined SIGN1R
- $\lambda_1$ , according to eqs. (G-13) and (G-14)
- $\dot{\psi}_1$ , according to eq. (G-15)
- $V_{S1/T1R}$ , according to eq. (G-20)
- $s_{1R}$ , according to eq. (H-1) as adapted to mesh 1

For the round on flat phase, the following calculations are made:

- $\psi_1$ , according to eq. (G-29), and with the help of the previously determined SIGN1F
- $s_1$ , according to eq. (G-27)
- $\dot{\psi}_1$ , according to eq. (G-30)
- $V_{S1/T1F}$ , according to eq. (G-33)
- $s_{1F}$ , according to eq. (H-2) as adapted to mesh 1

(2) Mesh 2

The increment DDPHI2 for each round of computation is obtained with the help of the change in the angle  $\psi_1$  between the present and the previous computation, i.e., as shown at statement label no. 31

$$DDPHI2 = PSI1 - PSI1P \quad (I-17)$$

For the first round of computations, the "previous"  $\psi_1$ , i.e., PSI1P, is equal to PSI1I.

It must be recalled that gear 2 rotates in a positive direction, and therefore, the angle  $\phi_2$  increases with continued

motion. The angle PHI2 is re-indexed to PHI2I once it becomes larger than PHI2F.

As for mesh 1, comparison with the transition angle decides whether the mesh is in the round on round or in the round on flat regime.

The following round on round parameters are calculated:

- $\psi_2$ , according to eq. (G-58), and with the help of the previously determined SIGN2R
- $\lambda_2$ , according to eqs. (G-59) and (G-60)

Note that the "input angular velocity" for mesh 2, i.e.,  $\dot{\phi}_2$ , equals the momentary value of  $\dot{\psi}_1$ .

- $\dot{\phi}_2$ , according to eq. (G-61)
- $V_{S2/T2R}$ , according to eq. (G-63)
- $s_{2R}$ , according to eq. (H-1) as adapted to mesh 2

For the round on flat phase, the following calculations are made:

- $\psi_2$ , according to eq. (G-71), and with the help of the previously determined SIGN2F
- $g_2$ , according to eq. (G-69)

Again,  $\dot{\phi}_2$  equals the momentary value of  $\dot{\psi}_1$

- $\dot{\phi}_2$ , according to eq. (G-72)
- $V_{S2/T2F}$ , according to eq. (G-74)
- $s_{2F}$ , according to eq. (H-2) as adapted to mesh 2

(3) Mesh 3

The increment DDPHI3, for each round of computation, is obtained with the help of the change in the angle  $\psi_2$  between the present and the previous computation, i.e., as shown at statement label no. 33:

$$\text{DDPHI3} = \text{PSI2} - \text{PSI2P} \quad (\text{I-18})$$

For the first round of computations, the "previous"  $\psi_2$ , i.e., PSI2P, is equal to PSI2I.

Gear 3 rotates in a negative (clockwise) direction, and therefore, the angle  $\varphi_3$  decreases with continued rotation. The angle PHI3, which represents this angle, is re-indexed to PHI3I once it becomes smaller than PHI3F.

As for meshes 1 and 2, comparison with the applicable transition angle decides whether the mesh is in the round on round or in the round on flat regime.

The following round on round parameters are calculated:

- $\psi_3$ , according to eq. (G-87), and with the help of the previously determined SIGN3R
- $\lambda_3$ , according to eqs. (G-89) and (G-90)

Note that the "input angular velocity" for mesh 3, i.e.,  $\dot{\psi}_3$ , equals the momentary value of  $\dot{\psi}_2$ .

- $\dot{\psi}_3$ , according to eq. (G-91)
- $V_{S3/T3R}$ , according to eq. (G-92)
- $s_{3R}$ , according to eq. (H-1) as adapted to mesh 3

For the round on flat phase, the following calculations are made:

$\psi_3$ , according to eq. (G-94), and with the help of the previously determined SIGN3F

$\xi_3$ , according to eq. (G-95)

Again,  $\dot{\phi}_3$  is equal to the momentary value of  $\dot{\psi}_2$ .

$\dot{\psi}_3$ , according to eq. (G-96)

$V_{S3/T3F}$ , according to eq. (G-97)

$s_{3F}$ , according to eq. (H-2) as adapted to mesh 3

#### B. Moment Computations, Point and Cycle Efficiencies

Regardless of the combination of contact conditions, the point efficiency is computed according to eq. (3), i.e.,

$$\epsilon_p = \text{POINTEF} = K_{\text{ratio}} \frac{M_{o41}}{M_{1n}} \quad (\text{I-19})$$

where, with  $\dot{\phi}_1 = -1$ ,

$$K_{\text{ratio}} = |\dot{\psi}_3| \quad (\text{I-20})$$

The cycle efficiency determination is based on eq. (C-10) in Appendix C, which represents an adaptation of eq. (4):

$$\epsilon_c = \frac{\Delta\phi_1 \Sigma \epsilon_p}{\phi_{1FIN} - \phi_{1IN}} \quad (\text{I-21})$$

(See page C-18.) The associated expression in the program, at statement label no. 45 becomes

$$\text{CYCLEPF} = -\text{MTOT} * \text{DDPHI1} / (\text{PHI1F} - \text{PHI1I}) \quad (\text{I-22})$$

where

$$\text{MTOT} = \text{MTOT} + \text{POINTEF} \quad (\text{I-23})$$

The moment computations begin with the statement label no. 35 ,and initially consist of the determination of the variables A1 to A64 and C1 to C32 of section 1 of Appendix H. The governing contact combination (see also Table H-1) is determined with the help of the 8 moment control statements, which start with card no.737 . Once the appropriate combination is established, the program is directed to one of the 8 associated moment expressions. These expressions for  $M_{041}$  coincide in nomenclature with those given by eqs. (H-81), (H-118), (H-158), (H-180), (H-216), (H-218), (H-239) and (H-241). They are listed in the above order, beginning with statement label no. 36 and ending with statement label no. 43 .

In devising the control statements, the manner of rotation of the individual mesh input gears had to be taken into account. Thus:

For mesh 3:

Round on round (R) corresponds to

$$\text{PHI3I} > \text{PHI3} > \text{PHI3T}$$

Round on flat (F) corresponds to

$$\text{PHI3T} > \text{PHI3} > \text{PHI3F}$$

For mesh 2:

Round on round (R) corresponds to

$\text{PHI2I} < \text{PHI2} < \text{PHI2T}$

Round on flat (F) corresponds to

$\text{PHI2T} < \text{PHI2} < \text{PHI2F}$

For mesh 1:

Round on round (R) corresponds to

$\text{PHI1I} > \text{PHI1} > \text{PHI1T}$

Round on flat (F) corresponds to

$\text{PHI1T} > \text{PHI1} > \text{PHI1F}$

c. Output (see Program CLOCK 3, below)

The output of the program is best explained with the help of the sample problem at the end of the program.

I. Input Parameters

Mesh 1

$\text{CAPRP1} = R_{p1} = .47725 \text{ in. (1.212 cm)}$

$\text{RP2} = r_{p2} = .09085 \text{ in. (0.231 cm)}$

$\text{ACG1} = a_{G1} = .47725 \text{ in. (1.212 cm)}$

$\text{ACP1} = a_{p1} = .09085 \text{ in. (0.231 cm)}$

$\text{RHOG1} = r_{G1} = .03870 \text{ in. (0.098 cm)}$

$\text{RHOP1} = r_{p1} = .01740 \text{ in. (0.044 cm)}$

$\text{TG1} = t_{G1} = .03480 \text{ in. (0.088 cm)}$

$\text{TP1} = t_{p1} = .02800 \text{ in. (0.071 cm)}$

$\text{NG1} = n_{G1} = 42$

$\text{NP2} = n_{p2} = 8$

### Mesh 2

CAPRP2 =  $R_{P2}$  = .20670 in. (0.525 cm)  
RP3 =  $r_{P3}$  = .06890 in. (0.175 cm)  
ACG2 =  $a_{G2}$  = .20670 in. (0.525 cm)  
ACP2 =  $a_{P2}$  = .06890 in. (0.175 cm)  
RHOG2 =  $r_{G2}$  = .02070 in. (0.053 cm)  
RHOP2 =  $r_{P2}$  = .01040 in. (0.026 cm)  
TG2 =  $t_{G2}$  = .02520 in. (0.064 cm)  
TP2 =  $t_{P2}$  = .02080 in. (0.053 cm)  
NG2 =  $n_{G2}$  = 27  
NP3 =  $n_{P3}$  = 9

### Mesh 3

CAPRP3 =  $R_{P3}$  = .17560 in. (0.446 cm)  
RP4 =  $r_{P4}$  = .05905 in. (0.150 cm)  
ACG3 =  $a_{G3}$  = .17560 in. (0.446 cm)  
ACP3 =  $a_{P3}$  = .05905 in. (0.150 cm)  
RHOG3 =  $r_{G3}$  = .01910 in. (0.049 cm)  
RHOP3 =  $r_{P3}$  = .00875 in. (0.022 cm)  
TG3 =  $t_{G3}$  = .02170 in. (0.055 cm)  
TP3 =  $t_{P3}$  = .01750 in. (0.044 cm)  
NG3 =  $n_{G3}$  = 27  
NP4 =  $n_{P4}$  = 9

### In addition

MU =  $\mu$  = .2  
RPM = 1000  
M1 =  $m_1$  =  $.69515 \times 10^{-4}$  lb-sec<sup>2</sup>/in. (12.171 g)

$M_2 = m_2 = .97028 \times 10^{-5} \text{ lb-sec}^2/\text{in.} (1.699 \text{ g})$   
 $M_3 = m_3 = .70027 \times 10^{-5} \text{ lb-sec}^2/\text{in.} (1.226 \text{ g})$   
 $M_4 = m_4 = .79188 \times 10^{-6} \text{ lb-sec}^2/\text{in.} (0.139 \text{ g})$   
 $R_1 = R_1 = .750 \text{ in.} (1.905 \text{ cm})$   
 $R_2 = R_2 = .750 \text{ in.} (1.905 \text{ cm})$   
 $R_3 = R_3 = .750 \text{ in.} (1.905 \text{ cm})$   
 $R_4 = R_4 = .750 \text{ in.} (1.905 \text{ cm})$   
 $RHO_1 = P_1 = .060 \text{ in.} (0.152 \text{ cm})$   
 $RHO_2 = P_2 = .030 \text{ in.} (0.076 \text{ cm})$   
 $RHO_3 = P_3 = .025 \text{ in.} (0.064 \text{ cm})$   
 $RHO_4 = P_4 = .020 \text{ in.} (0.051 \text{ cm})$   
 $MD = md^2 = .15 \times 10^{-4} \text{ lb-sec}^2 \text{ in.} (16.944 \text{ g - cm}^2)$   
 $K = 25$

## II. Computed Values

At the beginning of the output, one finds  $MIN = M_{in}$ .

Subsequently, the following are listed for each mesh:

$f_{P_1}$ , the length of the pinion flats

$\beta_1$ , the fuse body pivot to pivot line angles

$\psi_{T_1}$  and  $\phi_{T_1}$ , the transition angles as well as the associated subsidiary tests

$\phi_{IN_1}$  and  $\psi_{IN_1}$ , the initial angles

$\phi_{FIN_1}$  and  $\psi_{FIN_1}$ , the final angles

Finally, for the full range of the input angle  $\phi_1$ , the point efficiency  $POINTEF$  is listed, in addition to other parameters which are useful for checking purposes. Note that  $DPSI_1$ ,  $DPSI_2$

and DPSI3 represent  $\dot{\psi}_1$ ,  $\dot{\psi}_2$  and  $\dot{\psi}_3$ , respectively. The cycle efficiency CYCLEFF is found at the end of the output.

Program CLOCK 3

```

1      PROGRAM CLOCKS3(INPUT,OUTPUT,TAPES=INPUT,TAPE6=OUTPUT)
C
C      POINT AND CYCLE EFFICIENCIES FOR THREE PASS CLOCK (OGIVAL) STEP UP
C      GEAR TRAIN IN SPIN ENVIRONMENT
5
REAL MU,LANDA1,LANDA2,LANDA3,MO4,MO41,MO42,MO43,MO44,MO45,MO46,MO4
17,MO48,LX1,LY1,LT,LX2,LY2,L2,L3,L3,LY3,L3,RP2,RP3,RP4,NG1,NG2,NG3,NI
24,NI,NI2,NI3,NI4,NIOT,MO,LL1,LL2,LL3,K
1 READ (5,61) MU,ROM,CAPRP1,CAPRP2,CAPRP3,RP2,RP3,RP4,ACG1,ACG2,ACG3
1,ACP1,ACP2,ACP3,ISTOP
10 READ (5,62) R1,R2,R3,R4
READ (5,62) RHOG1,RHOG2,RHOG3,RHOP1,RHOP2,RHOP3
READ (5,63) TG1,TG2,TG3,TP1,TP2,TP3
READ (5,64) NG1,NG2,NG3,MP2,MP3,MP4
15 READ (5,65) NI,NI2,NI3,NI4
READ (5,65) RH01,RH02,RH03,RH04,MO,K
PI=3.14159
Z=PI/180.
OMEGA=RPM*2.*PI/60.
OM2=OMEGA*OMEGA
PH001=-1.
C
C      COMPUTATION OF GEAR TOOTH PARAMETERS
C
C
25      CKG1=RHOG1-TG1/2.
DELG1=ASIN(CKG1/CAPRP1)
CXP1=RHOP1-TP1/2.
DELP1=ASIN(CXP1/RP2)
GAMP1=ASIN(RHOP1/RP2)
ALPH1=GAMP1-DELP1
30      FP1=ACP1-COS(GAMP1)
R1=LAPRP1-RP2
CKG2=RHOG2-TG2/2.
DELG2=ASIN(CKG2/CAPRP2)
CXP2=RHOP2-TP2/2.
DELP2=ASIN(CXP2/RP3)
GAMP2=ASIN(RHOP2/RP3)
ALPH2=GAMP2-DELP2
35      FP2=ACP2-COS(GAMP2)
R2=CAPRP2+RP3
CKG3=RHOG3-TG3/2.
DELG3=ASIN(CKG3/CAPRP3)
CXP3=RHOP3-TP3/2.
DELP3=ASIN(CXP3/RP4)
GAMP3=ASIN(RHOP3/RP4)
ALPH3=GAMP3-DELP3
40      FP3=ACP3-COS(GAMP3)
R3=CAPRP3+RP4
C
C      COMPUTATION OF MIN, GAMMAS AND BETAS
C
50      MIN=MO+OM2
52      DELTA2=ACOS(((CAPRP1+RP2)*(CAPRP1+RP2)+R1-R1-R2-R2)/(2.*R1*(CAPRP1
53

```

```

55 1+RP2)))
    DELTA3=ACOS(((CAPRP2+RP3)*(CAPRP2+RP3)+R2-R2-R3+R3)/(2.*R2*(CAPRP2
1+RP2)))
    DELTA4=ACOS(((CAPRP3+RP4)*(CAPRP3+RP4)+R3-R3-R4+R4)/(2.*R3*(CAPRP3
1+RP4)))
60 GAMMA2=ACOS((R1+R1+R2+R2-(CAPRP1+RP2)*(CAPRP1+RP2))/(2.*R1+R2))
    GAMMA3=ACOS((R2+R2+R3+R3-(CAPRP2+RP3)*(CAPRP2+RP3))/(2.*R2+R3))
    GAMMA4=ACOS((R3+R3+R4+R4-(CAPRP3+RP4)*(CAPRP3+RP4))/(2.*R3+R4))
    GAMMA5=ACOS((R4+R4+R5+R5-(CAPRP4+RP5)*(CAPRP4+RP5))/(2.*R4+R5))
65 BETAI=PI-DELTA2
    BETA2=GAMMA2+PI-DELTA3
    BETA3=GAMMA3+PI-DELTA4
    BETAI0=BETAI/Z
    BETA20=BETA2/Z
    BETA30=BETA3/Z
70 WRITE (6.66) MIN,BU,RPM,CAPRP1,CAPRP2,CAPRP3,RP2,RP3,RP4,ACG1,ACG2
    I,ACG3,ACP1,ACP2,ACP3
    WRITE (6.83) R1,R2,R3,R4
    WRITE (6.67) RHOG1,RHOG2,RHOG3,RHOP1,RHOP2,RHOP3
    WRITE (6.68) TGI,TG2,TG3,TP1,TP2,TP3
    WRITE (6.69) MGI,NC2,NC3,MP2,MP3,MP4
    WRITE (6.66) M1,M2,M3,M4
    WRITE (6.70) RHQ1,RHQ2,RHQ3,RHQ4,MD,K,PHOBT1
    WRITE (6.84) FP1,FP2,FP3
    WRITE (6.71) BETA10,BETA20,BETA30
80 COMPUTATION OF OTHER PARAMETERS
    C
    C
    C
    DPH11=360./NG1+Z
    DPS11=360./MP2+Z
    DPH12=360./NG2+Z
    DPS12=360./MP3+Z
    DPH13=360./NG3+Z
    DPS13=360./MP4+Z
    L1=RHOG1+RHOP1
    L2=RHOG2+RHOP2
    L3=RHOG3+RHOP3
    Q1=M1+R1+OM2
    Q2=M2+R2+OM2
    Q3=M3+R3+OM2
    Q4=M4+R4+OM2
95 PRELIMINARY COMPUTATIONS FOR MESH 1
    C
    C
    C
    C
    DETERMINATION OF TRANSITION ANGLE OF MESH 1
    A1T=RHOG1+COS(BETA1+ALPH1)+FP1+SIN(BETA1+ALPH1)
    B1T=RHOG1+SIN(BETA1+ALPH1)+FP1+COS(BETA1+ALPH1)
    C1T=(ACG1+ACG1-RHOG1+RHOG1-B1+B1-FP1+FP1)/(2.*B1)
    ROOT1T=A1T+B1T-B1T-C1T+C1T
    Y1T1=A1T+SQRT(ROOT1T)
    Y1T2=A1T-SQRT(ROOT1T)
100
105

```

```

110 X1F=B1F+C1F
    PSI11=2.*ATAN2(V111,X11)
    PSI12=2.*ATAN2(Y12,X11)
    PSITE11=PSI11
    PSITE12=PSI12
    IF (PSI11.GT.PI) PSITE11=PSI11-2.*PI
    IF (PSI11.LT.-PI) PSITE11=PSI11+2.*PI
    IF (PSI12.GT.PI) PSITE12=PSI12-2.*PI
    IF (PSI12.LT.-PI) PSITE12=PSI12+2.*PI
    IF (PSITE11.GE.0.) TEST11=ABS(PI-BETA1+PSITE11-ALPH1)/Z
    IF (PSITE12.GE.0.) TEST12=ABS(PI-BETA1+PSITE12-ALPH1)/Z
    IF (PSITE11.LT.0.) TEST11=ABS(PI+BETA1-(PSITE11+2.*PI-ALPH1))/Z
    IF (PSITE12.LT.0.) TEST12=ABS(PI+BETA1-(PSITE12+2.*PI-ALPH1))/Z
    IF (PSI11.LT.0.) PSITE11=PSI11+2.*PI
    IF (PSI12.LT.0.) PSITE12=PSI12+2.*PI
    PSITE10=PSITE11/Z
    PSITE20=PSITE12/Z
    WRITE (6,46) PSITE10,TEST11
    WRITE (6,47) PSITE20,TEST12
    CALL TRANS1 (RHOGL,ALPH1,BETA1,ACG1,B1,DELG1,Z,PSITE11,PHI11,
111)
    IF (G12.GT.FP1) GO TO 2
    PHIE=PHI11
    PSIE=PSIE11
    GO TO 4
120 2 CALL TRANS1 (RHOGL,ALPH1,BETA1,FP1,ACG1,B1,DELG1,Z,PSITE12,PHI12,
    IG12)
    IF (G12.LT.FP1) GO TO 3
    WRITE (6,72)
    STOP
130 3 PHIE=PHIE12
    PSIE=PSIE12
140 4 IF (PHIE.LT.0.) PHIE=PHIE+2.*PI
    IF (PSIE.LT.0.) PSIE=PSIE+2.*PI
    PHITD=PHIE/Z
    PSITD=PSIE/Z
    WRITE (6,73) PHITD,PSITD
145 C DETERMINATION OF CORRECT SIGN FOR ROUND ON FLAT REGIME OF MESH 1
    C
    C
    A1F=ACG1*COS(PHIE12-DELG1+ALPH1)-B1*COS(BETA1+ALPH1)
    B1F=-ACG1*SIN(PHIE12-DELG1+ALPH1)+B1*SIN(BETA1+ALPH1)
    C1F=RHO31
    RQ11F=A1F+B1F-B1F-C1F+C1F
    Y1F=A1F+SQRT(RQ11F)
    Y2F=A1F-SQRT(RQ11F)
    X1F=B1F+C1F
    PSIF1=2.*ATAN2(Y1F,X1F)
    PSIF2=2.*ATAN2(Y2F,X1F)
    IF (PSIF1.LT.0.) PSIF1=PSIF1+2.*PI
    IF (PSIF2.LT.0.) PSIF2=PSIF2+2.*PI
    IF (ABS(PSIF1-PSIE11).LT.ABS(PSIF2-PSIE11)) GO TO 5
    SIGN1F=-1.
155

```

```

160 GO TO 6
161 5 SIGNIF=1.
162
163 C COMPUTATION OF FINAL AND INITIAL VALUES OF PHI AND PSI FOR MESH 1
164 C
165 8 DO 7 I=1,2000
166 PHID1=PHI1D-(I-1)/100.
167 PH11=PHID1*Z
168 A1F=ACG1*COS(PHI1+DELGI+ALPHP1)-B1*COS(BETA1+ALPHP1)
169 B1F=-ACG1*SIN(PHI1+DELGI+ALPHP1)+B1*SIN(BETA1+ALPHP1)
170 C1F=RHO*G1
171 ROOT1F=A1F+B1F+C1F
172 Y1F=A1F+SIGN1F*SQRT(ROOT1F)
173 X1F=B1F+C1F
174 PSI1F=2.*ATAN2(Y1F,X1F)
175 IF (PSI1F.LT.0.) PSI1F=PSI1F+2.*PI
176 LX1=B1*COS(BETA1)+ACPI+COS(PSI1F-DPSI1+DELPI)-ACG1*COS(PHI1+DPHI1+
177 DELGI)
178 LY1=B1*SIN(BETA1)+ACPI+SIN(PSI1F-DPSI1+DELPI)-ACGI*SIN(PHI1+DPHI1+
179 DELGI)
180 LL1=SQRT(LX1*LX1+LY1*LY1)
181 DELEL1=LL1-1
182 IF (DELEL1.LE.0.) GO TO 8
183 7 CONTINUE
184 8 PH1F=PHI1
185 PS1FF=PSI1F
186 PH11=PH1F+DPHI1
187 PS11=PS1FF-DPSI1
188 IF (PS11.LT.0.) PS11=PS11+2.*PI
189 PH11D=PH11/Z
190 PS11D=PS11/Z
191 PH1FD=PH1F/Z
192 PS1FD=PS1FF/Z
193 WRITE (6,74) PH11D,PS11D,PH11FD,PS11FD
194
195 C DETERMINATION OF CORRECT SIGN FOR ROUND ON ROUND REGIME OF MESH 1
196 C
197 A1R=ACG1*SIN(PHI1+DELGI-DELPI)-B1*SIN(BETA1-DELP1)
198 B1R=ACG1*COS(PHI1+DELGI-DELPI)-B1*COS(BETA1-DELP1)
199 C1R=(ACPI-ACPI+ACG1+ACGI+B1*B1-L1*L1-2.*ACGI*B1*COS(PHI1+DELGI-DE
200 LTA1))/(2.*ACPI)
201 ROOT1R=A1R+B1R+C1R
202 Y1R1=A1R+SQRT(ROOT1R)
203 Y1R2=A1R-SQRT(ROOT1R)
204 X1R=B1R+C1R
205 PSI1R1=2.*ATAN2(Y1R1,X1R)
206 PSI1R2=2.*ATAN2(Y1R2,X1R)
207 IF (PSI1R1.LT.0.) PSI1R1=PSI1R1+2.*PI
208 IF (PSI1R2.LT.0.) PSI1R2=PSI1R2+2.*PI
209 IF (ABS(PSI11-PSI1R1).LT.ABS(PSI11-PSI1R2)) GO TO 9
210 SIGN1R=-1.
211 GO TO 10
212 9 SIGN1R=1.

```

```

215 C PRELIMINARY COMPUTATIONS FOR MESH 2
216 C DETERMINATION OF TRANSITION ANGLE OF MESH 2
217 C
218 C
219 C
220 C 10 A21=-RHOG2*COS(BETA2-ALPHP2)+FP2*SIN(BETA2-ALPHP2)
      B21=RHOG2*SIN(BETA2-ALPHP2)+FP2*COS(BETA2-ALPHP2)
      C21=(ACG2*ACG2-RHOG2-RHOG2-B2*B2-FP2*FP2)/(2.*B2)
      ROOT21=A21+A21*B21*B21-C21*C21
      Y211=A21+SQRT(ROOT21)
      Y212=A21-SQRT(ROOT21)
      X21=B21+C21
      PSI211=2.*ATAN2(Y211,X21)
      PSI212=2.*ATAN2(Y212,X21)
      PSI2E21=PSI211
      PSI2E22=PSI212
      IF (PSI211.GT.PI) PSI2E21=PSI211-2.*PI
      IF (PSI211.LT.PI) PSI2E21=PSI211+2.*PI
      IF (PSI212.GT.PI) PSI2E22=PSI212-2.*PI
      IF (PSI212.LT.PI) PSI2E22=PSI212+2.*PI
      IF (PSI2E21-GE.0.) TEST21=ABS(PI-BETA2+PSI2E21+ALPHP2)/Z
      IF (PSI2E21-LT.0.) TEST21=ABS(BETA2+PI-(PSI2E21+2.*PI+ALPHP2))/Z
      IF (PSI2E22-GE.0.) TEST22=ABS(PI-BETA2+PSI2E22+ALPHP2)/Z
      IF (PSI2E22-LT.0.) TEST22=ABS(BETA2+PI-(PSI2E22+2.*PI+ALPHP2))/Z
      IF (PSI211.LT.0.) PSI2T1=PSI211+2.*PI
      IF (PSI212.LT.0.) PSI2T2=PSI212+2.*PI
      PSI2I10=PSI2T1/Z
      PSI2I20=PSI2T2/Z
      WRITE (6,48) PSI2I10,TEST21
      WRITE (6,49) PSI2I20,TEST22
      CALL TRANS2 (RHOG2,ALPHP2,BETA2,FP2,ACG2,B2,DELG2,Z,PSI2T1,PHI2T1,
1G21)
      IF (G21-GE.FP2) GO TO 11
      PHI2T=PHI2T1
      PSI2T=PSI2T1
      GO TO 13
245 C 11 CALL TRANS2 (RHOG2,ALPHP2,BETA2,FP2,ACG2,B2,DELG2,Z,PSI2T2,PHI2T2,
      1G22)
      IF (G22-LT.FP2) GO TO 12
      WRITE (6,75)
      STOP
250 C 12 PHI2T=PHI2T2
      PSI2T=PSI2T2
255 C 13 IF (PHI2T-LT.0.) PHI2T=PHI2T+2.*PI
      IF (PSI2T-LT.0.) PSI2T=PSI2T+2.*PI
      PHI2TD=PHI2T/Z
      PSI2TD=PSI2T/Z
      WRITE (6,76) PHI2TD,PSI2TD
260 C DETERMINATION OF CORRECT SIGN FOR ROUND ON FLAT REGIME OF MESH 2
261 C
262 C
263 C
264 C
265 C A2F=ACG2*COS(PHI2T-DELG2-ALPHP2)-B2*COS(BETA2-ALPHP2)
      B2F=-ACG2*SIN(PHI2T-DELG2-ALPHP2)+B2*SIN(BETA2-ALPHP2)

```



```

320      1TA21)/(2.*ACP2)
      ROOT2R=A2R+A2R+B2R+B2R-C2R-C2R
      Y2R1=A2R+SQRT(ROOT2R)
      X2R=B2R+C2R
      PS12R1=2.*ATAN2(Y2R1,X2R)
      PS12R2=2.*ATAN2(Y2R2,X2R)
      IF (PS12R1.LT.0.) PS12R1=PS12R1+2.*PI
      IF (PS12R2.LT.0.) PS12R2=PS12R2+2.*PI
      IF (ABS(PS121-PS12R1).LT.ABS(PS121-PS12R2)) GO TO 18
      SIGN2R=-1.
      GO TO 19
      18 SIGN2R=1.
      C
      C
      C
      C
330      PRELIMINARY COMPUTATIONS FOR MESH 3
      DETERMINATION OF TRANSITION ANGLE OF MESH 3
      19 A3T=RHO63*COS(BETA3+ALPHP3)+FP3-SIN(BETA3+ALPHP3)
      B3T=-RHO63*SIN(BETA3+ALPHP3)+FP3-COS(BETA3+ALPHP3)
      C3T=(ACG3*ACG3-RHO63-RHO63*B3*B3-FP3*FP3)/(2.*B3)
      Y3T1=A3T+SQRT(ROOT3T)
      X3T1=B3T+C3T
      PS13T1=2.*ATAN2(Y3T1,X3T)
      PS13T2=2.*ATAN2(Y3T2,X3T)
      PSITE31=PSI3T1
      PSITE32=PSI3T2
      IF (PSI3T1.GT.PI) PSITE31=PSI3T1-2.*PI
      IF (PSI3T1.LT.-PI) PSITE31=PSI3T1+2.*PI
      IF (PSI3T2.GT.PI) PSITE32=PSI3T2-2.*PI
      IF (PSI3T2.LT.-PI) PSITE32=PSI3T2+2.*PI
      IF (PSITE31-GE.0.) TEST31=ABS(PI-BETA3+PSITE31-ALPHP3)/Z
      IF (PSITE31.LT.0.) TEST31=ABS(PI+BETA3-(PSITE31+2.*PI-ALPHP3))/Z
      IF (PSITE32-GE.0.) TEST32=ABS(PI-BETA3+PSITE32-ALPHP3)/Z
      IF (PSITE32.LT.0.) TEST32=ABS(PI+BETA3-(PSITE32+2.*PI-ALPHP3))/Z
      IF (PSI3T1.LT.0.) PSI3T1=PSI3T1+2.*PI
      IF (PSI3T2.LT.0.) PSI3T2=PSI3T2+2.*PI
      PS13T1D=PSI3T1/Z
      PS13T2D=PSI3T2/Z
      WRITE (6,50) PS13T1D,TEST31
      WRITE (6,51) PS13T2D,TEST32
      CALL TRANS1 (RHO63,ALPHP3,BETA3,FP3,ACG3,B3,DEL63,Z,PSI3T1,PHI3T1,
      1G31)
      IF (G31.GT.FP3) GO TO 20
      PHI3T=PHI3T1
      PS13T=PSI3T1
      GO TO 22
      20 CALL TRANS1 (RHO63,ALPHP3,BETA3,FP3,ACG3,B3,DEL63,Z,PSI3T2,PHI3T2,
      1G32)
      IF (G32.LT.FP3) GO TO 21
      WRITE (6,78)

```

A 319  
A 320  
A 321  
A 322  
A 323  
A 324  
A 325  
A 326  
A 327  
A 328  
A 329  
A 330  
A 331  
A 332  
A 333  
A 334  
A 335  
A 335  
A 337  
A 338  
A 339  
A 340  
A 341  
A 342  
A 343  
A 344  
A 345  
A 346  
A 347  
A 348  
A 349  
A 350  
A 351  
A 352  
A 353  
A 354  
A 355  
A 356  
A 357  
A 358  
A 359  
A 360  
A 361  
A 362  
A 363  
A 364  
A 365  
A 366  
A 367  
A 368  
A 369  
A 370  
A 371



```

425 IF (PSI3I.LT.0.) PSI3I=PSI3I+2.*PI
    PHI3ID=PHI3I/Z
    PSI3ID=PSI3I/Z
    PHI3FD=PHI3F/Z
    PSI3FD=PSI3FF/Z
    WRITE (6,80) PHI3ID,PSI3ID,PHI3FD,PSI3FD
430
431 C
432 C
433 C
434 DETERMINATION OF CORRECT SIGN OF ROUND ON ROUND REGIME FOR MESH 3
435
436 A3R=ACG3*SIN(PHI3I+DELG3-DELP3)-B3*SIN(BETA3-DELP3)
437 B3R=ACG3*COS(PHI3I+DELG3-DELP3)-B3*COS(BETA3-DELP3)
438 C3R=(ACP3*ACP3+ACG3*ACG3+B3*B3-L3*L3-2.*ACG3*B3*COS(PHI3I+DELG3-
439 1TA3))/(2.*ACP3)
440 ROOT3R=A3R*A3R+B3R*B3R-C3R*C3R
441 Y3R1=A3R+SQRT(ROOT3R)
442 Y3R2=A3R-SQRT(ROOT3R)
443 X3R=B3R+C3R
444 PSI3R1=2.*ATAN2(Y3R1,X3R)
445 PSI3R2=2.*ATAN2(Y3R2,X3R)
446 IF (PSI3R1.LT.0.) PSI3R1=PSI3R1+2.*PI
447 IF (PSI3R2.LT.0.) PSI3R2=PSI3R2+2.*PI
448 IF (ABS(PHI3I-PSI3R1)-LT.ABS(PHI3I-PSI3R2)) GO TO 27
449 SIGN3R=-1.
450 GO TO 28
451 SIGN3R=1.
452
453 GEAR TRAIN MOTION MODEL, KINEMATICS
454
455 DOPHI1=NP2*MP3*(PHI3I-PHI3F)/(K*NG1*MG2)
456 PHI11=PHI11+DOPHI1
457 WRITE (6,52)
458 PHI11=PHI11-DOPHI1
459 PHI1D=PHI1/Z
460 IF (PHI11.LE.PHI1F+DOPHI1) GO TO 45
461 MESH 1
462
463 IF (PHI11.LE.PHI1T) GO TO 30
464 A1R=ACG1*SIN(PHI11+DELG1-DELP1)-B1*SIN(BETA1-DELP1)
465 B1R=ACG1*COS(PHI11+DELG1-DELP1)-B1*COS(BETA1-DELP1)
466 C1R=(ACPI*ACPI+ACG1*ACG1+B1*B1-L1*L1-2.*ACG1*B1*COS(PHI11+DELG1-BET
467 1A1))/(2.*ACPI)
468 ROOT1R=A1R*A1R+B1R*B1R-C1R*C1R
469 Y1R=A1R+SIGN1R*SQRT(ROOT1R)
470 X1R=B1R+C1R
471 PSI11=2.*ATAN2(Y1R,X1R)
472 IF (PSI11.LT.0.) PSI11=PSI11+2.*PI
473 PSI1D=PSI1/Z
474 IF (ABS(PHI11-PHI1T)-LT.0.0001) PSI11=PSI1
475 IF (ABS(PHI11-PHI1T)-LT..0001)PSI1P=PSI1T
476 SLAM1=(B1*SIN(BETA1)+ACPI*SIN(PHI11+DELP1)-ACG1*SIN(PHI11+DELG1))/L1
477 CLAM1=(B1*COS(BETA1)+ACPI*COS(PHI11+DELG1)-ACG1*COS(PHI11+DELG1))/L1
478 LAMDA1=ATAN2(SLAM1,CLAM1)

```

1  
4  
53

```

480 IF (LAMBDA1.LT.0.) LAMBDA1=LAMBDA1+2.*PI
PSDOT1=PHOG1*ACG1*(B1/ACPI*SIN(PHI1+DELG1-BETA1))+SIN(PHI1-PSI1)+DE
1LG1-DELP1)/(ATR*COS(PSI1))-B1R*SIN(PSI1)
VST1R=PHOOT1*(ACG1*COS(PHI1+DELG1-LAMBDA1)+RHOG1)-PSDOT1*(ACP1*COS(
1PSI1+DELP1-LAMBDA1))-RHOP1)
S1R=VST1R/ABS(VST1R)
GO TO 31
485 A1F=ACG1*COS(PHI1+DELG1+ALPHP1)-B1*COS(BETA1+ALPHP1)
B1F=-ACG1*SIN(PHI1+DELG1+ALPHP1)+B1*SIN(BETA1+ALPHP1)
C1F=RHOG1
ROOT1F=A1F+A1F+81F+81F-C1F-C1F
Y1F=A1F+SIGN1F*SQRT(ROOT1F)
X1F=B1F+C1F
PSI1=2.*ATAN2(Y1F,X1F)
IF (PSI1.LT.0.) PSI1=PSI1+2.*PI
PSI1D=PSI1/Z
G1=(ACG1*SIN(PHI1+DELG1)+RHOG1*COS(PSI1-ALPHP1)-B1*SIN(BETA1))/SIN
1(PSI1-ALPHP1)
PSDOT1=PHOOT1*(ACG1*COS(PHI1-PSI1+DELG1+ALPHP1))/(A1F*COS(PSI1))-B1
1F*SIN(PSI1)
VST1F=PHOOT1*(ACG1*SIN(PSI1-ALPHP1-PSI1-DELG1)-RHOG1)
S1F=VST1F/ABS(VST1F)
C
C
C
31 DOPHI2=PSI1-PSI1P
IF (ABS(PHI1-PHI11).LT.0.0001) PHI2=PHI2I
PHI2=PHI2+DOPHI2
PSI1P=PSI1
IF (PHI2.GT.PHI2F) PHI2=PHI2I
PHI2D=PHI2/Z
IF (PHI2.GE.-PHI2I) CD TO 32
A2R=B2*SIN(BETA2+DELP2)-ACG2*SIN(PHI2-DELG2+DELP2)
B2R=B2*COS(BETA2+DELP2)-ACG2*COS(PHI2-DELG2+DELP2)
C2R=(L2-L2-B2-B2-ACG2*ACG2-ACP2*ACP2+2.*ACG2*B2*COS(PHI2-DELG2-BET
1A2))/2.*ACP2)
ROOT2R=A2R+A2R+B2R+B2R-C2R-C2R
Y2R=A2R+SIGN2R*SQRT(ROOT2R)
X2R=B2R+C2R
PSI2=2.*ATAN2(Y2R,X2R)
IF (PSI2.LT.0.) PSI2=PSI2+2.*PI
PSI2D=PSI2/Z
IF (ABS(PHI2-PHI2I).LT.0.0001) PSI2I=PSI2
IF (ABS(PHI2-PHI2I).LT.0.0001) PSI2P=PSI2I
SLAW2=(B2*SIN(BETA2)+ACP2*SIN(PSI2-DELP2)-ACG2*SIN(PHI2-DELG2))/L2
CLAW2=(B2*COS(BETA2)+ACP2*COS(PSI2-DELP2)-ACG2*COS(PHI2-DELG2))/L2
LAMBDA2=ATAN2(SLAW2,CLAW2)
IF (LAMBDA2.LT.0.) LAMBDA2=LAMBDA2+2.*PI
PHOOT2=PSOOT1
PSDOT2=PHOOT2*ACG2*(-SIN(PHI2-PSI2-DELG2+DELP2)-B2/ACP2*SIN(PHI2-B
1ELG2-BETA2))/(A2R*COS(PSI2))-B2R*SIN(PSI2)
VST2R=PHOOT2*(ACG2*COS(PHI2-DELG2-LAMBDA2)+RHOG2)-PSDOT2*(ACP2*COS(
1PSI2-DELP2-LAMBDA2)-RHOP2)

```



```

585 ROOT3F=A3F+A3F*B3F+B3F*B3F-C3F-C3F
    Y3F=A3F+SIGK3F*SQRT(RODT3F)
    X3F=B3F+C3F
    PS13=2.*ATAN2(Y3F,X3F)
    IF (PS13.LT.0.) PS13=PS13+2.*PI
    G3=(ACG3+SIN(PHI3+DELG3)+RHO3-COS(PS13-ALPHA3)-B3-SIN(DELTA3))/SIN
    1(PS13-ALPHA3)
    PHODT3=PSODT2
    PSODT3=PHODT3+ACG3-COS(PHI3-PS13+DELG3+ALPHA3)/(A3F+COS(PS13)-B3F+
    1SIN(PS13))
    VST3F=PHODT3*(ACG3+SIN(PS13-ALPHA3-DELG3)-RHO3)
    S3F=VST3F/ABS(VST3F)

C
C MOMENT COMPUTATIONS
C
600 DM=1.-MU*BU
    A1=ABS((MU*SIN(GAMMA4)+COS(GAMMA4))/DM)
    A2=ABS((MU*(S3R-1.)+SIN(LAMDA3)-(1.+MU*BU*S3R)+COS(LAMDA3))/DM)
    A3=ABS((SIN(GAMMA4)-MU*COS(GAMMA4))/DM)
    A4=ABS(((1.+MU*BU*S3R)+SIN(LAMDA3)+MU*(S3R-1.))+COS(LAMDA3))/DM)
    A5=ABS(((1.-MU*BU*S3R)+COS(LAMDA3)-MU*(1.+S3R)+SIN(LAMDA3))/DM)
    A6=ABS((MU*(1.+S2R)+SIN(LAMDA2)-(1.-MU*BU*S2R)+COS(LAMDA2))/DM)
    A7=ABS((MU*SIN(GAMMA3)-COS(GAMMA3))/DM)
    A8=ABS(((1.-MU*BU*S3R)+SIN(LAMDA3)+MU*(1.+S3R)+COS(LAMDA3))/DM)
    A9=ABS(((MU*BU*S2R-1.)+SIN(LAMDA2)-MU*(1.+S2R)+COS(LAMDA2))/DM)
    A10=ABS((SIN(GAMMA3)+MU*COS(GAMMA3))/DM)
    A11=ABS(((1.+MU*BU*S2R)+COS(LAMDA2)-MU*(S2R-1.))+SIN(LAMDA2))/DM)
    A12=ABS((MU*(S1R-1.))+SIN(LAMDA1)-(1.+MU*BU*S1R)+COS(LAMDA1))/DM)
    A13=ABS((-COS(GAMMA2)-MU*SIN(GAMMA2))/DM)
    A14=ABS(((1.-MU*BU*S2R)+SIN(LAMDA2)-MU*(1.-S2R)+COS(LAMDA2))/DM)
    A15=ABS((MU*(1.-S1R)+COS(LAMDA1)-(1.+MU*BU*S1R)+SIN(LAMDA1))/DM)
    A16=ABS((MU*COS(GAMMA2)-SIN(GAMMA2))/DM)
    A17=ABS(((1.-MU*BU*S1R)+COS(LAMDA1)-MU*(1.+S1R)+SIN(LAMDA1))/DM)
    A18=ABS(1./DM)
    A19=ABS(((1.-MU*BU*S1R)+SIN(LAMDA1)+MU*(1.+S1R)+COS(LAMDA1))/DM)
    A20=ABS(MU/DM)
    A21=ABS((MU*(1.-S2R)+SIN(LAMDA2)+(1.+MU*BU*S2R)+COS(LAMDA2))/DM)
    A22=ABS(((1.-MU*BU*S1F)+SIN(PS11-ALPHA1)-MU*(1.+S1F)+COS(PS11-ALPH
    1P1))/DM)
    A23=ABS((MU*SIN(GAMMA2)+COS(GAMMA2))/DM)
    A24=ABS(((1.-MU*BU*S2R)+SIN(LAMDA2)-MU*(1.-S2R)+COS(LAMDA2))/DM)
    A25=ABS((-MU*(1.+S1F)+SIN(PS11-ALPHA1)+{MU*BU*S1F-1.}*COS(PS11-ALP
    1HP1))/DM)
    A26=ABS((-SIN(GAMMA2)+MU*COS(GAMMA2))/DM)
    A27=ABS((-1.+MU*BU*S1F)+SIN(PS11-ALPHA1)+MU*(S1F-1.))+COS(PS11-ALP
    1HP1))/DM)
    A28=ABS(1./DM)
    A29=ABS((MU*(S1F-1.))+SIN(PS11-ALPHA1)+(1.+MU*BU*S1F)+COS(PS11-ALPH
    1P1))/DM)
    A30=ABS(MU/DM)
    A31=ABS(((1.-MU*BU*S3R)+COS(LAMDA3)-MU*(1.+S3R)+SIN(LAMDA3))/DM)
    A32=ABS((-MU*(1.+S2F)+COS(PS12+ALPHA2)-(1.-MU*BU*S2F)+SIN(PS12+ALP

```

640 A 637 1HP2)) / DM  
 A 638 A33=ABS((MU\*SIN(GAMMA3)-COS(LAMDA3)) / DM)  
 A 639 A34=ABS((MU\*(1.+S3R)\*COS(LAMDA3)+(1.-MU\*RU\*S3R)\*SIN(LAMDA3)) / DM)  
 A 640 A35=ABS(((1.-MU\*RU\*S2F)\*COS(PSI2+ALPH2)-MU\*(1.+S2F)\*SIN(PSI2+ALPH  
 1P2)) / DM)  
 A 641 A36=ABS((SIN(GAMMA3)+MU\*COS(GAMMA3)) / DM)  
 A 642 A37=ABS(((1.-MU\*RU\*S2F)\*SIN(PSI2+ALPH2)+MU\*(S2F-1.)\*COS(PSI2+ALPH  
 1P2)) / DM)  
 A 643 A38=ABS(((1.-MU\*RU\*S1F)\*SIN(PSI1-ALPH1)-MU\*(1.+S1F)\*COS(PSI1-ALPH  
 1P1)) / DM)  
 A 644 A39=ABS((RU\*SIN(GAMMA2)+COS(GAMMA2)) / DM)  
 A 645 A40=ABS((RU\*(S2F-1.)\*SIN(PSI2+ALPH2)-(1.+RU\*RU\*S2F)\*COS(PSI2+ALPH  
 1P2)) / DM)  
 A 646 A41=ABS((-RU\*(1.+S1F)\*SIN(PSI1-ALPH1)+(RU\*RU\*S1F-1.)\*COS(PSI1-ALPH  
 1P1)) / DM)  
 A 647 A42=ABS((RU\*COS(GAMMA2)-SIN(GAMMA2)) / DM)  
 A 648 A43=ABS(((1.+RU\*RU\*S2F)\*SIN(PSI2+ALPH2)-MU\*(1.-S2F)\*COS(PSI2+ALPH  
 1P2)) / DM)  
 A 649 A44=ABS((RU\*(S1R-1.)\*SIN(LAMDA1)-(1.-RU\*RU\*S1R)\*COS(LAMDA1)) / DM)  
 A 650 A45=ABS((RU\*SIN(GAMMA2)+COS(GAMMA2)) / DM)  
 A 651 A46=ABS((RU\*(S2F-1.)\*SIN(PSI2+ALPH2)-(1.+RU\*RU\*S2F)\*COS(PSI2+ALPH  
 1P2)) / DM)  
 A 652 A47=ABS((-1.-RU\*RU\*S1R)\*SIN(LAMDA1)+MU\*(1.-S1R)\*COS(LAMDA1)) / DM)  
 A 653 A48=ABS((-SIN(GAMMA2)+MU\*COS(GAMMA2)) / DM)  
 A 654 A49=ABS(((1.-RU\*RU\*S3F)\*SIN(PSI3-ALPH3)-MU\*(1.+S3F)\*COS(PSI3-ALPH  
 1P3)) / DM)  
 A 655 A50=ABS((-RU\*SIN(GAMMA4)-COS(GAMMA4)) / DM)  
 A 656 A51=ABS((-RU\*(1.+S3F)\*SIN(PSI3-ALPH3)-(1.-RU\*RU\*S3F)\*COS(PSI3-ALPH  
 1HP3)) / DM)  
 A 657 A52=ABS((-SIN(GAMMA4)+MU\*COS(GAMMA4)) / DM)  
 A 658 A53=ABS((-1.-RU\*RU\*S3F)\*SIN(PSI3-ALPH3)+MU\*(S3F-1.)\*COS(PSI3-ALPH  
 1HP3)) / DM)  
 A 659 A54=ABS((RU\*RU\*S2F-1.)\*SIN(PSI2+ALPH2)-MU\*(1.+S2F)\*COS(PSI2+ALPH  
 1P2)) / DM)  
 A 660 A55=ABS((RU\*SIN(GAMMA3)-COS(GAMMA3)) / DM)  
 A 661 A56=ABS((RU\*(S3F-1.)\*SIN(PSI3-ALPH3)+(1.-RU\*RU\*S3F)\*COS(PSI3-ALPH  
 1P3)) / DM)  
 A 662 A57=ABS((-RU\*(1.+S2F)\*SIN(PSI2+ALPH2)+(1.-RU\*RU\*S2F)\*COS(PSI2+ALPH  
 1HP2)) / DM)  
 A 663 A58=ABS((-SIN(GAMMA3)-MU\*COS(GAMMA3)) / DM)  
 A 664 A59=ABS((-1.-RU\*RU\*S3F)\*SIN(PSI3-ALPH3)+MU\*(S3F-1.)\*COS(PSI3-ALPH  
 1HP3)) / DM)  
 A 665 A60=ABS((RU\*(1.+S2R)\*SIN(LAMDA2)+(MU\*RU\*S2R-1.)\*COS(LAMDA2)) / DM)  
 A 666 A61=ABS((RU\*SIN(GAMMA3)-COS(GAMMA3)) / DM)  
 A 667 A62=ABS((RU\*(S3F-1.)\*SIN(PSI3-ALPH3)+(1.-RU\*RU\*S3F)\*COS(PSI3-ALPH  
 1P3)) / DM)  
 A 668 A63=ABS(((RU\*RU\*S2E-1.)\*SIN(LAMDA2)-MU\*(1.+S2R)\*COS(LAMDA2)) / DM)  
 A 669 A64=ABS((-SIN(GAMMA3)-MU\*COS(GAMMA3)) / DM)  
 A 670 A65=C1=RU\*RHO4=(A1+A3)  
 A 671 C2=ACP3=(RU\*S3R+COS(PSI3+DELPH3)-SIN(PSI3+DELPH3-LAMDA3))-RU\*  
 A 672 1(RHOP3+S3R+RHO4\*(A2+A4))  
 A 673 C3=RU\*RHO3=(A5+A8)-RU\*S3R+RHO3+ACG3=(SIN(PHI3+DELG3-LAMDA3))-RU\*S3  
 A 674 1R-COS(PHI3+DELG3-LAMDA3))  
 A 675 A 676  
 A 677  
 A 678  
 A 679  
 A 680  
 A 681  
 A 682  
 A 683  
 A 684  
 A 685  
 A 686  
 A 687  
 A 688  
 A 689

690 C4=RU+RHO3\*(A7+A10)  
 691 C5=RU+RHO3\*(A6+A9)-RU+S2R+RHOP2+ACP2\*(RU+S2R+COS(PSI2-DELP2-LAMDA2  
 1)-SIN(PSI2-DELP2-LAMDA2))  
 692 C6=ACG2\*(SIN(PHI2-DELG2-LAMDA2))-RU+S2R+COS(PHI2-DELG2-LAMDA2))-RU+  
 693 RH02\*(A11+A14)-RU+RH02\*S2R  
 694 C7=RU+RH02\*(A13+A16)  
 695 CB=-ACP1\*(SIN(PSI1+DELP1-LAMDA1))-RU+S1R+COS(PSI1+DELP1-LAMDA1))+RU  
 696 C9=RU+RHO1\*(A18+A20)  
 697 C10=RU+RHO1\*(A17+A19)+ACG1\*(SIN(PHI1+DELGI-LAMDA1))-RU+S1R+COS(PHI1  
 1+DELGI-LAMDA1))-RU+S1R+RH01  
 698 C11=ACG2\*(SIN(PHI2-DELG2-LAMDA2))-RU+S2R+COS(PHI2-DELG2-LAMDA2))-RU  
 700 1+RH02\*(A21+A24)-RU+RH02\*S2R  
 C12=RU+RH02\*(A23+A26)  
 C13=GI-RU+RH02\*(A27+A25)  
 705 C14=RU+RHO1\*(A28+A30)  
 C15=RU+RHO1\*(A27+A29)+RU+S1F+RH01+ACG1\*(RU+S1F+SIN(PHI1+DELGI-PSI  
 1+ALPH1))-COS(PHI1+DELGI-PSI1+ALPH1))  
 C16=RU+RHO3\*(A31+A34)+ACG3\*(SIN(PHI3+DELG3-LAMDA3))-RU+S3R+COS(PHI3  
 1+DELG3-LAMDA3))-RH03\*RU+S3R  
 710 C17=RU+RHO3\*(A33+A36)  
 C18=RU+RHO3\*(A32+A35)-G2  
 C19=-RU+RH02\*(A37+A40)+ACG2\*(COS(PHI2-DELG2-PSI2-ALPH2))+RU+S2F\*SI  
 1M(PHI2-DELG2-PSI2-ALPH2))-RU+S2F+RH02  
 715 C20=RU+RH02\*(A39+A42)  
 C21=-RU+RH02\*(A38+A41)+G1  
 C22=-RU+RH02\*(A43+A46)+ACG2\*(COS(PHI2-DELG2-PSI2-ALPH2))+RU+S2F\*SI  
 1M(PHI2-DELG2-PSI2-ALPH2))-RU+S2F+RH02  
 720 C23=RU+RH02\*(A45+A48)  
 C24=-RU+RH02\*(A44+A47)+ACP1\*(RU+S1R+COS(PSI1+DELP1-LAMDA1))-S1R(PSI  
 1+DELP1-LAMDA1))-RU+S1R+RHOP1  
 C25=RU+RH04\*(A50+A52)  
 C26=GI-RU+RH04\*(A49+A51)  
 C27=RU+RHO3\*(A53+A56)+ACG3\*(-COS(PHI3+DELG3-PSI3+ALPH3))+RU+S3F\*SI  
 1M(PHI3+DELG3-PSI3+ALPH3))+RU+S3F+RH03  
 725 C28=RU+RHO3\*(A55+A58)  
 C29=RU+RHO3\*(A54+A57)-G2  
 C30=RU+RHO3\*(A59+A62)-ACG3\*(COS(PHI3+DELG3-PSI3+ALPH3))-RU+S3F\*SIN  
 1(PHI3+DELG3-PSI3+ALPH3))-RU+S3F+RH03  
 C31=RU+RHO3\*(A61+A64)  
 C32=RU+RHO3\*(A60+A63)-ACP2\*(SIN(PSI2-DELP2-LAMDA2))-RU+S2R+COS(PSI2  
 1-DELP2-LAMDA2))-RU+S2R+RHOP2  
 730 C  
 735 C  
 740 C  
 IF ((PHI1-GE.PHI1T).AND.(PHI2-LE.PHI2T).AND.(PHI3-GE.PHI3T)) GO TO  
 1 36  
 IF ((PHI1-LE.PHI1T).AND.(PHI2-LE.PHI2T).AND.(PHI3-GE.PHI3T)) GO TO  
 1 37  
 IF ((PHI1-LE.PHI1T).AND.(PHI2-GE.PHI2T).AND.(PHI3-GE.PHI3T)) GO TO  
 1 38  
 IF ((PHI1-GE.PHI1T).AND.(PHI2-GE.PHI2T).AND.(PHI3-GE.PHI3T)) GO TO  
 1 39



```

42 MD47=MIN=C0+C26-C32/(C6+C19+C30)-01+C8+C9+C26-C32/(C6+C19+C30)-02*
1C7+C26-C32/(C6+C30)-03+C26-C31/C30-Q4-C25
MD4=MD47
POINTEF=ABS(PSOOT3)*MD4/MIN
WRITE (6.50) PHI1D,PHI2D,PHI3D,PSI1D,PSI2D,PSI3D,PSOOT1,PSOOT2,PSO
1073,S1R,S2R,S3F,G3,POINTEF
GO TO 44
43 MD48=MIN=C13+C26+C32/(C11+C30)-01+C15+C30)-01+C13+C14+C26-C32/(C11+C15+C30
1)-02+C12+C26-C32/(C11+C30)-03+C26-C31/C30-Q4-C25
MD4=MD48
POINTEF=ABS(PSOOT3)*MD4/MIN
WRITE (6.60) PHI1D,PHI2D,PHI3D,PSI1D,PSI2D,PSI3D,PSOOT1,PSOOT2,PSO
1073,S2R,S1F,G1,S3F,G3,POINTEF
44 NTOT=NTOT+POINTEF
GO TO 29
45 CYCLEFF=NTOT*DDPHI1/(PHI1F-PHI1I)
WRITE (6.01) CYCLEFF
NTOT=0.
IF (ISTOP.NE.0) GO TO 1
STOP
C
46 FORELT (6X,9#PSI1I1D =,F9.4,3X,0#TESTI1 =,F9.4)
47 FORMAT (6X,9#PSI1I2D =,F9.4,3X,0#TESTI12 =,F9.4//)
48 FORMAT (6X,9#PSI2I1D =,F9.4,3X,0#TESTI21 =,F9.4)
49 FORMAT (6X,9#PSI2I2D =,F9.4,3X,0#TESTI22 =,F9.4//)
50 FORMAT (6X,9#PSI3I1D =,F9.4,3X,0#TESTI31 =,F9.4)
51 FORMAT (6X,9#PSI3I2D =,F9.4,3X,0#TESTI32 =,F9.4//)
52 FORMAT (120#0 PHI1 PHI2 PHI3 PSI1 PSI2 PSI3 DPSI1 DPSI2
1 DPSI3 S1R S2R S3R S1F G1 S2F G2 S3F G3 POINTEF
2/)
53 FORMAT (6X,6(F4.0,2X),3(F5.0,2X),3(F3.0,2X),3(X,3),F5.3)
54 FORMAT (6X,5(F4.0,2X),3(F5.0,2X),5(X,3)(F3.0,2X),F5.3,2(X,F5.3)
55 FORMAT (6X,6(F4.0,2X),3(F5.0,2X),10(X,F3.0,2X),F3.0,2(X,F5.3,2X),F3.0,
12X,F5.3,14X,F5.3)
56 FORMAT (6X,6(F4.0,2X),3(F5.0,2X),F3.0,7(X,F3.0,14X),F3.0,2(X,F5.3,14X
1,F5.3)
57 FORMAT (6X,6(F4.0,2X),3(F5.0,2X),15(X,3)(F3.0,2X),F5.3,2(X,F5.3)
58 FORMAT (6X,6(F4.0,2X),3(F5.0,2X),F3.0,2(X,F3.0,2X),F3.0,2(X,F3.0,2X,
1F5.3,2X,F5.3)
59 FORMAT (6X,6(F4.0,2X),3(F5.0,2X),2(F3.0,2X),2(X,F3.0,2X),F5.3,2(X,F5
1,3)
60 FORMAT (6X,6(F4.0,2X),3(F5.0,2X),5(X,F3.0,7(X,F3.0,2(X,F5.3,14X),F3.0,
12X,F5.3,2X,F5.3)
61 FORMAT (F10.3,F10.0/6F10.5/11)
62 FORMAT (6F10.4)
63 FORMAT (6F10.4)
64 FORMAT (6F10.0)
65 FORMAT (4F10.4/F10.4/F10.6)
66 FORMAT (1H1,5X,5#MIN =,F8.4,3X,4#MU =,F6.3,3X,5#RPM =,F6.0//6X,0#C
1APR:1 =,F8.5,3X,0#CAPR2 =,F8.5,3X,0#CAPR3 =,F8.5//6X,5#RPM2 =,F8.
25,3X,5#RPM3 =,F8.5,3X,5#RPM4 =,F8.5//6X,0#ACC1 =,F8.5,3X,0#ACC2 =,F8
3-5,3X,0#ACC3 =,F8.5//6X,0#ACP1 =,F8.5,3X,0#ACP2 =,F8.5,3X,0#ACP3 =

```



```

1  SUBROUTINE TRANS1 (RHOG,ALPHP,BETA,FP,ACG,B,DELG,Z,PSIT,PHIT,G)
    PI=3.14159
    SI=(-RHOG*COS(PSIT-ALPHP)+B*SIN(BETA)+FP*SIN(PSIT-ALPHP))/ACG
    CT=(RHOG*SIN(PSIT-ALPHP)+B*COS(BETA)+FP*COS(PSIT-ALPHP))/ACG
5  PHIT=ATAN2(ST,CT)-DELG
    PHINEX1=PHIT-.1*Z
    AF=ACG*COS(PHINEX1+DELG+ALPHP)-B*COS(BETA+ALPHP)
    BF=-ACG*SIN(PHINEX1+DELG+ALPHP)+B*SIN(BETA+ALPHP)
    CF=RHOG
10  ROOTF=AF+BF+BF-CF*CF
    YF1=AF+SQRT(ROOTF)
    YF2=AF-SQRT(ROOTF)
    XF=BF+CF
    PSINEX1=2.*ATAN2(YF1,XF)
    PSINEX2=2.*ATAN2(YF2,XF)
15  IF (PSINEX1.LT.0.) PSINEX1=PSINEX1+2.*PI
    IF (PSINEX2.LT.0.) PSINEX2=PSINEX2+2.*PI
    IF (ABS(PSINEX1-PSIT).LT.ABS(PSINEX2-PSIT)) GO TO 1
    PSINEX1=PSINEX2
    GO TO 2
20  1 PSINEX1=PSINEX1
    2 G=(ACG*SIN(PHINEX1+DELG)+RHOG*COS(PSINEX1-ALPHP)-B*SIN(BETA))/SIN(
    1PSINEX1-ALPHP)
    RETURN
    END
25

```

```

1 SUBROUTINE TRANS2 (RHOG,ALPHP,BETA,FP,ACG,B,DELG,Z,PSIT,PHIT,G)
  PI=3.14159
  ST=(RHOG*COS(PSIT+ALPHP)+B*SIN(BETA)+FP*SIN(PSIT+ALPHP))/ACG
  CT=(-RHOG*SIN(PSIT+ALPHP)+B*COS(BETA)+FP*COS(PSIT+ALPHP))/ACG
  PHIT=ATAN2(ST,CT)+DELG
  PHINEXT=PHIT+.1*Z
  AF=ACG*COS(PHINEXT-DELG-ALPHP)-B*COS(BETA-ALPHP)
  BF=-ACG*SIN(PHINEXT-DELG-ALPHP)+B*SIN(BETA-ALPHP)
  CF=-RHOG
  ROOTF=AF*AF+BF*BF-CF*CF
  YF1=AF+SQRT(ROOTF)
  YF2=AF-SQRT(ROOTF)
  XF=BF+CF
  PSINEX1=2.*ATAN2(YF1,XF)
  PSINEX2=2.*ATAN2(YF2,XF)
  IF (PSINEX1.LT.0.) PSINEX1=PSINEX1+2.*PI
  IF (PSINEX2.LT.0.) PSINEX2=PSINEX2+2.*PI
  IF (ABS(PSINEX1-PSIT).LT.ABS(PSINEX2-PSIT)) GO TO 1
  PSINEX1=PSINEX2
  GO TO 2
  1 PSINEX1=PSINEX1
  2 G=(ACG*SIN(PHINEXT-DELG)-RHOG*COS(PSINEX1+ALPHP)-B*SIN(BETA))/SIN(
  1PSINEX1+ALPHP)
  RETURN
  END
  
```

MIN = .1645 BU = .200 RPM = 1000.  
 CAPRP1 = .47725 CAPRP2 = .20670 CAPRP3 = .17560  
 RP2 = .09085 RP3 = .06890 RP4 = .05905  
 ACG1 = .47725 ACG2 = .20670 ACG3 = .17560  
 ACP1 = .09085 ACP2 = .06850 ACP3 = .05905  
 R1 = .75000 R2 = .75000 R3 = .75000 R4 = .75000  
 RHOG1 = .03870 RHOG2 = .02870 RHOG3 = .01910 RHOP1 = .01740 RHOP2 = .01040 RHOP3 = .00875  
 TGI = .03480 TGI2 = .02520 TGI3 = .02170 TPI = .02800 TPI2 = .02080 TPI3 = .01750  
 MGI = 42. MG2 = 27. MG3 = 27. MP2 = 8. MP3 = 9. MP4 = 9.  
 M1 = .69515E-04 M2 = .97028E-05 M3 = .70027E-05 M4 = .79188E-06  
 RH01 = .060 RH02 = .030 RH03 = .025 RH04 = .020  
 WD = .1500E-04  
 K = 25.0  
 PHO0T1 = -1.0  
 FP1 = .08917 FP2 = .06811 FP3 = .05840  
 BETA1D = 112.2552 BETA2D = 145.0978 BETA3D = 164.6850  
 PS11T1D = 305.6017 TEST11 = 4.4495  
 PS11T2D = 343.6259 TEST12 = 42.4736  
 PHI11D = 113.5016 PS11T0 = 305.6017 PSI11FD = 107.4216 PSI11FD = 337.4283  
 PHI11D = 115.9930 PS11T0 = 292.4283  
 PS12T1D = 286.9442 TEST21 = 29.4719  
 PS12T2D = 312.0785 TEST22 = 4.3377  
 PHI2TD = 142.0461 PS12TD = 312.0785 PSI2FD = 150.1161 PSI2FD = 290.9521  
 PHI2TD = 136.7828 PS12TD = 330.9531  
 PS13T1D = 357.5003 TEST31 = 4.2938  
 PS13T2D = 25.1346 TEST32 = 31.9282  
 PHI3TD = 166.7857 PS13TD = 357.5003 PSI3FD = 160.3457 PSI3FD = 15.8610  
 PHI3TD = 173.6791 PS13TD = 336.8610  
 PHI1 PHI2 PHI3 PS11 PS12 PS13 DPS11 DPS12 DPS13 S1R S2R S3R S1F G1 S2F G2 S3F G3 POINTEF  
 116. 137. 174. 292. 331. 337. 5. -16. 59. 1. -1. 1.



114.	148.	167.	304.	297.	356.	5.	-16.	47.	-1.	-1.	1.	.066	1.	.526
114.	148.	167.	304.	297.	356.	5.	-16.	47.	-1.	-1.	1.	.066	1.	.520
114.	148.	166.	304.	296.	360.	5.	-16.	48.	-1.	-1.	1.	.066	1.	.515
114.	148.	166.	304.	296.	360.	5.	-16.	48.	-1.	-1.	1.	.066	1.	.509
114.	149.	165.	304.	295.	3.	5.	-15.	47.	-1.	-1.	1.	.066	1.	.504
114.	149.	164.	304.	295.	4.	5.	-15.	47.	-1.	-1.	1.	.066	1.	.499
114.	149.	164.	305.	294.	6.	5.	-15.	47.	-1.	-1.	1.	.066	1.	.494
114.	149.	163.	305.	294.	8.	5.	-15.	46.	-1.	-1.	1.	.066	1.	.490
114.	149.	162.	305.	293.	9.	5.	-15.	46.	-1.	-1.	1.	.066	1.	.485
114.	150.	162.	305.	292.	11.	5.	-15.	45.	-1.	-1.	1.	.066	1.	.480
114.	150.	161.	305.	292.	12.	5.	-15.	44.	-1.	-1.	1.	.066	1.	.475
114.	150.	161.	305.	292.	14.	5.	-15.	44.	-1.	-1.	1.	.067	1.	.470
113.	138.	173.	307.	329.	340.	5.	-16.	48.	-1.	-1.	1.	.066	1.	.465
113.	138.	172.	307.	328.	342.	5.	-16.	49.	-1.	-1.	1.	.066	1.	.461
113.	137.	161.	306.	331.	15.	5.	-16.	48.	-1.	-1.	1.	.066	1.	.456
113.	137.	160.	306.	330.	17.	5.	-16.	47.	-1.	-1.	1.	.066	1.	.451
113.	137.	174.	306.	330.	337.	5.	-16.	51.	-1.	-1.	1.	.066	1.	.446
113.	137.	173.	306.	329.	339.	5.	-16.	50.	-1.	-1.	1.	.066	1.	.441
113.	138.	173.	307.	329.	340.	5.	-16.	50.	-1.	-1.	1.	.066	1.	.436
113.	138.	172.	307.	328.	342.	5.	-16.	49.	-1.	-1.	1.	.066	1.	.431
113.	138.	171.	307.	328.	344.	5.	-16.	48.	-1.	-1.	1.	.066	1.	.426
113.	138.	171.	307.	327.	345.	5.	-16.	48.	-1.	-1.	1.	.066	1.	.421
113.	138.	170.	307.	327.	347.	5.	-16.	48.	-1.	-1.	1.	.066	1.	.416
113.	138.	170.	308.	326.	348.	5.	-16.	48.	-1.	-1.	1.	.066	1.	.411
113.	139.	169.	308.	325.	350.	5.	-16.	48.	-1.	-1.	1.	.066	1.	.406
113.	139.	168.	308.	325.	352.	5.	-16.	48.	-1.	-1.	1.	.066	1.	.401
113.	139.	168.	308.	324.	353.	5.	-16.	49.	-1.	-1.	1.	.066	1.	.396
113.	139.	168.	308.	324.	355.	5.	-16.	49.	-1.	-1.	1.	.066	1.	.391
113.	139.	167.	308.	323.	357.	5.	-16.	49.	-1.	-1.	1.	.066	1.	.386
113.	140.	166.	309.	323.	358.	5.	-16.	49.	-1.	-1.	1.	.066	1.	.381
113.	140.	166.	309.	322.	3.	5.	-16.	50.	-1.	-1.	1.	.066	1.	.376
113.	140.	165.	309.	322.	2.	5.	-16.	50.	-1.	-1.	1.	.066	1.	.371
113.	140.	165.	309.	321.	3.	5.	-16.	50.	-1.	-1.	1.	.066	1.	.366
113.	140.	164.	309.	320.	5.	5.	-16.	50.	-1.	-1.	1.	.066	1.	.361
113.	140.	164.	310.	320.	7.	5.	-16.	50.	-1.	-1.	1.	.066	1.	.356
113.	141.	163.	310.	319.	9.	5.	-16.	50.	-1.	-1.	1.	.066	1.	.351
113.	141.	163.	310.	319.	10.	5.	-16.	50.	-1.	-1.	1.	.066	1.	.346
113.	141.	162.	310.	318.	12.	5.	-16.	49.	-1.	-1.	1.	.066	1.	.341
113.	141.	162.	310.	318.	14.	5.	-16.	48.	-1.	-1.	1.	.066	1.	.336
113.	141.	161.	310.	317.	15.	5.	-16.	48.	-1.	-1.	1.	.066	1.	.331
113.	142.	160.	311.	317.	17.	5.	-17.	47.	-1.	-1.	1.	.066	1.	.326
113.	142.	174.	311.	316.	337.	5.	-17.	51.	-1.	-1.	1.	.066	1.	.321
113.	142.	173.	311.	316.	337.	5.	-17.	51.	-1.	-1.	1.	.066	1.	.316
113.	142.	173.	311.	315.	339.	6.	-17.	51.	-1.	-1.	1.	.066	1.	.311
112.	142.	173.	311.	315.	340.	6.	-17.	50.	-1.	-1.	1.	.066	1.	.306
112.	142.	172.	311.	314.	342.	6.	-17.	50.	-1.	-1.	1.	.066	1.	.301
112.	143.	171.	312.	314.	344.	6.	-17.	50.	-1.	-1.	1.	.066	1.	.296
112.	143.	171.	312.	314.	345.	6.	-17.	50.	-1.	-1.	1.	.066	1.	.291
112.	143.	170.	312.	313.	347.	6.	-17.	50.	-1.	-1.	1.	.066	1.	.286
112.	143.	170.	312.	313.	349.	6.	-17.	50.	-1.	-1.	1.	.066	1.	.281
112.	143.	169.	312.	311.	350.	6.	-17.	50.	-1.	-1.	1.	.066	1.	.276
112.	143.	169.	312.	311.	350.	6.	-17.	50.	-1.	-1.	1.	.066	1.	.271
112.	143.	169.	313.	311.	352.	6.	-17.	50.	-1.	-1.	1.	.066	1.	.266
112.	144.	168.	313.	310.	354.	6.	-17.	50.	-1.	-1.	1.	.066	1.	.261
112.	144.	167.	313.	310.	356.	6.	-17.	51.	-1.	-1.	1.	.066	1.	.256
112.	144.	166.	313.	309.	357.	6.	-17.	51.	-1.	-1.	1.	.066	1.	.251
112.	144.	166.	313.	309.	359.	6.	-17.	52.	-1.	-1.	1.	.066	1.	.246
112.	144.	166.	313.	308.	1.	6.	-17.	52.	-1.	-1.	1.	.066	1.	.241
112.	145.	165.	314.	307.	2.	6.	-17.	52.	-1.	-1.	1.	.066	1.	.236
112.	145.	165.	314.	307.	4.	6.	-17.	52.	-1.	-1.	1.	.066	1.	.231
112.	145.	164.	314.	306.	6.	6.	-17.	52.	-1.	-1.	1.	.066	1.	.226
112.	145.	163.	314.	306.	8.	6.	-17.	52.	-1.	-1.	1.	.066	1.	.221
112.	145.	163.	314.	305.	10.	6.	-17.	52.	-1.	-1.	1.	.066	1.	.216
112.	145.	162.	315.	305.	11.	6.	-17.	51.	-1.	-1.	1.	.066	1.	.211

112.	146.	162.	315.	304.	13.	6.	-17.	50.	1.	-.84	1.	.066	1.	.056	-.472
112.	146.	161.	315.	303.	15.	6.	-17.	49.	1.	-.84	1.	.066	1.	.056	-.467
112.	146.	161.	315.	303.	16.	6.	-17.	48.	1.	-.84	1.	.066	1.	.056	-.461
112.	146.	174.	315.	302.	337.	6.	-17.	52.	1.	-.84	1.	.066	1.	.056	-.473
112.	146.	173.	316.	301.	339.	6.	-17.	51.	1.	-.84	1.	.066	1.	.056	-.476
112.	147.	173.	316.	301.	340.	6.	-17.	50.	1.	-.84	1.	.066	1.	.056	-.479
112.	147.	172.	316.	301.	342.	6.	-17.	50.	1.	-.84	1.	.066	1.	.056	-.482
112.	147.	171.	316.	300.	344.	6.	-17.	49.	1.	-.84	1.	.066	1.	.056	-.484
112.	147.	171.	316.	299.	345.	6.	-17.	49.	1.	-.84	1.	.066	1.	.056	-.484
112.	147.	170.	316.	299.	347.	6.	-17.	49.	1.	-.84	1.	.066	1.	.056	-.487
111.	148.	170.	317.	298.	349.	6.	-17.	49.	1.	-.84	1.	.066	1.	.056	-.489
111.	148.	169.	317.	298.	350.	6.	-16.	49.	1.	-.84	1.	.066	1.	.056	-.491
111.	148.	168.	317.	297.	352.	6.	-16.	49.	1.	-.84	1.	.066	1.	.056	-.493
111.	148.	168.	317.	297.	354.	6.	-16.	49.	1.	-.84	1.	.066	1.	.056	-.488
111.	148.	167.	318.	296.	355.	6.	-16.	48.	1.	-.84	1.	.066	1.	.056	-.480
111.	148.	167.	318.	296.	357.	6.	-16.	48.	1.	-.84	1.	.066	1.	.056	-.475
111.	149.	166.	318.	295.	359.	6.	-16.	48.	1.	-.83	1.	.066	1.	.058	-.469
111.	149.	166.	318.	294.	0.	6.	-16.	48.	1.	-.83	1.	.066	1.	.058	-.464
111.	149.	165.	318.	294.	2.	6.	-16.	48.	1.	-.83	1.	.066	1.	.057	-.459
111.	149.	165.	318.	293.	4.	6.	-16.	48.	1.	-.83	1.	.066	1.	.057	-.455
111.	149.	164.	319.	293.	5.	6.	-15.	48.	1.	-.83	1.	.066	1.	.056	-.450
111.	150.	164.	319.	292.	7.	6.	-15.	47.	1.	-.83	1.	.066	1.	.056	-.446
111.	150.	163.	319.	292.	8.	6.	-15.	46.	1.	-.83	1.	.067	1.	.056	-.442
111.	150.	163.	319.	291.	10.	6.	-15.	46.	1.	-.83	1.	.067	1.	.056	-.437
111.	137.	163.	319.	331.	10.	6.	-17.	51.	1.	-.83	1.	.056	1.	.056	-.451
111.	137.	162.	320.	330.	13.	5.	-17.	50.	1.	-.83	1.	.056	1.	.056	-.449
111.	137.	161.	320.	329.	15.	5.	-17.	49.	1.	-.83	1.	.056	1.	.056	-.447
111.	137.	161.	320.	329.	17.	5.	-17.	48.	1.	-.83	1.	.056	1.	.056	-.445
111.	138.	160.	320.	329.	17.	5.	-17.	47.	1.	-.83	1.	.056	1.	.056	-.444
111.	138.	174.	320.	328.	337.	5.	-17.	51.	1.	-.83	1.	.056	1.	.056	-.456
111.	138.	173.	320.	328.	339.	5.	-17.	51.	1.	-.83	1.	.056	1.	.056	-.462
111.	138.	173.	321.	327.	340.	5.	-16.	50.	1.	-.83	1.	.056	1.	.056	-.469
111.	138.	172.	321.	326.	342.	5.	-16.	49.	1.	-.83	1.	.056	1.	.056	-.475
111.	138.	171.	321.	326.	344.	5.	-16.	49.	1.	-.83	1.	.056	1.	.056	-.481
111.	139.	171.	321.	325.	345.	5.	-16.	49.	1.	-.83	1.	.056	1.	.056	-.487
111.	139.	170.	321.	325.	347.	5.	-16.	49.	1.	-.83	1.	.056	1.	.056	-.492
111.	139.	170.	321.	324.	349.	5.	-16.	48.	1.	-.83	1.	.056	1.	.056	-.498
111.	139.	169.	322.	324.	350.	5.	-16.	48.	1.	-.83	1.	.056	1.	.056	-.503
111.	139.	169.	322.	323.	352.	5.	-16.	48.	1.	-.83	1.	.056	1.	.056	-.508
111.	140.	168.	322.	323.	353.	5.	-16.	48.	1.	-.83	1.	.056	1.	.056	-.505
110.	140.	168.	322.	322.	355.	5.	-16.	48.	1.	-.82	1.	.056	1.	.056	-.502
110.	140.	167.	322.	321.	357.	5.	-16.	49.	1.	-.82	1.	.056	1.	.056	-.499
110.	140.	166.	323.	321.	358.	5.	-16.	49.	1.	-.82	1.	.056	1.	.056	-.499
110.	140.	166.	323.	320.	0.	5.	-16.	49.	1.	-.82	1.	.056	1.	.056	-.496
110.	140.	165.	323.	320.	2.	5.	-16.	50.	1.	-.82	1.	.056	1.	.056	-.494
110.	141.	165.	323.	319.	3.	5.	-16.	50.	1.	-.82	1.	.057	1.	.057	-.491
110.	141.	164.	323.	319.	5.	5.	-16.	50.	1.	-.82	1.	.056	1.	.056	-.489
110.	141.	164.	323.	318.	7.	5.	-16.	49.	1.	-.82	1.	.056	1.	.056	-.487
110.	141.	163.	324.	318.	8.	5.	-16.	49.	1.	-.82	1.	.056	1.	.056	-.485
110.	141.	163.	324.	318.	10.	5.	-16.	49.	1.	-.82	1.	.056	1.	.056	-.482
110.	142.	162.	324.	317.	12.	5.	-16.	49.	1.	-.82	1.	.056	1.	.056	-.480
110.	142.	162.	324.	316.	13.	5.	-16.	47.	1.	-.82	1.	.056	1.	.056	-.477
110.	142.	161.	324.	315.	15.	5.	-16.	47.	1.	-.82	1.	.056	1.	.056	-.480
110.	142.	160.	325.	315.	17.	5.	-16.	46.	1.	-.82	1.	.056	1.	.056	-.475
110.	142.	160.	325.	315.	17.	5.	-16.	46.	1.	-.82	1.	.056	1.	.056	-.470
110.	142.	174.	325.	314.	337.	5.	-16.	50.	1.	-.82	1.	.056	1.	.056	-.479
110.	142.	173.	325.	314.	339.	5.	-16.	49.	1.	-.82	1.	.056	1.	.056	-.482
110.	143.	173.	325.	313.	340.	5.	-16.	49.	1.	-.82	1.	.056	1.	.056	-.486
110.	143.	172.	325.	313.	342.	5.	-16.	48.	1.	-.82	1.	.056	1.	.056	-.488
110.	143.	171.	325.	312.	343.	5.	-16.	48.	1.	-.82	1.	.056	1.	.056	-.491
110.	143.	171.	325.	312.	345.	5.	-16.	48.	1.	-.82	1.	.056	1.	.056	-.493
110.	143.	170.	325.	311.	347.	5.	-16.	48.	1.	-.82	1.	.056	1.	.056	-.495



108.	140.	167.	336.	320.	357.	5.	-14.	41.	-1.	-1.	1.	.084	1.	.058	.470
108.	140.	167.	336.	320.	358.	5.	-14.	41.	-1.	-1.	1.	.084	1.	.058	.467
108.	141.	166.	337.	320.	359.	4.	-13.	41.	-1.	-1.	1.	.084	1.	.057	.465
108.	141.	166.	337.	319.	1.	4.	-13.	41.	-1.	-1.	1.	.084	1.	.057	.464
108.	141.	165.	337.	319.	2.	4.	-13.	41.	-1.	-1.	1.	.085	1.	.057	.462
108.	141.	165.	337.	318.	3.	4.	-13.	41.	-1.	-1.	1.	.085	1.	.057	.460
107.	141.	164.	337.	318.	5.	4.	-13.	41.	-1.	-1.	1.	.085	1.	.057	.458
107.	141.	164.	337.	317.	6.	4.	-13.	41.	-1.	-1.	1.	.085	1.	.056	.456

CYCLE EFFICIENCY = .491

2. Program CLOCK 4: Point and Cycle Efficiencies for Two Pass  
Clock (Oxival) Step-Up Gear Train in  
Spin Environment

The kinematics of program CLOCK 4 is again based on the work in Appendix G. The moment input-output relationships are derived in section 2 of Appendix H. This program is in many ways very similar to CLOCK 3 with the exception that only two meshes are involved, and therefore, wherever possible, reference will be made to CLOCK 3. Again, it is assumed that the two meshes will have been tested by program CLOCK 1 for their geometric suitability. The format of the following is identical to that used in section 1 of this appendix. For the sake of clarity, it will be helpful to refer to these parallel descriptions.

a. Input Parameters (see Program CLOCK 4, below)

The following parameters represent the input data for the program (for explanation, refer to section 1a of this appendix):

MU

RPM

CAPRP1, CAPRP2, RP2, RP3

RHOG1, RHOG2, RHOP1, RHOP2

ACG1, ACG2, ACP1, ACP2

R1, R2, R3

TG1, TG2, TP1, TP2

NG1, NG2, NP2, NP3

RHO1, RHO2, RHO3

M1, M2, M3

MD

K

FHDOT1 = -1

b. Computations (see also COMMENT cards in program)

I. Computation of Gear Tooth Parameters

The required computations are identical to those in CLOCK 3.

II. Computation of MIN, GAMMAS and BETAS

The input moment is computed in the manner of eq. (I-1).

In addition, the angles  $\gamma_2$ ,  $\gamma_3$ ,  $\beta_1$  and  $\beta_2$  are found according to the expressions given in section 6b of Appendix A.

III. Computation of Other Parameters

The computation of the angles  $\Delta\phi_1$  and  $\Delta\psi_1$ , the length  $L_1$  as well as the centrifugal forces  $Q_1$ ,  $Q_2$  and  $Q_3$  (called  $Q_{3p}$  by eq. (H-245)) are identical to those described in the parallel section dealing with CLOCK 3.

IV. Preliminary Computations for Mesh 1

The preliminary computations for mesh 1 are identical to those given in section 1-IV of this appendix.

V. Preliminary Computations for Mesh 2

The preliminary computations for mesh 2 are identical to those given in section 1-V of this appendix.

## VI. Gear Train Motion Model: Kinematics, Point and Cycle Efficiencies

The simulation of the gear train model, which is necessary for the determination of both POINTEF and CYCLEFF, is found in a loop starting with statement label no.20 and ending with card no.531. The motions of the individual driving gears are initialized at their respective angles PHI1I and PHI2I. The meshes will be in round on round contact until they reach their respective transition angles PHI1T and PHI2T. After the transition angles are passed, the meshes will be in round on flat contact. These regimes continue until the final angles PHI1F and PHI2F are reached.

The increment DDPHI1 of the input gear 1 is obtained from an adaptation of eqs. (A-207) and (A-208), in which tooth numbers, rather than base circle radii are used. The increment DDPHI2 of gear 2 is related to the increment of the pinion angle PSI1.

While the motion of gear 1 is terminated when the angle PHI1 reaches the magnitude PHI1F (or rather PHI1F + DDPHI1 for moment summation purposes), gear 2 must be reset to its starting angle PHI2I whenever its final angle PHI2F has been reached.

The appropriate choice of moment equation depends upon which of the four possible combinations of contact conditions, as indicated by Table H-2, is applicable.

The following discusses the kinematics of the individual meshes as well as the determination of the point and cycle efficiencies where they differ from the description in section 1 of this appendix.

### A. Kinematics

The program only utilizes the kinematics of meshes 1 and 2. These are identical with those for program CLOCK 3, as given in section 1.

### B. Moment Computations, Point and Cycle Efficiencies

Regardless of the combination of contact conditions, the point efficiency is computed according to eq. (3), i.e.,

$$\eta_p = \text{POINTEP} = K_{\text{ratio}} \frac{M_{031}}{M_{1n}} \quad (\text{I-24})$$

where, with  $\dot{\phi}_1 = -1$

$$K_{\text{ratio}} = |\dot{\psi}_2| \quad (\text{I-25})$$

The cycle efficiency determination is based on eqs. (I-21) to (I-23).

The moment computations begin with the statement label no.24, and initially consist of the determination of selected variables between A11 and A72 and selected variables between C6 and C36, as applicable to the analyses of section 2 of Appendix H. The governing contact combination (see also Table H-2) is determined with the help of the four moment control statements, which start with card no.498. Once the appropriate combination is established, the program is directed to one of the four associated moment expressions. These expressions for  $M_{031}$  coincide with those given by eqs. (H-260), (H-261), (H-277) and (H-278). They are listed in the above

order beginning with statement label no.25 and ending with statement label no.28 .

The rationale of the control statements for meshes 1 and 2 is identical to that given for program CLOCK 3 (see section 1-VIIB of this appendix).

c. Output (see Program CLOCK 4, below)

The output of the program is best explained with the help of the sample problem at the end of the program.

I. Input Parameters

Mesh 1

CAPRP1 =  $R_{P1}$  = .47725 in. (1.212 cm)  
RP2 =  $r_{P2}$  = .09085 in. (0.231 cm)  
ACG1 =  $a_{G1}$  = .47725 in. (1.212 cm)  
ACP1 =  $a_{P1}$  = .09085 in. (0.231 cm)  
RHOG1 =  $\rho_{G1}$  = .03870 in. (0.098 cm)  
RHOP1 =  $\rho_{P1}$  = .01740 in. (0.044 cm)  
TG1 =  $t_{G1}$  = .03480 in. (0.088 cm)  
TP1 =  $t_{P1}$  = .02800 in. (0.71 cm)  
NG1 =  $n_{G1}$  = 42  
NP2 =  $n_{P2}$  = 8

Mesh 2

CAPRP2 =  $R_{P2}$  = .20670 in. (0.525 cm)  
RP3 =  $r_{P3}$  = .06890 in. (0.175 cm)  
ACG2 =  $a_{G2}$  = .20670 in. (0.525 cm)  
ACP2 =  $a_{P2}$  = .06890 in. (0.175 cm)

RHOG2 =  $\rho_{G2}$  = .02070 in. (0.053 cm)  
 RHOP2 =  $\rho_{P2}$  = .01040 in. (0.026 cm)  
 TG2 =  $t_{G2}$  = .02520 in. (0.064 cm)  
 TP2 =  $t_{P2}$  = .02080 in. (0.053 cm)  
 NG2 =  $n_{G2}$  = 27  
 NP3 =  $n_{P3}$  = 9

In addition

MU = .2  
 RPM = 1000  
 M1 =  $m_1$  =  $.69515 \times 10^{-4}$  lb-sec<sup>2</sup>/in. (12.171 g)  
 M2 =  $m_2$  =  $.97028 \times 10^{-5}$  lb-sec<sup>2</sup>/in. (1.699 g)  
 M3 =  $m_3$  =  $.10780 \times 10^{-5}$  lb-sec<sup>2</sup>/in. (0.189 g)  
 R1 =  $R_1$  = .750 in. (1.905 cm)  
 R2 =  $R_2$  = .750 in. (1.905 cm)  
 R3 =  $R_3$  = .750 in. (1.905 cm)  
 RHO1 =  $\rho_1$  = .060 in. (0.152 cm)  
 RHO2 =  $\rho_2$  = .030 in. (0.076 cm)  
 RHO3 =  $\rho_3$  = .025 in. (0.051 cm)  
 MD =  $md^2$  =  $.15 \times 10^{-4}$  lb-sec<sup>2</sup> in. (16.944 g - cm<sup>2</sup>)  
 K = 25

II. Computed Values

At the beginning of the output, one finds MIN =  $M_{in}$ .  
 Subsequently, the following are listed for each mesh:

$f_{P1}$ , the length of the pinion flats  
 $\beta_1$ , the fuze body pivot to pivot line angles

$\psi_{T1}$  and  $\varphi_{T1}$ , the transition angles as well as the associated subsidiary tests

$\varphi_{IN1}$  and  $\psi_{IN1}$ , the initial angles

$\varphi_{FIN1}$  and  $\psi_{FIN1}$ , the final angles

Finally, for the full range of the input angle  $\varphi_1$ , the point efficiency POINTEF is listed, in addition to other parameters which are useful for checking purposes. Note that DPSI1 and DPSI2 represent  $\dot{\psi}_1$  and  $\dot{\psi}_2$ , respectively. The cycle efficiency CYCLEFF is found at the end of the output.

Program CLOCK 4

I-57

```

1          PROGRAM CLOCK4(INPUT,OUTPUT,TAPES=INPUT,TAPES=OUTPUT)
C          A 1
C          A 2
C          A 3
C          A 4
C          A 5
5          A 6
          A 7
          A 8
          A 9
          A 10
          A 11
          A 12
          A 13
          A 14
          A 15
          A 16
          A 17
          A 18
          A 19
          A 20
          A 21
          A 22
          A 23
          A 24
          A 25
          A 26
          A 27
          A 28
          A 29
          A 30
          A 31
          A 32
          A 33
          A 34
          A 35
          A 36
          A 37
          A 38
          A 39
          A 40
          A 41
          A 42
          A 43
          A 44
          A 45
          A 46
          A 47
          A 48
          A 49
          A 50
          A 51
          A 52
          A 53

          PROGRAM CLOCK4(INPUT,OUTPUT,TAPES=INPUT,TAPES=OUTPUT)
          POINT AND CYCLE EFFICIENCIES FOR TWO PASS CLOCK (OGIVAL) STEP-UP
          GEAR TRAIN IN SPIN ENVIRONMENT

          REAL MU, LAMDA1, LAMDA2, LK1, LV1, LV2, LY2, L2, NP2, NP3, NG1, NG2, MIN, M1
          1 READ (5,40) MU, RPM, CAPRP1, CAPRP2, RP2, RP3, ACG1, ACG2, ACP1, ACP2, ISTOP
          READ (5,58) R1, R2, R3
          READ (5,41) RHOG1, RHOE2, RHOP1, RHOP2
          READ (5,42) TGI, TG2, TPI, TP2
          READ (5,43) NG1, NG2, NP2, NP3
          READ (5,61) M1, M2, M3
          READ (5,44) RHOT, RHO2, RHO3, MO, K, J1, J2
          PI=3.14159
          Z=PI/180.
          OMEGA=RPM*2.*PI/60.
          CM2=OMEGA*OMEGA
          PHO011=-1.

          COMPUTATION OF GEAR TOOTH PARAMETERS FOR BOTH MESHES

          CXG1=RHOG1-TGI/2.
          DELG1=ASIN(CXG1/CAPRP1)
          CXPI=RHOP1-TP1/2.
          DELP1=ASIN(CXPI/RP2)
          GAMMP1=ASIN(RHOP1/RP2)
          ALPHI1=GAMMP1-DELP1
          FPI=ACP1*COS(GAMMP1)
          B1=CAPRP1*RP2
          CXG2=RHOG2-TG2/2.
          DELG2=ASIN(CXG2/CAPRP2)
          CXPI2=RHOP2-TP2/2.
          DELP2=ASIN(CXPI2/RP3)
          GAMMP2=ASIN(RHOP2/RP3)
          ALPHI2=GAMMP2-DELP2
          FPI2=ACP2*COS(GAMMP2)
          B2=CAPRP2*RP3

          COMPUTATION OF MIN, GAMMAS AND BETAS

          MIN=4D*OM2
          DELTA2=ACOS(((CAPRP1+RP2)*(CAPRP1+RP2)+R1+R1-R2*R2)/(2.*R1*(CAPRP1
          1+RP2)))
          DELTA3=ACOS(((CAPRP2+RP3)*(CAPRP2+RP3)+R2+R2-R3*R3)/(2.*R2*(CAPRP2
          1+RP3)))
          GAMMA2=ACOS((R1+R1+R2-R2-(CAPRP1+RP2)*(CAPRP1+RP2))/(2.*R1*R2))
          GAMMA3P=ACOS((R2+R2+R3-R3-(CAPRP2+RP3)*(CAPRP2+RP3))/(2.*R2*R3))
          GAMMA3=GAMMA2+GAMMA3P
          BETA1=PI-DELTA2
          BETA2=GAMMA2+PI-DELTA3
          BETA1D=BETA1/Z
          BETA2D=BETA2/Z

```

```

55 WRITE (6,45) MIN,MU,RPM,CAPRP1,CAPRP2,RP2,RP3,ACG1,ACG2,ACPI,ACP2
   WRITE (6,59) R1,R2,R3
   WRITE (6,46) RHOG1,RHOG2,RHOP1,RHOP2
   WRITE (6,47) TGI,IG2,TP1,TP2
   WRITE (6,48) NG1,NG2,NP2,NP3
   WRITE (6,62) M1,M2,M3
   WRITE (6,49) RHO1,RHO2,RHO3,MO,K,PHOOT1
   WRITE (6,60) FPI,FP2
   WRITE (6,50) BETA10,BETA20
60
65 C COMPUTATION OF OTHER PARAMETERS
   C
   C
   DPHI1=360./NG1*Z
   DPSI1=360./MP2*Z
   DPHI2=360./NG2*Z
   DPSI2=360./MP3*Z
   L1=RHOG1+RHOP1
   L2=RHOG2+RHOP2
   Q1=M1*R1*OM2
   Q2=M2*R2*OM2
   Q3=M3*R3*OM2
70
75 C PRELIMINARY COMPUTATIONS FOR MESH 1
   C
   C
   C
   C
   C
   DETERMINATION OF TRANSITION ANGLE OF MESH 1
   A1T=RHOG1*COS(BETA1+ALPH1)+FPI*SIN(BETA1+ALPH1)
   B1T=-RHOG1*SIN(BETA1+ALPH1)+FPI*COS(BETA1+ALPH1)
   C1T=(ACG1*ACG1-RHOG1*RHOG1-81*81-FPI*FPI)/(2.*81)
   ROOT11=A1T+AT1+B1T*B1T-C1T*C1T
   Y1T1=A1T+SORT(ROOT11)
   Y1T2=A1T-SORT(ROOT11)
   X1T=81T+C1T
   PS11T1=2.*ATAN2(Y1T1,X1T)
   PS11T2=2.*ATAN2(Y1T2,X1T)
   PS11E11=PS11T1
   PS11E12=PS11T2
90 IF (PS11T1.GT.PI) PS11E11=PS11E11-2.*PI
   IF (PS11T1.LT.-PI) PS11E11=PS11E11+2.*PI
   IF (PS11T2.GT.PI) PS11E12=PS11E12-2.*PI
   IF (PS11T2.LT.-PI) PS11E12=PS11E12+2.*PI
   IF (PS11E11.GE.0.) TEST11=ABS(PI-BETA1+PS11E11-ALPH1)/Z
   IF (PS11E11.LT.0.) TEST11=ABS(PI+BETA1-(PS11E11+2.*PI-ALPH1))/Z
   IF (PS11E12.GE.0.) TEST12=ABS(PI-BETA1+PS11E12-ALPH1)/Z
   IF (PS11E12.LT.0.) TEST12=ABS(PI+BETA1-(PS11E12+2.*PI-ALPH1))/Z
100 IF (PS11T1.LT.0.) PS11T1=PS11T1+2.*PI
   IF (PS11T2.LT.0.) PS11T2=PS11T2+2.*PI
   PS11I10=PS11T1/Z
   PS11I20=PS11T2/Z
   WRITE (6,31) PS11I10,TEST11
   WRITE (6,32) PS11I20,TEST12
105 CALL TRANS1 (RHOG1,ALPH1,BETA1,FPI,ACG1,B1,DELGI,Z,PS11T1,PHI1T1,
   TE11)

```

```

110 IF (G11.GT.FP1) GO TO 2
    PHIIT=PHIIT1
    PSIIIT=PSIIIT1
    GO TO 4
111 2 CALL TRANS1 (RHOG1,ALPHP1,BETA1,FP1,ACG1,B1,DELG1,Z,PSIIIT2,PHIIT2,
    1G12)
112 IF (G12.LT.FP1) GO TO 3
    WRITE (6,51)
113 STOP
114 3 PHIIT=PHIIT2
    PSIIIT=PSIIIT2
115 4 IF (PHIIT.LT.0.) PHIIT=PHIIT+2.*PI
    IF (PSIIIT.LT.0.) PSIIIT=PSIIIT+2.*PI
120 PHIITD=PHIIT/Z
    PSIIITD=PSIIIT/Z
    WRITE (6,52) PHIITD,PSIIITD
125 C DETERMINATION OF CORRECT SIGN FOR ROUND ON FLAT REGIME OF MESH 1
    C
    C A1F=ACG1*COS(PHIIT+DELG1+ALPHP1)-B1*COS(BETA1+ALPHP1)
    B1F=-ACG1*SIN(PHIIT+DELG1+ALPHP1)+B1*5.*Y(BETA1+ALPHP1)
    C1F=RHOG1
130 ROOT1F=A1F+A1F*B1F*B1F-C1F*C1F
    Y1F=A1F+SORT(ROOT1F)
    X1F=B1F+C1F
    PSI1F1=2.*ATAN2(Y1F1,X1F)
    PSI1F2=2.*ATAN2(Y1F2,X1F)
135 IF (PSI1F1.LT.0.) PSI1F1=PSI1F1+2.*PI
    IF (PSI1F2.LT.0.) PSI1F2=PSI1F2+2.*PI
    IF (ABS(PSI1F1-PSI1F2)-LT.ABS(PSI1F2-PSI1F1)) GO TO 5
    SIGN1F=-1.
    GO TO 6
140 5 SIGN1F=1.
    C
    C COMPUTATION OF FINAL AND INITIAL VALUES OF PHI AND PSI FOR MESH 1
    C
    C 6 DO 7 I=1,2000
    PHID1=PHIITD-(I-1.)/100.
    PHI1=PHID1*Z
    A1F=ACG1*COS(PHI1+DELG1+ALPHP1)-B1*COS(BETA1+ALPHP1)
    B1F=-ACG1*SIN(PHI1+DELG1+ALPHP1)+B1*SIN(BETA1+ALPHP1)
    C1F=RHOG1
145 ROOT1F=A1F+A1F*B1F*B1F-C1F*C1F
    Y1F=A1F+SIGN1F*SORT(ROOT1F)
    X1F=B1F+C1F
    PSI1F=2.*ATAN2(Y1F,X1F)
    IF (PSI1F.LT.0.) PSI1F=PSI1F+2.*PI
150 LX1=B1*COS(BETA1)+ACPI*COS(PSI1F-DPSI1+DELPI)-ACG1*COS(PHI1+DPHI1+
    1DELGI)
    LY1=B1*SIN(BETA1)+ACPI*SIN(PSI1F-DPSI1+DELPI)-ACG1*SIN(PHI1+DPHI1+
    1DELGI)
    LL1=SORT(LX1*LY1+LY1*LY1)
    .53
154 A 154
155 A 155
156 A 156
157 A 157
158 A 158
159 A 159

```

```

160 DELEL1=LL1-L1
    IF (DELEL1.LE.0.) GO TO 8
7 CONTINUE
8 PH11F=PH11
  PSI1FF=PSI1F
  PH11I=PH11F+DPHI1
  PSI1I=PSI1FF-DPSI1
  IF (PSI1I.LT.0.) PSI1I=PSI1I+2.*PI
  PH11ID=PH11I/Z
  PSI1ID=PSI1I/Z
  PH11FD=PH11F/Z
  PSI1FD=PSI1FF/Z
  WRITE (6,53) PH11ID,PSI1ID,PH11FD,PSI1FD
C
175 DETERMINATION OF CORRECT SIGN FOR ROUND ON ROUND REGIME OF MESH 1
C
    A1R=ACG1*SIN(PHI1I+DELG1-DELP1)-B1*SIN(BETA1-DELP1)
    B1R=ACG1*COS(PHI1I+DELG1-DELP1)-B1*COS(BETA1-DELP1)
    C1R=(ACP1*ACP1+ACG1*ACG1+B1*B1-L1*L1-2.*ACG1*B1*COS(PHI1I+DELG1-DE
    L1I))/2.*ACP1
    ROOT1R=A1R+B1R+C1R
    Y1R=A1R+SORT(ROOT1R)
    Y1R2=A1R-SORT(ROOT1R)
    X1R=B1R+C1R
    PSI1R1=2.*ATAN2(Y1R1,X1R)
    PSI1R2=2.*ATAN2(Y1R2,X1R)
    IF (PSI1R1.LT.0.) PSI1R1=PSI1R1+2.*PI
    IF (PSI1R2.LT.0.) PSI1R2=PSI1R2+2.*PI
    IF (ABS(PSI1I-PSI1R1).LT.ABS(PSI1I-PSI1R2)) GO TO 9
    SIGN1R=-1
    GO TO 10
9 SIGN1R=1.
C
195 PRELIMINARY COMPUTATIONS FOR MESH 2
C
    DETERMINATION OF TRANSITION ANGLE OF MESH 2
C
10 A2I=-RHOG2*COS(BETA2-ALPHP2)+FP2*SIN(BETA2-ALPHP2)
    B2I=-RHOG2*SIN(BETA2-ALPHP2)+FP2*COS(BETA2-ALPHP2)
    C2I=(ACG2*ACG2-RHOG2*RHOG2-B2*B2-FP2*FP2)/(2.*B2)
    ROOT2I=A2I+A2I+B2I*B2I-C2I
    Y2I=A2I+SORT(ROOT2I)
    Y2I2=A2I-SORT(ROOT2I)
    X2I=B2I+C2I
    PSI2I1=2.*ATAN2(Y2I1,X2I)
    PSI2I2=2.*ATAN2(Y2I2,X2I)
    PSI2E1=PSI2I1
    PSI2E2=PSI2I2
    IF (PSI2I1.GT.PI) PSI2E1=PSI2E1-2.*PI
    IF (PSI2I1.LT.PI) PSI2E1=PSI2E1+2.*PI
    IF (PSI2I2.GT.PI) PSI2E2=PSI2E2-2.*PI
    IF (PSI2I2.LT.PI) PSI2E2=PSI2E2+2.*PI
    IF (PSI2E1.GE.0.) TEST2I=ABS(PI-BETA2+PSI2E1+ALPHP2)/Z

```

```

215 IF (PSITE21.LT.0.) TEST21=ABS(PI+BETA2-(PSITE21+2.*PI+ALPHP2))/Z
    IF (PSITE22.GE.0.) TEST22=ABS(PI-BETA2+PSITE22-ALPHP2)/Z
    IF (PSITE22.LT.0.) TEST22=ABS(PI+BETA2-(PSITE22+2.*PI+ALPHP2))/Z
    IF (PSI2T1.LT.0.) PSI2T1=PSI2T1+2.*PI
    IF (PSI2T2.LT.0.) PSI2T2=PSI2T2+2.*PI
    PSI2TD=PSI2T1/Z
    PSI2FD=PSI2T2/Z
220 WRITE (6,33) PSI2T1D,TEST21
    WRITE (6,34) PSI2TD,TEST22
    CALL TRANS2 (RHOG2,ALPHP2,BETA2,FP2,ACG2,B2,DELG2,Z,PSI2T1,PHI2T1,
    1G2)
    IF (G21.GT.FP2) GO TO 11
    PHI2T=PHI2T1
    PSI2T=PSI2T1
    GO TO 13
225
11 CALL TRANS2 (RHOG2,ALPHP2,BETA2,FP2,ACG2,B2,DELG2,Z,PSI2T2,PHI2T2,
    1G22)
    IF (G22.LT.FP2) GO TO 12
    WRITE (6,54)
    STOP
12 PHI2T=PHI2T2
    PSI2T=PSI2T2
235 13 IF (PHI2T.LT.0.) PHI2T=PHI2T+2.*PI
    IF (PSI2T.LT.0.) PSI2T=PSI2T+2.*PI
    PHI2TD=PHI2T/Z
    PSI2TD=PSI2T/Z
    WRITE (6,55) PHI2TD,PSI2TD
240
C
C
C DETERMINATION OF CORRECT SIGN FOR ROUND ON FLAT REGIME OF MESH 2
A2F=ACG2-COS(PHI2T-DELG2-ALPHP2)-B2*CGS(BETA2-ALPHP2)
B2F=-ACG2-SIN(PHI2T-DELG2-ALPHP2)+B2*SIN(BETA2-ALPHP2)
C2F=-RHOG2
ROOT2F=A2F+A2F+82F+82F-C2F+C2F
Y2F1=A2F+SQRT(ROOT2F)
Y2F2=A2F-SQRT(ROOT2F)
X2F=B2F+C2F
PSI2F1=2.*ATAN2(Y2F1,X2F)
PSI2F2=2.*ATAN2(Y2F2,X2F)
IF (PSI2F1.LT.0.) PSI2F1=PSI2F1+2.*PI
IF (PSI2F2.LT.0.) PSI2F2=PSI2F2+2.*PI
IF (ABS(PSI2F1-PSI2T)-LT.ABS(PSI2F2-PSI2T)) GO TO 14
PSI2FD=PSI2F1/Z
PSI2FD=PSI2F2/Z
SIGN2F=-1.
GO TO 15
14 SIGN2F=1.
250
C
C
C COMPUTATION OF FINAL AND INITIAL VALUES OF PHI AND PSI FOR MESH 2
15 DO 16 I=1,1000
    PHI2D=PHI2TD*(I-1.)/100.
    PHI2=PHI2D+Z
255
260
265

```

```

A 256 A2F=ACG2*CGS(PHI2-DELG2-ALPHP2)-B2*CGS(BETA2-ALPHP2)
A 267 B2F=-ACG2*SIN(PHI2-DELG2-ALPHP2)+B2*SIN(BETA2-ALPHP2)
A 268 C2F=-RHGG2
A 269 ROOT2F=A2F+A2F*B2F+B2F*C2F
A 270 Y2F=A2F+SIGN2F*SQR(ROOT2F)
A 271 X2F=B2F+C2F
A 272 PSI2F=2.*ATAN2(Y2F,X2F)
A 273 IF (PSI2F.LT.0.) PSI2F=PSI2F+2.*PI
A 274 LX2=B2*CGS(BETA2)+ACP2*CGS(PSI2F+DPSI2-DELP2)-ACG2*CGS(PHI2-DPHI2-
A 275 1DELG2)
A 276 LY2=B2*SIN(BETA2)+ACP2*SIN(PSI2F+DPSI2-DELP2)-ACG2*SIN(PHI2-DPHI2-
A 277 1DELG2)
A 278 LL2=SQRT(LX2*LX2+LY2*LY2)
A 279 DELEL2=LL2-L2
A 280 IF (DELEL2.LE.0.) GO TO 17
A 281 16 CONTINUE
A 282 17 PHI2F=PHI2
A 283 PSI2FF=PSI2F
A 284 PHI2I=PHI2F-DPHI2
A 285 PSI2I=PSI2FF+DPSI2
A 286 IF (PSI2I.GT.2.*PI) PSI2I=PSI2I-2.*PI
A 287 PHI2ID=PHI2I/Z
A 288 PSI2ID=PSI2I/Z
A 289 PHI2FD=PHI2F/Z
A 290 PSI2FD=PSI2FF/Z
A 291 WRITE (6,56) PHI2ID,PSI2ID,PHI2FD,PSI2FD
A 292
A 293 C
A 294 C
A 295 DETERMINATION OF CORRECT SIGN FOR ROUND ON ROUND REGIME OF MESH 2
A 296 A2R=B2*SIN(BETA2+DELP2)-ACG2*SIN(PHI2I-DELG2+DELP2)
A 297 R2R=B2*CGS(BETA2+DELP2)-ACG2*CGS(PHI2I-DELG2+DELP2)
A 298 C2R=(L2-L2-B2*B2-ACG2*ACG2-ACP2*ACP2+2.*ACG2*B2*CGS(PHI2I-DELG2-BE
A 299 1TA2))/(2.*ACP2)
A 300 ROOT2R=A2R+A2R*B2R+B2R*C2R
A 301 Y2R1=A2R+SQRT(ROOT2R)
A 302 Y2R=A2R-SQRT(ROOT2R)
A 303 X2R=B2R+C2R
A 304 PSI2R1=2.*ATAN2(Y2R1,X2R)
A 305 PSI2R2=2.*ATAN2(Y2R2,X2R)
A 306 IF (PSI2R1.LT.0.) PSI2R1=PSI2R1+2.*PI
A 307 IF (PSI2R2.LT.0.) PSI2R2=PSI2R2+2.*PI
A 308 IF (ABS(PSI2I-PSI2R1).LT.ABS(PSI2I-PSI2R2)) GO TO 18
A 309 SIGN2R=-1.
A 310 GO TO 19
A 311 18 SIGN2R=1.
A 312 C
A 313 C
A 314 C
A 315 19 DDPHI1=NP2*(PHI2F-PHI2I)/((K*NG1)
A 316 PHI1=PHI1+DDPHI1
A 317 WRITE (6,35)
A 318 20 PHI1D=PHI1-DDPHI1
A 319 PHI1D=PHI1/Z

```

```

320 C IF (PHI1.LE.PHI1F+DDPHI1) GO TO 30
325 C MESH: 1
330 C IF (PHI1.LE.PHI1F) GO TO 21
A 319 AIR=ACG1*SIN(PHI1+DELGI-DELP1)-B1*SIN(BETA1-DELP1)
A 320 B1R=ACG1*COS(PHI1+DELGI-DELP1)-B1*COS(BETA1-DELP1)
A 321 CIR=(ACPI*ACPI+ACG1*ACG1+B1*B1-L1*L1-2.*ACG1*B1*COS(PHI1+DELGI-BET
A 322 1A1))/2.*ACPI
A 323 ROOT1R=AIR*AIR+A1R*B1R+C1R*C1R
A 324 X1R=B1R*C1R
A 325 Y1R=A1R*SIGNR*SQRT(ROOT1R)
A 326 PSI1=2.*ATAN2(Y1R,X1R)
A 327 IF (ABS(PHI1-PHI1I).LT.0.0001)PSI1I=PSI1
A 328 IF (ABS(PHI1-PHI1I).LT.0.0001)PSI1P=PSI1I
A 329 PSI1D=PSI1/Z
A 330 SLAM1=(B1*SIN(BETA1)+ACPI*SIN(PSI1+DELP1)-ACG1*SIN(PHI1+DELGI))/L1
A 331 CLAM1=(B1*COS(BETA1)+ACPI*COS(PSI1+DELP1)-ACG1*COS(PHI1+DELGI))/L1
A 332 LAMDA1=ATAN2(SLAM1,CLAM1)
A 333 IF (LAMDA1.LT.0.) LAMDA1=LAMDA1+2.*PI
A 334 PSDOT1=PHOOT1*ACG1-(B1/ACPI*SIN(PHI1+DELGI-BETA1)+SIN(PHI1-PSI1+DE
A 335 1LGI-DELP1))/(A1R*COS(PSI1)-B1R*SIN(PSI1))
A 336 VST1R=PHOOT1*(ACG1*COS(PHI1+DELGI-LAMDA1)+RHOG1)-PSOOT1*(ACPI*COS(
A 337 1PSI1+DELPI-LAMDA1)-RHOP1)
A 338 STR=VST1R/ABE(VST1R)
A 339 GO TO 22
A 340 21 A1F=ACG1*COS(PHI1+DELGI+ALPHP1)-B1*COS(BETA1+ALPHP1)
A 341 B1F=-ACG1*SIN(PHI1+DELGI+ALPHP1)+B1*SIN(BETA1+ALPHP1)
A 342 C1F=RHOG1
A 343 ROOT1F=A1F+A1F+B1F*B1F-C1F*C1F
A 344 Y1F=A1F+SIGN1F*SQRT(ROOT1F)
A 345 X1F=B1F+C1F
A 346 PSI1=2.*ATAN2(Y1F,X1F)
A 347 IF (PSI1.LT.0.) PSI1=PSI1+2.*PI
A 348 PSI1D=PSI1/Z
A 349 GI=(ACG1*SIN(PHI1+DELGI)+RHOG1*COS(PSI1-ALPHP1)-B1*SIN(BETA1))/SIN
A 350 1(PSI1-ALPHP1)
A 351 PSDOT1=PHOOT1*(ACG1*COS(PHI1+DELGI+ALPHP1)-B1*SIN(BETA1)-B1
A 352 1F*SIN(PSI1))
A 353 VST1F=PHOOT1*(ACG1*SIN(PSI1-ALPHP1)-PHI1-DELGI)-RHOG1
A 354 S1F=VST1F/ABS(VST1F)
A 355 MESH 2
A 356 22 DDPHI2=PSI1-PSI1P
A 357 IF (ABS(PHI1-PHI1I).LT.0.0001) PHI2=PHI2I
A 358 PHI2=PHI2+DDPHI2
A 359 PSI1P=PSI1
A 360 IF (PHI2.GT.PH12F) PHI2=PHI2I
A 361 PH12D=PHI2/Z
A 362 IF (PHI2.GE.PHI2I) GO TO 23
A 363 A2R=B2-SIN(BETA2+DELP2)-ACG2*SIN(PHI2-DELG2+DELP2)
A 364
A 365
A 366
A 367
A 368
A 369
A 370
A 371

```

```

375      B2R=B2+COS(BETA2+DEL P2)-ACG2+COS(PHI2-DELG2+DEL P2)
        C2R=(L2-L2-B2-B2-ACG2+ACG2-ACP2+ACP2+2.*ACG2+B2+COS(PHI2-DELG2-BET
        1A2))/L2.*ACP2)
        ROOT2R=A2R+A2R+B2R+B2R-C2R+C2R
        Y2R=A2R+SIGM2R*SQRT(ROOT2R)
        X2R=B2R+C2R
        PS12=2.*ATAN2(Y2R,X2R)
        IF (PS12.LT.0.) PS12=PS12+2.*PI
        IF (ABS(PHI2-PHI2I).LT.0.0001) PS12I=PS12
        IF (ABS(PHI2-PHI2I).LT.0.0001) PS12P=PS12I
        PS12B=PS12/Z
        SLAB2=(B2+*SIN(BETA2)+ACP2+*SIN(PS12-DEL P2)-ACG2+*SIN(PHI2-DELG2))/L2
        CLAB2=(B2+*COS(BETA2)+ACP2+*COS(PS12-DEL P2)-ACG2+*COS(PHI2-DELG2))/L2
        LAMBDA2=ATAN2(SLAB2,CLAB2)
        IF (LAMBDA2.LT.0.) LAMBDA2=LAMBDA2+2.*PI
        PHDOT2=PSDOT1
        PSDOT2=PHDOT2+ACG2*(-*SIN(PHI2-PS12-DELG2+DEL P2)-B2/ACP2+*SIN(PHI2-0
        1ELG2-BETA2))/(A2R+*COS(PS12)-B2R+*SIN(PS12))
        VST2R=PHDOT2*(ACG2+*COS(PHI2-DELG2-LAMBDA2)+RHOG2)-PSDOT2*(ACP2+*COS(
        1PS12-DEL P2-LAMBDA2)-RHOP2)
        S2R=VST2R/ABS(VST2R)
        GO TO 24
23      A2F=ACG2+*COS(PHI2-DELG2-ALPHP2)-B2+*COS(BETA2-ALPHP2)
        B2F=-ACG2+*SIN(PHI2-DELG2-ALPHP2)+B2+*SIN(BETA2-ALPHP2)
        C2F=-RHOG2
        ROOT2F=A2F+A2F+B2F+B2F-C2F+C2F
        Y2F=A2F+SIGM2F*SQRT(ROOT2F)
        X2F=B2F+C2F
        PS12=2.*ATAN2(Y2F,X2F)
        IF (PS12.LT.0.) PS12=PS12+2.*PI
        PS12B=PS12/Z
        G2=(ACG2+*SIN(PHI2-DELG2)-RHOG2+*COS(PS12+ALPHP2)-B2+*SIN(BETA2))/SIN
        1(PS12+ALPHP2)
        PHDOT2=PSDOT1
        PSDOT2=(PHDOT2+ACG2+*COS(PHI2-DELG2-ALPHP2-PS12))/(A2F+*COS(PS12)-B2
        1F+*SIN(PS12))
        VST2F=PHDOT2*(ACG2+*SIN(PS12+ALPHP2-PHI2+DELG2)+RHOG2)
        S2F=VST2F/ABS(VST2F)
C
C
C      MOMENT COMPUTATIONS
24      DN=1.-*MU+*MU
        A12=ABS((MU+*(S1R-1.)+*SIN(LAMBDA1)-(1.+*MU+*MU+*S1R)*COS(LAMBDA1))/DN)
        A11=ABS(((1.+*MU+*MU+*S2R)*COS(LAMBDA2)-*MU+*(S2R-1.)+*SIN(LAMBDA2))/DN)
        A13=ABS((-*COS(GAMMA2)-*MU+*SIN(GAMMA2))/DN)
        A14=ABS(((1.+*MU+*MU+*S2R)*SIN(LAMBDA2)-*MU+*(1.-*S2R)+*COS(LAMBDA2))/DN)
        A15=ABS((MU+*(1.-*S1R)*COS(LAMBDA1)-(1.+*MU+*MU+*S1R)*SIN(LAMBDA1))/DN)
        A16=ABS((MU+*COS(GAMMA2)-*SIN(GAMMA2))/DN)
        A17=ABS(((1.-*MU+*MU+*S1R)*COS(LAMBDA1)-*MU+*(1.+*S1R)*SIN(LAMBDA1))/DN)
        A18=ABS(1./DN)
        A19=ABS(((1.-*MU+*MU+*S1R)*SIN(LAMBDA1)+*MU+*(1.-*S1R)*COS(LAMBDA1))/DN)
        A20=ABS(MU/DN)
        A21=ABS((MU+*(1.-*S2R)*SIN(LAMBDA2)+*(1.+*MU+*MU+*S2R)*COS(LAMBDA2))/DN)

```

A 372

A 373

A 374

A 375

A 376

A 377

A 378

A 379

A 380

A 381

A 382

A 383

A 384

A 385

A 386

A 387

A 388

A 389

A 390

A 391

A 392

A 393

A 394

A 395

A 396

A 397

A 398

A 399

A 400

A 401

A 402

A 403

A 404

A 405

A 406

A 407

A 408

A 409

A 410

A 411

A 412

A 413

A 415

A 416

A 417

A 418

A 419

A 420

A 421

A 422

A 423

A 424

425 A22=ABS(((1.-MU\*BU\*S1F)\*SIN(PSI1-ALPHP1)+SIN(PSI1-ALPHA))\*COS(PSI1-ALPHA) A 425  
 1P1))/DN A 426  
 A23=ABS((MU\*SIN(GAMMA2)+COS(GAMMA2))/DN) A 427  
 A24=ABS(((1.-MU\*BU\*S2R)\*SIN(LAMDA2)-MU\*(1.-S2R)\*COS(LAMDA2))/DN) A 428  
 A25=ABS(((1.-MU\*BU\*S1F)\*SIN(PSI1-ALPHP1)+(MU\*BU\*S1F-1.)\*COS(PSI1-ALP A 429  
 1HP1))/DN A 430  
 A26=ABS((-SIN(GAMMA2)+MU\*COS(GAMMA2))/DN) A 431  
 A27=ABS((-1.-MU\*BU\*S1F)\*SIN(PSI1-ALPHP1)+MU\*(S1F-1.)\*COS(PSI1-ALP A 432  
 1HP1))/DN A 433  
 A28=ABS(1./DN) A 434  
 A29=ABS((MU\*(S1F-1.)\*SIN(PSI1-ALPHP1)+(1.-MU\*BU\*S1F)\*COS(PSI1-ALPHA A 435  
 1P1))/DN A 436  
 A30=ABS(MU/DN) A 437  
 A37=ABS(((1.-MU\*BU\*S2F)\*SIN(PSI2+ALPHP2)+MU\*(S2F-1.)\*COS(PSI2+ALPHA A 438  
 1P2))/DN A 439  
 A38=ABS(((1.-MU\*BU\*S1F)\*SIN(PSI1-ALPHP1)-MU\*(1.+S1F)\*COS(PSI1-ALPHA A 441  
 1P1))/DN A 442  
 A39=ABS((MU\*SIN(GAMMA2)+COS(GAMMA2))/DN) A 443  
 A40=ABS((MU\*(S2F-1.)\*SIN(PSI2+ALPHP2)-(1.-MU\*BU\*S2F)\*COS(PSI2+ALPHA A 444  
 1P2))/DN A 445  
 A41=ABS((-MU\*(1.+S1F)\*SIN(PSI1-ALPHP1)+(MU\*BU\*S1F-1.)\*COS(PSI1-ALP A 446  
 1HP1))/DN A 447  
 A42=ABS((MU\*COS(GAMMA2)-SIN(GAMMA2))/DN) A 448  
 A43=ABS(((1.-MU\*BU\*S2F)\*SIN(PSI2+ALPHP2)-MU\*(1.-S2F)\*COS(PSI2+ALPHA A 449  
 1P2))/DN A 450  
 A44=ABS((MU\*(S1R-1.)\*SIN(LAMDA1)-(1.-MU\*BU\*S1R)\*COS(LAMDA1))/DN) A 451  
 A45=ABS((MU\*SIN(GAMMA2)+COS(GAMMA2))/DN) A 452  
 A46=ABS((MU\*(S2F-1.)\*SIN(PSI2+ALPHP2)-(1.-MU\*BU\*S2F)\*COS(PSI2+ALPHA A 453  
 1P2))/DN A 454  
 A47=ABS((-1.-MU\*BU\*S1R)\*SIN(LAMDA1)+MU\*(1.-S1R)\*COS(LAMDA1))/DN) A 455  
 A48=ABS((-SIN(GAMMA2)+MU\*COS(GAMMA2))/DN) A 456  
 A65=ABS((MU\*(1.+S2R)\*SIN(LAMDA2)+(MU\*BU\*S2R-1.)\*COS(LAMDA2))/DN) A 457  
 A66=ABS((MU\*SIN(GAMMA3)-COS(GAMMA3))/DN) A 458  
 A67=ABS((MU\*BU\*S2R-1.)\*SIN(LAMDA2)-MU\*(1.+S2R)\*COS(LAMDA2))/DN) A 459  
 A68=ABS((-SIN(GAMMA3)-MU\*COS(GAMMA3))/DN) A 460  
 A69=ABS(((BU\*BU\*S2F-1.)\*SIN(PSI2+ALPHP2)-MU\*(1.+S2F)\*COS(PSI2+ALPHA A 461  
 1P2))/DN A 462  
 A70=ABS((MU\*SIN(GAMMA3)-COS(GAMMA3))/DN) A 463  
 A71=ABS((-MU\*(1.+S2F)\*SIN(PSI2+ALPHP2)+(1.-MU\*BU\*S2F)\*COS(PSI2+ALP A 464  
 1HP2))/DN A 465  
 A72=ABS((-SIN(GAMMA3)-MU\*COS(GAMMA3))/DN) A 466  
 C6=ACG2\*(SIN(PHI2-DELG2-LAMDA2)-MU\*S2R\*COS(PHI2-DELG2-LAMDA2))-MU\* A 467  
 RHQ2\*(A11+A14)-MU\*RHO2\*S2R A 468  
 C7=MU\*RHO2\*(A13+A16) A 469  
 C8=-1\*ACPI\*(SIN(PSI1+DELP1-LAMDA1)-MU\*S1R\*COS(PSI1+DELP1-LAMDA1))+M A 470  
 U\*RHO2\*(A12+A15)+MU\*S1R\*RHOPI A 471  
 C9=BU\*RHO1\*(A18+A20) A 472  
 C10=BU\*RHO1\*(A17+A19)+ACG1\*(SIN(PHI1+DELG1-LAMDA1)-MU\*S1R\*COS(PHI1 A 473  
 1+DELG1-LAMDA1))-MU\*S1R\*RHO1 A 474  
 C11=ACG2\*(SIN(PHI2-DELG2-LAMDA2)-MU\*S2R\*COS(PHI2-DELG2-LAMDA2))-MU A 475  
 1+PHC2\*(A21+A24)-MU\*RHO2\*S2R A 476  
 C12=BU\*RHO2\*(A23+A26) A 477  
 C13=G1-MU\*RHO2\*(A22+A25)



```

GO TO 20
30 CYCLEFF=-BTOT*DDPHI1/(PHI1F-PHI1I)
WRITE (6,57) CYCLEFF
BTOT=0.
IF (ISTOP-.ME.0) GO TO 1
STOP

C
C
535
540
545
550
555
560
565
570
575
580

31 FORMAT (6X,9#PSI11TD =,F9.4,3X,8#TEST11 =,F9.4)
32 FORMAT (6X,9#PSI112D =,F9.4,3X,8#TEST12 =,F9.4//)
33 FORMAT (6X,9#PSI212D =,F9.4,3X,8#TEST21 =,F9.4)
34 FORMAT (6X,9#PSI212D =,F9.4,3X,8#TEST22 =,F9.4//)
35 FORMAT (85H PSI1 PSI2 PSI1 PSI2 DPS11 DPS12 SIR S2R S
11F G1 S2F G2 POINTEFF//)
36 FORMAT (6X,4(F4.0,2X),2(F5.0,2X),2(F3.0,2X),24X,F5.3)
37 FORMAT (6X,4(F4.0,2X),2(F5.0,2X),5X,F3.0,2X,F3.0,2X,F5.3,14X,F5.3)
38 FORMAT (6X,4(F4.0,2X),2(F5.0,2X),10X,2(F3.0,2X,F5.3,2X),F5.3)
39 FORMAT (6X,4(F4.0,2X),2(F5.0,2X),F3.0,19X,F3.0,2X,F5.3,2X,F5.3)
40 FORMAT (F10.3,F10.0/4F10.5/4F10.5//)
41 FORMAT (4F10.4)
42 FORMAT (4F10.4)
43 FORMAT (4F10.0)
44 FORMAT (3F10.4/F10.6/F10.4)
45 FORMAT (1H1,5X,5#MIN =,F8.4,3X,4#MU =,F6.3,3X,5#RPM =,F6.0//6X,8#C
LAPRPI =,F8.5,3X,8#CAPR2 =,F8.5//6X,5#R2 =,F8.5,3X,5#R3 =,F8.5//
26X,6#ACG1 =,F8.5,3X,6#AC2 =,F8.5,3X,6#ACP1 =,F8.5,3X,6#ACP2 =,F8.
35//)
46 FORMAT (6X,7#HDG1 =,F8.5,3X,7#HDG2 =,F8.5,3X,7#HDOP1 =,F8.5,3X,7
1#RHCP2 =,F8.5//)
47 FORMAT (6X,5#TGI =,F8.5,3X,5#IG2 =,F8.5,3X,5#TPI =,F8.5,3X,5#TP2 =
1,F8.5//)
48 FORMAT (6X,5#MG1 =,F5.0,3X,5#MG2 =,F5.0,3X,5#MP2 =,F5.0,3X,5#MP3 =
1,F5.0//)
49 FORMAT (6X,6#HD1 =,F6.3,3X,6#HD2 =,F6.3,3X,6#HD3 =,F6.3//6X,4#M
1D =,F10.6//6X,3#K =,F6.1//6X,8#PHD11 =,F5.1//)
50 FORMAT (6X,8#ETA1D =,F8.4,3X,8#ETA2D =,F8.4//)
51 FORMAT (6X,30#SOMETHING IS WRONG WITH MESH 1)
52 FORMAT (6X,8#PHI1TD =,F8.4,3X,8#PSI1TD =,F8.4)
53 FORMAT (6X,8#PHI1TD =,F8.4,3X,8#PSI1TD =,F8.4,3X,8#PHI1FD =,F8.4,3
1X,8#PSI1FD =,F8.4//)
54 FORMAT (6X,30#SOMETHING IS WRONG WITH MESH 2)
55 FORMAT (6X,8#PHI2TD =,F8.4,3X,8#PSI2TD =,F8.4)
56 FORMAT (6X,8#PHI2TD =,F8.4,3X,8#PSI2TD =,F8.4,3X,8#PHI2FD =,F8.4,3
1X,8#PSI2FD =,F8.4//)
57 FORMAT (1#0,5X,1#MCYCLE EFFICIENCY =,F5.3)
58 FORMAT (3F10.5)
59 FORMAT (6X,4#R1 =,F8.5,3X,4#R2 =,F8.5,3X,4#R3 =,F8.5//)
60 FORMAT (6X,5#F1 =,F8.5,3X,5#F2 =,F8.5//)
61 FORMAT (3E15.5)
62 FORMAT (6X,4#M1 =,E15.5,3X,4#M2 =,E15.5,3X,4#M3 =,E15.5//)
END

```

```

1  SUBROUTINE TRANS1 (RHOG,ALPHP,BETA,FP,ACG,B,DELG,Z,PSIT,PHIT,G)
    PI=3.14159
    ST=(-RHOG+COS(PSIT-ALPHP)+B*SIN(BETA)+FP+SIN(PSIT-ALPHP))/ACG
    CT=(RHOG+SIN(PSIT-ALPHP)+B*COS(BETA)+FP+COS(PSIT-ALPHP))/ACG
    PHIT=ATAN2(ST,CT)-DELG
    PHINEXT=PHIT-.1*Z
    AF=ACG+COS(PHINEXT+DELG+ALPHP)-B*COS(BETA+ALPHP)
    BF=-ACG+SIN(PHINEXT+DELG+ALPHP)+B*SIN(BETA+ALPHP)
    CF=RHOG
    ROOT=AF+BF+BF-CF+CF
    YF1=AF+SQRT(ROOTF)
    YF2=AF-SQRT(ROOTF)
    XF=BF+CF
    PSINEX1=2.*ATAN2(YF1,XF)
    PSINEX2=2.*ATAN2(YF2,XF)
    IF (PSINEX1.LT.0.) PSINEX1=PSINEX1+2.*PI
    IF (PSINEX2.LT.0.) PSINEX2=PSINEX2+2.*PI
    IF (ABS(PSINEX1-PSIT).LT.ABS(PSINEX2-PSIT)) GO TO 1
    PSINEX=PSINEX2
    GO TO 2
2  PSINEX=PSINEX1
    G=(ACG+SIN(PHINEXT+DELG)+RHOG+COS(PSINEX-ALPHP)-B*SIN(BETA))/SIN(
1PSINEX-ALPHP)
    RETURN
    END
    
```

```

1  SUBROUTINE TRANS2 (RHOG,ALPHP,BETA,FP,ACG,B,DELG,Z,PSIT,PHIT,G)
   PI=3.14159
   ST=(RHOG*COS(PSIT+ALPHP)+B*SIN(BETA)+FP*SIN(PSIT+ALPHP))/ACG
   CT=(-RHOG*SIN(PSIT+ALPHP)+B*COS(BETA)+FP*COS(PSIT+ALPHP))/ACG
   PHIT=ATAN2(ST,CT)+DELG
   PHINEXT=PHIT+.1*Z
   AF=ACG*COS(PHINEXT-DELG-ALPHP)-B*COS(BETA-ALPHP)
   BF=-ACG*SIN(PHINEXT-DELG-ALPHP)+B*SIN(BETA-ALPHP)
   CF=-RHOG
   ROOTF=AF+BF+CF
   YF1=AF+SQRT(ROOTF)
   YF2=AF-SQRT(ROOTF)
   XF=BF+CF
   PSINEX1=2.*ATAN2(YF1,XF)
   PSINEX2=2.*ATAN2(YF2,XF)
   IF (PSINEX1.LT.0.) PSINEX1=PSINEX1+2.*PI
   IF (PSINEX2.LT.0.) PSINEX2=PSINEX2+2.*PI
   IF (ABS(PSINEX1-PSIT).LT.ABS(PSINEX2-PSIT)) GO TO 1
   PSINEX1=PSINEX2
   GO TO 2
   1 PSINEX1=PSINEX1
   2 G=(ACG+SIN(PHINEXT-DELG)-RHOG*COS(PSINEX1+ALPHP)-B*SIN(BETA))/SIN(
   RETURN
   END

```

```

C 1
C 2
C 3
C 4
C 5
C 6
C 7
C 8
C 9
C 10
C 11
C 12
C 13
C 14
C 15
C 16
C 17
C 18
C 19
C 20
C 21
C 22
C 23
C 24
C 25-

```

MIN = .1645 MJ = .200 RPM = 1000.  
 CAPRP1 = .47725 CAPRP2 = -.20670  
 RP2 = .09085 RP3 = -.06890  
 ACG1 = .47725 ACG2 = .20670 ACP1 = .09085 ACP2 = -.06890  
 R1 = .75000 R2 = .75000 R3 = .75000  
 RHOC1 = .03870 RHOC2 = .02070 RHOP1 = .01740 RHOP2 = .01040  
 TG1 = .03480 TG2 = .02520 TP1 = .02800 TP2 = .02060  
 NG1 = 42. MC2 = 27. NP2 = 8. NP3 = 9.  
 M1 = .69514E-04 M2 = .97028E-05 M3 = .10780E-05  
 RHO1 = .060 RHC2 = .030 RHC3 = .025  
 MD = .000015  
 K = 25.0  
 PHO0T1 = -1.0  
 FP1 = .08917 FP2 = .06811  
 BETA10 = 112.2552 BETA20 = 145.0978  
 PSI1T10 = 305.6017 TEST11 = 4.4495  
 PSI1T20 = 343.6259 TEST12 = 42.4736  
 PHI1T0 = 113.5016 PSI1T10 = 305.6017  
 PHI1T10 = 115.9930 PSI1T10 = 292.4283 PHI1FD = 107.4216 PSI1FD = 337.4283  
 PSI2T20 = 286.9442 TEST21 = 29.4719  
 PSI2T20 = 312.0785 TEST22 = 4.3377  
 PHI2T0 = 143.0461 PSI2T0 = 312.0785  
 PHI2T0 = 136.7828 PSI2T0 = 330.9521 PHI2FD = 150.1161 PSI2FD = 290.9521  
 PHI1 PHI2 PS11 PS12 DPS11 DPS12 S1R S2R S1F G1 S2F G2 POINTEF  
 116. 137. 292. 331. 5. -16. 1. -1. .617  
 116. 137. 293. 329. 5. -16. 1. -1. .626  
 116. 138. 294. 328. 5. -16. 1. -1. .634  
 116. 138. 294. 326. 5. -16. 1. -1. .642  
 116. 139. 295. 324. 5. -16. 1. -1. .650  
 115. 139. 295. 323. 5. -16. 1. -1. .657  
 115. 140. 296. 321. 5. -16. 1. -1. .665  
 115. 141. 296. 320. 5. -16. 1. -1. .672  
 115. 141. 297. 318. 5. -16. 1. -1. .679  
 115. 142. 297. 316. 5. -16. 1. -1. .686  
 115. 142. 298. 315. 5. -16. 1. -1. .693  
 115. 143. 298. 313. 5. -16. 1. -1. .689  
 115. 143. 299. 312. 5. -16. 1. .068 .685



108.	150.	333.	291.	5.	-13.	1.	.083	1.	.067	.531
108.	137.	333.	331.	5.	-15.	1.	.083	1.		.551
108.	137.	334.	329.	5.	-15.	1.	.083	1.		.555
108.	138.	334.	328.	5.	-14.	1.	.083	1.		.559
108.	138.	334.	327.	5.	-14.	1.	.084	1.		.563
108.	139.	335.	325.	5.	-14.	1.	.084	1.		.566
108.	139.	335.	324.	5.	-14.	1.	.084	1.		.569
108.	140.	336.	322.	5.	-14.	1.	.084	1.		.572
108.	140.	336.	321.	5.	-14.	1.	.084	1.		.575
108.	141.	337.	320.	4.	-13.	1.	.084	1.		.578

CYCLE EFFICIENCY = .620

DISTRIBUTION LIST

Commander  
U.S. Army Armament Research and Development Command  
ATTN: DRDAR-LCN, F. Tepper (30)  
DRDAR-TSS (5)  
Dover, NJ 07801

Commander  
Harry Diamond Laboratories  
ATTN: Library  
DRXDO-DAB, D. Overman  
Washington, DC 20418

Defense Technical Information Center (2)  
Cameron Station  
Alexandria, VA 22314

Weapon System Concept Team/CSL  
ATTN: DRDAR-ACW  
Aberdeen Proving Ground, MD 21010

Technical Library  
ATTN: DRDAR-CLJ-L  
Aberdeen Proving Ground, MD 21010

Director  
U.S. Army Ballistic Research Laboratory  
ARRADCOM  
ATTN: DRDAR-TSB-S (STINFO)  
Aberdeen Proving Ground, MD 21005

Benet Weapons Laboratory  
Technical Library  
ATTN: DRDAR-LCB-TL  
Watervliet, NY 12189

Commander  
U.S. Army Armament Materiel Readiness Command  
ATTN: DRSAR-LEP-L  
Rock Island, IL 61299

Director  
U.S. Army TRADOC Systems Analysis Activity  
ATTN: ATAA-SL (Tech Lib)  
White Sands Missile Range, NM 88002

THIS REPORT HAS BEEN DELIMITED  
AND CLEARED FOR PUBLIC RELEASE  
UNDER DOD DIRECTIVE 5200.20 AND  
NO RESTRICTIONS ARE IMPOSED UPON  
ITS USE AND DISCLOSURE.

DISTRIBUTION STATEMENT A

APPROVED FOR PUBLIC RELEASE;  
DISTRIBUTION UNLIMITED.